Cranfield University at Silsoe
National Soil Resources Institute

Ph.D. Thesis
2009

Sorche O'Keefe

The Recovery of Soils after Compaction:

A laboratory investigation into the effect of wet/dry cycles on bulk density and soil hydraulic functions

Principal Supervisor: Dr. Cedric Kechavarzi
Associate Supervisor: Professor Richard J. Godwin

September 2009

This thesis is submitted in fulfilment of the requirement for the degree of Doctor of Philosophy

Abstract

Van den Akker *et al.* (2003) stated that "European subsoils are more threatened than ever in history" in an editorial referring to the results of the European Union concerted action "Experiences with the impact of subsoil compaction on soil crop growth and environment and ways to prevent subsoil compaction". Compaction of agricultural soils not only reduces yields but can lead to pollution of surface waters and the release of greenhouse gases. Understanding, therefore, how, and to what extent, subsoil compaction may be reversed seems of vital importance.

The literature suggests that soils with a range of textures could recover structural properties such as total and macro-porosity, infiltration rate and stability, although the extent and depth of these changes varies greatly. Factors affecting the extent and depth of changes are the rate of wetting and drying and the matric potentials achieved during drying (influenced by crop cover and irrigation practices as well as climate), organic matter content and tillage history.

There is, however, a limited amount of information regarding changes to the pore-size distribution and unsaturated hydraulic conductivity of soils with wet/dry cycles. Although there are models able to predict the compaction that would occur for a given set of conditions, as well as the compactibility of soils and surface crack generation, there are no predictive models that describe structural changes due to wet/dry cycles.

The aims of this study were to assess the changes in bulk density and hydrological parameters of a range of soils, of varying texture and other physical and chemical properties, with wet/dry cycles and to explore the relationships between any measured changes and the measured soil properties. A series of laboratory experiments were designed to measure changes to the total porosity and pore size distribution and hydraulic functions of soil samples. Changes to bulk density and moisture content of undisturbed soil cores at field capacity with wet/dry cycles were monitored. Changes to the moisture release curve and hydraulic conductivity curve (as well as bulk density) of remoulded clayey subsoil samples, with wet/dry cycles, were estimated using the multi-step outflow method. The surface cracking of the samples during the wetting and drying process was also explored. Changes to these parameters were statistically compared between soils and between initial bulk densities, and related to soil properties such as texture, organic matter content and Atterberg limits with a general linear model for repeated measures.

Changes to the bulk density of the soils after three wet/dry cycles were found to be significantly different (at the 95 % probability level) between soils and between initial bulk densities. It was found that 90 % of the changes in bulk density could be predicted from the initial bulk density and the liquid limit of soils alone.

The porosity gained or lost during wet/dry cycles was not confined to the macro-pore region, but included changes to pores that were undrained at pressures up to and including 100 m of water. Changes in the pore size distribution, as described by the parameters of the water

release curve, modelled with the van Genuchten-Mualem equation, were found to be statistically related to soil texture and Atterberg limits.

Changes to the hydraulic conductivity function of the soils were found to be affected by changes to the connectivity of the pore network, not just to changes in the volume of conducting pores. This was particularly true of the saturated hydraulic conductivity which was found to increase the most in soil samples that experienced a concomitant increase in bulk density and decrease in macro-porosity.

Changes to the area of surface cracks were found to be significantly related to changes in the saturated hydraulic conductivity and to changes in the parameters of the van Genuchten-Mualem equation. It was also found that cracks did not close up entirely when the samples were saturated and there were many instances where wetting increased the area of surface cracks, relative to the preceding dry event, implying that the wetting phase was as important in structural formation as the drying phase.

There is a strong suggestion that it would be possible to construct a relatively simple model, based on easily measurable parameters, which could be used to predict the changes to soil structure achievable with wet/dry cycles. Further research is needed, therefore, that extends the data set upon which the predictive model designed in this study was constructed. Refinement of the model to include information on the rates of wetting and drying would also contribute greatly to its applicability to the field situation. However, important steps have

been made by this study towards a more comprehensive understanding of soil structural dynamics.

Acknowledgments

The author is very grateful to Cranfield University, National Soil Research Institute and the Douglas Bomford Trust for sponsoring this research.

Many thanks to Dr. Kim Blackburn, Dr. Terence Richards, Mrs. Gabriela Lovelace, Mr. Richard Andrews, Mr Allen Hilton, Mr. Roger Swatland, Mr. Roy Newman, Mr. Simon Stranks and many other members of University staff, for their technical advice and assistance.

Special thanks are also expressed to Dr Mike Hann and Dr. Richard Whalley for their invaluable contributions.

Deepest gratitude is expressed to Dr. Cedric Kechavarzi, Professor Dick Godwin, Professor Peter Leeds-Harrison and Dr. Marc Dresser, for their insights, guidance, supervision and unerring patience and encouragement.

To all my family and friends, who have supported and encouraged me throughout the course of my studies, many, many thanks.

Finally, thank you to my partner Chris who has been my rock, especially in these last months when I needed him most.

Table of Contents

Abstract i

Acknowledgments v

Table of Contents vi

Table of Figures xi

Table of Tables xix

Table of Equations xxi

Nomenclature and Abbreviations xxiii

1 Introduction 1

1.1 Soil functions 1

1.2 Understanding of the issues relating to compaction and soil structural dynamics 5

1.2.1 The causes of compaction 5

1.2.2 Current understanding of the persistence of compaction and the recovery of soil structure 6

1.2.3 The focus of this study 8

1.3 Aim and objectives 10

2 Soil structure, its Degradation and Amelioration 12

2.1 Issues relating to the compaction of soils 12

2.2 The causes of compaction 16
2.3 The vulnerability of soils to compaction 20
2.4 Recovery of soil structure after compaction 22
2.4.1 Field studies 25
2.4.2 Laboratory studies 35
2.4.3 Summary 50
2.5 Multi-step outflow method – estimating changes in the van Genuchten-Mualem parameters 55
2.5.1 Summary 69
3 Materials and Methods 71
3.1 Overview 71
3.2 Soil selection and sampling 75
3.3 Construction of subsoil samples with a range of bulk densities 80
3.4 Soil physical and chemical characteristics 82
3.4.1 Particle-size distribution 83
3.4.2 Organic matter content lost on ignition 84
3.4.3 Oxidisable organic matter content 84
3.4.4 Plastic limit 85
3.4.5 Liquid limit 85
3.4.6 Shrinkage limit 86
3.4.7 Cation exchange capacity 86
3.5 Changes in bulk density and macro-porosity of the undisturbed samples 87

3.6 Saturated hydraulic conductivity – falling head method 92

3.7 Multi-step outflow method – estimating changes in the van Genuchten-Mualem parameters 94

3.7.1 Measurement of outflow 94

3.7.2 Modelling 104

3.8 Image analysis 111

3.8.1 Background 111

3.8.2 Application 118

4 Results and Discussion 121

4.1 Soils' physical and chemical properties 121

4.1.1 Particle-size distribution 121

4.1.2 Physical and chemical properties 124

4.2 Changes to the bulk density and available water with wet/dry cycles 129

4.2.1 Changes to the saturated volumetric moisture content 131

4.2.2 Changes in the volumetric moisture content at tension 138

4.2.3 Changes in saturated volumetric moisture content and the relation of these changes to soil parameters 143

4.2.4 Conclusions on changes to bulk density and available water 154

4.3 Testing the predictive model against a range of initial bulk densities 154

4.3.1 Changes in bulk density with wet/dry cycles 157

4.4 Equilibrium bulk density and 'D' value 160

4.5 Changes in saturated hydraulic conductivity with wet/dry cycles 163
4.6 Changes to the water retention and hydraulic conductivity functions 168
4.6.1 SS/2 169
4.6.2 SS/3 172
4.6.3 SS/4 178
4.6.4 General statistical trends in changes to the parameters of the van Genuchten-Mualem Equation with wet/dry cycles 181
4.6.5 Conclusions on the results of the transient outflow experiments 185
4.7 Dexter's index of soil physical quality 189
4.8 Surface crack generation with wet/dry cycles 192
4.8.1 The cracking of SS/2 193
4.8.2 The cracking of SS/3 198
4.8.3 The cracking of SS/4 201
4.8.4 Correlations between the area of surface cracks and other soil characteristics 204
4.8.5 Statistical analysis of surface cracks 208
5 Summary of Results and Discussions and Directions of Further Research 217
5.1 Summary of results and discussions 217
5.2 Further research 230
6 Conclusion 235
References 238
Appendix 1 255
Appendix 2 258

Appendix 3 261

Appendix 4 264

Appendix 5 268

SS/2 269

Low density group 269

Medium density group 275

High density group 279

SS/3 285

Low density group 285

Medium density group 291

High density group 295

SS/4 299

Low density group 299

Medium density group 305

High density group 311

Appendix 6 315

Table of Figures

Figure 1. Soil damage by agricultural machinery. Taylor, 2003. 12

Figure 2. The stages of compaction as visualised by Horn et al., 2003. 16

Figure 3. Formation of soil aggregates (Lesley Dampier & Distance Education and Technology Continuing Studies, The University of British Columbia). 24

Figure 4. Simple correlations between mean weight diameter and some soil parameters (after Grant *et al.,* 1995). 43

Figure 5. Influence of peat amendment and wet/dry cycles on soil structure on mechanical behaviour (after Zang *et al.*, 2005). 46

Figure 6. Map of the farm from which the soil samples were taken. 76

Figure 7. Example of one of the profile pits dug in order to establish appropriate depths from which to take samples. 78

Figure 8. Soil sampling with the coring device. 79

Figure 9. Experimental equipment used in the multi-step outflow method.....96

Figure 10. Layout of the equipment used in to measure the cumulative outflow of water, at given pressure heads, with time. 97

Figure 11. Example of the graphs that were produced to monitor drainage as it was occurring. 99

Figure 12. Flow diagram illustrating the experimental procedure of the Multi-Step Outflow experiment.....103

Figure 13. Screen shot showing an example of the HYDRUS-1D user interface. 108

Figure 14. Screen shot showing profile discretization in HYDRUS-1D. 111

Figure 15. Screen shot showing the different stages of image processing. 119

Figure 16. Textural triangle showing the particle size distribution of the soils investigated created using the soil texture calculator provided by NRCS (http://soils.usda.gov/technical/aids/investigations/texture/). 122

Figure 17. Particle size distribution of the investigated soils. 123

Figure 18. The measured physical and chemical parameters of the investigated soils. 126

Figure 19. Initial mean bulk density of soils.....130

Figure 20. Changes in the volumetric moisture content of the plough layer of soil 2 (PP/2). 133

Figure 21. Changes in the volumetric moisture content of the subsoil of soil 2 (SS/2). 134

Figure 22. Changes in the volumetric moisture content of the plough layer of soil 3 (PP/3). 134

Figure 23. Changes in the volumetric moisture content of the subsoil of soil 3 (SS/3). 135

Figure 24. Changes in the volumetric moisture content of the plough layer of soil 4 (PP/4). 135

Figure 25. Changes in the volumetric moisture content of the subsoil of soil four (SS/4)....136

Figure 26. Changes in the volumetric moisture content of the plough layer of soil 1(PP/1). 136

Figure 27. Changes in the volumetric moisture content of the subsoil of soil 1 (SS/1). 137

Figure 28. Changes in the volumetric moisture content of the plough layer of soil 5 (PP/5). 137

Figure 29. Changes in the volumetric moisture content of the subsoil of soil five (SS/5). ...138

Figure 30. The observed and the predicted saturated volumetric moisture content of the samples at the third saturation, based on the first run of the general linear model for repeated measures.....145

Figure 31. The observed and the predicted saturated volumetric moisture content of the samples at the third saturation, based on the second run of the general linear model for repeated measures. 147

Figure 32. The observed and the predicted saturated volumetric moisture content of the samples at the third saturation, based on the fourth run of the general linear model for repeated measures. 150

Figure 33. A comparison between the observed bulk density at the third saturation and that predicted by the model.....151

Figure 34. Predicted changes in the bulk density of the clayey soils, assuming a wide range of initial bulk densities. 152

Figure 35. Predicted changes in the bulk density of the sandier soils, assuming a wide range of initial bulk densities.....153

Figure 36. Initial bulk density of individual soil samples plotted against the bulk density to which the soil blocks from which they were taken were compressed. 156

Figure 37. Changes in the bulk density of individual soil samples with wet/dry cycles. 158

Figure 38. Comparisons between measured and modelled bulk density at the third saturation. 160

Figure 39. Critical limits for plant growth for 1 - loamy sand, 2 - light loam, 3 - silty loam, 4 - clay loam. Håkansson and Lipiec, 2000. 161

Figure 40. Changes in saturated hydraulic conductivity with time, grouped by initial bulk density. 164

Figure 41. Diagram showing the direction of crack propagation during both the wetting and the drying phase. 166

Figure 42. Hydraulic properties of sample 3 of SS/2 (initial bulk density 1.23 g cm^{-3}) estimated with HYDRUS-1D. 170

Figure 43. Total volume of water filled pores of sample 3 of SS/2 during cycles 1 and 3.... 172

Figure 44. Hydraulic properties of sample 1 of SS/3 (initial bulk density 0.90 g cm^{-3}) estimated with HYDRUS-1D. 173

Figure 45. Total volume of water filled pores of sample 1 of SS/3 during cycles 1 and 3.... 174

Figure 46. A simplified model of soil structure. 176

Figure 47. A simplification of the possible changes to the pore network that would result in a loss of total porosity but an increase in hydraulic conductivity. 177

Figure 48. Hydraulic properties of sample 8 of SS/4 (initial bulk density 1.43 g cm^{-3}) estimated with HYDRUS-1D. 179

Figure 49. Total volume of water filled pores of sample 8 of SS/4 during cycles 1 and 3.... 180

Figure 50. Changes in Dexter's Soil Quality Index between cycles 1 and 3. 191

Figure 51. An example of one of the samples of SS/2 (initial bulk density 1.48 g cm^{-3})..... 194

Figure 52. The total area of crack on the surface of the samples of SS/2, averaged for the initial bulk density class. 195

Figure 53. An example of SS/3 (initial bulk density 1.44 g cm^{-3}). 199

Figure 54. The total area of crack on the surface of the samples of SS/3, averaged for the initial bulk density class. 200

Figure 55. An example of SS/4 (initial bulk density 1.40 g cm^{-3}). 202

Figure 56. The total area of crack on the surface of the samples of SS/4, averaged for the initial bulk density class. 203

Figure 57. Correlations between surface crack area and bulk density, changes in bulk density and saturated hydraulic conductivity. 207

Figure 58. An example of the compression data gathered for sub-soils two, three and four. 259

Figure 59. Graph showing all data obtained from compressing six samples of each soil, assuming a particle density of 2.65 g cm^{-3}. 260

Figure 60.SS/2, sample 1. Total volume of water filled pores during drainage cycles 1 and 3. 269

Figure 61. SS/2, sample 1. Hydraulic properties estimated with HYDRUS-1D. 270

Figure 62. SS/2, sample 2. Total volume of water filled pores during drainage cycles 1 and 3. 271

Figure 63. SS/2, sample 2. Hydraulic properties estimated with HYDRUS-1D. 272

Figure 64. SS/2, sample 3. Total volume of water filled pores during drainage cycles 1 and 3. 273

Figure 65. SS/2, sample 3. Hydraulic properties estimated with HYDRUS-1D. 274

Figure 66. SS/2, sample 4. Total volume of water filled pores during drainage cycles 1 and 3. 275

Figure 67. SS/2, sample 4. Hydraulic properties estimated with HYDRUS-1D. 276

Figure 68. SS/2, sample 5. Total volume of water filled pores during drainage cycles 1 and 3. 277

Figure 69. SS/2, sample 5. Hydraulic properties estimated with HYDRUS-1D. 278

Figure 70. SS/2, sample 6. Total volume of water filled pores during drainage cycles 1 and 3. 279

Figure 71. SS/2, sample 6. Hydraulic properties estimated with HYDRUS-1D. 280

Figure 72. SS/2, sample 7. Total volume of water filled pores during drainage cycles 1 and 3. 281

Figure 73. SS/2, sample 7. Hydraulic properties estimated with HYDRUS-1D. 282

Figure 74. SS/2, sample 8. Total volume of water filled pores during drainage cycles 1 and 3. 283

Figure 75. SS/2, sample 8. Hydraulic properties estimated with HYDRUS-1D. 284

Figure 76. SS/3, sample 1. Total volume of water filled pores during drainage cycles 1 and 3. 285

Figure 77. SS/3, sample 1. Hydraulic properties estimated with HYDRUS-1D. 286

Figure 78. SS/3, sample 2. Total volume of water filled pores during drainage cycles 1 and 3. 287

Figure 79. SS/3, sample 2. Hydraulic properties estimated with HYDRUS-1D. 288

Figure 80. SS/3, sample 3. Total volume of water filled pores during drainage cycles 1 and 3. 289

Figure 81. SS/3, sample 3. Hydraulic properties estimated with HYDRUS-1D. 290

Figure 82. SS/3, sample 4. Total volume of water filled pores during drainage cycles 1 and 3. 291

Figure 83. SS/3, sample 4. Hydraulic properties estimated with HYDRUS-1D. 292

Figure 84. SS/3, sample 5. Total volume of water filled pores during drainage cycles 1 and 3. 293
Figure 85. SS/3, sample 5. Hydraulic properties estimated with HYDRUS-1D. 294
Figure 86. SS/3, sample 6. Total volume of water filled pores during drainage cycles 1 and 3. 295
Figure 87. SS/3, sample 6. Hydraulic properties estimated with HYDRUS-1D. 296
Figure 88. SS/3, sample 7. Total volume of water filled pores during drainage cycles 1 and 3. 297
Figure 89. SS/3, sample 7. Hydraulic properties estimated with HYDRUS-1D. 298
Figure 90. SS/4, sample 1. Total volume of water filled pores during drainage cycles 1 and 3. 299
Figure 91. SS/4, sample 1. Hydraulic properties estimated with HYDRUS-1D. 300
Figure 92. SS/4, sample 2. Total volume of water filled pores during drainage cycles 1 and 3. 301
Figure 93. SS/4, sample 2. Hydraulic properties estimated with HYDRUS-1D. 302
Figure 94. SS/4, sample 3. Total volume of water filled pores during drainage cycles 1 and 3. 303
Figure 95. SS/4, sample 3. Hydraulic properties estimated with HYDRUS-1D. 304
Figure 96. SS/4, sample 4. Total volume of water filled pores during drainage cycles 1 and 3. 305
Figure 97. SS/4, sample 4. Hydraulic properties estimated with HYDRUS-1D. 306
Figure 98. SS/4, sample 5. Total volume of water filled pores during drainage cycles 1 and 3. 307

Figure 99. SS/4, sample 5. Hydraulic properties estimated with HYDRUS-1D. 308

Figure 100. SS/4, sample 6. Total volume of water filled pores during drainage cycles 1 and 3.....309

Figure 101. SS/4, sample 6. Hydraulic properties estimated with HYDRUS-1D. 310

Figure 102. SS/4, sample 7. Total volume of water filled pores during drainage cycles 1 and 3.....311

Figure 103. SS/4, sample 7. Hydraulic properties estimated with HYDRUS-1D. 312

Figure 104. SS/4, sample 8. Total volume of water filled pores during drainage cycles 1 and 3.....313

Figure 105. SS/4, sample 8. Hydraulic properties estimated with HYDRUS-1D. 314

Table of Tables

Table 1. The particle size distribution of the investigated soils in % mass of total mineral content.....122

Table 2. The Plasticity Index, calculated as the difference between the liquid and the plastic limits, of the investigated soils.....127

Table 3. Significance of changes in volumetric moisture content. 132

Table 4. First run of the general linear model for repeated measures.....144

Table 5. Second run of the general linear model for repeated measures. 147

Table 6. Fourth run of the general linear model for repeated measures. 149

Table 7. The interactions between the cycle and the area of surface cracks when considering the value of α of the selected data set. 208

Table 8. The statistical dependence of *n* on surface cracks. 210

Table 9. The interaction between cycle and the area of surface cracks in determining *n* for the selected data set.....211

Table 10. The statistical dependence of *l* on surface cracks. 211

Table 11. The interaction between cycle and the area of surface cracks in determining *l* for the whole data set.....212

Table 12. The statistical dependence of K_{sat} of the whole data set on surface cracks. 213

Table 13. The interaction between cycle and the area of surface cracks in determining K_s for the selected data set.....213

Table 14. The effect of surface cracks in determining Dexter's S value and how it changed with wet/dry cycles, for the whole data set. 214

Table 15. The interaction between parameters and cycle in determining the value of S of the selected data set 215

Table of Equations

Equation 1.The strain on individual springs (Vogel *et al.,* 2005). 41

Equation 2. The net force acting on a node (Vogel *et al.,* 2005).....41

Equation 3.The total energy at a node (Vogel *et al.,* 2005).....42

Equation 4. Relationship between swelling pressure and percentage swell (Sridharan and Gurtug, 2004) 49

Equation 5. Richards' equation (after Kool *et al.,* 1985).....56

Equation 6. Boundary condition applied to Richards' Equation (after Kool *et al.,* 1985).....56

Equation 7. Boundary condition applied to Richards' Equation (after Kool *et al.,* 1985).....57

Equation 8. Boundary condition applied to Richards' Equation (after Kool *et al.,* 1985).....57

Equation 9. Pressure state in a draining soil column (after Kool *et al.,* 1985).....57

Equation 10. Galerkin finite element model of van Genuchten (Kool *et al.,* 1985).....57

Equation 11. Cumulative outflow (Kool *et al*., 1985).....58

Equation 12. van Genuchten's model (after van Genuchten, 1980).....58

Equation 13. The objective function used by Kool *et al.* (1985).....59

Equation 14. Root mean square used by Hwang and Powers (2003).....68

Equation 15. Bulk density.....89

Equation 16. Gravimetric moisture content.....89

Equation 17. Volumetric moisture content.....89

Equation 18. Mass to volume ratio of water at 20 ^{o}C at sea level.....89

Equation 19. Change in mass of water between cycles 1 and 3.....89

Equation 20. The initial volume of soil.....90

Equation 21. Mass of soil.....90

Equation 22. Calculating cycle 3 bulk density from volumetric moisture content.....90

Equation 23. Saturated hydraulic conductivity – falling head.....93

Equation 24. Modified form of Richards' equation (Šimůnek *et al.*, 2005).....104

Equation 25. Unsaturated hydraulic conductivity function (Šimůnek *et al.*, 2005).....105

Equation 26. Objective function to be minimised when solving the inverse problem (Šimůnek *et al.*, 2005).....106

Equation 27. Air dry soil water pressure (Slatyer, 1967).....109

Equation 28. Prediction equation produced by the first run of the general linear model for repeated measures.....145

Equation 29. Prediction equation produced by the second run of the general linear model for repeated measures.....148

Equation 30. Prediction equation produced by the fourth run of the general linear model for repeated measures.....150

Equation 31. Dexter's S value (Dexter, 2004).....189

Nomenclature and Abbreviations

Abbreviation	Description
mm	Millimetres
cm	Centimetres
m	Metres
g	Grams
kg	Kilogram
Mg	Megagram
ha	Hectare
kPa	Kilopascal
s	Second
min	Minute
h	Hour
d	Day
yr	Year
BD	The bulk density of a soil.
LL	The liquid limit of a soil i.e. the gravimetric moisture content at which a soil begins to behave as a liquid.

PL	The plastic limit of a soil i.e. the gravimetric moisture content at which a soil deforms in a plastic, rather than a brittle, manner.
PI	The plasticity index of a soil i.e. the difference between its plastic and liquid limits.
SL	The shrinkage limit of a soil i.e. the percentage reduction in the length of a sample slowly dried from its liquid limit to oven dry.
CEC	The cation exchange capacity of a soil.
OC	The organic carbon content of a soil.
OM	The organic matter content of a soil.
LOI	The organic matter content of a soil lost on ignition.
OX	The oxidisable organic matter content of a soil.
K_s	The saturated hydraulic conductivity of a soil.
K	The unsaturated hydraulic conductivity of a soil.
θ	The moisture content of a soil.
θ_s	The saturated moisture content of a soil.
θ_r	The residual moisture content of a soil i.e. the moisture content of a soil at infinite matric potential.
D-value	The bulk density of a soil as a percentage of the Proctor test value at 200 kPa.

MSO	The multi-step outflow method i.e. the estimation of the parameters of the van Genuchten-Mualem Equation from transient outflow data.
S-value	Dexter's index of soil quality i.e. the modulus of the slope of a soil's moisture release curve at the inflection point.
Threshold	When referring to image analysis, a threshold is a point on the histogram of pixel intensity, on a grey scale image, selected to differentiate cracks from the soil surface. All pixels to the left of this threshold are shown as black (cracks), all pixels to the right of this threshold are shown as white (soil surface).
Thresholding	The process of applying a threshold to an image for analysis.
Thresholded image	An image to which a threshold has been applied.

1 Introduction

Soil is a fundamental component of the global environment. It is the medium for plant growth, an integral part of the water and nutrient cycle, the bio-habitat for micro-organisms to mammals and the foundations upon which our towns and cities are built. Therefore it is of paramount importance that our understanding of soil services and functions, and how our actions impinge upon them, be increased. Compaction by agricultural machinery is one of the effects that human activity has had on soils during the last 150 years. In an editorial referring to the results of the European Union concerted action "Experiences with the impact of subsoil compaction on soil crop growth and environment and ways to prevent subsoil compaction", Van den Akker *et al.* (2003) states that "European subsoils are more threatened than ever in history". Understanding therefore how and to what extent subsoil compaction may be reversed seems of vital importance tot he future wellbeing of our agricultural systems.

1.1 Soil functions

A medium for plant growth is one of the foremost functions of soil for consideration. The soil is required to act as an anchor for the plant roots and to be a storage vessel for water and nutrients, while at the same time allowing air to reach the roots. A healthy soil is essential to optimise crop growth, whether that be for food production, raw materials for industry such as timber, bamboo, or hemp, biofuel production, trees and flowers in ornamental gardens, or the

grass in parks. In addition to being the medium for plant growth, soils also act as a storage medium for future plants i.e. the seed bank. Unsuitable soil conditions can degrade the seeds and prevent germination. However, ideal soil conditions will vary with the application. Even between different food crops, what would be considered perfect growing conditions for one would be unsuitable for another. For example, corn production requires a well aerated soil profile, whereas the early stages of rice production is in flooded, anaerobic conditions. Other plants, either in the natural environment or grown for aesthetic reasons, demand every extreme, from acid to alkali, marsh to desert, and everything in between. Whatever the requirements of a particular crop, however, understanding soil structural dynamics is an important part of maintaining ideal hydrological conditions.

Soil water status is not only important for plant growth, but is an integral part of the water cycle. A porous soil with rapid hydraulic conductivity allows precipitation to infiltrate the soil profile, prolonging the time taken for excess water to reach drains and surface water courses. Without soil to retard the rate of runoff to surface waters, flooding can occur with potentially catastrophic consequences. Soil properties are, therefore, included in flood prediction models (Jorgeson and Julien, 2005). As water travels over the soil surface and through a well structured soil profile, nutrients and potential pollutants within the water are intercepted, preventing contamination of the aquatic environment, such as fertilisers applied to agricultural fields, reaching rivers, lakes and streams (Jones *et al.*, 2003). The structure of the soil will affect the opportunities that exist for bonding between the soil particles and substances potentially detrimental to the aquatic environment.

Nutrients also enter the soil through the decomposition of organic matter, through nitrogen fixers such as legumes and through atmospheric precipitation. One element of particular concern to today's society is carbon. It is estimated that the total world carbon stock held in just the top 30 cm of soil is 2157–2293 x 10^{15} g (Batjes, 1996). The current rate of loss from UK soils is estimated to be 13 x 10^{12} g yr^{-1}, equivalent to approximately a tenth of the carbon emissions from industry in the UK (Bellamy *et al.,* 2005) and is equal to the reductions in UK CO_2 emissions achieved between 1990 and 2002 (Schulze and Freibauer, 2005). The structure of the soil will affect carbon additions and losses (Brevick *et al.,* 2002; Pengthamkeerati *et al.,* 2005) and the flux of other gasses that contribute to the greenhouse effect (Jones *et al.,* 2003; Teepe *et al.,* 2004).

The decomposition of organic matter can be considered a soil function in itself, not just as a means of nutrient cycling and storage; soil can be considered a medium of waste disposal. Dead animals and plants and faecal matter are broken down by micro fauna and flora that live within soil. Soil must, therefore, provide an appropriate habitat for these communities i.e. a suitable level of moisture, aeration, temperature and nutrient balance (Pengthamkeerati *et al.,* 2005).

Although this study will concentrate on agricultural soils, the structure of soil is also important to the other functions it performed. Soils are also directly utilised for the disposal of anthropogenic waste, for example sewage sludge and landfill leachate (Tyrrel *et al.,* 2002). Moreover, soil material is an integral part of the landfill construction. Landfill liners and caps are often constructed from compacted clay layers and it is vital that they be both stable and

impervious to the movement of water and gasses (Yessiller *et al.*, 2000). Failure of these soil based liners to contain waste waters and gasses would result in the release of highly polluting leachate and the virulent greenhouse and explosive gas, methane. Other constructions also require stable soil foundations and models exist that describe the interaction between soil structure and construction stability (Capuani *et al.*, 1995). It is important that the soil under buildings, roads and airstrips is stable (Sridharan and Gurtug, 2004). Whilst all soils around newly constructed areas are likely to be required to provide the functions and services of plant growth, and water and nutrient storage and cycling, they must also be resistant to movement; a landslide onto a road or path could result in serious accident or injury and in some cases results in the total loss of soil material. This is a phenomenon which is linked to the structure of soils and changes to that structure (Chen and Martin, 2002). Inappropriate soil conditions on sports pitches can increase incidents of injury to players (Nigg, 1990). Conditions can be improved by engineering the soil structure, however more research is needed in order to attain and maintain optimal conditions (Stiles *et al.*, 2009).

The ramifications of soil compaction depend on the soil service or function considered. Equally, whether changes to soil structure are considered positive or negative will depend on the function or service. For example, a reduction in bulk density experienced by a soil that was supporting a man-made construction is likely to be deleterious to the integrity of that structure. Conversely, a reduction in bulk density and an increase in the proportion of macro-pores of a compacted agricultural soil would be likely to have a positive effect on yields. This study has concentrated on changes in soil structure experienced by agricultural soils, but its findings have also improved understanding of all soil functions and services.

1.2 Understanding of the issues relating to compaction and soil structural dynamics

1.2.1 The causes of compaction

Compaction of agricultural soils, caused by trafficking with machinery heavy enough to exceed the bearing capacity of the soil, has been studied by various authors. Horn *et al.* (2003), for example, investigated changes to the structure of soil caused by compaction and found that compaction increased bulk and aggregate density, made the soil structure become coherent and increased the proportion of horizontal to vertical pores. This reduces the infiltration rate of the soil, which leads to increased runoff, soil erosion and the pollution of surface waters (Jones *et al.*, 2003). Compaction can also pose other environmental problems. It can reduce the amount of carbon (Brevick *et al.*, 2002) and methane stored by the soil, increase nitrous oxide emissions (Teepe *et al.*, 2004). It also increases the resistance posed by the soil to root elongation (Etana and Håkansson, 1994; Alakukku, 1996b) and decreases porosity, and hence the water available for plant growth and aeration, (Blackwell *et al.*, 1985; Arvidsson and Håkansson, 1996). This in turn leads to reduced yields (Arvidsson and Håkansson, 1996; Abu-Hamdeh, 2003; Hamza and Anderson, 2003; Radford *et al.*, 2007).

The stress distribution under a variety of tyre pressures, configurations and axle loads have been studied by many researchers, for example; Arvidsson and Ristic (1996), Botta *et al.* (2002), Çarmen (2002), Alakukku *et al.* (2003), Chamen *et al.* (2003), Keller and Arvidsson

(2004) and Sarifi (2004). Most importantly, perhaps, was Soehne (1958) who developed equations used to describe these stress distributions. What makes a soil vulnerable to compaction has also been studied by Leeson and Campbell (1983) Weirmann *et al.* (2000), Jones *et al.* (2003), and Gregory *et al.* (2007). Such studies have contributed to the models of prediction of compaction developed by O'Sullivan *et al.* (1999), Jones *et al.* (2003), Poodt *et al.* (2003) and van den Akker (2004). The causes of compaction, the effects that compaction has on soil structure and the consequences of compaction to agriculture and the environment will be reviewed in greater detail in Chapter 2.

1.2.2 Current understanding of the persistence of compaction and the recovery of soil structure

Recovery of soil structure, both through tillage and through natural mechanisms of recovery, in the field and in the laboratory, has also been explored by many researchers. Croke *et al.* (2001) and Rab (2004) investigated changes in bulk density and infiltration rate of soils compacted by E*ucalyptus* harvesting. Alakukku (1996a), Alakukku (1996b), Alakukku *et al*. (2003) and Chamen *et al*. (2003) reported the results of long term field experiments in an area with deep freeze-thaw cycles that assessed structural changes to the soil profile realised as changes to total and macro-porosity, penetration resistance and saturated hydraulic conductivity. Similar studies were also reported by Etana and Håkansson (1994) and Arvidsson and Håkansson (1996). Shorter term studies were also conducted by Halvorson *et*

al. (2003) and Radford *et al.* (2007) who measured changes in bulk density, shear strength and penetration resisitance.

The effects of subsoil tillage on compacted soils were explored by Horn *et al.* (1995), Abu-Hamdeh (2003), Hamza and Anderson (2003), Motavalli *et al.* (2003) and Dexter *et al.* (2004) with reference to changes in bulk density, infiltration rate and yield. They found that the reductions in bulk density and increases in yield achieved were variable and short lived, and that infiltration rate could be reduced. The role that vegetation played in ameliorating compacted soils was investigated by measuring changes in bulk density, porosity, saturated hydraulic conductivity by Lister *et al.* (2004). Bushamuka and Zobel (1998), Williams and Weil (2004) and Whalley *et al.* (2005) all looked at the potential of different crops to penetrate compacted soil. They reported that certain crops could indeed penetrate compacted soils, creating a pore network that was utilised by successive crops.

Laboratory studies have investigated changes to aggregate bulk density (Horn and Dexter, 1989), and infiltration rate with wet/dry cycles (Saramah *et al.,* 1996). The effect of crops on the efficacy of wet/dry cycles were investigated by Pillai and McGarry, 1999. Changes in porosity with wet/dry cycles were investigated by Hussein and Adey, 1998 and the changes in the meanweight diameter of soil aggregates with wet/dry cycles by Grant *et al.,* 1995. Changes in pore size distribution with wet/dry cycles were investigated by Pires *et al.,* 2005. The results of these laboratory studies were more conclusive than those studies conducted in the field and showed than wet/dry cycles reduce bulk density and increase infiltration rates. Inclusion of a cover crop accentuated observed effects.

The emergence of cracks with wet/dry cycles has also been studied (Yesiller *et al.,* 2000; Velde, 2001; Vogel *et al.,* 2005). It was found that it was possible to predict surface cracking patterns the suggestion was made that this could be related to changes in other soil properties.

Current understanding of the recovery of soil structure after a compaction event will be reviewed in greater detail in Chapter 2. The following section describes the focus of this study.

1.2.3 The focus of this study

The mechanisms of soil recovery are predominantly tillage (Arvidsson and Håkansson, 1996; Abu-Hamdeh, 2003;Motavalli *et al.*, 2003) , the creation of bio-pores (Bushamuka and Zobel, 1998; Williams and Weil, 2004), freeze/thaw cycles (Alakukku, 1996a) and wet/dry cycles (Alakukku, 1996a). This study, however, will focus specifically on the changes to soil structure that can be achieved through wet/dry cycles as these are likely to contribute to the efficacy of most of the other mechanisms.

Models have been developed by O'Sullivan *et al.* (1999); Jones *et al.* (2003); Poodt *et al.* (2003); and van den Akker (2004) that predict the changes to soil structure, experienced during a compaction event, but not how the soil structure changes after that event. Being able

to predict changes induced by successive wet/dry cycles, based on measurable soil properties, would be a valuable resource to farmers and land managers and to others working with the engineering properties of soils. This study attempts to relate soil structural changes experienced , as a result of wet/dry cycles, to various measurable soil properties.

Where changes to soil hydraulic properties, such as infiltration rate, have been investigated by other researchers (for example, Croke *et al.*, 2001), changes to these properties have been detected where changes to bulk density were not necessarily apparent. This suggests that a more detailed understanding of the changes to soil structure induced by wet/dry cycles may be gained from investigating changes to hydraulic properties than from investigating changes to bulk density alone. However, few studies have monitored changes to moisture release characteristics, or hydraulic conductivity curves, factors that would affect the ability of the soil to fulfil functions, such as providing the crop available water (held between field capacity and permanent wilting point), the pore network available to accommodate root elongation and the movement of fluids through the soil profile at less than saturation (which is linked to leaching, and hence diffuse pollution, and infiltration during a rainfall event, that affects flood risk and surface erosion). Changes in bulk density are indicative of changes to available water and the movement of water through the soil profile, but insufficient in themselves to really describe them. This study, therefore, will look in detail at the changes to the moisture release and hydraulic conductivity curves of a selection of soils, induced by a series of wet/dry cycles.

It has been suggested that the cracking of soils is a phenomenon that will contribute to changes to other soil structural properties, particularly hydrological ones. Exploring this further could improve understanding of soil structural dynamics. The relationship between surface cracks and hydrological parameters has also been investigated.

1.3 Aim and objectives

Aim

To assess the changes in bulk density and hydrological parameters of a range of soils, varying in texture and other physical and chemical properties, with wet/dry cycles and to explore the relationships between any measured changes and the measured soil properties.

Specific objectives

1. To review the literature relating to the recovery of soils after compaction.
2. To measure the changes in bulk density and the water filled porosity at field capacity of a range of soils, varying in texture and other measureable parameters, after three wet/dry cycles.
3. To assess the contribution of soil texture and other physical and chemical soil parameters to the measured changes.

4. To be able to predict changes from these parameters.
5. To conduct a more detailed study on clayey subsoils, detailing changes to their moisture release and unsaturated hydraulic conductivity curves after three wet/dry cycles.
6. To measure changes to the saturated hydraulic conductivity of these clayey subsoils after three wet/dry cycles.
7. To monitor the emergence of surface cracks on these clayey subsoils during the wetting and drying process.
8. To explore relationships between the emergence of cracks and changes to the bulk density and hydrological parameters of these soils.

The literature is reviewed in detail such that factors which influence structural changes with wet/dry cycles might be identified and an appreciation of the extent of these changes that might be expected in different situations gained (Chapter 2). A series of experiments are described that focus on changes to the structure of soils with wet/dry cycles (Chapter 3). The first of these experiments relates changes in the simplest measures of compaction, bulk density, to other measurable soil properties. More detailed experiments are then described that look at changes to the hydrological functions of the soils, and how the initial bulk density affects these changes. Experiments will also be described that investigate the emergence of surface cracks and relate this to changes to the hydrological properties of the soils. The results of these experiments will be reported and discussed in Chapter 4 and drawn together in overall summaries and conclusions in Chapter 5.

2 Soil structure, its Degradation and Amelioration

2.1 Issues relating to the compaction of soils

Methods of agricultural production have changed rapidly over the last century. These changes have included the advent of inorganic fertilisers, extended tillage practices and the increase in size and weight of agricultural machinery used for tillage and cropping (van den Akker *et al.*, 2003). What has progressed less rapidly is the understanding of the long term consequences of these changes. This chapter reviews the progress that has been made in understanding the consequences of using heavy machinery on soil and the ramifications of this for agriculture.

Figure 1. Soil damage by agricultural machinery. Taylor, 2003.

The damage caused to a soil by trafficking results in compaction. Compaction has been defined as the densification of the soil, measured as an increase in the bulk density. However,

this definition does not describe the structural dynamics involved, nor why compaction may be viewed as problematic by the agriculturalist. Two soils may have very similar bulk densities, but vary greatly in pore size distribution and connectivity of soils. For example, a soil with only very large cracks and a high aggregate density may be a less suitable medium for plant growth than the same soil with smaller cracks, less dense aggregates and smaller pores, yet both soils could have the same overall bulk density. It therefore seems reasonable to accept bulk density as an indicator of compaction, but not as the definitive parameter. Other authors, when quantifying the extent and persistence of soil compaction have measured variously bulk density (for example: Etana and Håkansson, 1994; Arvidsson and Håkansson, 1996; Croke *et al.,* 2001; Halvorson *et al.,* 2003; Horn *et al.,* 2003; and Motavalli *et al.,* 2003), aggregate bulk density (Horn *et al.,* 2003), aggregate stability (Arvidsson and Håkansson, 1996), porosity (for example: Blackwell *et al.,* 1985; (Alakukku, 1996a; Arvidsson and Håkansson, 1996; Hussein and Adey, 1998; Velde, 2001; Horn *et al.,* 2003; Rab, 2004; Pires *et al.,* 2005; Whalley *et al.,* 2005; and Zang *et al.,* 2005), pore size distribution (Alakukku, 1996a; and Zang *et al.,* 2005), pore connectivity (Werner and Werner, 2001; and Jones *et al.,* 2003), hydraulic conductivity (both vertical and horizontal) (Alakukku, 1996b; Chamen *et al.,* 2003; Halvorson *et al.,* 2003; Jones *et al.,* 2003; Dexter *et al.,* 2004; Lister *et al.,* 2004; and Drewry, 2006), infiltration rate (Sarmah *et al.,* 1996; Croke *et al.,* 2001; Hamza and Anderson, 2003; and Jones *et al.,* 2003), penetration resistance (Etana and Håkansson, 1994; and Alakukku, 1996b) and moisture release characteristics (Horn and Dexter, 1989; and Pires *et al.,* 2005).

In order to decide upon the most informative method of quantifying soil compaction and, therefore, the structural recovery of the soil from the compaction event, the perceived repercussions of compaction, and the associated problems, must be discussed.

Two answers readily present themselves to the question "why is compaction a problem?" These are that compaction results in reduction in yield and environmental pollution. The reduction in yield caused by compaction has been measured by various researchers. Arvidsson and Håkansson (1996), for example, conducted 21 long term field experiments into the effects of compaction on crop yield on a variety of soil types (clay contents ranging from 11 to 65 %). Compaction reduced yields on average 4 % when an extra 120 Mg km ha^{-1} $year^{-1}$ were applied to the fields, 11 % when an extra 350 Mg km ha^{-1} $year^{-1}$. However, under wet conditions, yield was depressed by 22 %.

Soil compaction can cause significant detriment to the environment via changes to the soil's hydraulic properties. Relative increases in lateral hydraulic conductivity (caused by the collapse of vertical pores) decrease the proportion of the applied nutrients that are either held by the soil, or taken up by plants. The potential consequence of this is the pollution of surface waters because reduced infiltration increases effective runoff (Jones *et al.*, 2003). This increases the risk of flooding and the risk of water shortages to crops as less rainfall penetrates the surface to augment the soil water store. Increased runoff can also increase soil erosion, leading to sedimentation of water bodies and phosphorus pollution (Jones *et al.*, 2003).

Reduced porosity and pore connectivity also increases greenhouse gas production through processes of denitrification, associated with anaerobic conditions (Jones *et al.,* 2003). Teepe *et al.* (2004) measured the difference in greenhouse gas fluxes between the skid trail in a forested area and the non-compacted areas. They found that compaction increased N_2O emissions up to 40 times and the CH_4 consumption by the soil was reduced by 90 % and was even released in some areas. One element of particular concern to today's society is carbon. It is estimated that the total world carbon stock held in just the top 30 cm of soil is 2×10^{18} g (Batjes, 1996). The current rate of loss from UK soils is estimated to be 13×10^{12} g C yr^{-1}, equivalent to approximately a tenth of the carbon emissions from industry in the UK (Bellamy *et al.,* 2005) and equal to the estimated reductions in UK CO_2 emissions achieved between 1990 and 2002 (Schulze and Freibauer, 2005). Although compacting a soil can retard the rate of carbon mineralisation by reducing soil macro-porosity, hence decreasing aeration and altering the activity soil microbial communities (Pengthamkeerati *et al.,* 2005), it can also decrease the amount of carbon that is stored within that soil by restricting root growth and, therefore, the addition of new organic matter to the pool (Brevick *et al.,* 2002). This implies that compaction reduces the amounts of carbon sequestered and stored by soil and hence has a negative impact on levels of greenhouse gases in the atmosphere.

The literature has reported that yield reductions, pollution and greenhouse gas emissions are seriously problematic results of compaction that have potentially significant economic and environmental consequences. It is prudent, therefore, to resolve the structural parameters of compaction that are restrictive to plant growth and that inhibit drainage and aeration.

2.2 The causes of compaction

Compaction is caused by forces applied to a soil causing the arrangement of soil particles to fail in a brittle, or a plastic, manner. Soil particles realign themselves to form a new soil structure (Horn *et al.*, 2003). On agricultural soils, the compaction is caused by heavy agricultural machinery, driven on the land when it is vulnerable. Similarly, heavy harvesting machinery compacts forest soils.

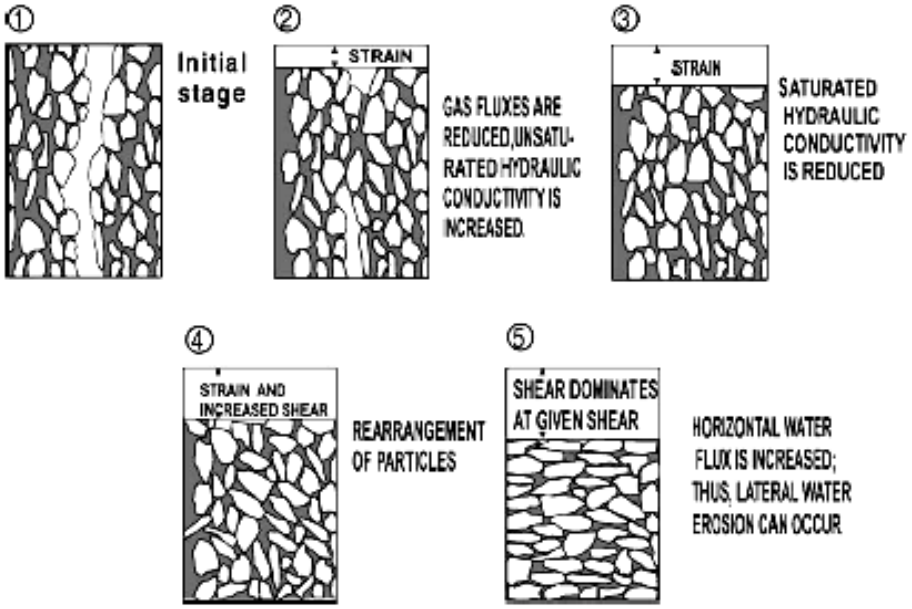

Figure 2. The stages of compaction as visualised by Horn et al., 2003.

After ten passes with a tractor with a front wheel load of 3.8 Mg, a rear wheel load of 5.5 Mg and tyre pressures of 120 kPa, Horn *et al.* (2003) demonstrated that the bulk density

consistently reached a value of 1.69 g cm^{-3}, exceeding the Proctor test value of 1.62 g cm^{-3}. The top layer of soil (60 - 100 mm) went from a crumb structure to a massive one. The 200 - 240 mm layer went from a subangular to a blocky/massive structure, whereas the 350 - 390 mm layer went from a massive to a platy/blocky structure after four passes and then returned to a coherent structure after ten passes. The inter-aggregate pore volume in the 350 -390 mm layer displayed similar behaviour going from 0 to 4.5 to 0 %. Bulk density and aggregate bulk density in this layer, however, increased with the number of passes (Horn *et al.*, 2003).

When considering the stress distribution under various wheel configurations, Keller and Arvidsson (2004) found that dual tyres (two tyres next to each other on each side of the vehicle) were most effective at reducing the extent of soil compaction. This is because the axle load is spread over several wheels and, therefore, a greater surface area. Even though the wheels in their experiment were positioned only 100 mm apart, there was no interaction of stresses between the wheels. As each wheel carries less of the load, the tyre inflation pressure could be reduced. This was found to significantly reduce vertical stress in the soil to a depth of 300 mm. Below this depth, however, inflation pressure had no effect and stress was completely dependent on wheel load (Keller and Arvidsson, 2004).

These findings are similar to the earlier work of Arvidsson and Ristic (1996), who also found that inflation pressure increased the rut depth, but that the effects of inflation pressure were not significant at depth. Other researchers have also observed this phenomenon. Botta *et al.* (2002) go so far as to say that compaction at depth is independent of ground pressure and purely a result of axle load. However, they do not consider this true of surface compaction,

which can be reduced with dual tyre configuration. Sharifi (2004) also found that the effect of tyre inflation pressure on soil compaction appeared to be most evident at the soil surface and diminish at depth. When axles with high loads (4500 kg) were studied, the effects of pressure were evident to a depth of 400 mm. The rate at which an applied pressure reduces with depth has also been found to diminish with increase in wheel load (Chamen *et al.*, 2003). Alakukku *et al.* (2003) goes further to state the load alone will affect the normal stress levels below 1000 m m, but that this will never exceed the maximum ground contact pressure.

This effect is exaggerated by considering a narrow tyre. Çarmen (2002) found that narrow, high pressure tyres with high lugs caused more damage to the soil structure than wider, low pressure tyres with a smoother surface. The carcass stiffness also has an effect on the rut depth (Arvidsson and Ristic, 1996), the bias ply tyre tested producing a greater rut depth than a slightly narrower, higher pressure radial tyre. This is attributed to an uneven distribution of pressure across the width of the tyre.

Interestingly, the vertical normal stress in the plough layer and at depth was significantly affected by both tyre type, and by inflation pressure (Arvidsson and Ristic, 1996). These measurements were made in a soil bin packed with dry sand and therefore were not subject to the in field heterogeneity that the measurements of some other researchers such that smaller differences would have been detectable.

These results suggest that compaction is caused by high axle load, but that the compactive effect of that axle load can be reduced by lower tyre inflation pressures and dual tyre

configurations. However, the benefits of these measures appear to diminish with depth, implying that subsoil compaction may occur, even if the structure of the plough layer remains relatively in tact. This in turn suggests that the only way to avoid subsoil compaction is to reduce the axle load, not just the applied pressure.

Shear stress can also damage the subsoil (Alakukku *et al.,* 2003). Horn *et al.* (2003) state that the process of shearing is more detrimental to soil structure than applied vertical load because it deteriorates and homogenizes the pore system. They also stated that the vertical stress component will deform weak subsoil, even if the plough layer is behaving elastically and investigated this hypothesis through a series of experiments conducted on an undisturbed clay loam in a soil bin. Stress state transducers and displacement transducer systems were inserted into the soil in order to measure stress and particle movement at various depths.

Horn *et al.,* 2003 found that the octahedral shear stress and the major principal stress increased with the number of wheelings, while the mean normal stress remains approximately constant. The vertical displacement from the original position increased with every wheel pass, but the magnitude of the additional displacement decreased between one pass and the next. This was also true of horizontal displacement. With increasing number of passes, bulk density and aggregate density increased and inter aggregate pore volume decreased, suggesting that the changes in porosity experienced by the soil were primarily attributable to shear forces.

2.3 The vulnerability of soils to compaction

A soil with a high water content will be more prone to deformation than an air dry soil. Soehne (1958) conducted experiments comparing the deformation of soils under confined, uniaxial compression at different water contents. He found that it took 2 % of the pressure required to compress a wet clay loam to a given porosity that it took to compress an air dry clay loam to the same extent. He also showed that there is a limit to the compaction that can be achieved by a given pressure, applied for short durations, at a given water content. If this pressure were to be applied for a longer period, however, he stated that water would be squeezed from the soil pores, allowing further deformation of the soil. Soehne (1958) also showed that more deformation will occur, at the same water content and pressure, if the soil is kneaded (i.e., allowed to bulge round the area of applied pressure) rather than subject to a static pressure. This form of pressure application is a better representation of a field soil tyre system and deformation also varied with soil texture and type.

Jones *et al.* (2003) state that the shape of the soil pores can affect the soil's vulnerability to compaction. Vertical pores are resistant to vertical loads, but are vulnerable to shearing, whereas horizontal pores are more likely to be affected by vertical loads. However, Werner and Werner (2001) state that soil compaction increases the proportion of horizontal pores to vertical pores, the pores becoming compressed and elongated before finally collapsing and reducing the pore connectivity.

Gregory *et al.* (2007) conducted field trials on a sandy loam, a sandy clay loam and a clay soil. The field plots were subjected to a compaction event and then monitored for soil strength and crop growth over the following 16 months. They found that soil strength was increased and crop yield severely depressed in the sandy loam and sandy clay loam, but that the clay (initial bulk density estimated to be 1.0 g cm^{-3}) was unaffected by the treatment, generally retaining a penetration resistance that was less than 3 MPa, except at depths in excess of 400 mm; the other two soils had penetration resistances greater than this at a depth of 100 mm, an increase from the non compacted state. The resistance to compactive effort of the clay soil was attributed to the buoyancy effect of pore water pressure. It was also thought that because the clay soil was able to retain more water, it was weak enough for roots to penetrate, which in turn maintained the low strength of the soil, possibly by creating a network of macro-pores/root channels and causing small fractures due to drying (Gregory *et al.*, 2007).

Weirmann *et al.* (2000) compared the vulnerability of a silty loam that had been in conservation tillage and conventional tillage for 25 years. They found that the conventionally tilled system was far more vulnerable to compaction than the soils under conservation tillage. They also found that fragments of channels were preserved in the conservation tillage plots, implying that these plots would be more likely to experience structural recovery by physical and/or biological processes (Weirmann *et al.*, 2000).

Leeson and Campbell (1983) investigated the variation in soil physical behaviour under stress with moisture content, as described by critical state theory. They found that the gradient of

the virgin compression line and the recompression line differed. They also found that as the water content of the soil increased, the gradient of the virgin compression line and the recompression line also increased linearly (although there was more variation in the latter).

Soil compaction has since been predicted by O'Sullivan *et al.* (1999), Poodt *et al.* (2003) and van den Akker (2004), based on critical state theory, as a function of moisture content, cohesion, angle of internal friction and preconsolidation stress. Jones *et al.* (2003) developed a method by which a soil's vulnerability to compaction could be assessed by giving the soil a score based on its packing density (a function of bulk density and clay content), soil texture, number of days at field capacity and potential soil moisture deficit. They then applied this score to soil maps of Europe to create a map of estimated soil vulnerability (Appendix 1). If these factors can be used to assess a soil's vulnerability to compaction and, hence, the damage caused by compaction, it seems possible that they could also influence the soils structural recovery after a compaction event.

2.4 Recovery of soil structure after compaction

The mechanisms of soil recovery are predominantly; tillage (Arvidsson and Håkansson, 1996; Abu-Hamdeh, 2003; Motavalli *et al.*, 2003) , the creation of bio-pores (Bushamuka and Zobel, 1998; Williams and Weil, 2004), freeze/thaw cycles (Alakukku, 1996a) and wet/dry cycles (Alakukku, 1996a). Tillage can be a very effective means of alleviating compaction.

However, it is not always an appropriate option as it can be costly and time consuming, causing further damage to the soil structure by decreasing aggregate stability, and potentially further compaction to an already vulnerable soil if conducted under inappropriate conditions (Arvidsson and Håkansson, 1996).

The creation of bio-pores is an important factor in the natural recovery of soils from compaction. Worm burrows and root channels can provide a network of macro-pores that are important for drainage and that can be utilised by the roots of crops (Alakukku, 1996b; Bushamuka and Zobel, 1998; Williams and Weil, 2004). Root channels can significantly enhance a soil's recovery after compaction (dependent upon plant species). A strong rooted species can penetrate some compacted soil layers, allowing the movement of water and gases, and accelerating the rate of soil drying (Bushamuka and Zobel, 1998; Williams and Weil, 2004). However, there will be limits to the pressure that can be exerted by a root on resistant soil structure, and it may be the case that for a severely compacted soil, physical processes are required to initiate the process of recovery, before biological mechanisms can accelerate this process. The limit of penetration resistance employed by Håkansson and Lipiec (2000) was 3 MPa; the penetration resistance of the field plots used in these experiments approached 5 MPa at depth, despite wet conditions (34 % w/w).

Dexter (1988) comprehensively reviewed soil aggregation processes, stating that surface tension of water menisci are great enough to pull soil particles together to form micro aggregates as the soil dries (after Dexter and Spoor, 1988, unpublished). As the clay platelets are drawn together, the cations between them will attract the negatively charged surfaces of

the platelets, forming a bond. A clay domain is formed when several platelets bond together in this way. These clay domains, along with charged organic colloids, form bridges which bond to each other and to fine silt particles creating micro-aggregates (Brady and Weil, 1999). Micro-aggregates are bound together by fungal hyphae and microbial secretions to form macro-aggregates (Figure 3). With each wet/dry cycle, swelling pressures tend to consolidate aggregates. Cracks always remain planes of weakness, propagating with each cycle, creating smaller and better defined peds. Hence, structure is created by particles clustering together and the clusters being separated along the planes of weakness. After a number of years, an equilibrium level of natural aggregation is reached (Dexter, 1988 after Horn and Dexter, 1988, unpublished).

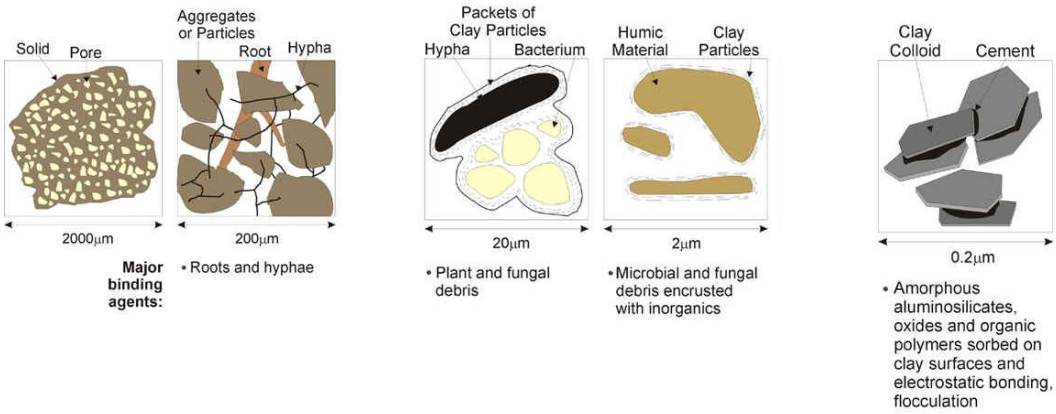

Figure 3. Formation of soil aggregates (Lesley Dampier & Distance Education and Technology Continuing Studies, The University of British Columbia).

The following sections will review the research that has been conducted, both in the field and in the laboratory, on the rates and extent of recovery of soil structure after a compaction event.

2.4.1 Field studies

Various studies have investigated the recovery of soil structure after a compaction event and a proportion of these have been conducted on commercially cropped forest soils. Forest harvesting equipment can be very heavy; John Deere manufacture skidders (large tractors used in forest harvesting) that weigh up to approximately 15 tonnes (John Deere, 2010). Croke *et al.* (2001) investigated the recovery of a coarse textured soil with an organic rich surface layer; a strongly structure loam, overlying a clay loam with a light clay subsoil; and a gravelly clay loam soil. These soils are located in New South Wales, Australia, in an area prone to bush fires and planted with *Eucalyptus* that was harvested every 20 to 40 years. Croke *et al.* (2001) found that there was no change in bulk density up to five years after compaction caused by harvesting equipment, in either the snig tracks, or in the general harvesting areas. However, surface infiltration in the snig tracks more than doubled in this period, although there was no change in the infiltration rate of the harvested areas, despite dry conditions. The degree of surface compaction and its recovery did not vary significantly with soil type (Croke *et al.*, 2001).

Rab (2004) also looked at the recovery of soils in commercial *Eucalyptus* forestry in Australia. The area in question was cool, temperate, with annual rainfall of 1900 mm. The soil was a silty clay loam. The author found that 10 years after logging, macro porosity was up to 60 % lower, to a depth of 300 mm, in the heavily disturbed sites, compared with those that were undisturbed. However, this was over a 100 % improvement in macro-porosity since the initial compaction event. The bulk density of the sites receiving minimal disturbance was

not significantly different from those with no disturbance. In the primary snig tracks and those areas receiving deep disturbance, bulk density was greater by approximately 51 % and 68 % respectively at the surface and 22 % and 37 % at 300 mm. There was no significant difference in bulk density between sampling dates, except in the secondary snig tracks (21 %) (Rab, 2004).

Lister *et al.* (2004) looked at the role of vegetation in ameliorating soil compaction in a wet pine flat, intensively managed for loblolly pine production, situated on the Coastal Plain of South Carolina. The soil was a poorly drained loam. They found that there was a marginal difference in soil quality between treatments of no vegetation control, operational control and total control. Vegetated treatment plots were generally more aerated, had lower bulk densities and higher aggregate stabilities, but saturated hydraulic conductivity was not effected (Lister *et al.*, 2004).

Whalley *et al.* (2005) also looked at the effects of roots on soil porosity. Germinated seeds of wheat, maize, or barley were planted in pots of homogenized silty clay loam and allowed to grow for six weeks. The bulk and rhizosphere soil was then separated an analysed. They found that there was no difference in total porosity between the rhizosphere and the bulk soil, but the rhizosphere soil had a greater proportion of macro pores. They also found that plant species had an effect on porosity, maize having the highest porosity and barley the lowest.

Bushamuka and Zobel (1998) discovered that different cultivars of the same species of crop will respond to compaction in different ways, with regard to root growth. Some of the

cultivars investigated produced tap roots, or basal roots, that were capable of penetrating the compacted layer. They suggested, therefore, that plants that were tolerant to soil compaction could be bred and further that these plants could be used in crop rotation to ameliorate compaction by providing a macro-pore network.

Williams and Weil (2004) also suggested that plants could be used in a rotation to ameliorate compaction. They found that soya bean roots took direct advantage of the root channels left by forage radish in a compacted soil and that yield was improved when compared to a system that had no cover crop. This view is supported by Hamza and Anderson (2005), who conclude in their review of the nature, causes and possible solutions to soil compaction, that crop rotations with deep, strong roots may alleviate some of the effects of compaction.

Worms can also significantly contribute to the structure of a compacted soil. Lanrink *et al.*, (2001) investigated how worms might regenerate a compacted loess. Worms were introduced to field plots after a compaction event. The worm casts were found to have 10 to 20 % higher porosity than the surrounding soil aggregates. The casts also had approximately a 50 % higher swelling value, but were less water stable (Larink *et al.*, 2001). In conjunction with the pore network that the worms would have produced, the effect of the worms would be to create a soil profile that was more penetrable by plant roots, which would in turn accentuate the drying process and so further contribute to structural regeneration.

One of the most comprehensive of the studies of the recovery of agricultural soil from compaction was conducted by the Agricultural Research Centre of Finland, as reported by

Alakukku (1996a), Alakukku (1996b), Alakukku *et al*. (2003) and Chamen *et al*. (2003). Field experiments were established in 1981 and continued for nine years (Alakukku, 1996b) on a Vertic Cambisol and a Mollic Gleysol (Alakukku, 1996a). Three treatments were considered; no wheeling, one pass of a tractor trailer combination and four passes of a tractor trailer combination. The tandem axle load of the trailer was 19 tonnes on the clay soil and 16 tonnes on the organic soil. The tyre inflation pressure was 700 kPa. The front axle load of the tractor was 1.5 tonnes, the rear 6.5 tonnes on the clay and 5.5 tonnes on the organic soil. The clay soil was just below field capacity and the organic soil just above when trafficked (Alakukku, 1996a).

The results of this study were interesting. Compaction was persistent, despite the study area being subject to annual frosts (up to 1000 mm deep, 500 mm mean average) and cracking during the summer (700 mm deep). The topsoil of the clay (10 - 20 mm) still showed signs of compaction three years after multiple wheeling, despite being annually cropped and ploughed (Alakukku, 1996a). Compaction was still measurable in all experiments after nine years (Alakukku, 1996b).

Compaction of the clay reduced total porosity, both in the plough layer and in the subsoil. On the organic soil, pore size distribution was affected more than total porosity; the quantity of macro pores was decreased but total porosity was more stable. Compared with the clay soil, however, the volume of macro pores in the organic soil was large, despite compaction (Alakukku, 1996a).

Penetration resistance of the subsoil (at approximately field capacity) in the clay plots was 22 % greater in the heavily wheeled plots than in the control (Alakukku, 1996b). The penetration resistance of the organic soil was 11 % and 26 % greater in the 'one' and 'four' pass plots, respectively, than in the control, nine years after compaction. After six years, the penetration resistance in the loam soil was 11 % and 58 % greater in the 'one' and 'four' wheeling plots than in the control. Saturated hydraulic conductivity showed no significant difference between either of the treatments and the control, although the author suggests that this is due to the in-field heterogeneity (Alakukku, 1996b).

Arvidsson and Håkansson (1996) also conducted long term field experiments into the effects of compaction on crop yield on a variety of soil types (clay contents ranging from 11 to 65 %). They found that, especially for clay soils, although ploughing loosened the soil and reduced bulk density, the structure of the soil remained coarse for up to two years after the compaction treatment. Porosity in the plough layer was also negatively correlated with applied load, despite annual ploughing. This effect was exaggerated below the plough layer. There was no correlation with clay content and the change in porosity. They also found that the compacted soils behaved more like remoulded soils than the control, i.e. compacted soils had increased aggregate strength when dry, but reduced aggregate stability when wet. These findings are reflected by the work of McGovern (2002), who also found that soil aggregates in ploughed systems were less stable than those under minimal tillage. She also found that soils under minimal tillage had greater elasticity and a higher plastic limit than ploughed soils.

In general, Arvidsson and Håkansson (1996) found that although mouldboard ploughing removed the physical indicator of compaction, such as increased bulk density, yield losses persisted three to four years after the compaction event and were approximately linearly correlated with the amount of trafficking. Yield loss was also correlated with clay content of the soil, wetness of the soil at time of trafficking and tyre inflation pressure used. Since there was very little persistent change in bulk density, they suggest that yield losses were attributable to increased mechanical resistance to roots and lower pore continuity.

Blackwell *et al.* (1985) found that some recovery of the structure of a compacted, swelling clay (38 %) occurred in the second growing season after the compaction event. Their findings were based on field trials, conducted in Oxfordshire. The compaction decreased porosity to a depth of at least 300 mm and cracking occurred to depths of 250 mm, which was thought to contribute significantly to the recovery of porosity. Wetting and drying due to rainfall and evapotranspiration was monitored between October and June after the compaction event. Six wet/dry cycles were detected over this period. At the 150 mm depth, sufficient wetting/drying occurred to equate to a change in volumetric moisture content of 5 %. Below this depth, however, changes were much smaller (Blackwell *et al.,* 1985). Although the changes to the structure of the compacted soil reported here were minimal, they were monitored over less than a year and differences in the soil moisture content were small. Practices that exaggerated the wetting and drying process may have resulted in more extensive recovery and improved crop growth.

Motavalli *et al.* (2003) investigated the effects of subsoiling on compaction on sandy and silty soils in a damp, temperate North American, climate. Surprisingly, they found that subsoiling had no effect on bulk density in the compacted fields, but did increase nitrogen uptake and possibly, leaching. Abu-Hamdeh (2003) found that subsoiling a clay loam soil in an arid, North African climate increased yields, even in the control field where no compaction had taken place, but that the increase in yields in compacted fields that had been subsoiled were still less than in the control field which had received no treatment. Dexter *et al.* (2004) found that subsoil tillage of three sandy loam soils and on silt loam soil in a temperate, European climate could cause significant reductions in saturated hydraulic conductivity as the process destroyed biopores and concluded that the practice could have serious environmental consequences unless repeated periodically.

Motovalli *et al.* (2003) also suggested that the recompaction of physically loosened soil may be relatively rapid. Horn *et al.* (1995) found that three to five years after the initial loosening, subsoils were even denser than before loosening. In addition to this, Motovalli *et al.* (2003) suggested that subsoiling may mix the subsoil, with a low organic matter content, with the topsoil, reducing organic matter near the surface. Considering the results of Zang *et al.* (2005), this implies that subsoiling would increase the vulnerability of a soil to compaction and reduce its ability to recover from that compaction under certain conditions. Mechanical impact on the soil has also been discovered to have a significant, negative effect on the tensile strength of aggregates and this effect persists after ploughing (Arvidsson and Håkansson, 1996; Munkholm and Schjønning, 2004).

Hamza and Anderson (2003) suggest that the recompaction of deep ripped soil may be retarded by the inclusion of an aggregating agent, such as gypsum. They investigated the effect of deep ripping, with and without gypsum, of a compacted loamy sand and compacted sandy clay loam, on yield and infiltration. Deep ripping with gypsum increased yields on both soil types, but deep ripping without gypsum resulted in yield reductions in the third and subsequent years. The deep ripping and gypsum treatment also resulted in an increase in infiltration rate of 90 % on the loamy sand and of more than 130 % on the sandy clay loam, four years after the application of the treatment. The economic viability of the deep ripping and gypsum treatment was also assessed and found to return profits of \$53 and \$69 ha^{-1} above the control on the loamy sand and the sandy clay loam respectively (Hamza and Anderson, 2003).

Etana and Håkansson (1994) reported findings on the persistence of subsoil compaction, based on the results of nine, long term field experiments conducted in Sweden. The soils involved ranged in clay content from 6 to 85 %. The vehicle used to compact the soil had a front axle load of 10 tonne and a rear axle load of 16 tonne. The treatments were one pass per plot, the whole plot surface wheeled once, the whole plot surface wheeled four times and a control (no traffic). All trafficking was done at moisture contents close to field capacity. After the initial treatment, the plots were all treated in 'accordance with normal farm practice, including mouldboard ploughing to a depth of 250 mm every autumn', with machines of axle loads less than 5 tonnes.

Results showed that the experimental traffic had caused compaction down to a depth of at least 500 mm. Based on measurements of shear strength, bulk density and penetration resistance, it was found that practically no alleviation of compaction in the subsoil (below 350 mm) had occurred 11 years after the initial treatment (Etana and Håkansson, 1994). This was despite annual frosts reaching a mean depth of 640 mm, but it appears that no hydrological measurements were made. Other studies have shown that soil hydraulic properties can be more sensitive to structural changes than bulk density, for example Croke *et al.* (2001) and Halvorson *et al.* (2003).

Håkansson and Reeder (1994) reviewed the extent and persistence of subsoil compaction under high axle loads and concluded that compaction was virtually permanent at depths of more than 400 mm, even in clay soils with annual freezing. However, they did conclude that in shrink-swell soils, it would be unlikely that subsoil compaction would restrict plant roots to the plough layer (Håkansson and Reeder, 1994).

Halvorson *et al.* (2003) investigated the over-winter changes to the structure of soils that had been compacted by tracked military vehicles. The soils studied were a silt loam and a very rocky silt loam on two military sites. They found that the bulk density of the compacted soils did not change significantly with time, but that the saturated hydraulic conductivity did increase significantly with time and approached levels of the uncompacted soil. The steady state runoff from the compacted soil plots also indicated that significant recovery of structure had occurred over the winter. Halvorson *et al.* (2003) concluded that recovery of structure of

a silt loam was detectable, especially near the soil surface, after only one year, but that bulk density was not a sensitive enough measure to detect this.

Drewry (2006) reviewed the natural recovery of soils that had been subjected to treading damage in New Zealand and Australia. Only the top 50 - 100 mm of soil were considered, but significant recovery of macro-porosity, hydraulic conductivity and infiltration rate was reported after durations ranging between just four and eight months. Drewry (2006) concluded, however, that rapid recovery of soil structure is likely to be limited to these shallow depths.

Radford *et al.* (2007) investigated the recovery of a Vertisol (50 % clay) in a semi-arid area of Australia. The treatments applied were: 10 tonnes and 6 tonnes applied to wet soil for five years and 6 tonnes applied to dry soil over five years. They found that the shear strength of the plots receiving the load only when dry showed no difference from the control. Shear strength of the other plots was significantly increased, and persisted down to 300 mm for 3 years and 2 years after the final compaction event for the for the '10 tonne wet' and the '6 tonne wet' treatments, respectively. At depths of 70 – 100 mm, increases in shear strength persisted for 5 and 3 years. Grain yield was comparable to the control on the '10 tonne wet' treatment at the sixth harvest, but was unaffected by the other treatments. Radford *et al.* (2007) concluded that unusually low rainfall had contributed to the persistence of compaction in the most severely degraded plots and that in such an instance, other methods of alleviating compaction should be considered.

The processes of structural formation in the B horizon (subsoil) were discussed by van de Graff (1978). After examining cores taken from the field, it was observed that, in clayey soils, the less than 8 µm fraction appeared to be responsible for promoting the formation of large structural units, while the 16-32 µm fraction promoted the formation of small structural units. The author added that smaller units were produced by rapid stress development, further suggesting that the structure of a soil could be modified by rapid wetting and drying, as had been shown by the effect of tile drains. This could be further enhanced by incorporating planes of weakness through the soil profile in the form of crop residues or well flocculated, stable granules of montmorillonitic clay.

2.4.2 Laboratory studies

Horn and Dexter (1989) investigated the aggregation of a desert loess under flood irrigation. Their research was based on lysimeters filled with disturbed, homogenised soil (19 % clay and 25 % sand) with a single almond tree planted in them. The lysimeters were sampled 1.5 and 2.5 years after the beginning of the experiment and the tensile strength and dry bulk density of the aggregates were measured and compared to older, undisturbed soil. They found that the more often a soil had shrunk and swollen, the higher the tensile strength was for a given water content. They also found that the bulk density of the aggregates first increased but, that after a long period, if undisturbed, the bulk density decreased again, possibly reaching some equilibrium state. The moisture release curve also displayed a cyclic change;

after one year, the soil retained much less water at all but the highest tensions; after two years, the soil retained more water in the macro and micro-pores (although retention in the meso-pores was similar to the original, homogenised state). The aggregate size distribution tended to be more skewed towards smaller diameters, the more negative the water suction had been and the more intensively the aggregates had been dried, the more irreversible the change in the pore sizes created during swelling (Horn and Dexter, 1989).

Sarmah *et al.* (1996) investigated the effect of wet/dry cycles on a compacted Vertisol from which soil cores 300 mm in diameter and 500 mm deep were taken from wheeled areas (48 cores) and from the adjacent beds (36 cores). The soil was 48 % clay and 34 % sand and had 1 % organic carbon. The cores were dried by evaporation and wetted either through flooding (a head of 15 to 20 mm of water applied to the surface for 30 minutes), or through simulated rainfall (63 mm h^{-1} for 30 minutes).

In general, wet/dry cycles increased the proportion of smaller cracks (less than 4 mm diameter, measured from digitised photographs of the soil surface taken at maximum soil dryness) and decreased shear strength and clod size, as well as increasing infiltration rates. Most of the increase in infiltration rate occurred during the first wet/dry cycle. Flood wetting had a greater effect on the measured parameters than rain wetting, except at the surface where flood wetting caused some slaking to occur. Overall, the authors concluded that the Vertisol investigated had a low to moderate ability to self repair under wet/dry cycles. They also state that none of the methods of assessing soil structure were found to be more reliable than the

others and that it was necessary to develop a robust and readily interpretable method of assessing soil structure (Sarmah *et al.,* 1996).

These studies were extended by Pillai and McGarry (1999), who compared the effect of four crops (sorghum, lablab, wheat and mung bean) on the efficacy of wet/dry cycles on compacted samples of the same Vertisol. The inclusion of crops improved shrinkage of the soil samples. This was particularly true of legume crops, an effect that was exaggerated by progressive cycles, although three wet/dry cycles were enough to demonstrate significant improvement in structure to at least a depth of approximately 200 mm. Binary images showed that wet/dry cycles created porosity inside of soil clods and promoted small clod formation. The soil was deemed to show good structural repair with wet/dry cycles under crops, based on increases in porosity shown by the binary images, as opposed to the moderate to low levels of structural repair shown without crops (Pillai and McGarry, 1999).

Changes in the structure of a Vertisol with wet/dry cycles, and how this was effected by the rate of wetting, were also investigated by Hussein and Adey (1998). The porosity observable in thin sections (greater than 5 µm) increased from 2.5 % to 23.9, 13.7, 12.8 and 12.3 % for the samples wetted by fast capillary, rainfall, slow capillary and flood wetted samples respectively after just one wet/dry cycle. Capillary wetting was executed at a height of 70 mm above the water table, the slow wetting being achieved through a kaolin tension table, the fast via a porous cloth that acted as a wick. Rainfall was applied at 32 mm h^{-1} and flooding under a head of 16 mm of water. The void structure went from predominantly planar to predominantly compound voids after all methods of wetting. The structure of the undisturbed

soil was most closely approached, however, by the fast capillary wetted samples (Hussein and Adey, 1998). These results differ from those of Sarmah *et al.* (1996), who found that flood wetting provoked the most rapid change to soil structure. However, the parameters measured were different, as Sarmah *et al.* (1996) monitored infiltration rates, rather than porosity. An increase in infiltration rate may be a better measure of an improvement of soil structure as it indicates an improved flow of water and gases through the soil profile, implying a greater potential for augmentation of the soil water store, and a reduced risk of runoff and the potential for pollution associated with this.

Grant and Dexter (1986) also found that the rate of wetting of a soil was significant in determining structural regeneration, based on assessments of the tensile strength of remoulded soil samples with 17 % clay. They found that there was a critical wetting rate for their samples of 6.1×10^{-2} $gg^{-1}h^{-1}$ (grams of water per gram of soil per hour), below which no reduction in the tensile strength of the soils occurred.

Pires *et al.* (2005) used gamma ray computed tomography to evaluate the changes to the structure of samples of three soils containing 28, 43 and 48 % clay and having initial bulk densities of 1.56, 1.62 and 1.33 g cm^{-3} respectively. Six samples of each soil, 300 mm deep and 480 mm in diameter, were subjected to none, three and nine wet/dry cycles. Soils were wetted from the bottom up for 24 hours and dried by the application of 4 MPa (approximately 400 m water). The increase in porosity between none and nine cycles of the 28 and 43 % clays was 6 and 7 % respectively. The 48 % clay soil behaved more erratically, with less consistency between samples. It demonstrated a mean increase in porosity of 4 % between

none and three cycles, but remained constant between three and nine cycles (Pires *et al.*, 2005). However, the initial bulk density of the 48 % clay soil was much lower than the other soils and would, therefore, have been expected to demonstrate a lesser change (if any) in porosity.

Differences in the moisture release curves of the three soils between three and nine cycles were also considered and the individual points on the curve analysed for statistical differences. The soil containing 28 % clay showed significant differences at pressures over 1 m (~ 10 KPa), more water being retained after nine cycles, although differences were greatest at high pressures. The 43 % clay soil also retained more water, but this was only significant at pressures equal to and in excess of 15 m of water (~150 kPa) and the differences were marginal. The soil with 48 % clay displayed significant increases in retained water at all pressures. The differences of this soil's moisture retention curve were greatest at low pressures, indicating that the soil had experienced an increase in macro-porosity (Pires *et al.*, 2005).

Velde (2001) examined the pore space that was developed by a clay rich Rendzina during one wet/dry cycle in the field. The field plot was initially dry from the summer climate. It was then gradually wetted until saturation occurred with slight puddling. Surface photographs were taken during the drying process, as were 70 mm diameter cores from 30, 60 and 90 mm depths that were taken to the lab and impregnated with a fluorescent resin. The observed area of surface cracks increased linearly with time to approximately 10 % after 10 days. As drying progressed, the crack length increased initially and then after seven days, existing cracks

widened. After 10 days, the porosity of the cores taken from depths of 30 and 60 mm was 26 and 18 % respectively, but negligible at 90 mm. Velde (2001) concludes that the presence of aggregates determines pore structure more than surface cracks, but that when water stable aggregates are not present, surface cracking will be the dominant pore forming mechanism.

Surface cracking was also explored by Yesiller *et al.* (2000). Three soils with clay contents of 30 (soil 1), 42 (soil 2) and 11 (soil 3) % clay were compacted to densities of 1.79, 1.87 and 1.88 g cm^{-3} in tanks 1.0 m by 1.5 m by 0.5 m deep. The final depth of soil was 170 mm. The soils were then air dried, wetted to saturation with simulated rainfall with an intensity of 25 mm h^{-1} and allowed to air dry again. The 42 % clay soil was wetted and dried a further two times. Some cracking of soils 1 and 2 occurred during the first drying cycle (to approximately 1 % of the surface area), but not for soil 3, but soils cracked during the second drying cycle. The first two soils (with the higher clay contents) achieved areas of cracks of approximately 5.5 and 5 % , the third soil approximately 2.5 %. The area of cracks visible on the surface of soil two rose to 6.9 and 6.7 % on the second and third drying cycles. The second wetting reduced the area of cracks to virtually zero, but the third wetting only reduced the area of cracks to 2.3 %. The authors concluded that most of the cracking of all three soils occurred at suction of less than 1000 kPa (100 m of water). The critical suctions for the soils were reported as 800, 200 and 300 kPa for soils one, two and three respectively. Yesiller *et al.* (2000) also suggested that very little further cracking would be likely after the second drying cycle.

A model of crack formation was developed by Vogel *et al.* (2005), based on a lattice of Hookean springs (idealised, massless springs that obey Hooke's Law) and reproduced characteristic of natural crack patterns and dynamics, as described by Minkowski functions (a non-negative, positively homogeneous, convex function with zero as a real number, that maps quadratic irrationals to rational numbers on the unit interval) and the distribution of bifurcation angles. The clay layer was represented by a two-dimensional network of simple Hookean springs. As the soil layer dries, the natural length of the springs is reduced, increasing the strain between the nodes. When the strain reached a critical threshold, the spring broke and the energy was redistributed around the remaining springs; a crack emerged when the critical threshold was exceeded. The strain of each individual spring connecting to nodes at the positions x_i and x_j respectively was given as:

$$\in_{ij} = \frac{|x_i - x_j|}{\lambda} - 1 \qquad (1)$$

Where: λ*= the natural (relaxed) length of the spring.*

The net force acting on node *i* through its N_i neighbours was given as:

$$F_i = -\sum_{j \in N_i} K_{ij} \frac{(x_i - x_j)}{|x_i - x_j|} \left[|x_i - x_j| - \lambda \right] \qquad (2)$$

Where: *K = the spring constant.*

The total energy at each node was given by:

$$E_i = \frac{1}{2}\sum_{j \in N_i} K_{ij} \left[\left|x_i - x_j\right| - \lambda\right]^2 \quad (3)$$

Vogel *et al.* (2005) state that the parameters of the model have direct, physical meaning (related to Youngs modulus, critical stress failure and interfacial energy) and can, therefore, be directly linked to physical properties and boundary conditions. Although their model was only applicable in two dimensions (i.e. at the soil surface), they proposed that the model could be extended into three dimensions and coupled with transport models to simulate phenomena such as preferential flow along macro-pores. They also suggest that bulk density dynamics of aggregates could be used for scaling the hydraulic properties of the matrix domain. Since the properties of soil structure most relevant to crop growth are described by the hydraulic functions, it is implied that this model has the potential to be developed to describe changes to soil structure with wet/dry cycles.

Grant *et al*. (1995) investigated the ability of remoulded soil samples to fragment under wet/dry cycles. The soils investigated were from the plough layer and subsoil and ranged in clay content from 29 to 74 %. 11 soils were sampled in total. The mean-weight diameter of four of the 11 soils (containing 71, 74, 55, and 56 % clay) dropped from 35 mm to approximately 5 mm after three wet/dry cycles. The effect of wet/dry cycles had varied effects on the other soils. The mean-weight diameter of these soils started at approximately 40 mm and ranged between 40 and 10 mm after three wet/dry cycles.

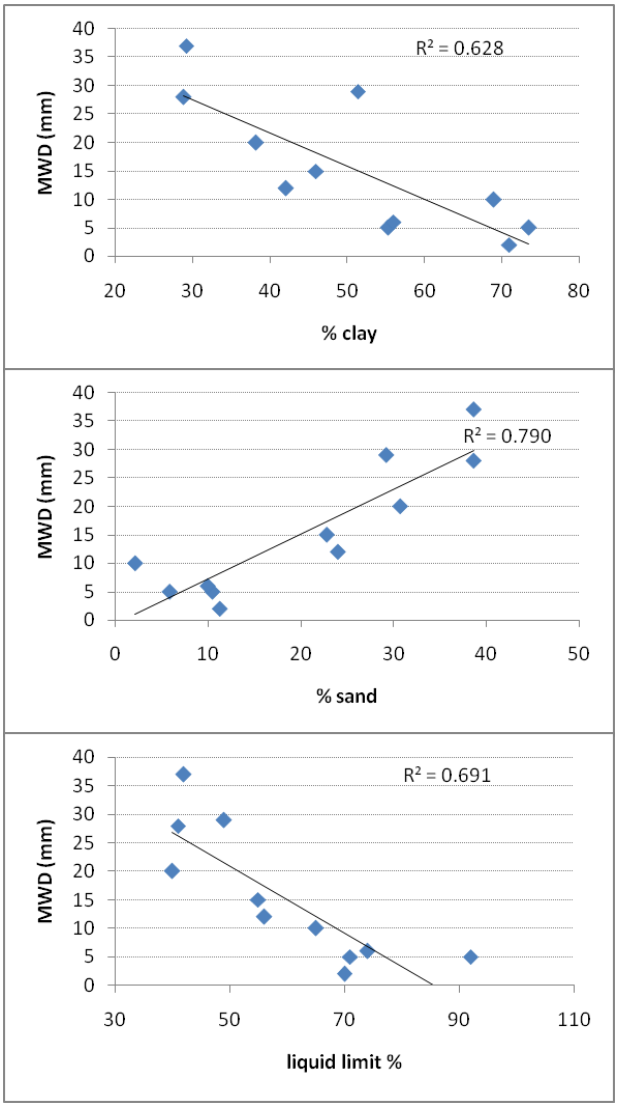

Figure 4. Simple correlations between mean weight diameter and some soil parameters (after Grant *et al.*, 1995).

The soil which experienced no overall reduction in mean-weight diameter of aggregates with wet/dry cycles had a clay content of 29 %, the soil which experienced the greatest reduction in mean-weight diameter of aggregates (to 10 mm) has a clay content of 69 %, a greater clay content than other soils that had smaller aggregates. Grant *et al.* (1995) did not correlate the

mean-weight diameter of the soils with other measured parameters reported, but simple regressions were drawn, based on tabulated data (clay and sand fractions and liquid limits) and the mean-weight diameter of soil aggregates after three wet/dry cycles, estimated from graphs (Figure 4).

Wagner *et al.* (2007) found that the aggregation of soil was based primarily on clay content but that the development of water stable aggregates with wet/dry cycles was improved by the addition of organic matter (in the form of straw) to the soil profile. After three wet/dry cycles, the mean-weight diameters of aggregates were increased by 70% and 140% with the organic matter additions of 3.1 t ha^{-1} and 12.4 t ha^{-1} respectively, and by 160% and 290% after six wet/dry cycles, compared to samples without organic amendments; the addition of organic matter increased the size of water stable aggregates developed during wet/dry cycles. This could be considered an improvement to soil structure if the initial structure of the soil was massive and the inclusion of organic matter promoted the formation of a granular structure.

Zang *et al.* (2005) investigated the use of peat as a soil amendment to increase soil resilience and explored the effects of wet/dry cycles on a degraded soil structure, following differing proportions of peat amendment. They tested the hypothesis (drawing on the theories of Gupta *et al.*, 1987 and Dexter, 1988) that organic matter in the soil would act as spring, increasing the rebound, or resilience of a soil after the removal of a compressive stress and that mechanic resistance to shear stress would also be positively affected (Zang *et al.*, 2005). They also hypothesized, however, that with increasing numbers of wet/dry cycles, the organic matter would be incorporated into aggregates, reducing its effectiveness as a spring.

The soil used in the experiment was kaolinitic, clayey and acidic, containing 20.6 % sand, 33.6 % silt, 45.8 % clay, 4.6 pH (2:1 soil:water), 0.68 % soil organic carbon, 103.0 mmol (+) kg^{-1} cation exchange capacity. The soil was severely degraded after having been in cultivation under peanut cropping for 30 years in China (28^o 15' N, 166^o 55' E). The organic matter that was used to amend the samples was a highly decomposed peat, selected because it was considered resistant to biological decay during incubation. 0, 10 or 50 g kg^{-1} of peat were mixed with homogenized soil samples. The constructed soil cores were subjected to 0, 4 or 10 cycles of 12 hour saturation, followed by 24 hours drainage on a -30 kPa suction plate and 10 hours of drying at 40^o C (the average soil temperature in summer in the sampling area). Total porosity was calculated from bulk and particle densities. Pore size distribution was calculated from soil water retention curves. Normal stresses of 20, 40, 70,100, 200, 400 kPa were applied to the cores, for three hours, in free draining conditions. The settlement and the recovery in the subsequent hour were recorded.

Zang *et al.* (2005) found that total porosity increased with organic matter content, but was not significantly affected by the number of wet/dry cycles. Pore size distribution, however, was affected by both organic matter content and the number of wet dry cycles. The proportion of pores that had diameters of < 6 μm increased with the increase in both parameters. The compressibility index (ratio of the gradient of the virgin compression line to that of the recompression line) increased with number of wet dry cycles. It was also higher for that soil with 10 g kg^{-1} organic matter than for the 50 g kg^{-1} amended soil. The rebound height after the applied load was removed increased with increasing organic matter, but tended to be

higher after four wet/dry cycles than after either one, or ten. Surface soil cohesion tended to decrease with increases in wet/dry cycles and organic matter content. Friction, however, increased with wet/dry cycles for the 10 g kg^{-1} amended soil. For the 50 g kg^{-1} amended soil, friction was slightly higher generally than for the 10 g kg^{-1} amended soil, but was not affected by the number of wet/dry cycles. There was very little difference in the direct shear tests between any of the samples, other than the highest organic matter, wet/dry scenario which had a low value of cohesion.

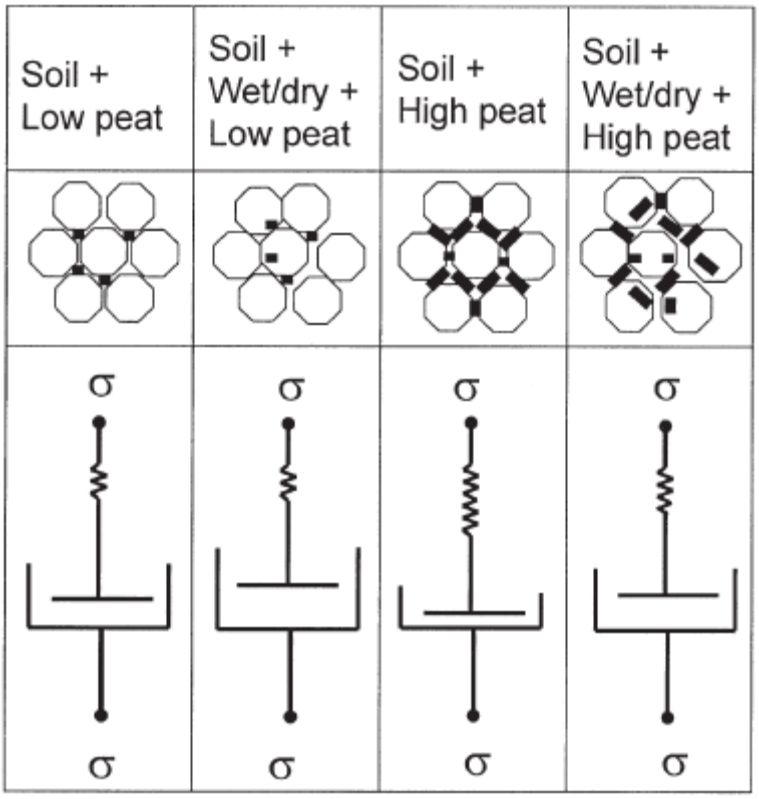

Figure 5. Influence of peat amendment and wet/dry cycles on soil structure on mechanical behaviour[1] (after Zang *et al.*, 2005).

[1] "A conceptual diagram of how peat amendment and wet/dry cycles influence soil structure and mechanical behaviour. At the top of the figure, the lightly textured blocks represent soil aggregates and the thick lines peat. At the bottom of the figure, the size of spring represents elastic deformation that is recoverable once the stress is

Zang *et al.* (2005) conclude that the addition of organic matter did increase elastic deformation of the soil, but also the mechanical resilience of the soil after the applied load had been removed. They also concluded, however, that wet/dry cycles diminished this effect as they increased aggregation, leading to coarser pores, which were more easily compressed, but not recovered on unloading (Figure 5).

Zang *et al.* (2005) also suggested that the observed effects were purely mechanical as the experiments were conducted over a short period. They state that other researchers may have had more exaggerated results because the experiments were conducted over a longer time scale, allowing biological factors, such as microbial and fungal aggregation of the soil and suggest that further research is necessary, comparing the results of experiments conducted after differing incubation periods. This is supported by the results of McGovern (2002) who found that fungal and microbial growths effected soil aggregation and hydraulic characteristics.

Peng and Horn (2006) investigated the shrinkage and swelling of undisturbed cores (10 cm in diameter and 6.1 cm in height) from the subsoils of: a Eutric Histosol, 11.5 % clay, 22.2 % organic C (soil 1); a Histic Gleysol, 39.9 % clay, 20.1 % organic C (soil 2); a Calcic Gleysol, 34.9.% clay,1.4 % organic C (soil 3); and a Dystric Gleysol, 64.9 % clay, 0.5 % organic C (soil 4). The soil cores were wetted by capillary rise, air dried, oven dried, rewetted by vapour

removed. The size of the dashpot represents plastic deformation that is not recoverable when the stress is removed" (Zang *et al.*, 2005).

and saturated by capillary rise again. Vertical and horizontal displacements were measured during this process. They found that there was very little difference between the behaviour of soils 1 and 2 and between soils 3 and 4, despite differences in their clay content. They found that the two inorganic soils only lost 10 to 26 % of their volume on drying, whereas the organic soils lost 77 to 78 % of their volume. They concluded that it was the organic C content of the soils that was the predominant factor in determining behaviour (Peng and Horn, 2006).

Reeve and Earl (1989) explored the effects of organic matter content and the proportion of silt+clay on the moisture content at which the soil reached its plastic limit. Clear trends were identified. There was a strong, positive, linear relationship with organic matter content and moisture content at the plastic limit (Reeve and Earl, 1989). This is significant as it implies that the moisture content at which damage would occur with trafficking is increased with organic matter content, increasing the trafficability window. The proportion of silt+clay also had a positive effect on the water content at which the soil behaved plastically, but the trend was not linear. The data points were evenly scattered under a maximum line (Reeve and Earl, 1989). Verheijen et al. (2005) related clay content, whether the soil was under permanent grassland, ley-arable, or arable farming to an indicative upper limit of soil organic matter content. It could be that the form of Reeve and Earl's (1989) graph relating plastic limit and clay + silt content was a result of this relationship. If this is the case, it could be used to indicate how resilient a soil could be made to compaction by the amount of organic carbon the soil contains.

The liquid and plastic limits of soils have been significantly correlated to the compactability of soils (Ball *et al.,* 2000), which were found to be in turn correlated the readily oxidisable organic matter, whereas clay content was found to be only weakly correlated with compactibility. These findings were based on the maximum density that could be achieved by the Proctor test on soils from 156 different sites, ranging in clay content from 2.5 to 49 % and in sand from 1.7 to 93.5 %. The dry bulk densities achieved ranged from 0.76 to 1.82 g cm^{-3}.

Sridharan and Gurtug (2004) investigated the swelling behaviour of five fine grained soils, varying in clay content and mineralogy. Samples of the soils were compacted at their optimum moisture content, at three different compactive energies, and then the swelling pressure they exerted when they were wetted was measured. Swelling pressure was found to vary between soils and between compactive energies: as the plasticity of the soils increased, so did the swelling pressure; as the compactive energy increased, so did the selling pressure. Most importantly, however, a very strong linear relationship was found between swelling pressure and percent swell, up to 1000 kPa of swelling pressure, regardless of soil or compactive energy (R = 0.98). The relationship discovered was:

$$\textit{Swelling pressure (kPa)} = 48.32 \times \textit{percent swell} \qquad (4)$$

These findings are very important to this thesis as swelling amounts to a change in bulk density, changes in which have been shown to be linearly related to swelling pressure, which in turn has been shown to be related to plasticity and compressibility of the soils. This

strongly suggests that it should be possible to predict changes in bulk density induced by wet/dry cycles.

Although this thesis is focussing on the recovery of soil structure after a compaction event, rather than the compactibility of soils, the findings of Ball *et al.* (2000) could have relevance as they show that it is possible to predict the behaviour of soils from readily measurable parameters, especially considering the results of Sridharan and Gurtug (2004). Organic matter has been associated with soil resilience (Zang *et al.*, 2005) and with extent of shrinkage and swelling (Peng and Horn, 2006). Another factor found to effect shrinkage and swelling curves was the initial structure of the soil (Reeve and Hall, 1978; Peng and Horn, 2005). The rate of wetting and drying has also been found to be important. When considered in conjunction with observations made on the findings of Grant *et al.* (1995), it seems plausible that some measure of soils structure may also be predictable from such parameters.

2.4.3 Summary

Recovery of soil structure has been measured and recorded, both in the field and the laboratory. Croke *et al.* (2001) found that after five years, the bulk density of soil compacted by snig tracks, created during harvesting of *Eucalyptus*, had not changed, but the surface infiltration had more than doubled. Similarly, Rab (2004) found that there was no change in bulk density of compacted snig tracks 10 years after harvesting, but did observe over 100 %

improvement in macro-porosity. Long term field studies have shown that penetration was still greater the control in compacted plots of clay and organic soils nine years after the compaction event, despite deep, annual freezing. However, differences in saturated hydraulic conductivity (K_s) were undetectable due to infield heterogeneity (Alakukku, 1996a; Alakukku, 1996b; Alakukku *et al*., 2003; and Chamen *et al*., 2003). Etana and Håkansson (1994) also found that there was no change in the bulk density, shear strength or penetration resistance of subsoil 11 years after the compaction event despite deep, annual freezing. Blackwell *et al.* (1985) detected some recovery of the structure of a swelling, compacted clay in the second growing season after the compaction event. Radford *et al.* (2007) noted that yields from their compacted plot were comparable with the control at the sixth harvest after the compaction event. Halvorson *et al.* (2003) found that the bulk density of a compacted silt loam did not change, but that saturated hydraulic conductivity approached levels of the uncompacted soil after just one year. Drewry (2006) observed significant recovery of macro-porosity, hydraulic conductivity and infiltration rate at the surface of a puddled soil after just four months.

Arvidsson and Håkansson (1996) found that although mould-board ploughing removed the physical indicator of compaction, such as increased bulk density, yield losses persisted three to four years after the compaction event and were approximately linearly correlated with the amount of trafficking. Subsoiling has been found to increase yields (Abu-Hamdeh, 2003) but has also been found to leave the soil vulnerable to re-compaction (Horn *et al.,* 1995; Motovalli *et al.,* 2003), although gypsum additions may alleviate this (Hamza and Anderson, 2003), and reduce saturated hydraulic conductivity (Dexter *et al.,* 2004). Mechanical impact on the soil has also been discovered to have a significant, negative effect on the tensile

strength of aggregates and this effect persists after ploughing (Arvidsson and Håkansson, 1996; Munkholm and Schjønning, 2004).

Horn and Dexter (1989) showed that the more rapid the drying of a disturbed, leoss soil, the smaller the structural units that were produced by wet/dry cycles. This finding was also made by van de Graff (1978), who also suggested that the less than 8 µm particles were responsible for promoting the formation of large structural units, while the 16–32 µm particles promoted formation of smaller structural units. Sarmah *et al.* (1996) reported that flood wetting produced a greater increase in infiltration rate than rain wetting during wetting and drying of a compacted Vertisol. Hussein and Adey (1998) found fast capillary rise the method of wetting that increased porosity the most. A critical rate of wetting of 6.1 x 10^{-2} $gg^{-1}h^{-1}$ was found for a soil with 17 % clay by Grant and Dexter (1986). Pires *et al.* (2005) reported that wet/dry cycles increased porosity, but that the pore size class where this increased occurred varied between soils with different clay contents.

Pillai and McGarry (1999) found that the inclusion of crops increased shrinkage and hence structural formation in the same soil studied by Sarmah *et al.* (1996). Lister *et al.* (2004) found that vegetated compacted plots generally had lower bulk densities and higher aggregate stabilities than those where vegetation had been totally controlled. Bushamuka and Zobel (1998) and Williams and Weil (2004) also found that strong rooted plants could be used to ameliorate compaction by penetrating the compacted layer, creating a pore network that was utilised by successive crops, as could worms (Larink *et al.*, 2001).

Velde (2001) suggested that when water stable aggregates are not present, surface cracking will be the predominant pore forming mechanism. When Yesiller *et al.* (2000) considered the cracking of homogenised, compacted clays they observed that there were critical suctions, below which all the cracking occurred and suggested that very little further cracking would occur after the second drying cycle. Vogel *et al.*(2005) developed a model of crack emergence that they proposed could be extended and coupled with transport models to simulate preferential flow along macro-pores.

The work of Grant *et al.* (1995) implied that the mean-weight diameter of the aggregates produced as a result of wet/dry cycles could be predicted from easily measurable soil parameters, such as the liquid limit. Wagner *et al.* (2007) observed that although the development of water stable aggregates with wet/dry cycles was based primarily on clay content, organic matter inclusions significantly increased the mean-weight diameter of those aggregates. The investigations of Zang *et al.* (2005) showed that organic matter amendments also increased the mechanical resilience of the soil, but this effect diminished with wet/dry cycles, as the cycles promoted aggregation and increased the proportion of macro-pores, which were more easily compressed. Peng and Horn (2006) found that organic matter was more important than clay content in determining the extent of shrinkage of soils upon drying, a higher organic matter implying greater shrinkage. Organic matter has also been found to have a strong, positive correlation with the plastic and liquid limits of soils (Reeve and Earl, 1989; Ball *et al.,* 2000). Ball *et al.* (2000) also found that the liquid of soils and their oxidisable organic matter could be used to predict their compactibility.

The results of the studies reported above suggest that some recovery of soil structure may occur in the field, but that it can be a lengthy process, especially when considering subsoils. In some instances changes to the surface soil have been relatively rapid. Mostly, these studies have focussed on changes in the bulk density of the soils and little attention has been paid to hydraulic properties. However, where properties such as infiltration rate have been investigated, research has elucidated changes to soil structure that were not necessarily apparent from bulk density measurements. Soil hydraulic parameters are also directly related to environmental and food production functions of the soil, dictating levels of water storage and availability, aeration status and amounts of runoff. This confirms the view that it was fruitful to further investigate changes to the hydraulic properties of soils with wet/dry cycles in this thesis.

Soil parameters affecting the extent/rate of structural change, which are highlighted in the literature reported above, are clay content, organic matter content and the liquid and plastic limits. Models have been found that predict compaction under a given set of conditions, as has a model which predicts surface cracking. No evidence has been found, however, for predictive equations that describe the recovery of soil structure after the compaction event. The following chapter will describe experiments designed to elucidate changes to the bulk density and hydrological parameters of soils with wet/dry cycles and to relate these to measured soil properties, thus addressing a key aim of this thesis.

2.5 Multi-step outflow method – estimating changes in the van Genuchten-Mualem parameters

One of the methods used in this thesis to assess changes to soil structure was to examine changes to the moisture release and the hydraulic conductivity functional parameters. These parameters may be estimated relatively rapidly by using the multi-step outflow method. The following section will review the development of the multi-step outflow method and explain the theory behind it. The specific methods used by this thesis will then be described in Chapter 3.

A method for calculating diffusivity and capillary conductivity from instantaneous outflow data was first published by Gardner in 1956 (after Doering, 1965). The method has since been developed by a series of researchers from single-step, transient outflow experiments to multi-step transient outflow experiments, which can simultaneously estimate soil water retention parameters and hydraulic conductivity functions. The method has the advantage over equilibrium measurements of being relatively rapid and of having no limitations on sample size. The findings of these researchers, relating to the reliability and development of the method, will be reported in the following section.

Kool *et al.* (1985) tested the proposition that soil hydraulic properties could be estimated from transient flow data, based on the assumption that these could be described by mathematical functions with a small number of parameters that could be optimised by

minimising the error between measured transient flow data and that obtained numerically by solving Richards' Equation (Equation 5). Transient flow from a single pressure step was measured and then simulated with estimates of soil hydraulic parameters for two hypothetical soils (a sandy loam and a clay loam). Simulations were then evaluated with a nonlinear least-squares fitting of predicted and observed cumulative outflow with time.

Richards' Equation was written for the one dimensional case with vertical distance x taken positive downward and with pneumatic potentials translated to the lower boundary condition as:

$$C(h)\frac{\partial h}{\partial t} = \frac{\partial}{\partial x}[K(h)(\partial h / \partial x - 1)] \quad (5)$$

Where: $C = d\theta / dh$ *is the water holding capacity*

The initial boundary conditions are: when time is 0, the pressure is 0 all through the soil column; at a time greater than 0, the difference in pressure in the column between two depths is equal to the difference in height; and the pressure in the soil core is the pressure at the bottom of the porous plate minus the pressure applied to the soil column divided by gravity time the density of water, i.e.:

$$h=h_0(x),\ t=0,\ 0\leq x\leq L \quad (6)$$

$$dh/dx=1,\ t>0,\ x=0 \quad (7)$$

$$h=h_L-h^a,\ t>0,\ x=L \quad (8)$$

where: $x=0$ *is the top of the core*

$x=L$ *is the bottom of the porous plate*

h_L *= the pressure head at the bottom of the porous plate*

and:

$$h^a=\Delta p/\rho g \quad (9)$$

where: Δp *= the gas gauge pressure applied to the core*

g *= gravity*

ρ *= the density of water.*

The solution to this equation was obtained by a modified version of Galerkin finite element model of van Genuchten:

$$h(x,t) \cong h(x,t) = \sum_{j=1}^{n} \varphi_j(x) a_j(t) \quad (10)$$

Where: $\varphi_j(x)$*= the selected basic functions*

a_j (t)= the associated, unknown, time-dependent coefficients which represent solutions of Equation 5 at specified nodes within the solution domain.

Cumulative outflow was calculated as:

$$Q(t) = A\int_0^L [\theta(x,0) - \theta(x,t)]dx \qquad (11)$$

Where: *A = the area of the soil core perpendicular to flow*

It was also assumed that the soil hydraulic properties could be described by van Genuchten's model (after van Genuchten, 1980):

$$S_e = \frac{\theta - \theta_r}{\theta_s - \theta_r} = \frac{1}{\left[1 + |\alpha h|^n\right]^m} \qquad (12.1)$$

$$K = K_s S_e^{1/2}\left[1 - \left(1 - S_e^{n/(n-1)}\right)^m\right]^2 \qquad (12.2)$$

Where: S_e = *normalised water content*

θ = *actual water content*

θ_r = *residual water content*

θ_s = *saturated water content*

h = *the pressure head*

α *and* n = *empirical parameters*

m = *1-1/n*

K = *unsaturated hydraulic conductivity*

K_s = *saturated hydraulic conductivity*

Although in the true case, the residual water content will always be zero, Kool *et al.* (1985) treated it as a fitting parameter. The saturated water content (θ_s) and the saturated hydraulic conductivity (K_s) were measured and l was fixed as 0.5; residual water content (θ_r), α and n were sought by numerical inversion of the flow problem. The objective function $E(\mathbf{b})$ which was minimised during the parameter estimation describes the differences between observed, $Q_o(t_i)$, and predicted cumulative outflow, $Q_c(t_i, \mathbf{b})$, at time t_i:

$$E(\mathbf{b}) = \sum_{i=1}^{i=n} \{ w_i [Q_o(t_i) - Q_c(t_i, \mathbf{b})] \}^2 \qquad (13)$$

Where: w_i = *a weighing factor for individual measurements;*

n = *the number of observations (i.e. number of outflow data).*

$Q_o(t_i)$ = *observed cumulative outflow at time* t_i

$Q_c(t_i, \mathbf{b})$=*predicted cumulative outflow at time* t_i

For the clay loam, Kool *et al.* (1985) found that an applied pressure of 10 m resulted in more accurate estimates than an applied pressure of 1 m. They also found that measuring outflow for six hours instead of three improved accuracy and recommended that the outflow with time be measured until at least half of the total outflow for the pressure head had occurred. Inclusion of the total outflow also improved accuracy and the speed of convergence. However, the estimated release curves for the clay loam were sensitive to the initial parameter estimates and diverged at pressures of greater than 10 m.

Parker *et al.* (1985) continued the investigations of Kool *et al.* (1985) with experimental data. They took undisturbed soil cores (54 mm diameter by 40 mm deep), ranging in texture from sandy loam to clay, and subjected them to a series of wet/dry cycles to stabilise them during the drainage process. The samples were then saturated. A one-step pressure outflow test was performed with a pressure head of 10 m applied to the top of the soil core and cumulative outflow measured with time. The cores were then resaturated and equilibrium water contents measured at applied pressures of 0.1, 0.5, 1.0, 3.0, 6.0, 10, 30 and 150 m (~ 1, 5, 10, 30, 60, 100, 300, and 1500 kPa). The cores were saturated again and the saturated hydraulic conductivity measured (Parker *et al.*, 1985).

Parker *et al.* (1985) found that the method gave a reasonable estimation of soil parameters at low pressures, but tended to diverge at pressures much greater than 10 m (~100 kPa),

although it was improved by adding to the objective function the two measured equilibrium moisture contents obtained at pressures of 30 and 150 m (~ 300 and 1500 kPa). However, it was also found that it may be more appropriate to estimate hydraulic properties from transient data than from equilibrium moisture contents as equilibrium measurements predicted $\theta(h)$ data more accurately than the transient flow experiments but sometimes at the expense of accuracy in $K(h)$ and in predictions of transient flow (Parker *et al.,* 1985). This suggests that there may some advantages to the one-step outflow experiment over equilibrium moisture content experiments when considering the changes to the structure of a soil elucidated by the hydraulic conductivity curve. These authors went on to write a review of parameter estimation techniques (Kool *et al.,* 1987). They concluded that much work was left to be done in the development of parameter estimation methods, especially when considering field scale heterogeneity, but that the method would become increasingly useful.

Various other authors have also explored and evaluated the appropriateness of outflow methods in the estimation of soil hydraulic properties. Borcher *et al.* (1987), for example, successfully estimated the diffusivity of a silt loam using the one-step outflow model. Jaynes and Tyler (1980) tested parameter optimisation as a method for estimating hydraulic conductivity and found that the method was a good predictor at moisture contents less than saturation. The saturated hydraulic conductivity was not well predicted, however. These findings were corroborated by the findings of Green *et al.*, 1998, who concluded that the one-step outflow method could be successfully, routinely applied to estimate diffusivity and unsaturated hydraulic conductivity, but that the procedure could not be used to determine values of hydraulic conductivity very close to saturation due to the difficulty in determining

the derivative of the soil water characteristic at small suctions and because only stage III outflow data were used (the portion of the outflow where the boundary condition at the top of the soil core begins to influence flow). Such a limitation in the Mualem-van Genuchten Equation has also been noted by Schaap and van Genuchten (2005) and Ippisch *et al.* (2006), who state that predicting the conductivity curve from the moisture retention curve will result in errors close to saturation.

Van Dam *et al.*(1992) also predicted soil hydraulic functions from one-step outflow data and compared these to measured equilibrium data. They found that the model estimated the general shape of the measured moisture release curve well, provided that only the saturated moisture content or the residual moisture content were estimated, not both, as one of these points is needed to determine the range of the retention curve; if both were estimated, relative changes between them might be accurate, but the position of the curve on the graph would not. They also found that realistic initial estimates of the parameters were needed in order to avoid local minima. Importantly, they concluded that the accuracy of predictions could be improved by introducing data from a series of sequential pressure steps, rather than just one step, and went on to test this theory.

Van Dam *et al.* (1994) compared the results from a multi-step outflow experiment to the results gained from equilibrium measurements. After equilibrium measurements had been taken, the samples were re-wetted to an equilibrated at 0.3 m pressure (~ 3 kPa). Increasing pressure increments were applied daily, over five days, to 10 m and cumulative outflow with time was recorded. They also measured the moisture content of the medium textured soil at a

pressure of 160 m (~ 1600 kPa), to provide the model with a fixed point on the moisture retention curve.

Van Dam *et al*. (1994) found that parameter estimates from the multi-step outflow method corresponded well with those from equilibrium data. They also found that the model converged upon the same result when three different initial parameter estimates were used, where as the optimization results of the one step method depended on the original estimates; using more than one pressure step seemed to have solved problems of non-uniqueness in parameter estimates (van Dam *et al.,* 1994). They also tested different combinations of fitted parameters, but concluded that Mualem-van Genuchten model was flexible enough when the parameters α, n, K_s and l were optimised, whilst θ_s was fixed at its measured value and θ_r was assumed to be zero, although they did also recommend determining K_s independently. Fixing l was found to have a negative impact on the *K(h)* curve (van Dam *et al.*, 1994).

Eching and Hopmans (1993) tested the addition of soil water pressure head data to both one-step and multi-step outflow data to minimize uniqueness problems when estimating unsaturated soil hydraulic functions. They experimented upon four soils; a silt loam, a loam, a sandy loam and a fine sand. The soils were formed into remoulded samples of 82 mm diameter and 60 mm depth. For the one-step experiments, the samples were drained at a pressure/suction (both were applied in separate experiments) of 7 m (~ 70 kPa), except for the fine sand which was drained at 4 m. For the multi-step experiments, pressures/suctions of 0.4, 0.6, 0.8, 2, 4 and 7 m (~ 4, 6, 8, 20, 40 and 70 kPa) were applied to the soils, except for the fine sand which had pressures/suctions of 0.4, 0.6, 0.8 and 2 m (~ 4, 6, 8 and 20 kPa) applied

to it. Individual pressure steps were applied until outflow had decreased to approximately 0.05 ml h^{-1}. The parameters α, n, θ_r and K_s of the van Genuchten Equation were optimised. The results were then compared to equilibrium data. Eching and Hopmans (1993) concluded that when outflow data were used alone, the multi-step method returned better results than single-step outflow. However, when soil water pressure head data, measured with time during drainage by a tensiometer installed just below the soil surface, were included in the optimisation process, both the one-step and the multi-step experiments produced excellent results that correlated well with independently measured equilibrium data. They also found that the optimisation process converged on the same set of results, regardless of the initial parameter estimates (Eching and Hopmans, 1993). This suggests that either the multi-step method be used, or that soil water pressure head data be used with the single-step method to improve parameter estimates.

Eching *et al.* (1994) also tested the multistep outflow method as a means of estimating soil unsaturated hydraulic conductivity functions. The applied pressures ranged from 0.4 to 7 m (~ 4 to 70 kPa) to soils ranging in texture from fine-silty loam to fine sand. The duration of each pressure step ranged from six to 36 hours, pressure changes occurring when outflow decreased to 0.05 ml h^{-1}. Soil water pressure head readings were measured as a function of time with a tensiometer installed vertically 30 mm below the soil surface. Readings were recorded automatically every minute, but measurements taken every 3 ml during rapid flow and every 1 ml when flow rates decreased were found, in Eching *et al.'s* (1994) experience, to be most appropriate for use for both computer optimisation and direct estimation of $K(\theta)$. One of the problems they found was that the ceramic plate was impeding drainage at high

moisture contents/low pressures (i.e. the high flow rates associated with the soil conductivity close to saturation being greater than the conductivity of the ceramic plate) and that it could become blocked during the experiment by soil particles and/or bacterial growths. However, overall they found that the agreement between the results of the multi-step outflow experiment and directly measured hydraulic data were "excellent", although they did again suggest that non-uniqueness was reduced if soil water pressure head data (measured with a tensiometer installed just below the soil surface) were considered simultaneously with outflow data.

Vereecken *et al.* (1997) investigated which combination of the Mualem-van Genuchten model parameters would produce the best estimation of the soil hydraulic functions when optimised as part of the multi-step outflow experiment. They considered the results obtained from 57 undisturbed soil samples, taken from three soil horizons, having clay contents of 15.4, 19.6 and 21.9 %. Two suctions were applied to the soil samples (0.1 and 0.3 m, ~ 1 and 3 kPa) and four pressures (2, 4, 6, and 8 m, ~ 20, 40, 60 and 80 kPa). Each suction/pressure was applied for 24 hours, although it was stated that drainage must be continued beyond the first inflection point (i.e. the gradient of the tangent to the curve of cumulative outflow against time for that pressure step must have significantly decreased). In all optimisation runs, θ_r was set to zero and θ_s was calculated from bulk density measurements. The parameters α and n were optimised in every run with different combinations of K_s and l. They concluded that both K_s and l should be considered fitting parameters and optimised along with α and n (Vereecken *et al.,* 1997).

Vrugt *et al.* (2001) proposed that all six of the van Genuchten-Mualem parameters could be estimated from multi-step outflow data. The method they suggested was PIMLI (Parameter Identification Method based on the Localisation of Information). As the name implies, different parameters were estimated from different portions of the outflow data. The method was tested against artificial measurements calculated for a soil core with diameter of 50.4 mm and a depth of 50 mm, that had had pressure of 0.0030 m, 0.15 m, 0.50 m, 1.00 m, 3.00 m and 5.00 m (~ 0.03, 1.5, 5, 10, 30 and 50 kPa) applied to it. The method was then illustrated for a sandy and a clayey soil. They concluded that PIMLI could accurately predict all of the Mualem-van Genuchen parameters. Saturated water content was predicted from the average water content of the sample near the beginning of the experiment. The cumulative outflow at hydraulic equilibrium after the pressure step that was just past the air entry point was used to estimate the value of α, the equivalent information from later in the experiment was used to estimate n. The information content regarding K_s was contained within the flux density of outflow immediately after a pressure step in the high water content range, l in similar data at a low moisture content. The residual water content was estimated based on cumulative outflow near the end of the experiment (Vrugt *et al.*, 2001). The estimated and calculated results for the moisture retention curve presented for the clayey soil appeared almost indistinguishable from each other, although the two curves did begin to diverge at high pressures (greater than approximately 10 m), the PIMLI parameters marginally over estimating water content.

Other authors to have investigated the multi-step outflow method were Crescimanno and Iovino (1995). They considered whether the method would be applicable to shrink swell

clays. They found that the multi-step method was more reliable than the one-step method, but they also suggested that both methods needed to be supplemented by three fixed measured equilibrium values of $\theta(h)$. They recommended that these points be at pressures of 1, 4 and 7 kPa (~ 0.1, 0.4 and 0.7 m). They fitted θ_s and estimated θ_r directly from the measured data points. What is more interesting about the work of Crescimanno and Iovino (1995) was that the soils upon which they based their investigations were shrink-swell clays. They found that the soils remained in contact with the porous plate and that the shrinkage of these soils was not sufficient to distort parameter estimates (Crescimannoa and Iovino, 1995).

Other authors to have compared the multi-step outflow method with the direct estimation method of permeability functions are Lui *et al.* (1998). They also found the match in results to be good between the two methods, but felt that the results could be improved and calculations eliminated by replacing the porous plate with a nylon membrane with and air entry pressure large enough for the intended applied pressures (Lui *et al.*, 1998). Fujimaki and Inoue (2003) also suggested that there was an implied hydraulic resistance at the soil – porous plate interface that was distorting their estimates of soil parameters.

Similar experiments were conducted by Finsterle and Faybishenko (1999) on a loam soil and by Hwang and Powers (2003) on a sandy soil. Both concluded that the multi-step outflow method was suitable for estimating soil hydraulic properties. The use of nylon membranes was applied by Hwang and Powers (2003) who investigated the appropriateness of different soil hydraulic functions and different flow rates on the uniqueness of parameter estimates and their proximity to directly measured equilibrium data points. They found that the comparison

between measured and optimised results were good and improved by selecting pressure steps that resulted in a low flow rate. They also found that the lognormal distribution-Mualem had the lowest root of mean squared residuals (RMS, Equation 14) of the six functions considered, but failed to converge in several cases. The van Genuchten-Mualem function had generally higher RMS values, but always converged.

$$RMS = \sqrt{\frac{O(b)}{M + N + L}} \tag{14}$$

Where: *O(b) = the objective function and*

M = number of observations of outflow

N = number of observations of capillary pressure head

L = number of observations of volumetric moisture content

The multi-step outflow method was used by Mohanty on various occasions (Mohanty, 1999 and Mohanty *et al.*, 2002, for example). Mohanty *et al.*, 2002 used the numerical code HYDRUS-1D, a windows based finite element modelling environment for the analysis of one dimensional water flow written by Šimůnek, Šejna and van Genuchten in association with the Department of Environmental Sciences, University of California (Šimůnek *et al.*, 2005), to model soil hydraulic functions (using the multi-step outflow method) for comparison with measured soil water retention data. Their results indicated that the measured data and that estimated by HYDRUS-1D corresponded well, but that the modelled data diverged from the measured data at pressures greater than approximately 10 m (~ 100 kPa) of water when

equilibrium data were not included in the model's input data. At lower pressure, however, the measured and the modelled data were indistinguishable at the scale presented.

2.5.1 Summary

Although the work of these authors has only been described here in the briefest of detail, their findings and conclusions are all very similar. The consensus seems to be that soil hydraulic functions can be accurately estimated from transient flow data. Uniqueness of parameter estimates can be improved by including either tensiometer data or equilibrium data points, or by performing multi-step, rather than single-step, experiments (Eching and Hopmans, 1993). The parameters most appropriate for optimisation were found to be α, n, K_s and l (van Dam *et al.*, 1994; Vereecken *et al.*, 1997). All the authors appear to have selected pressure heads not exceeding 10 m (~ 100 kPa) of water. Outflow from the samples was measured at least until flow had significantly diminished, although rarely to equilibrium. Some authors also found that the use of a ceramic plate impeded drainage at high moisture contents/flow rates and that the plate may become blocked, suggesting that the use of a porous membrane may be more appropriate. The method was found to be applicable to shrink swell clay soils (Crescimannoa and Iovino, 1995). All the authors used the van Genuchten-Mualem model (Equation 12) and this model was found to be appropriate when tested by Hwang and Powers (2003). HYDRUS was considered an appropriate computer program to run the model by Mohanty *et al.* (2002), who achieved good results. Based on the findings of these authors, the multi-step outflow

method was deemed the most appropriate method for the estimation of soil hydraulic parameters and analysis of the changes to said during wet/dry cycles.

3 Materials and Methods

3.1 Overview

As stated in Chapter 1, the aim of this study was to assess the propensity of a range of soils to recover structure after a compaction event and the objective was to quantify the changes to the structure of a range of compacted soils with wet/dry cycles by measuring changes to their bulk density, moisture content at field capacity, saturated hydraulic conductivity, surface crack emergence and the parameters of the van Genuchten-Mualem Equation (Equation 12) which describes their characteristic moisture release and hydraulic conductivity curves. Steps were also made towards developing a predictive equation describing the changes in the simplest of these parameters (bulk density) with wet/dry cycles.

Changes to the above parameters could have been measured in field, or laboratory, studies. Field studies have the advantage that they are more easily transcribed into real life situations than laboratory studies, but they also have some distinct disadvantages. The time scales involved in conducting thorough field studied are prohibitively long; Alakukku (1996a), for example, studied changes in the field for nine years. In-field heterogeneity and the inability to repeat measurements on exactly the same sample of soil means that small changes will be undetectable against background 'noise' and, therefore, many years must elapse before changes to the soil structure can be reliably detected. The second major disadvantage with field studies is the inability to control climatic conditions and, therefore, the number of

wet/dry cycles experienced by the soils. It is also the case that it would be difficult to separate the effects of climate on structure from the effects of other recovery mechanisms, such as the creation of bio-pores.

Conversely, laboratory conditions can be tightly controlled. This means that the number of wet/dry cycles experienced by a soil can be greatly accelerated beyond that which would be experienced in the field. This means that the time period required to affect structural change can be significantly truncated. The method and rate of wetting can also be kept constant. In addition to this, the same samples can have parameters tested and retested, rather than a selection of random samples being taken in the field, allowing for much smaller changes in these parameters to be detected. For these reasons, it was decided to focus on laboratory studies.

Ten soils with contrasting properties were selected for investigation; five from the bottom of the plough layer and five from the subsoil. These soils were taken from various locations on College Farm, Silsoe and varied in soil series, texture and organic matter content. The rational for soil selection sampling procedure is described in detail in Section 3.2.

The evidence presented in the literature review suggests that the most devastating consequence of soil compaction, at least for agriculture, is the impedance of the flow of gasses and water through the soil profile. This is caused, primarily, by the collapse of macro-pores and an overall reduction in porosity/increase in bulk density, which results in reduced crop yields and the pollution of surface waters (Jones *et al.*, 2003). The selected

measurements would, therefore, have to be related to these factors. The physical and chemical characteristics of the soils also had to be measured so that they could be related to the degree and direction of any observed structural changes.

The physical and chemical characteristics of the soils measured were: particle-size distribution; the organic matter contents (both labile and occluded); the plastic and liquid limits; the shrinkage limits; and the cation exchange capacity. The methods used for these measurements are described in Section 3.4. Changes in the bulk density of the soils with wet/dry cycles were measured, as were changes to their macro-porosity, and experimentation is described in detail Section 3.5. A more detailed study of a smaller selection of the subsoils, taken from College Farm, Silsoe, was also conducted. The saturated hydraulic conductivity of theses samples was measured at various points during the wet/dry cycles (Section 3.6) and the moisture release and hydraulic conductivity curves estimated from transient outflow experiments (Section 3.7). In addition to this, photographs were taken of the surface of these samples during the wet/dry cycles and analysed for crack development (Section 3.8).

There are various methods by which compaction can be quantified. The most obvious of these is to measure bulk density. However, bulk density measurements do not directly measure the most problematic aspect of soil compaction because impeded drainage and gas exchange are not directly equable with bulk density. Despite this, bulk density is a useful measure as it is easily interpreted and can be related to soil porosity and water holding capacity. It is also strongly related to penetration resistance and, therefore, changes to the bulk density of samples with wet/dry cycles were measured. An indication of the macro-

porosity can be gained in the laboratory by measuring the drainable porosity that is the difference in moisture content between saturation and field capacity (usually measured at 5 kPa) of a soil sample; a change in the mass of a sample at field capacity can be equated with a change in the volume of macro-pores that have drained at this tension. This can be indicative of changes in the water available for crop growth and the proportion of air filled pores at field capacity, although shrinkage of a shrink/swell soil will complicate this.

A more complete picture of the changes in the hydrological properties of a compacted soil may be gained from measuring the moisture release characteristic curve of a soil. This can be done by pressure membrane apparatus and measuring the moisture content of the sample at equilibrium at a range of points along the curve (suction from 200 – 1500 kPa). However, this is a time consuming process that may take many days or even weeks, dependent on soil texture and structure. A faster method of simultaneously estimating the parameters of the moisture release curve and the unsaturated hydraulic conductivity curve is to apply the multi-step outflow method. Richards' Equation (Equation 5) is solved numerically in order to simulate transient outflow data obtained from pressure cell measurements obtained under controlled initial and boundary conditions using specific hydraulic functions, the parameters of which are optimised by minimising an objective function.

Various authors have suggested that when estimating the parameters of the van Genuchten-Mualem Equation (Equation 12) via the multi-step outflow method, the saturated hydraulic conductivity should be considered a fitting parameter (for example Eching and Hopmans, 1993), or that estimates of saturated hydraulic conductivity may be less accurate than other

parameter estimates (for example, Jaynes and Tyler, 1980). The saturated hydraulic conductivity of a soil is a good indicator of changes to a soil's macro-pore structure. This was, therefore, measured separately (Section 3.6). It was also used as an initial estimate in the parameter optimisation.

The shrink swell reactions of soils due to wet/dry cycles (associated with their structural regeneration) result in the appearance of surface cracks. It has been suggested that patterns of cracking may be related to structural changes at depth when there is a lack of water stable aggregates (Velde, 2001) and that modelling of surface cracking could be extended to simulate preferential flow along macro-pores (Vogel *et al.,* 2005). The emergence of cracks on the surface of the soil samples was, therefore, monitored throughout the imposed wet/dry cycles, so that they might be compared to other structural changes. Photographs were taken at key points in the cycles and analysed for the area of cracks. The area of cracks at various stages in the wet/dry cycles was then compared to other measured soil parameters (Section 3.8).

3.2 Soil selection and sampling

The soils selected for experimentation were located on the farm at Cranfield University's Silsoe site (Figure 6).

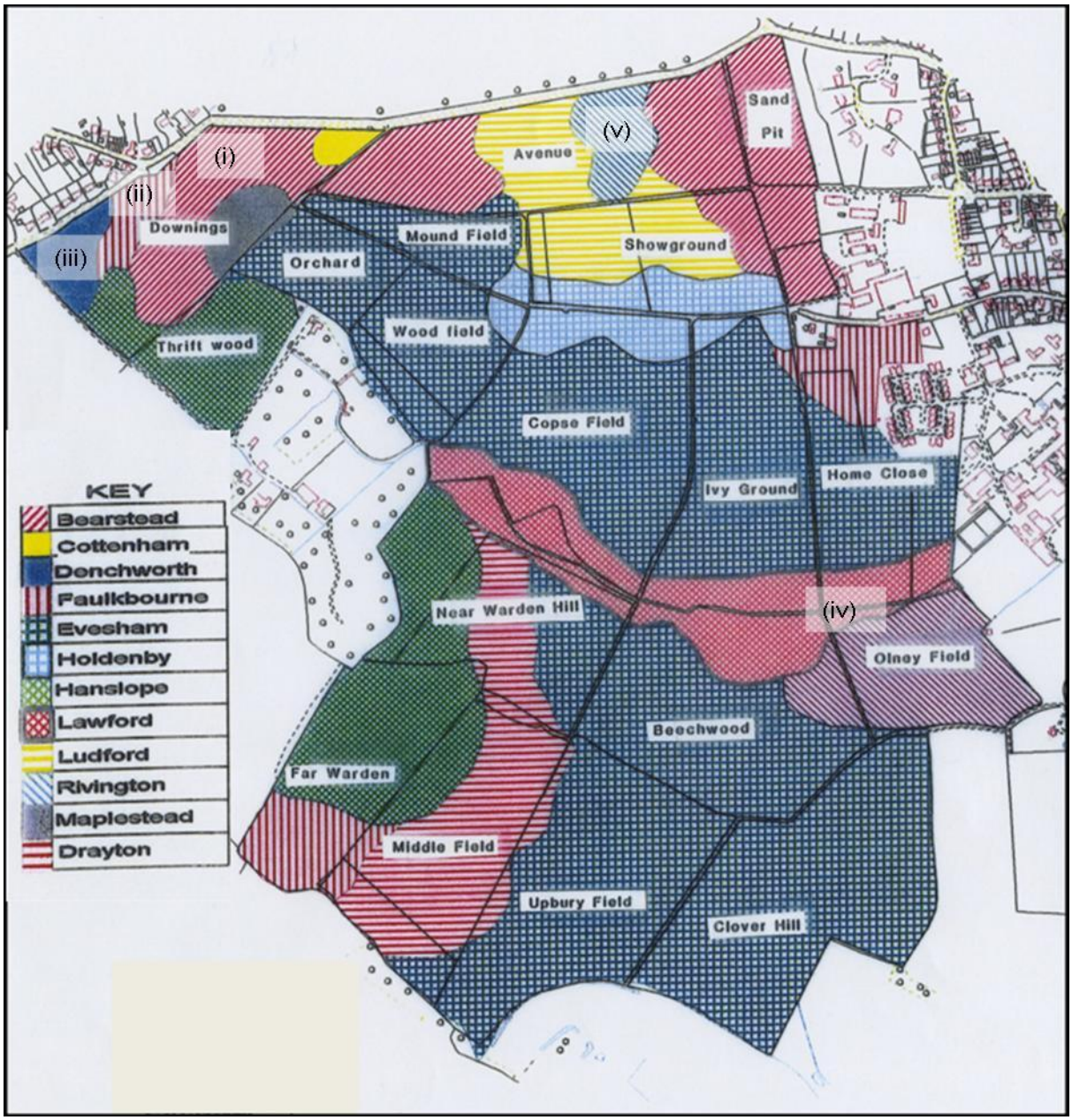

Figure 6. Map of the farm from which the soil samples were taken. [2]

[2] Soil series sampled were; (i) Bearstead (sandy loam), (ii) Faulkbourne (clay), (iii) Denchworth (clay), (iv) Lawford (clay) and (v) Rivington (sandy loam), (Bradley, unpublished).

A sandy loam, a clay loam low in organic matter and a clay loam high in organic matter (according to Wolharn, 2001) were located in the same field (shown as i, ii, iii in Figure 6). These soils were selected with the assistance of information on bore holes, taken from Wolharn, (2001) which gave details of the particle-size distribution, colour and ped form. The clay loams were chosen as they had similar particle-size distribution, but differed in the organic matter content, providing opportunity for the contribution of organic matter content to structural change to be analysed. A lighter sand (v) and a heavier clay (iv) were taken from elsewhere on the farm (Figure 6). These soils were selected, based on the maps of the farm and visual inspection, to provide a broader spectrum of textures.

Five undisturbed soil samples were taken from each of the locations described above (plough layer and subsoil) totalling 50 samples. This was done with a coring device at depths of approximately 300 and 500 mm, depending on where the density and the appearance of the soil were perceived to have changed when a profile pit, at least 500 mm deep, was dug and inspected (Figure 7). This was done at every sampling site. Samples from the plough layer of location (i) will denoted with PP/1 and the corresponding subsoil samples denoted with SS/1. This pattern is followed for all samples.

After the exact sampling depth had been selected, a trench was dug, the bottom of which was level with the sampling depth, from which the samples were taken (Figure 8). The coring device consisted of a sample ring holder mounted below a sliding hammer. The undisturbed cores were contained in metal cylindrical sleeves, 75 mm in diameter and 50 mm deep, with removable caps at both ends. The volume of the undisturbed cores was fixed at 222 cm^3. The

sleeve, with both caps removed, was inserted into the holder and capped with a cutting edge. This was then positioned on the soil surface at the bottom of the trench and hammered in. The coring device was then be removed and the sleeve containing the sample and cutting ring carefully removed. After the samples had been taken from the first depth, the bottom of the trench was cleared and levelled to the second sampling depth (based again on profile inspection) and the subsoil samples were taken in a similar manner.

Figure 7. Example of one of the profile pits dug in order to establish appropriate depths from which to take samples.

Figure 8. Soil sampling with the coring device.

It could be argued that it would have been more informative to have taken larger cores, spanning the soil from the surface to below the plough pan and encompassing whole, large soil aggregates. This would have been a closer approximation to the field situation as the subsoil portion of the sample would have subject to overburden pressure. Edge effects would also have been reduced. However, the time involved in saturating and draining core samples larger than 220 cm^3 under laboratory conditions would have been prohibitive. Therefore, a series of small cores, that could be wetted and dried at an accelerated rate, were taken from

the plough pan and the subsoil. Large (approximately 1 m^3), disturbed samples were also taken from these locations and depths, both for physical and chemical analysis and for the creation of additional samples.

3.3 Construction of subsoil samples with a range of bulk densities

As well as the experiments performed on the undisturbed soil samples taken from the field, more detailed experiments were conducted on constructed samples of the clay subsoils to: estimate changes in the moisture release curves and the unsaturated hydraulic conductivity curves; measure changes in saturated hydraulic conductivity; monitor changes in bulk density and surface cracking with wet/dry cycles. These experiments were designed not just to look at the differences in behaviour between the soils, but also how the initial bulk density of the soils effected changes with wet/dry cycles. Because a range of initial bulk densities was required, it was necessary to construct the samples under controlled conditions in the laboratory.

Large, bulk samples of subsoils 2, 3 and 4 were taken from College farm, Silsoe (Figure 6). These soils were of the Faulkbourne (ii), Denchworth (iii) and Lawford (iv) series. The soils were broken up, air dried and ground to pass through a 2 mm sieve and were then wetted to their approximate plastic limits. This was achieved by sprinkling a thin layer of soil into a bucket and then wetting it with a fine spray, followed by another thin layer of soil, which was

wetted in the same way, until all the soil had been wetted. It was then covered and left for 48 hours, at which point the soil was carefully stirred and a small sample taken and oven dried to check the moisture content. If the soil was found to have a moisture content less than its plastic limit, extra water was added. If it was found to have a moisture content greater than its plastic limit, it was spread out briefly to dry. The moisture content of the soils was then checked again.

After final checks of the moisture content had been made, the soils were weighed and poured into moulds containing three samples sleeves (75 mm diameter by 50 mm deep). The amount of soil poured into the moulds was calculated so that the target bulk density would be achieved when the soil was compressed to a known distance above the rim of the sample sleeves. The target bulk densities for the soils were 1.0, 1.3 and 1.6 g cm^{-3}. These bulk densities were selected as they span the range from loose to dense, allowing the contribution of initial bulk density to the extent of any changes in the structure of the soils to be assessed. It was also intended that this range of bulk densities might reveal the equilibrium bulk density to which the soils would naturally tend, as well as illustrating the structural changes to a soil which, although not necessarily compact, maybe devoid of structure.

A plate was placed on the surface of the soil. Force was applied to the plate at a steady rate of approximately 2 kN min^{-1} until the desired level of compaction had been achieved. Pressure was then removed and the sample sleeve carefully removed from the mould and surrounding soil and weighed. The samples were then ready to be saturated for saturated hydraulic conductivity measurements (Section 3.6), the transient flow experiments (Section 3.7) and

surface cracking to be monitored (Section 3.8). Changes in the bulk density of the samples with wet/dry cycles were monitored during the transient flow experiments.

3.4 Soil physical and chemical characteristics

As already stated, the soils were tested for particle-size distribution (pipette method), plastic and liquid limits, shrinkage limits, cation exchange capacity (CEC) and total and oxidisable organic matter. These parameters were selected for testing as they were considered to be the factors most likely to influence restructuring. Particle-size distribution is the most obvious test because texture is how soils are commonly identified. It is also the case that shrink/swell reactions are associated with clay content and mineralogy (Sridharan and Gurtug, 2003). Clay mineralogy is difficult and expensive to measure and special distribution is know at a very coarse scale, but the activity of a soil (plasticity index of a soil divided by the clay fraction) can be an indication of the predominant clay mineralogy (Lambe and Whitman, 1969). Plastic and liquid limits are also important because they relate to how the soil structure and stability are affected by moisture content i.e., at what moisture content the inter-particulate bonds sufficiently weakened to easily rearranged in plastic, rather than a brittle, manner (Lambe and Whitman, 1969). Shrinkage limits are an indication of the magnitude shrink/swell reactions, thought to be the driving force behind the restructuring of soils with wet/dry cycles (Etana and Håkansson, 1994; Sarmah *et.al.*, 1996; Pillai and McGarry, 1999 for example). CEC was thought to have the potential to influence restructuring as it is a

measure of charge and soil particles are thought to bind to one another via electrostatic forces (Brady and Weil, 1999). Total and available organic matter was considered to have the potential to influence restructuring as various studies have linked organic matter with soil resilience (for example, Alakukku, 1996) and plasticity index (Reeves and Earl, 1989). Organic matter is also associated with increased water holding capacity, without compromising aeration, which implies a more porous soil (Brady and Weil, 1999).

3.4.1 Particle-size distribution

The particle size distribution of the soils was measured by the pipette method (BS 1377:Part 2:1990). In brief, this method involves drying the soil and breaking down the aggregates in a pestle and mortar. The ground soil is then passed through a 2 mm sieve to remove the gravel fraction. The remaining soil is then mixed with a solution of H_2O_2 and the reaction observed for approximately 30 minutes. This is repeated twice, or until no further reaction occurs, and left to stand overnight. The solution is then heated at 90 ^{o}C for one hour. After the solution has cooled, it is shaken for 15 minutes at 2000 rpm. Sodium hexametaphosphate and Na_2CO_3 is added and the mixture is shaken for at least seven hours. It is then passed through a 63 µm sieve. The solution remaining in the sieve contains the sand fraction. This is oven dried and passed through 600, 212 and then 63 µm sieves to determine the coarse, medium and fine sand fraction respectively.

.

The soil solution that passes through the sieve contains the silt and clay fractions. This is poured into a beaker and allowed to sediment in a water bath at a constant temperature of 25 ^{o}C for eight hours. The mixture is then thoroughly mixed, being careful not to introduce air. A sample is immediately taken at a depth of 100 mm. This sample contains the less than 63 µm fraction. The solution is then allowed to sediment again for six hours and 23 minutes (as determined by look up tables relating sedimentation time to temperature) and a sample taken at a depth of 90 mm. This sample contains the less than 2 µm fraction. (BS 1377:Part 2:1990).

3.4.2 Organic matter content lost on ignition

The soil was ground to pass through a 2 mm sieve and dried overnight at 50 ^{o}C and then placed in an unheated furnace. The temperature of the furnace was set to 440 ^{o}C and heated. The soil was left in the furnace until constant mass was achieved and the loss of mass was the organic matter that had been removed from the sample (BS 1377:Part 3:1990).

3.4.3 Oxidisable organic matter content

Potassium dichromate followed by sulphuric acid was added to a flask containing the soil sample and allowed to stand. Distilled water, orthophosphoric acid and indicator solution

were then added. Ferrous sulphate solution was then added in increments until the solution turned green. More potassium dichromate was then added to turn the solution to a bluish black, followed by further incremental additions of ferrous sulphate to return the solution to green. The total volume of potassium dichromate and ferrous sulphate added are used to calculate the oxidisable organic matter. (BS 1377:Part3:1990).

3.4.4 Plastic limit

The soil was air dried and sieved. The soil was then mixed with distilled water to form a plasticine type consistency. The soil was then rolled into cylinders 3 mm thick. The moisture content at which the cylinders began to beak into pieces 6 to 12 mm in length was taken as the plastic limit. (BS 1377:Part2:1990).

3.4.5 Liquid limit

The soil was air dried, sieved and mixed with distilled water until it became a coherent, homogenous mass. The moist soil was placed in a brass cup with a palette knife, taking care not to trap air pockets. The cup of soil was placed under a penetrometer with a 35 mm cone, angle 30^{o}, on a sliding shaft of 80 g. The cone was positioned on the soil surface and released for 5 seconds. The penetration depth was recorded and the moisture content of the soil was

measured. The process was repeated for at least four moisture contents. The moisture content was plotted against the penetration depth and the moisture content corresponding to a penetration of 20 mm was taken as the liquid limit of the soil. (BS 1377:Part2:1990).

3.4.6 Shrinkage limit

The soil was air dried and ground to pass through a 2 mm sieve. It was then wetted with distilled water to its liquid limit. The wet soil put into a rectangular mould and allowed to dry. The percentage decrease in the length of the sample was the shrinkage limit (BS 1377:Part2:1990).

3.4.7 Cation exchange capacity

The soil was air dried and ground to pass through a 2 mm sieve. Barium chloride was then added and the mixture was left to stand overnight. The mixture was then centrifuged and the supernatant liquid discarded. Distilled water was then added, the mixture shaken to break up the soil cake and then centrifuged and the supernatant discarded again. Magnesium sulphate was then added and the mixture shaken periodically for two hours. 5 ml of this solution was pipette into a conical flask and six drops of 2N NH_4OH was added with two drops of indicator. The mixture was then titrated with EDTA solution until it went from wine red to inky blue. 5 ml of magnesium sulphate was then added with 2N NH_4OH and indicator

solution and the mixture was titrated again. The amount of EDTA used in the titration was used to calculate the cation exchange capacity of the soil (after Bascomb, 1964; Thompson, 1993).

3.5 Changes in bulk density and macro-porosity of the undisturbed samples

The changes in the bulk density and macro-porosity following successive wet/dry cycles were quantified by measuring change to the mass (and, therefore, the moisture content) of the undisturbed field samples as they drained on sand tables. The samples described in Section 3.2 were saturated and then subjected to two successive tensions (0.5 and 1.0 m of water, ~ 5 and 10 kPa). They were then air dried at 30 ^{o}C until equilibrium was reached. They were then re-saturated, drained and dried a further two times. The tensions 0.5 and 1.0 m of water (~ 5 and 10 kPa) were chosen as representative of field capacity so that changes in the drainable porosity (the difference in drained porosity between saturation and field capacity) could be estimated and macro-porosity defined in this case as the pore class comprising all the pores that were drained at a tension of 1.0 m. A temperature of 30 ^{o}C was chosen to dry the samples because it would provide the most accelerated drying rate, allowing the most efficient use of the experimental time available, without exceeding summer air temperatures. Air drying the samples also allowed the maximum shrinkage of the soils to occur.

The 50 samples were saturated by placing them in a bath of deionised water, where the water level was just below the top of the samples and covered to reduce evaporation. Deionised water was used as the local tap water contains calcium, which is a known flocculent and which is not present in rainwater. After an equilibrium mass had been reached, the samples were placed on sand tables. The samples were distributed amongst the sand tables such that any one sand table housed at least one of the five replicates from each location being investigated. This allowed any potential differences in equilibrium mass of the samples due to their position to be analysed statistically. The sand tables were set to a tension of 0.5 m and the samples allowed to equilibrate, weighing regularly. Having reached equilibrium, the tension was increased to 1.0 m. After equilibrium at 1.0 m had been reached, the samples were moved to an incubator and allowed to dry at 30 ^{o}C until equilibrium had been reached, as indicated by the mass being constant for a period of 24 hours. Reaching equilibrium could take in excess of two weeks. The majority of the moisture was lost, however, in the first five days, the mass of water lost after this being an order of magnitude smaller.

The wet/dry cycle described above was repeated a further two times on all the soil samples. The samples were then saturated once more, the soil that had swelled above the top of the soil ring carefully removed and both sections oven dried in order to calculate their exact bulk density at time of sampling and the decrease in bulk density between the first (where little or no swelling occurred) and the fourth saturation. During the experiment, changes to the bulk density were calculated, based on the saturated moisture content. It was assumed that an increase in water content was concomitant with an equal increase in porosity, taking the density of water to be 1 g cm^{-3}. The calculations are as follows:

Known quantities:

$$BD_1,\ MC_{v/v_1},\ MC_{v/v_s}$$

Where: BD_1 = *initial bulk density*

MC_{v/v_1} = *initial saturated volumetric moisture content*

MC_{m/m_s} = *saturated gravimetric moisture content at the third saturation.*

Known relationships:

$$BD = m_s/v_T \quad (15)$$

$$MC_{m/m} = m_s/m_w \quad (16)$$

$$MC_{v/v} = v_w/v_T \quad (17)$$

$$m_w = v_w \quad (18)$$

$$m_{w_c} = m_{w_s} - m_{w_1} \quad (19)$$

Where: m_s = *the mass of soil*

v_T = *total volume*

m_w = *mass of water*

v_w = *volume of water*

m_{w_c} = *change in the mass of water.*

Required quantity:

$$BD_3$$

Route:

If an initial total volume is assumed, then:

$$v_{s_1} = v_{T_1} - v_{w_1} = v_{T_1} - \left(v_{T_1} \times MC_{v/v_1}\right) \tag{20}$$

and

$$m_s = BD_1 \times v_{T_1} \tag{21}$$

All the initial values are then known and can be used to calculate BD_3 *as follows:*

$$MC_{v/v_3} = \frac{v_{w_3}}{v_{T_3}} = \frac{\left(m_{w_1} + m_{w_c}\right)}{v_{s_1} + m_{w_1} + m_{w_c}} \tag{22.1}$$

$$MC_{v/v_s}\left(v_{s_1} + m_{w_1} + m_{w_c}\right) - m_{w_1} - m_{w_c} = 0 \quad (22.2)$$

$$\left(MC_{v/v_s} \times v_{s_1}\right) + \left[m_{w_1} \times \left(MC_{v/v_s} - 1\right)\right] + \left[m_{w_c} \times \left(MC_{v/v_s} - 1\right)\right] = 0 \quad (22.3)$$

$$m_{w_c} = \frac{\left[-\left(MC_{v/v_s} \times v_{s_1}\right) - \left(m_{w_1} \times \left[MC_{v/v_s} - 1\right]\right)\right]}{MC_{v/v_s} - 1} \quad (22.4)$$

$$BD_3 = \frac{m_s}{v_{T_1} + m_{w_c}} \quad (22.5)$$

Where: MC_{v/v_s} *= volumetric moisture content at third saturation (%)*

v_{w_s} *= volume of water at third saturation*

v_{T_s} *= total volume at third saturation*

m_{w_1} *= mass of water at first saturation*

m_{w_c} *= change in mass of water between saturations 1 and 3*

v_{s_1} = *volume soil at first saturation*

v_{T_1} = *total volume at first saturation*

BD_3 = *bulk density at third saturation*

The results were then analysed for significant statistical differences between equilibrium points between cycles and between soils. This was done by applying a general linear model for repeated measures to the data set with Statistica 8.0. Changes in the bulk density of the samples were also compared to the measured physical and chemical parameters of the soil and a linear equation was produced by the analysis that predicted those changes. The results of these analyses are reported in the Chapter 4, Section 4.2.

3.6 Saturated hydraulic conductivity – falling head method

As has already been stated, a series of more detailed experiments than those described above were conducted on samples of the clay subsoils. One of these experiments investigated changes to the saturated hydraulic conductivity with wet/dry cycles of the samples constructed to have a range of initial bulk densities. The samples were saturated by connecting a tube to the outlet of the (Temp) pressure cells in which the samples were contained that went into a reservoir of deionised, de-oxygenated water, the surface of which

was level with the surface of the soil surface. The tops of the pressure cells were removed. This allowed for rapid, bottom up saturation of the soil samples, minimising the trapping of air within the samples. The samples were left in this configuration for a minimum of 48 hours. Deionised water was used to saturate the samples, rather than tap water, as the local tap water was high in calcium content and this was felt to be too dissimilar to rain/surface waters. The samples were then sealed inside Temp cells. Any gaps between the sample rings and the sides of the cells were plugged with a stiff silicone gel, to prevent preferential flow around the sides of the samples. A head of water was then applied to the samples via glass tubes of known diameter and the drop in water level measured with time. The saturated hydraulic conductivity was then calculated as:

$$K_s = \left[\frac{al}{A(t_2 - t_1)}\right] ln\left(\frac{h_1}{h_2}\right) \quad (23)$$

Where: K_s *= the saturated hydraulic conductivity*

a = the cross sectional area of the inlet tube

l = the length of the soil sample

A = the cross sectional area of the soil sample

t = time

h = height above the water table.

Differences in saturated hydraulic conductivity were analysed for statistical differences by calculating the 95 % confidence intervals for the mean result from each soil/bulk density

group. Correlations between the saturated hydraulic conductivity and crack emergence were also investigated with a general linear model for repeated measures. The results of these investigations are reported and discussed in Chapter 4, Section 4.8.

3.7 Multi-step outflow method – estimating changes in the van Genuchten-Mualem parameters

The multi-step outflow method is a method by which the parameters of the van Genuchten-Mualem Equation (Equation 12) are estimated from transient outflow experiments. A full explanation of the theory behind the method and how it developed is given in the last section of Chapter 2. The following section described the specific method used in this thesis.

3.7.1 Measurement of outflow

The multi-step outflow method was selected to estimate the parameters of the van Genuchten-Mualem Equation (Equation 12), and any changes to those parameters with wet/dry cycles, of samples with a range of initial bulk densities constructed from the clayey subsoils as described in Section 3.3. In brief, the soils were air dried and ground to pass through a 2 mm sieve. The samples (750 mm diameter by 50 mm deep) were formed at a gravimetric moisture content of approximately 25 % (close to the plastic limit of the soils)

and had bulk densities, ranging from approximately 1.0 to 1.6 g cm^{-3}. Three replicates of three soils at three bulk densities gave nine samples of each soil, 27 samples in total.

The samples were placed in (Temp) pressure cells. These cells had a push fitting for the inlet air tube at the top and were sealed on the bottom with a nitrocellulose semi-permeable membrane (0.45 µm pore diameter, flow rate of 40 ml min^{-1} cm^{-2} at 90 kPa, Fisher Scientific product number BDR-100-660J). This membrane was chosen as it retained its semi-permeable characteristics at pressures in excess of 20 m of water, but had a flow rate under the experimental boundary conditions that was always in excess of the saturated hydraulic conductivity of the soils. It was important that the flow rate through the membranes be high so as not to interfere with the outflow from the soil samples, since it was the *rate* of flow that was of importance to the model, rather than the total outflow that would have been measured during the conventional construction of a moisture release curve.

After the samples were saturated, the saturated hydraulic conductivity was measured, as described in Section 3.6. The pressure cells were then connected up to the pressurised air system. Pressurised air entered the system from a compressor and was divided into three separate lines, each line accommodating one replicate of each soil-bulk density combination, in a random order. Each line also had its own pressure regulator, flow regulator, bubble tube and pressure sensor (Figure 9). Dividing the samples into three separate groups allowed for two things. Firstly, if there was a problem in one of the lines (such as a faulty pressure sensor or a pressure surge), two replicates of each soil-bulk density combinations would remain in tact. Secondly, where outflow was rapid at the beginning of a cycle, it allowed for a smaller

sub-set of samples to be drained (i.e. one line), rather than all the samples having to be drained simultaneously. This allowed for greater accuracy of measurement during periods of rapid flow.

Figure 9. Experimental equipment used in the multi-step outflow method.

The bubbling tubes were required for the accurate measurement and regulation of low pressures, as the pressure regulators were only accurate at pressures above 1.0 m of water (~ 10 kPa) as were the pressure sensors (see attached data sheet, Appendix 3 and 4). A branch of the air line went from the pressure regulator to a flow regulator into a tube filled with water. By positioning the tube at depth below the surface of the water equal to the required pressure

and restricting the flow of air to the minimum that allowed bubbles to escape from the air tube, an accurate control of the pressure in the system could be achieved (Figure 10).

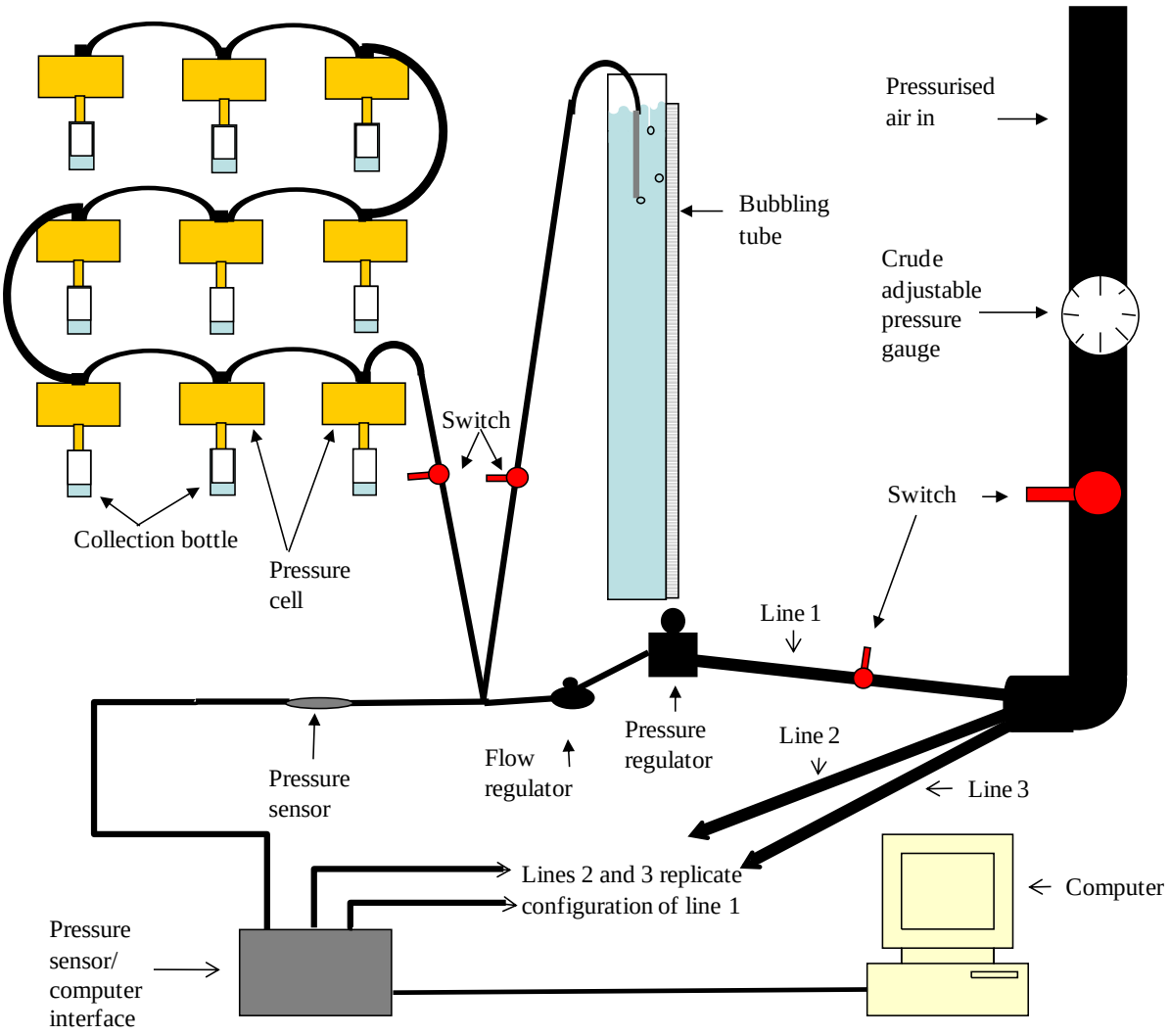

Figure 10. Layout of the equipment used in to measure the cumulative outflow of water, at given pressure heads, with time.

An alternative to this could have been to use a sand table for each sample for the low pressure readings and measure the outflow from the table. However, the sand table may have affected

the rate of outflow from the sample and it would have required that the samples be moved into the pressure cells half way through the experiment, which may have introduced errors. The case that the two different methods of applying force to the samples (applying air pressure from above and suction due to the surface tension of the water below) could also have resulted in some discontinuity between the two data sets, based on the work of Eching and Hopmans (1993), who compared transient flow experiments where outflow was induced by pressure and by suction. Although both methods of inducing outflow produced parameter estimates close to those estimated from measured retention data, there were subtle differences. It was therefore felt preferable to retain the same method of applying pressure to the samples throughout the experiment and hence the bubbling tubes were selected to regulate the pressure.

Pressure sensors were used throughout the duration of the experiment to monitor the pressures being applied to the samples. This was achieved via a routine written using DASYLab. DASYLab is data acquisition software produced by Adept Scientific (http://www.adeptscience.co.uk/products/dataacqu/dasylab/). Appropriate input or output, display and operator modules are selected and connected with virtual 'wires'. Data can be processed from multiple channels and the output logged and/or displayed in graphical and/or list form. DASYLab was used to convert and log changes in voltage registered by the sensors to a pressure in meters of water. To achieve this, the sensors first needed to be calibrated. A sensor of known accuracy was connected to the system. The pressure was set to a known level and the changes in voltage produced by the sensors were recorded over a period of time.

The results of this were then averaged and the necessary calculations made to convert the reading into a pressure.

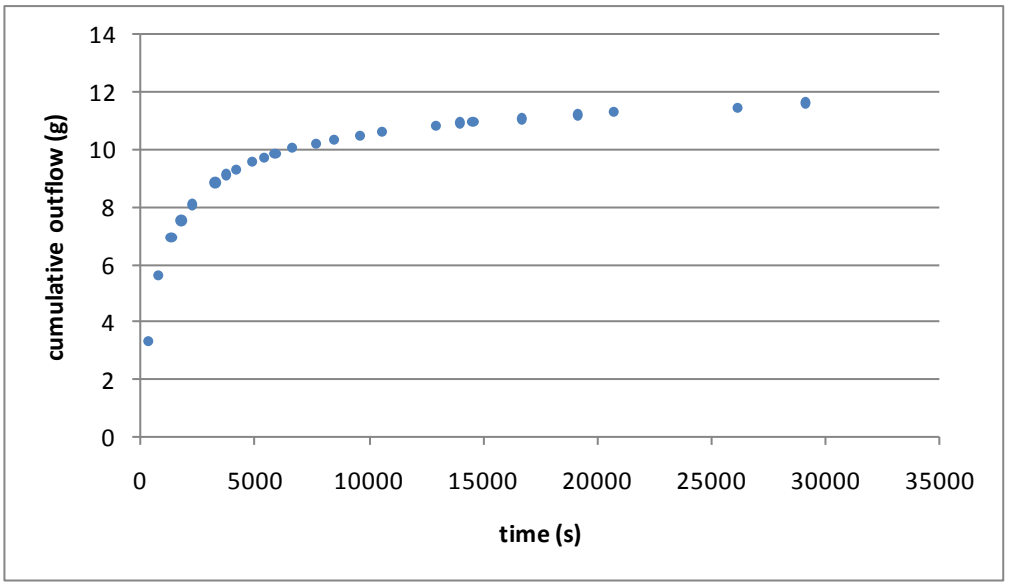

Figure 11. Example of the graphs that were produced to monitor drainage as it was occurring.

Each Temp cell drained into a collection bottle connected to the outlet tube. During the experiment, drainage was measured and logged manually. This was done by removing one bottle at a time and weighing it on an electronic balance with an accuracy of +/- 0.01 g. Whilst a bottle was being weighed, it was temporarily replaced by another bottle so that no water was lost. This bottle was weighed immediately after the cell's bottle had been returned to the outlet. Any drainage occurring in this time was added to the total drainage next time it was measured. As the air line to the Temp cells was opened, a stopwatch was started and the time on the computer clock noted. Every time a bottle was removed for weighing, the time was noted to the second and logged on a spread sheet. The spread sheet was constructed such that the data were automatically plotted on a graph as they were inputted (Figure 11).

Measurement of the cumulative drainage continued until the rate of drainage had obviously decreased from that at the start of the pressure step. The pressure was left on overnight and drainage allowed to continue until the next morning, when the final drainage measurement was taken, the stop watch reset and the next pressure step was begun.

The first stage was to equilibrate the samples at 0.1 m (~ 1 kPa). Of the literature cited in Chapter 2, a significant number of researchers commenced their experiments with soil cores equilibrated at a pressure greater than zero. Of those authors who quoted initial pressures, these pressures were: 0.035 m (~0.35 kPa) (Vrugt *et al.,* 2001); 0.04 m (~ 0.4 kPa) (Jaynes and Tyler, 1980); 0.1 m (~ 1 kPa) (Crescimanno and Iovino, 1995); 0.2 m (~ 2 kPa) (Finsterle and Faybishenko, 1999); 0.3 m (~ 3 kPa) (Eching and Hopmans, 1993). The justification for this, as cited by Eching and Hopmans (1993), van Dam *et al.* (1994), Crescimanno and Iovino (1995) and Lui *et al.* (1998), is that given by Hopmans *et al.* (1992). They showed, through analysis of x-ray tomography showing soil water distribution during the drainage process, that fluid flow could only be properly described if both wetting and non-wetting fluid were continuous throughout the outflow experiment and suggested that the results of transient flow experiments were improved by the initial state of the samples being less than saturation. They thought that this is what is assumed by Richards' Equation (Equation 5) and that continuous fluid flow was prevented by the presence of the ceramic plate at the pressurised end of the saturated sample. Other researchers reported in Chapter 2 began their drainage from the saturated state and zero applied pressure. It is also the case that the experiment described in this thesis used a nitrocellulose semi-permeable membrane, rather than a ceramic plate, and the air entry pressure of the soil was not known before hand (and so

could not be exceeded by the initial soil water pressure). An initial equilibrium pressure of 0.1 m (~1 kPa) was selected for this experiment to remove excess water from around the samples, because it was the initial equilibrium pressure selected by Crescimanno and Iovino (1995) who were also investigation shrink swell clays and because selecting a low initial equilibrium pressure allowed the maximum potential for drainage and, therefore, data acquisition.

The pressure was set using the bubble tubes as they had great accuracy at low pressures. Air flowed into the system from a compressor at approximately 150 m of water (~ 1500 kPa). At this point the system divided into three branches, one branch going to each set of soil sample replicates (Figure 10). The air then flowed through the pressure regulators which reduced it to approximately 1 m (~ 10 kPa) and then through the flow regulators to reduce the air flow, minimising disturbance to the surface of the water in the bubbling tubes and, hence, fluctuation in pressure. Each line branched again at this point, one branch going into a water filled tube, one to the line of pressure cells, another to a pressure sensor. The branch going into the water filled tube was positioned such that the end of the tube was 0.1 m below the surface of the water. After the pressure had been set, the switch was opened, allowing the air pressure to reach the top of the samples. The drained water was collected in bottles attached to the outlet on the pressure cells. When the mass of the water in the bottles ceased to increase over a period of 24 hours, the samples were considered to be equilibrated.

When the samples had ceased draining, the line to the pressure cells was closed while the pressure was reset to 0.5 m (~ 5 kPa) using the bubble tubes. The line to the pressure cells

was then opened and measurement of drainage commenced. This process was repeated at 1.0 m pressure with the bubble tubes and then at 3.0 m, 5.0 m, 10 m and 15 m (~ 10, 30, 50, 100 and 150 kPa) with the pressure regulators alone. At the end of the cycle, the tops of the Temp cells were removed and the samples were allowed to air dry for five days. At the end of this period, the samples were re-saturated and the cycle was begun again (Figure 12). The membranes were replaced between each cycle to minimise any blocking of the pores that might have occurred during drainage.

During the experiment, changes to the bulk density of the samples at saturation were monitored by measuring changes to the height of the samples. Although it would have been preferable to measure changes to the saturated mass of the samples directly and calculate changes in saturated moisture content from which changes in bulk density could have been inferred, this would have involved removing the samples from the Temp cells. Therefore, changes to the height of the samples, and hence the volume (as the sample rings prevented swelling beyond the original diameter in the horizontal direction at saturation), were recorded. At the end of the experiment, the samples were oven dried and their bulk densities at various stages calculated. The saturated hydraulic conductivity was also measured at the beginning of each cycle (see Section 3.6 for method) and the surface of the soil samples photographed (see Section 3.8 for method) at 0.1 m (close to saturation, but without surface water), at the end of the 15 m pressure step and after air drying (Figure 12).

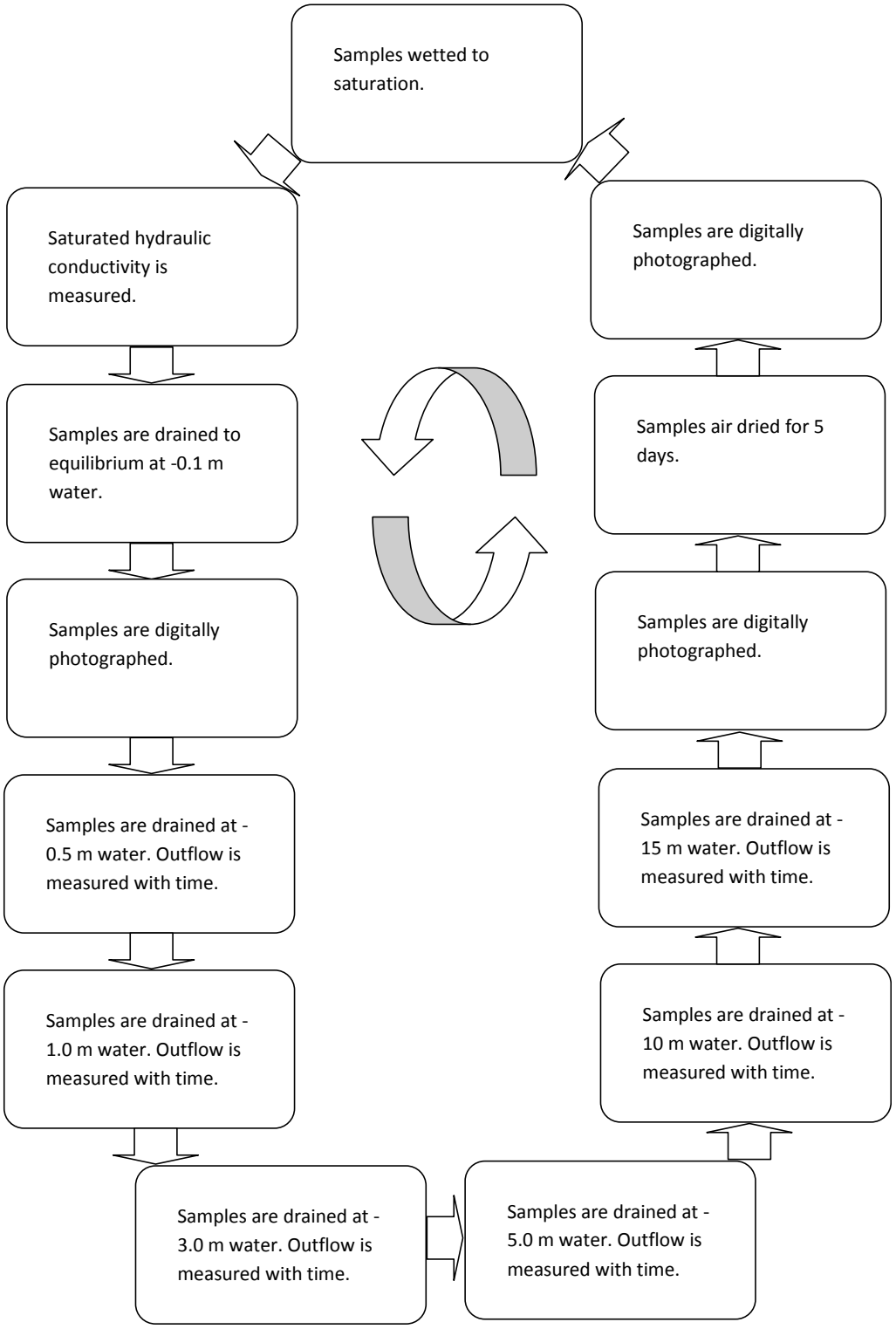

Figure 12. Flow diagram illustrating the experimental procedure of the Multi-Step Outflow experiment.

3.7.2 Modelling

The process described in the above section provided the cumulative drainage data for a number of sequential pressure steps, required to implement to the multi-step outflow method. The software used to implement the simultaneous optimisation of the parameters of the van Genuchten-Mualem Equation (Equation 12) was HYDRUS-1D. The HYDRUS-1D programme is a Windows-based finite element modelling environment for the analysis of one dimensional water flow and solute transport in variable saturated porous media, created by Šimůnek, Šejna and van Genuchten in association with the Department of Environmental Sciences, University of California (Šimůnek *et al.,* 2005).

The governing flow equation used to describe one-dimensional uniform water movement in a partially saturated rigid porous medium is a modified form of Richards' Equation (Equation 24) that assumes that under natural conditions, in the shallow subsurface the air phase pressure remains constant (because it is continuous with the atmosphere) and hence plays an insignificant role in the liquid flow process and that water flow due to thermal gradients can be neglected.

$$\frac{\delta\theta}{\delta t} = \frac{\delta}{\delta x}\left[K\left(\frac{\delta h}{\delta x} + cos\alpha\right)\right] - S \qquad (24)$$

Where: *h = the water pressure head*

θ = volumetric water content

t = time

x = the spatial coordinate (positive upward)

S = the sink term

α = the angle between the flow direction and the vertical axis

K = the unsaturated hydraulic conductivity function given by:

$$K(h,x) = K_s(x)K_r(h,x) \tag{25}$$

Where: K_r *= the relative hydraulic conductivity*

K_s *= the saturated hydraulic conductivity.*

The governing flow and transport equations are solved numerically using a Galerkin-type finite element schemes (Equation 10). One of the key features of HYDRUS-1D is that it can be used for inverse modelling. The modified form of Richard's Equation (Equation 24) is solved under given boundary and initial conditions and the parameters of, in this case, the van Genuchten-Mualem Equation are optimised by minimising an objective function (cumulative

outflow). Inverse estimation of flow from transient outflow data is achieved with a Marquardt-Levenberg type parameter optimisation algorithm (Equation 26).

$$\phi(b,q,p) = \sum_{j=1}^{m_q} v_j \sum_{i=1}^{n_{qj}} w_{i,j} \left[q_j^*(x,t_i) - q_j(x,t_i,b)\right]^2 + \sum_{j=1}^{m_p} \overline{v_j} \sum_{i=1}^{n_{pj}} \overline{w_{i,j}} \left[p_j^*(\theta_i) - p_j(\theta_i,b)\right]^2 + \sum_{j=1}^{n_b} \widehat{v_i} \left[b_j^* - b_j\right]^2 \quad (26)$$

The first term on the right hand side represents deviations between the measured and the calculated cumulative flux versus time across a boundary

Where: m_q *= the number of different sets of measurements*

n_{qj} *= the number of measurements in a particular measurement set*

$q_j^*(x,t_i)$ *represents specific measurements at time* t_i *for the jth measurements set at location x(r,z)*

$q_j(x,t_i,b)$ *= the corresponding model predictions for the vector of optimised parameters b (e.g.,* θ_r, θ_s, α, n, K_s, l*)*

v_j *and* w_{ij} *= weights associated with a particular measurement set or point, respectively.*

The second term on the right represents differences between independently measured and predicted soil hydraulic properties (e.g., retention, θ(h) and/or hydraulic conductivity, K(θ) or K(h) data).

The last term represents a penalty function for deviations between prior knowledge of the soil hydraulic parameters, b_j^*, and their final estimates b_j

Where: n_b *= the number of parameters with prior knowledge*

$\hat{v}_j$ *= pre-assigned weights*

The HYDRUS-1D model interface prompts for the required information in a series of steps (Figure 13). Firstly, it asks what problem is to be solved (water flow, heat transport, etc.). Secondly, it asks what is to be estimated (soil hydraulic parameters), whether to include internal weighting, the maximum number of iterations and the number of data points in the objective function. Next it asks for the number of soil materials, the number of layers, the angle of flow and the depth of the soil profile. After this comes time information, then tolerances for water content and pressure head, then the hydraulic model to be applied (van Genuchten-Mualem in this case, although other models are available), then which parameters are to be estimated and their initial estimates, then upper and lower boundary conditions, then the time information for the pressure steps followed by the actual data points in the objective function and finally information on the profile discretization (number and position of nodes,

Figure 14) and initial conditions (pressure head or moisture content). The output from the model includes a data sheet showing the initial and final parameter estimates with their 95 % confidence intervals, the measured and modelled cumulative outflow with an R^2 value showing goodness of fit between the two and a series of points for the retention and conductivity curves.

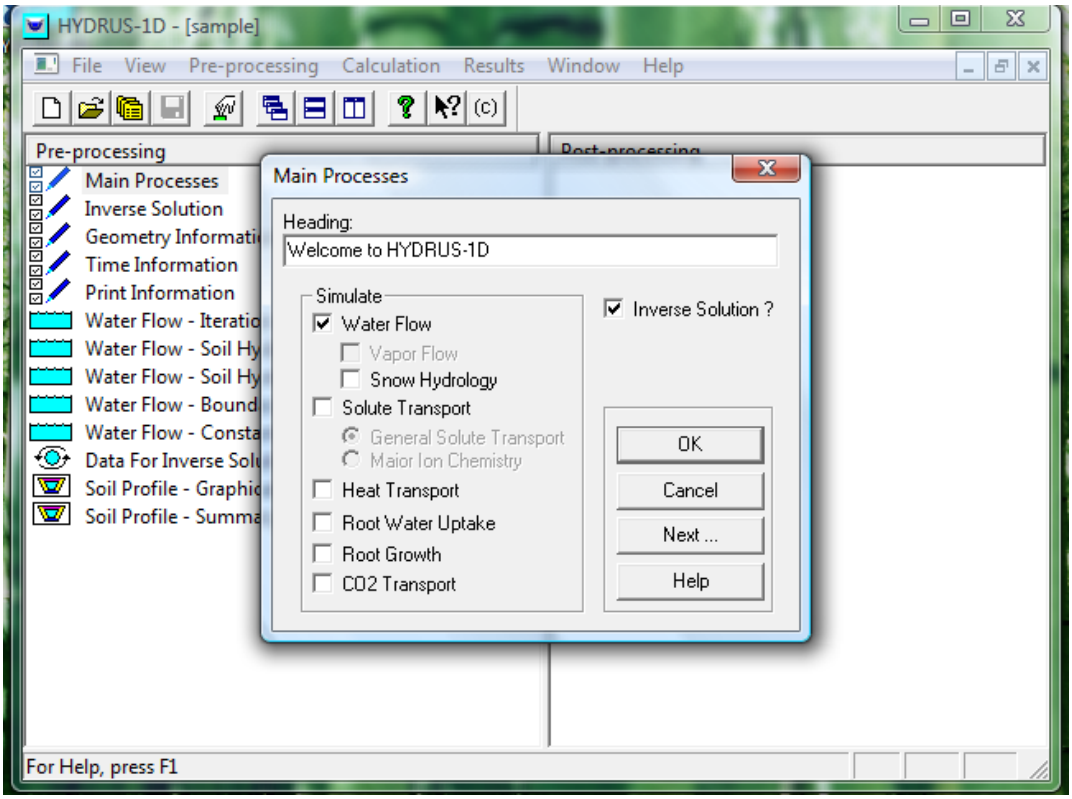

Figure 13. Screen shot showing an example of the HYDRUS-1D user interface.

Since the problem was one dimensional, there were only two boundaries; the time variable pressure boundary at the top where the air pressure was applied to the samples (but which remained constant until the next pressure step was initiated) and free drainage at the bottom

at atmospheric pressure. The initial condition in this instance was uniform soil moisture pressure at 0.1 m of water. The profile discretised into 300 elements, but with a greater density of elements at the bottom of the sample (Figure 14). The estimated parameters were α, n, K_s and l; the saturated moisture content was measured, as was the air dry moisture content, while the residual moisture content was set to zero, constraining both ends of the retention curve. The pressure at which the soil was air dried was calculated as:

$$\psi_t = -\frac{RT}{M_v} ln \left[\frac{P_v}{P_{vs}}\right] \quad (27)$$

Where: R = *the ideal gas constant*

T = *the absolute temperature*

M_v = *the molar volume of water,*

P_v = *the vapour pressure of water*

P_{vs} = *the saturated vapour pressure of water*

Although the model will provide its own initial estimates of the parameters to be optimised, predicted using neural networks and based on the bulk density of the sample and the particle size distribution, these initial estimates were found to be unsatisfactory as the results they produced were clearly the result of local minima in the optimisation process. Initial parameter estimates were therefore selected by analysing the drainage data. Microsoft Excel was used to plot the van Genuchten-Mualem retention curve though points that corresponded to the

moisture content of the samples at the end of the pressure step, estimating α and n by minimising the difference between the measured moisture content at a given pressure and that calculated with estimates of α and n. A curve was also created at this point by visual inspection to provided alternative initial estimates of α and n. The parameters calculated using Excel were then used as the initial parameters for the HYDRUS-1D model, which also optimised K_s (the initial estimate of which was taken as its measured value) and l (initial estimate taken as 0.5). The results produced by the first run of the model were then used as the initial parameters for a second run of the model. A third run of the model generally converged at the same set of parameter estimates and were attributed an R^2 value in excess of 0.99, based on the difference between the modelled and the calculated drainage outflow data. It was assumed that disparities between the modelled and the measured drainage data were due to experimental error when measuring the outflow from the samples, or possibly when measuring the saturated moisture content.

The model was run for the first and the third drainage cycle. The retention and hydraulic conductivity curves were compared between soils, cycles and initial bulk densities as were the individual parameters of the van Genuchten-Mualem equation. The total volume of water filled pores was also calculated for each sample and cycle (by multiplying the volumetric moisture content at a given tension by the total volume at saturation) so that the development of porosity could be investigated. The results of these analyses are described and discussed in Chapter 4, Section 4.6.

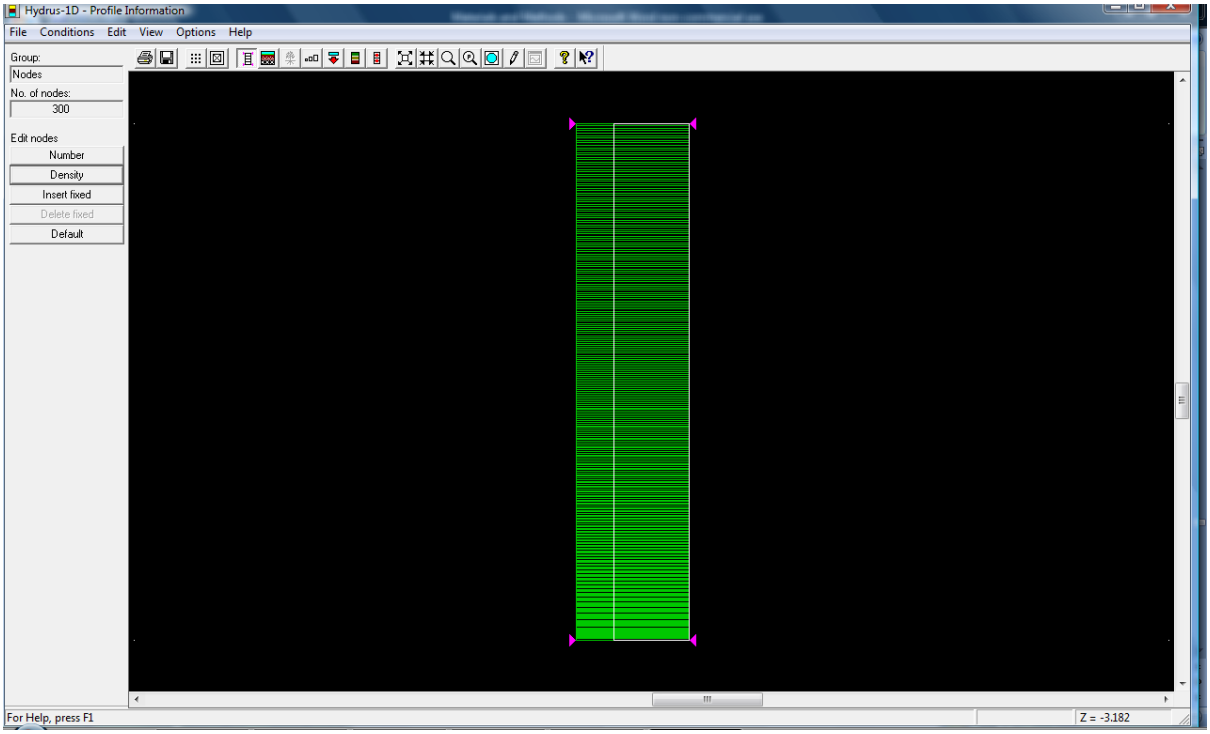

Figure 14. Screen shot showing profile discretization in HYDRUS-1D.

3.8 Image analysis

3.8.1 Background

Image analysis has been used by various authors to quantify the area of cracks on the surface of soil (for example, Yesiller *et al.*, 2000, and Vogel *et al.*, 2005) and the pore space visible in thin sections (for example Velde, 2001). Techniques such as fractal analysis can also be

used to describe features of cracking patterns in more detail. Whatever the intended analysis, the image must be converted to a binary image that separates the features of interest from the surrounding soil. Features of interest are commonly assigned the colour black and the surrounding soil white. The area of features of interest can then be calculated relative to the total area. Other analysis can also be performed, such as estimating crack length and width, the complexity of fractal patterns formed by the cracks and pore size distributions.

In order to obtain a binary image, features can be traced by hand, which is a laborious process, or the image can be thresholded. When thresholding an image, the histogram of pixel intensity of an 8 bit grey scale image is considered and a threshold grey scale intensity is selected. Pixels to the right of this threshold are set to value 255, or white, and pixels to the left, those representing the feature of interest, are converted to a value of 0, or black. The selection of this threshold is, therefore, fundamental in determining the final outcome of any analysis.

Different authors have used a variety of methods to select a threshold, ranging from manual to fully automatic techniques. This is commonly referred to as thresholding. The following section will review a selection of these techniques and describe the methods implemented in this study.

There are various automatic thresholding techniques that can be applied to digital images. Baveye *et al.* (1998) employed two iterative methods of thresholding images when considering the fractal dimensions of cracking patterns; the intermeans algorithm and the

minimum-error algorithm. The intermeans algorithm calculates the mean grey level for the pixels either side of an initial estimate. The mean of these two means is then calculated and used as the initial estimate for the next calculation. This process is repeated until the answers converge. The minimum-error algorithm assumes two normally distributed histogram of grey scale. As with the intermeans algorithm, an initial estimate of the threshold is made. The pixel fraction, means and variances of either side of this threshold are calculated and used to create a composite histogram, which is the weighted sum of the two initial normal distributions. Where these distributions are equal is taken as the initial estimate for the next iteration. This process continues until the solution converges. The final outcome of both these methods, however, is influenced by their initial estimates. Generally, the intermeans algorithm resulted in a lower threshold than the minimum-error algorithm, but the influence on the fractal dimension calculated was small (Baveye *et al.*, 1998).

Ringrose-Voase (1996) implemented the following thresholding technique to images of pore space with a bimodal distribution of grey levels. The portions of the distribution that were definitely pore and solid were identified and two thresholds applied. The edges of the objects within the image were then sharpened with a Laplacian filter; each pixel was compared to its immediate neighbours and adjusted according to the gradient of the difference in grey level. Two binary images were then created from the original. The first uses the threshold that identifies definite pore space, although narrow pore spaces are often missing. The second image uses the threshold that identified solid to create a binary image that includes pore space and the grey area between definite pore and definite solid. This image is then thinned to create a network of pore space that is an underestimate of the total pore space, but that does

include the narrow regions. The resulting two images are then combined using a logical OR operator (Ringrose-Voase, 1996).

Vogel *et al.* (2005) utilised a method of thresholding which allowed the threshold to vary over individual images, to measure the area of cracks on drying samples over time. The threshold for a segment 20 x 20 pixels was set at 0.65 x mean grey level of that segment. Problems were encountered when the cracks became large as light penetrated the cracks. This was overcome by comparing images with earlier images and attributing all points that were identified as cracks to the new image, except where they were on the edge of an aggregate. The method of selecting the threshold grey value described here seems arbitrary as no justification is given for the value of 0.65 x mean grey value. However, it does have the advantage of allowing for variation in colour across the image. It also allows for the automated processing of images, where as a completely manual inspection technique requires each image to be considered individually.

Velde (1999) also highlights problems associated with applying automatic thresholding techniques to images where grey levels vary over the surface of the image, specifically in the case the surface photographed is uneven. This variation is used as a justification for selecting a threshold based on inspection and then to manually edit the resulting binary image to achieve an accurate representation of the original (Velde, 1999). However, if this is the only barrier to using an automatic thresholding technique, the problem could be solved by segmenting the image and considering each segment separately, as suggested by Vogel *et al.* (2005).

Another draw back of the automatic thresholding techniques described here is that they all assume a bimodal distribution of grey levels. This is not always the case, although the fluorescent images studied by Marcelino *et al.* (2006) did not have clearly bimodal distributions. This could have contributed to the differences in the area of pores measured between the automatic and the semiautomatic and manual thresholding techniques.

Manual thresholding techniques are considered to be the most appropriate by some authors. Peng *et al.* (2006) used Adobe Photoshop and Windows Scion 4.02 to measure the horizontal shrinkage and surface cracking of soils. They began by using Adobe Photoshop to maximise the contrast of the images. The cracks were then outlined by hand using the "magic wand" tool, separating the cracks from the surface area of the soil and generating a threshold pixel intensity (Peng *et al.*, 2006). Thresholds are manually selected in Adobe Photoshop.

A new layer was created, from which pseudo cracks (soil particles whose pixel intensity was similar to that of the cracks) were erased. Subjective error in this procedure was considered to be negligible as the contrast between the soil surface and the cracks was great. When the thresholded image was considered to accurately represent the cracked area it was converted to a binary image, the cracks being white and the background and soil surface being black. The image was then inverted before being loaded into the Scion imaging software. This software then applied a threshold pixel intensity and measured the area of the image that was above this threshold (i.e. the black soil cracks) (Peng *et al.*, 2006). However, as the authors

appear to have already applied a threshold to the image using Adobe Photoshop, the second thresholding exercise seems extraneous; the images were effectively manually thresholded. Preston *et al.* (1997) do not state whether a manual or an automatic threshold was applied to their images, but the binary image was manually edited to match the original, which equates essentially to manual thresholding as the results were dependent on the observer processing the image. In a later study, Preston *et al.* (2001) found that it was impossible to threshold images of cracks and resorted to tracing the cracking patterns.

Marcelino *et al.* (2006) compared manual, semiautomatic and automatic methods of thresholding both fluorescent and backscattered electron (BSE) 2D images of pore space for analysis. The manual method simply required an observer to threshold the image by adjusting sliders until they considered the pores and the surrounding soil to be separated. The image was then converted to a binary image for analysis. The repeatability of this method was assessed by asking two observers to threshold the same set of images and on the observers to repeat the process after a period of one month. No smoothing or shape correction operations were performed. The interobserver difference between measures of total porosity was found to be 6.4%, the intraobserver difference 2.0% (Marcelino *et al.,* 2006). This suggests that, to make the analysis of images comparable between studies, that some level of automation is required although for comparison within a study, it may be acceptable to threshold manually if the images are all processed at the same time by the same observer and if the differences between images are large relative to the totality of features within an image.

The semiautomatic thresholding was a process of segmentation by hysteresis (Marcelino *et al.,* 2006). A similar set of images were used to determine "strong" and "weak" thresholds. The "strong" threshold identified areas that were definitely pores, but did not fill all the pore space. The "weak" threshold filled the pore space completely, but included noise. The "strong" and the "weak" images were then combined.

Before automatic thresholding was undertaken, the fluorescent images were subjected to an automatic histogram equalisation algorithm, which spread the 256 grey levels of the image evenly across the brightness range. The BSE images had their black pores enhanced by the reiterated mathematic addition of the images to themselves. Automatic thresholding was then applied. The threshold was calculated by assuming that the histogram was the sum of two normally distributed intensities (pores and soil). The point where these two distributions intersected was found by minimising the variances of the two distributions (Marcelino *et ai.,* 2006).

It was found that automatic thresholding systematically resulted in greater porosity measurements but very little difference was apparent between manual and semiautomatic thresholding techniques (Marcelino *et al.,* 2006). The small differences between the manual and the semiautomatic results imply that there is little benefit to be had from the semiautomatic thresholding method over the manual method, other than possible savings in time. It also suggests that manual methods have an acceptable level of accuracy.

The greater porosity implied by the automatic thresholding was explained by the histogram equalisation process, which artificially increased the pore area. The image addition, however, did not distort the image, merely enhanced the contrast between pore space and soil. The higher measured porosity in the BSE images was accounted for by the superior resolution of the BSE images, relative to the fluorescent images, hence more of the smallest pores were detected (Marcelino *et al.*, 2006).

Overall, it seems that although automatic thresholding techniques have their appeal because they are objective, rapid and repeatable, manually thresholding the images will give more representative results.

3.8.2 Application

The surface of the soil samples were photographed after equilibrium at 0.1 m (~1 kPa) and after air drying for five days at the end of each of the three drainage cycles using a digital camera with a four megapixel resolution. The camera was positioned at a fixed height above the samples at every photographing event. The samples were lit by an overhead light and by additional lamps positioned above and to the sides of the sample being photographed. After all the photographs had been taken they were ready to be processed and analysed for changes. It was felt preferable to process all the images together to minimise variations in results due to intraobserver differences.

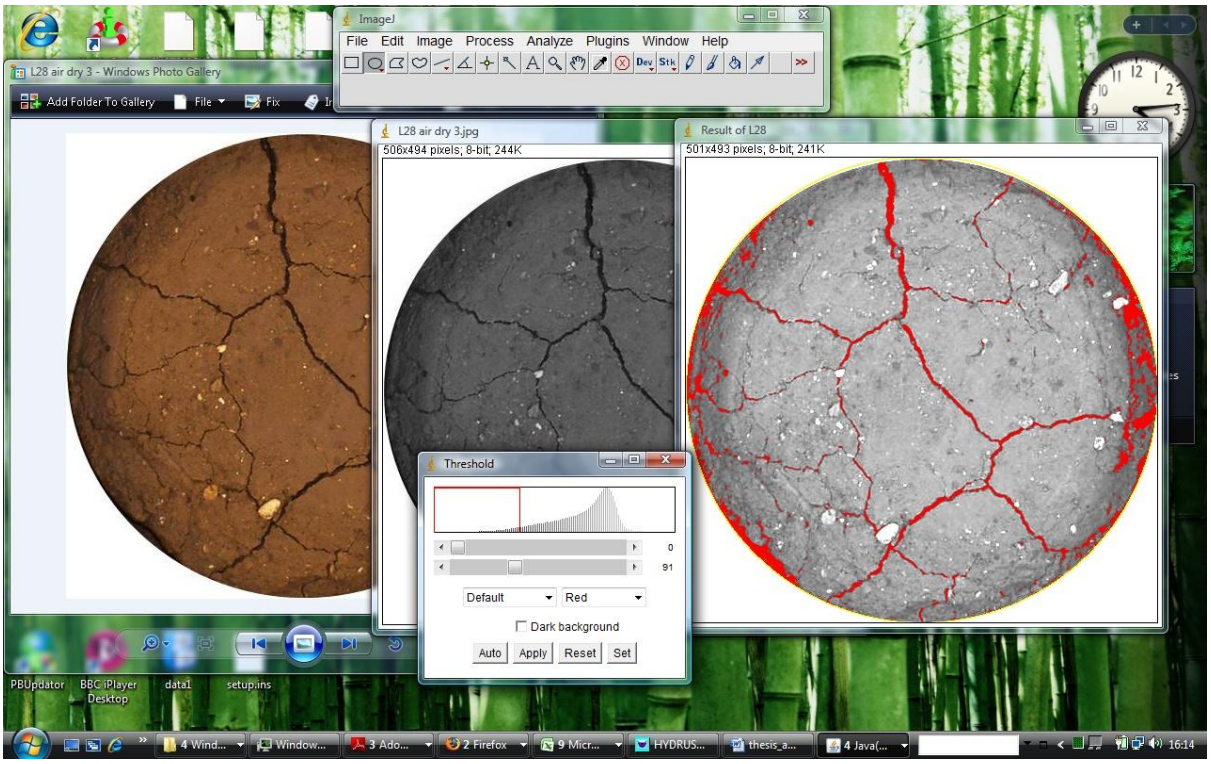

Figure 15. Screen shot showing the different stages of image processing. [3]

The images were processed with the programme ImageJ which is public domain software for analysing digital images developed by Wayne Rasband at the National Institute of Health, USA and is the successor to Scion Image. The first stage of processing the photographs was to crop the images, so that only the soil surface was visible. The next stage was to convert the images to an 8 bit black and white scale. The contrast of the black and white images was then enhanced by superimposing a copy of the 8 bit image onto itself, making the dark areas darker and the light areas lighter. The images were then ready to have the thresholds applied.

[3] From left to right; the cropped image, the 8 bit image and the enhanced image with thresholding slider.

The standard automatic thresholding function implements the Isodata algorithm. There are also plugins that contain other thresholding algorithms; Mixture Modelling, the Otsu algorithm and Maximum Entropy (http://rsb.info.nih.gov/ij/). As has already been discussed, however, automatic thresholding techniques alone cannot be relied upon to produce an accurate representation of the surface being considered in every instance. With wet/dry cycles, the surface of the samples considered in this study became increasingly uneven, introducing shadow effects. The application of the automatic thresholding techniques available for ImageJ was attempted, but all resulted in large errors when compared with visual inspection.

Each image was, therefore, individually thresholded manually. This was achieved by viewing the original image next to the enhanced grey scale image. A slider was then adjusted until all the visible surface cracks were highlighted (Figure 15). This threshold was applied and the image was converted to a black and white image, the cracks appearing black and the soil surface appearing white. This was used to calculate the area of the image that was assigned black and hence the total area of cracks. Every enhanced grey scale image was thresholded three times to monitor the consistency and repeatability of the technique and an average of the three readings were used in the statistical analysis. The total area of cracks was compared between cycles and between soils. How the area of cracks developed during wetting and drying was also investigated. Finally, correlations between the area of cracks and the physical and hydrological properties of the samples were explored. The results of these analyses are shown in final section of Chapter 4.

4 Results and Discussion

The following sections will describe and discuss the results of experiments, outlined in Chapter 3, designed to measure a range of the soils' physical and chemical properties, changes to the bulk density of soils with wet/dry cycles, changes in the saturated hydraulic conductivity of soils with wet/dry cycles, changes to their van Genuchten-Mualem parameters and the generation of surface cracks.

4.1 Soils' physical and chemical properties

4.1.1 Particle-size distribution

Figure 16 shows the texture of the soils, plotted on a triangular diagram. The colours assigned to the soils here will be used in all the following figures. The plough layers of soils 1 and 5 (PP/1 and PP/5) have a sandy loam texture. Their corresponding subsoils (SS/1 and SS/5) are loamy sands. Investigating these coarse textured soils provided a good comparison with the finer textured soils, especially for the purposes of statistical analysis. All the other soils were clay loams, apart from subsoil four (SS/4) which was a clay. The particle size distribution of the investigated soils is detailed in Table 1 and shown as bar graphs in Figure 17.

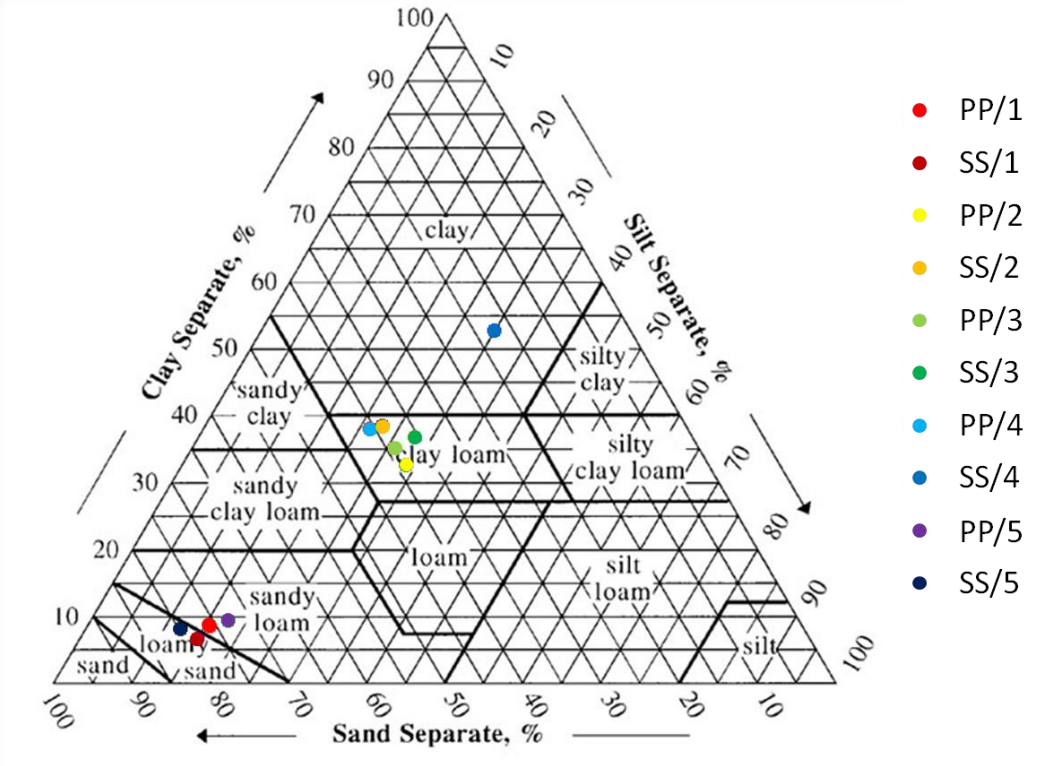

Figure 16. Textural triangle showing the particle size distribution of the soils investigated created using the soil texture calculator provided by NRCS (http://soils.usda.gov/technical/aids/investigations/texture/).

Table 1. The particle size distribution of the investigated soils in % mass of total mineral content.

	coarse sand %	medium sand %	fine sand %	total sand %	silt %	clay %
PP/1	6.08	49.83	20.58	76.49	14.49	9.03
SS/1	8.15	51.26	19.59	79.00	13.85	7.15
PP/2	2.75	31.67	4.88	39.30	27.57	33.13
SS/2	3.81	19.75	15.93	39.50	21.51	38.99
PP/3	3.69	22.17	13.66	39.52	24.79	35.70
SS/3	3.43	19.52	13.23	36.19	26.50	37.31
PP/4	4.62	24.77	11.84	41.23	20.15	38.62
SS/4	3.80	8.08	6.06	17.94	28.82	53.24
PP/5	14.55	42.44	16.63	73.62	16.44	9.95
SS/5	11.67	57.75	10.95	80.38	10.89	8.74

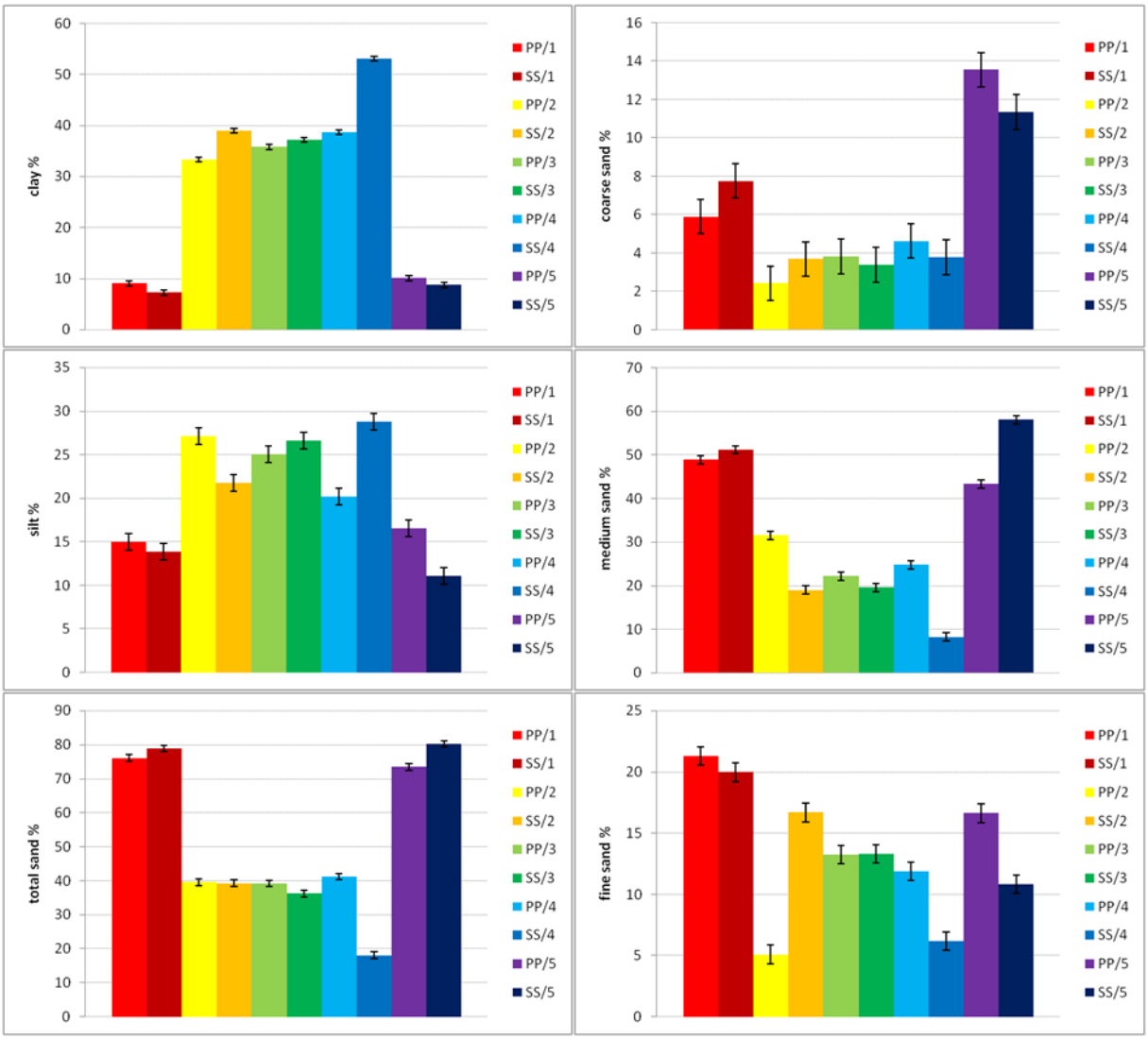

Figure 17. Particle size distribution of the investigated soils. [4]

[4] Error bars denote 95 % confidence intervals.

4.1.2 Physical and chemical properties

The plastic limit, liquid limit, shrinkage limit, organic matter lost on ignition, oxidisable organic matter and cation exchange capacity are shown in Figure 18. The plastic limit varied considerable between soils, even those with a similar texture. PP/4 had the highest plastic limit (approximately 33 %), followed by PP/3 and SS/4 (approximately 31 % and 29 % respectively). These values were statistically significantly different. SS/2 had a very similar plastic limit to PP/1 and PP/5 and was statistically insignificantly different from PP/1 (18 %, 19 % and 17 % respectively). This is surprising as PP/1 and PP/5 had much lower clay contents than SS/2 and would, therefore, be expected to have a much lower plastic limit (Reeve and Earl, 1989). These sandier soils did, however, have very low liquid limits (26 % and 23 %) compared to the finer textured soils. SS/4 had the highest liquid limit of approximately 67 %, closely followed by PP/3 and PP/4 with liquid limits of approximately 55 % and 56 %. Soil two had the lowest plastic and liquid limits of all the fine textured soils. As show in Table 2, the soil with the greatest difference between its liquid and its plastic limit (the greatest Plasticity Index) was SS/4, with a difference of approximately 37 %. The other fine texture soils had differences of between 21 and 25 %, the coarse textured soils between 3 and 6 %.

The soil that shrank the most upon drying (the greatest shrinkage limit) was PP/3 (approximately 25 % of its original length), despite having much less clay than SS/4, which shrank approximately 18 %, and a similar content to the other fine textured soils that shrank only 13 to 18 %. It did, however, have a higher organic matter content, shown to be important

in determining shrinkage by Peng and Horn, 2006. The coarse textured soils also shrank upon drying but, unsurprisingly, to a much lesser extent. SS/1 shrank the most out of the coarse textured soils (7 %). PP/1 shrank by 4 %. Soil 1 shrank more than soil 5, however, (PP/5 shrank approximately 2 % and the shrinkage of SS/5 was negligible) despite being almost identical in texture, the only difference being that soil 5 had a higher proportion of coarse sand.

Statistically, PP/2 and SS/2 had identical shrinkage limits, as did SS/3, PP/4 and SS/4. PP/5 and SS/5 were indistinguishable from each other, but has a significantly lower shrinkage limit than all the other soils. The shrinkage limit of SS/1 was significantly greater than that of PP/1, but less than that of the clay loams or the clay. The shrinkage limit of PP/3 was significantly and substantially greater than all the other soils.

The organic matter content lost on ignition varied between 1.4 and 8.6 %, PP/3 having the highest organic matter content and SS/1 the lowest. Generally, the sandier soils had a lower organic matter content than the clayey soils, although PP/1 and PP/5 had a very similar organic matter content to SS/2 (3.5, 3.0 and 3.7 % respectively). The soil with the highest clay content (SS/4) had an organic matter content of 4.9 %. The trend in organic matter contents closely, if not precisely, mirrored the trends in plastic limits, supporting the finding of Reeve and Earl (1989) who suggested that the plasticity of the soils was in part dependent upon their organic matter content as well as their clay content. The variation in organic matter content between soils of similar clay content (notably soils two and three) aided in the

separation of the effects of clay from organic matter content on changes to the structure of the samples with wet/dry cycles.

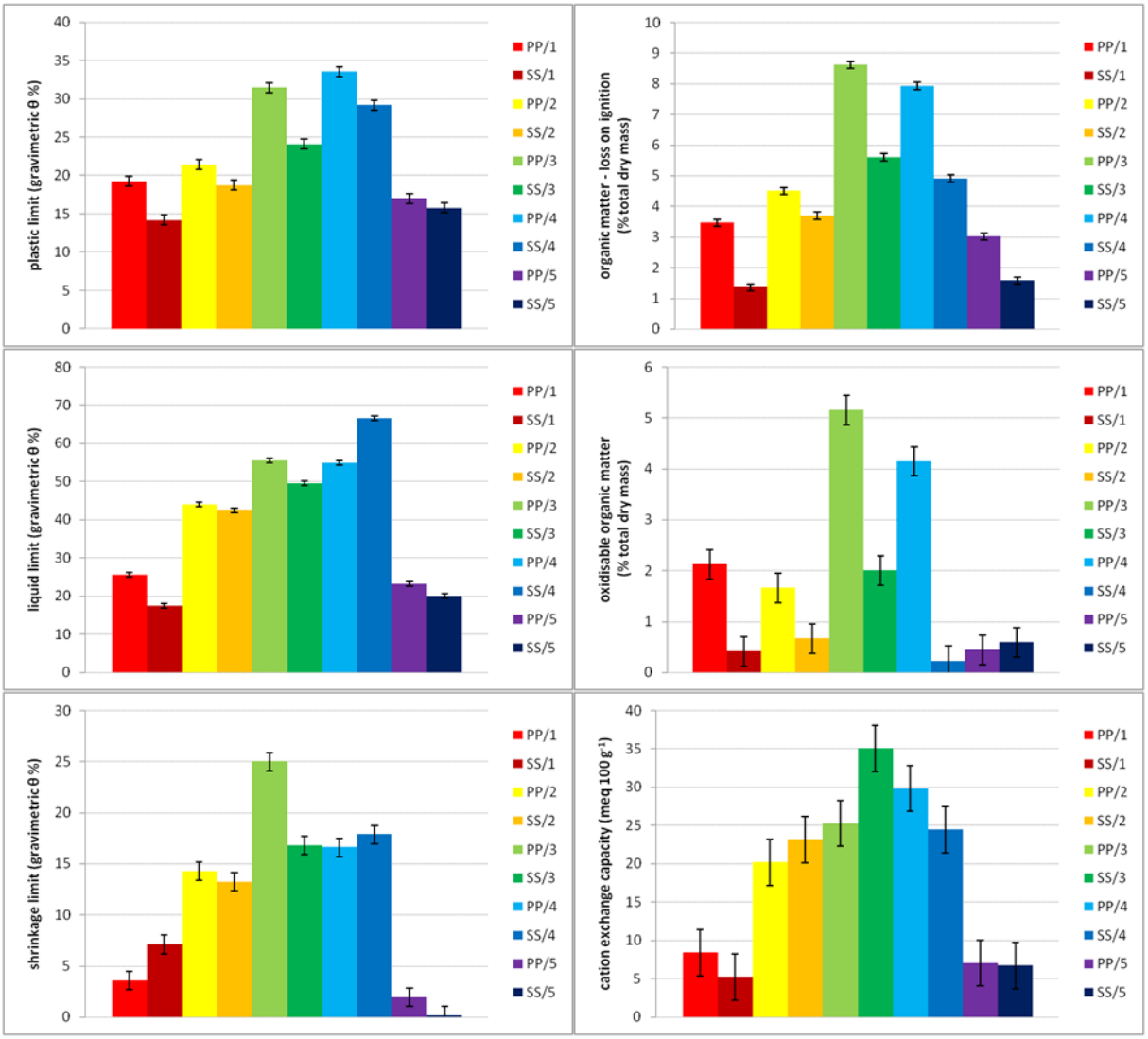

Figure 18. The measured physical and chemical parameters of the investigated soils. [5]

[5] Error bars denote 95 % confidence intervals.

The variation in the oxidisable organic matter content was greater than the variation in the organic matter lost on ignition. In general, the soils from the plough layer had more oxidisable organic matter than their subsoil counterparts. The difference in the oxidisable organic matter content between the sandier soils and the clayey soils was less pronounced than the differences in the organic matter lost on ignition. PP/3 had the highest oxidisable organic matter content (as well as the highest content of organic matter lost on ignition), approximately 5 %, although PP/4 had a similar oxidisable organic matter content of approximately 4 %. PP/1, PP/2 and SS/3 were similar in that they had oxidisable organic matter contents of approximately 2 % and the other soils had less than 1 % oxidisable organic matter.

Table 2. The Plasticity Index, calculated as the difference between the liquid and the plastic limits, of the investigated soils.

	Plasticity Index
PP/1	6.27
SS/1	3.33
PP/2	22.57
SS/2	23.76
PP/3	24.04
SS/3	25.39
PP/4	21.38
SS/4	37.34
PP/5	6.11
SS/5	6.16

The cation exchange capacity (CEC) of the soils varied between 5 and 10 meq 100 g^{-1} for the sandier soils and 20 and 35 meq 100 g^{-1} for the clayey soils. As was the case with the plastic limits, soils with a similar clay content, but different organic matter contents, differed in their cation exchange capacity, although unlike the plastic limits, SS/3 had the highest value (approximately 35 meq 100 g^{-1}). The other clayey soils had CEC's of between 20 and 30 meq 100 g^{-1}.

With the exception of subsoil 4 (SS/4) which was a clay soil, the soils selected for investigation fell into two textural classes; clay loam and sandy loam/loamy sand (Figure 16). The soils did exhibit differences in other parameters, however. The moisture content above which the soils behaved plastically varied between the clayey soils and, to a certain extent, between the sandy soils (Figure 18). The plough layer of soils three and four (PP/3 and PP/4) had a plastic limit 10 % greater than either the plough layer or the subsoil of soil two (PP/2 and SS/2), despite having a very similar clay content.

The variation in the liquid limit of the soils varies in a similar way to the plastic limit, but to a lesser extent (Figure 18). The subsoil of soil 4 (SS/4), however, had the greatest liquid limit of any of the soils. PP/3 shrank the most upon drying (Figure 18), despite SS/4 having a significantly ($p = 0.95$) greater clay content (Figure 17). PP/3 also had the highest occluded and available organic matter contents (Figure 18). SS/3 had the highest cation exchange capacity (Figure 18). The variation in these parameters allowed it to be ascertained whether the generation of soil structure was dependent exclusively on clay fraction, or whether other soil parameters contributed.

4.2 Changes to the bulk density and available water with wet/dry cycles

Undisturbed soil samples were repeatedly saturated and drained to equilibrium at 0.5 and 1.0 m of water on sand tables and then air dried at 30 ^{0}C in an incubator until there was no further water loss. The mass of the samples was measured at each tension. Changes in the mass of the samples at saturation were used as an indication of changes to the bulk density of the samples, changes in their mass at each tension as an indication of changes to the pore size distribution. The data set was considered as a whole and analysed for statistical differences in the variance of repeated measures using Statistica 8.0.

A change in the saturated moisture content of a sample can be related to a change in the bulk density of the sample. If the mass of the saturated sample increased, then the bulk density must experience a concomitant decrease to create the extra pore space indicated by the increased volume of water contained by an unchanging mass of soil. If it was the case that no increase in volume was observed, then it could be argued that the increase in saturated moisture content, if small, was attributable to pores that were previously air filled due to lack of pore connectivity becoming saturated, implying merely an increase in pore connectivity. However, a visible increase in the volume of the clayey soil samples was observed and changes to the saturated moisture content were large. Changes to the saturated moisture content were accepted, therefore, as a proxy for changes to the bulk density of the samples.

Although changes in the saturated moisture could have been used to calculate the changes in the bulk density, it was decided that statistical analysis would be performed directly on the

saturated moisture content as this would allow the initial bulk density to be included in the model predictors. This was felt to be important as the initial mean bulk density of the samples varied between soils (Figure 19). Soil two (PP/2 and SS/2) had a high bulk density relative to the other clayey soils, but similar to that of the sandy soils. Soil four (PP/4 and SS/4) had the lowest initial bulk density.

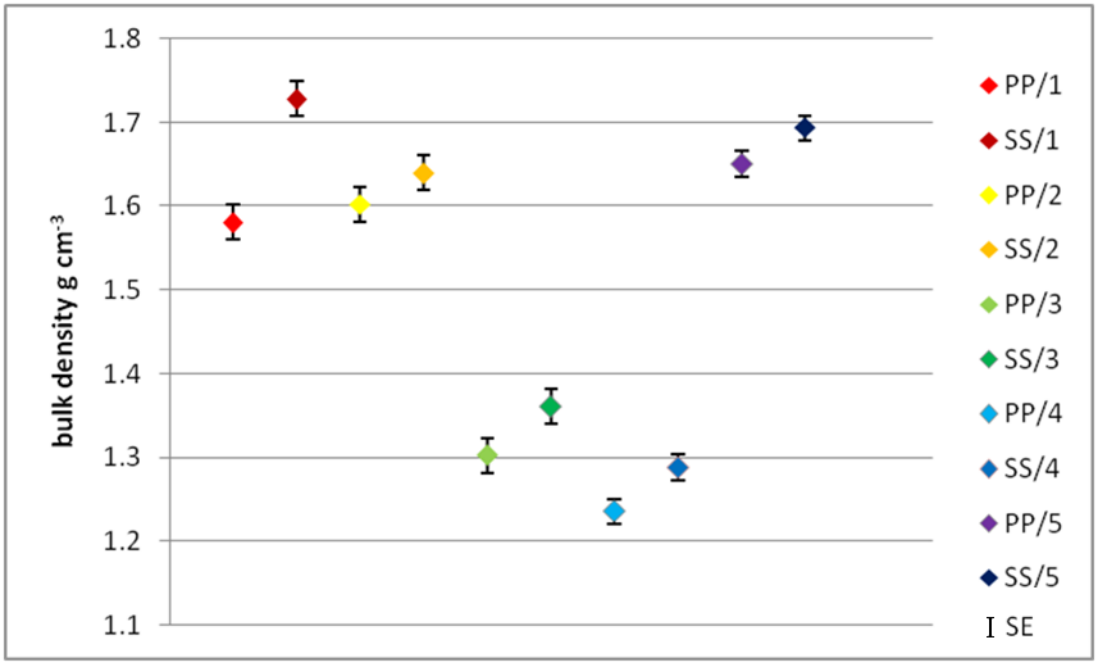

Figure 19. Initial mean bulk density of soils.

A general linear model for repeated measures was applied to the data in order to ascertain whether the changes with wet/dry cycles were significant, whether this was affected by the soil and whether the initial bulk density was significant in determining the changes. The error bars, calculated as part of the statistical analysis and displayed on following figures, should *not* be taken as measures of significance, but merely as an indication of the variation within

the data set. The confidence intervals associated with the data could not be accurately displayed in a two dimensions because more than one predictor was considered simultaneously and, therefore, extended into more than two dimensions. Changes with wet/dry cycles *were*, however, found to be significant at the 95 % level, as was the interactions between the cycle and the soil and the cycle and the initial bulk density. Probability levels are shown in Table 3.

4.2.1 Changes to the saturated volumetric moisture content

The general trend of the clayey samples was to decrease in bulk density (as indicated by changes in the volumetric moisture content), the sandy samples to increase, although the plough layer of soil 5 (PP/5) did decrease in bulk density. The magnitudes of these changes were not the same for all the soils. Changes to the volumetric moisture content of the clayey soils are shown in Figure 20 to Figure 25. The drainage cycle is shown on the *x* axis and the volumetric moisture content at saturation, equilibrium at 0.5 m and 1.0 m for that cycle is shown on the *y* axis. The range in volumetric moisture content displayed on the *y* axis is the same for all the figures to make the extent of any changes more easily comparable between soils. The significance of the changes to moisture content, as calculated by the statistical package, is reported separately in Table 3. The predictor column shows those factors which may affect the volumetric moisture content of the samples. The numbers are the probability that the moisture content was different at the measured tensions i.e. saturation, 0.5 m of water

and 1.0 m of water. The predictor 'cycle' is asking 'is there a difference in moisture content between cycle 1 and cycle 3'? The predictor 'cycle*initial bulk density' is asking 'is the difference in moisture content between cycles affected by the initial bulk density of the samples'? The predictor 'cycle*soil' is asking 'is the difference in moisture content between cycles 1 and 3 affected by the soil type'?

Table 3. Significance of changes in volumetric moisture content.

		p	
predictor	**saturation**	**0.5 m**	**1.0 m**
cycle	0.00303	0.00029	0.00093
cycle * initial bulk density	0.00214	0.00021	0.00093
cycle * soil	0.00000	0.01330	0.00014

Changes in the volumetric moisture content were found to be significantly different between cycles and how the moisture content changed was found to be affected by the initial bulk density and to be different between soils. The greatest increase in saturated volumetric moisture content and, therefore, the greatest reduction in bulk density, was experienced by PP/3 and SS/3 (Figure 22 and Figure 23). These soils had a similar texture to PP/2 and SS/2 and to PP/4, but had less clay than SS/4 (Figure 16). The differences between these soils and the other similar soils lay predominantly in the higher organic matter content and plasticity (Figure 18) of soil 3 and the initial bulk density (Figure 19), although SS/4 had a similar initial bulk density. Neither SS/3 (Figure 23) nor soil 4 (PP/4 and SS/4, Figure 24 and Figure 25) changed in bulk density after the second wetting and dying cycle. This implies that an equilibrium bulk density had been reached. Soil 2 (Figure 20 and Figure 21) also experienced

very little change in saturated moisture content and, therefore, bulk density. There was still a trend of reduction in bulk density, however, if less pronounced than that of soil 3. Variation in saturated moisture content within each soil was reduced by cycle 3, lending further weight to the argument that the soils were tending towards an equilibrium bulk density.

Changes in the volumetric moisture content of the sandy soils (PP/1, SS/1, PP/5 and SS/5) are shown in Figure 26 to Figure 29. All the sandy soils demonstrated a drop in saturated moisture content after the first wet/dry cycle, but this was followed by a marginal increase in saturated moisture content, apart from SS/5. SS/5 also experienced the greatest drop in saturated moisture content and had a similar organic matter content to SS/1, but had a lower initial bulk density than SS/1. As with the clayey soils, variation in moisture content within each soil was reduced by cycle 3.

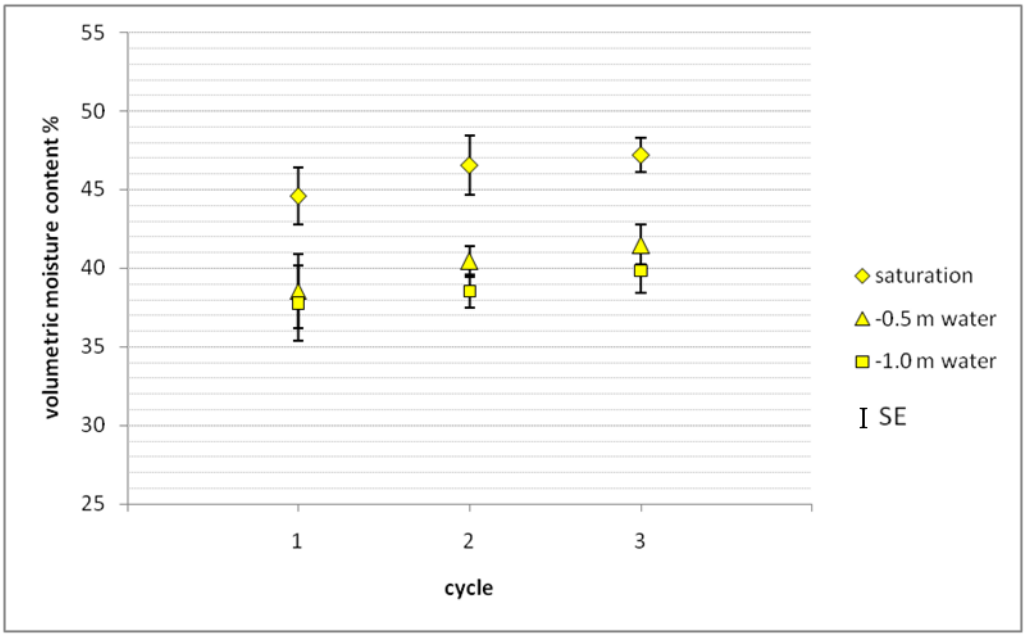

Figure 20. Changes in the volumetric moisture content of the plough layer of soil 2 (PP/2).

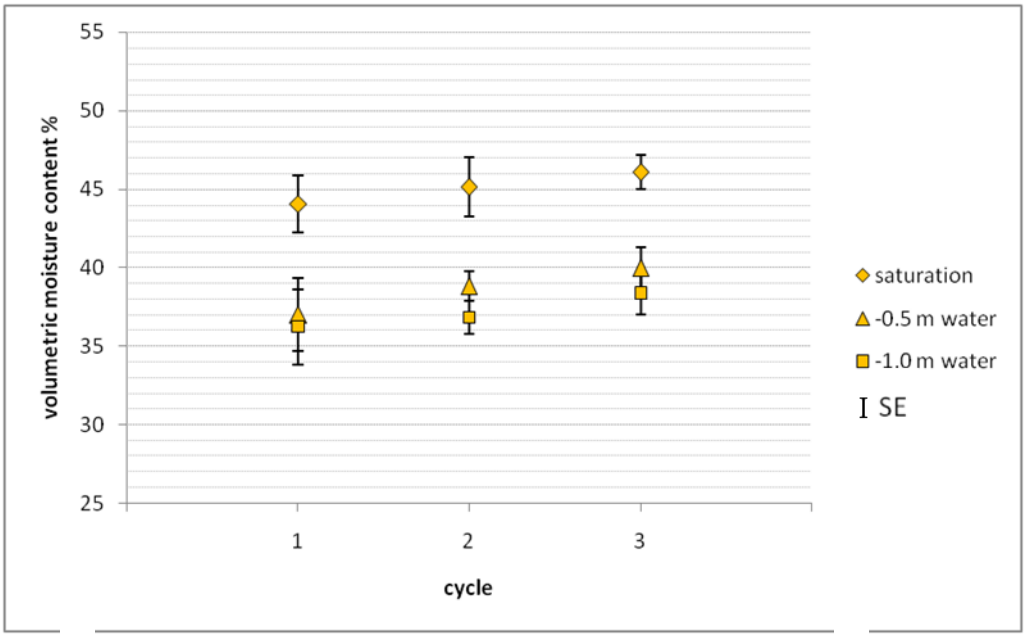

Figure 21. Changes in the volumetric moisture content of the subsoil of soil 2 (SS/2).

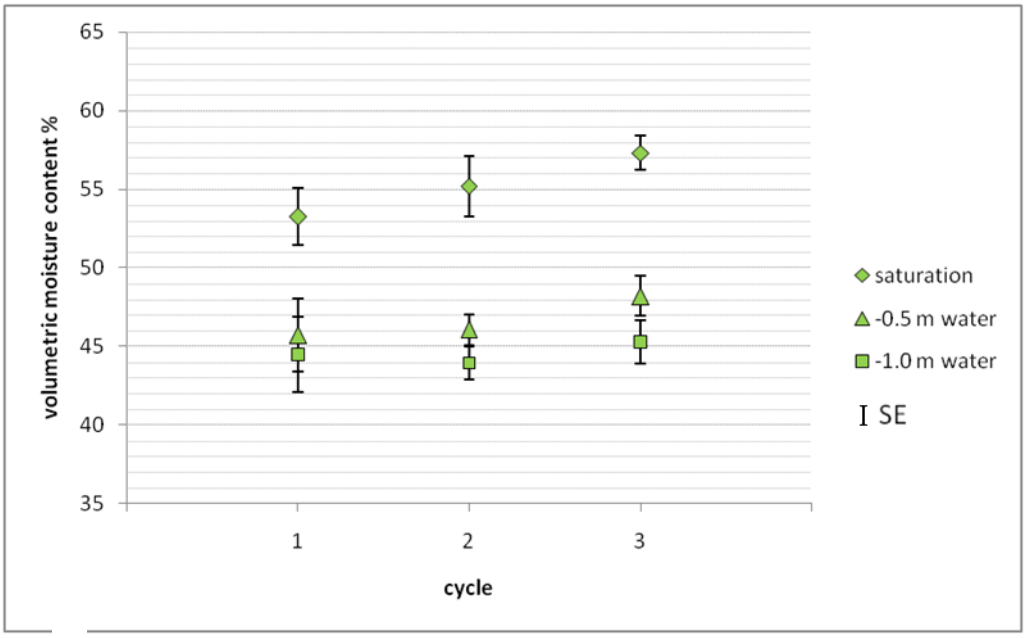

Figure 22. Changes in the volumetric moisture content of the plough layer of soil 3 (PP/3).

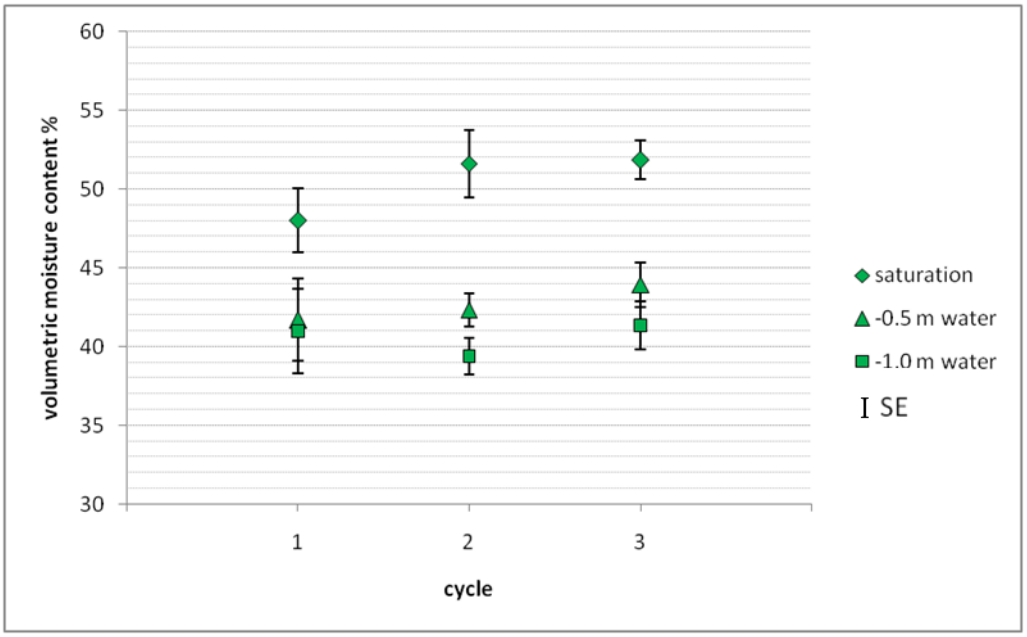

Figure 23. Changes in the volumetric moisture content of the subsoil of soil 3 (SS/3).

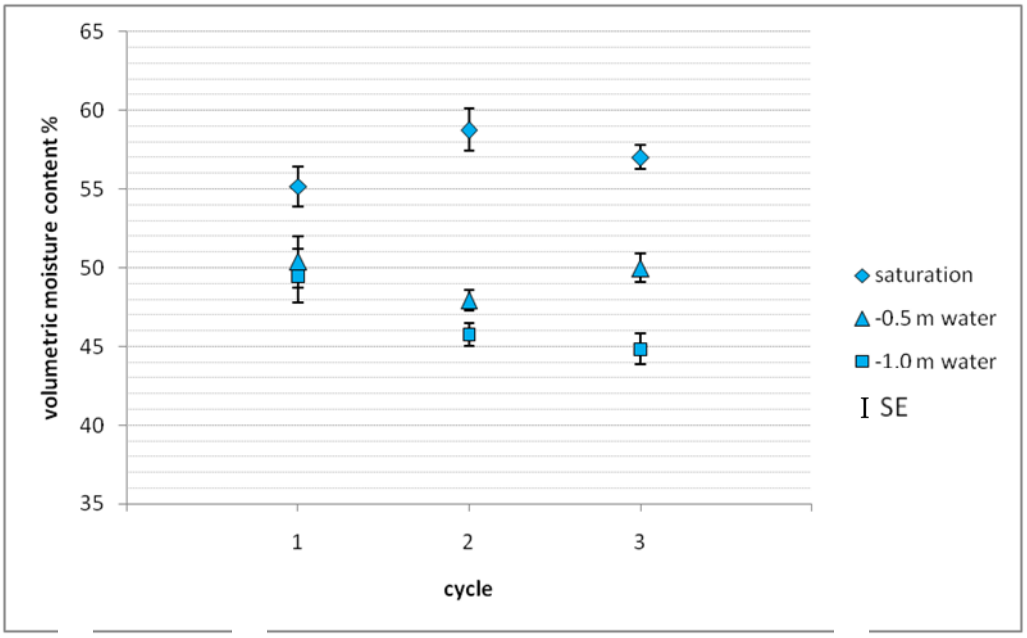

Figure 24. Changes in the volumetric moisture content of the plough layer of soil 4 (PP/4).

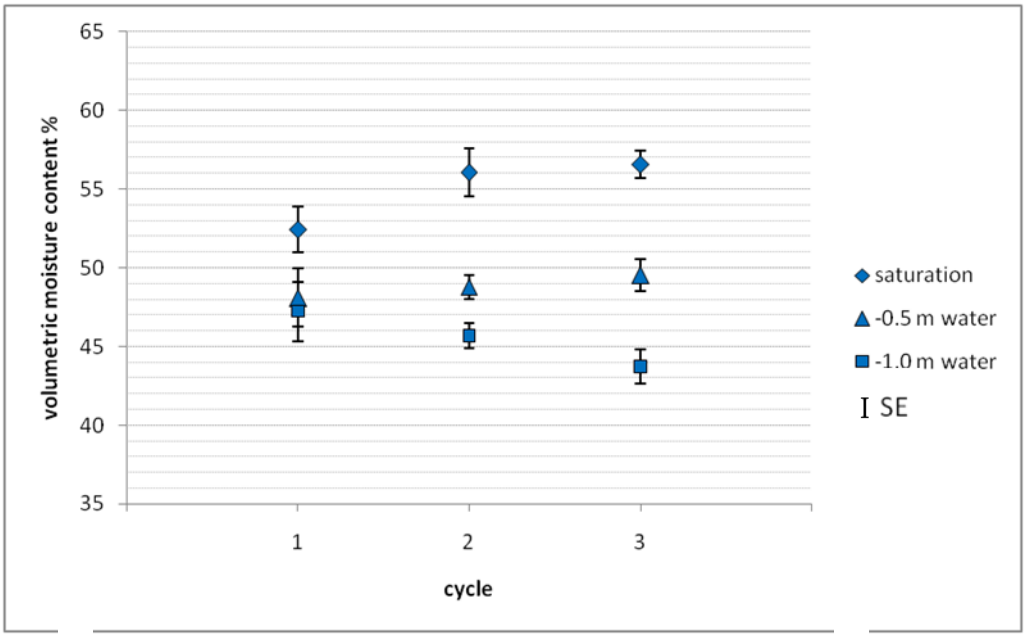

Figure 25. Changes in the volumetric moisture content of the subsoil of soil four (SS/4).

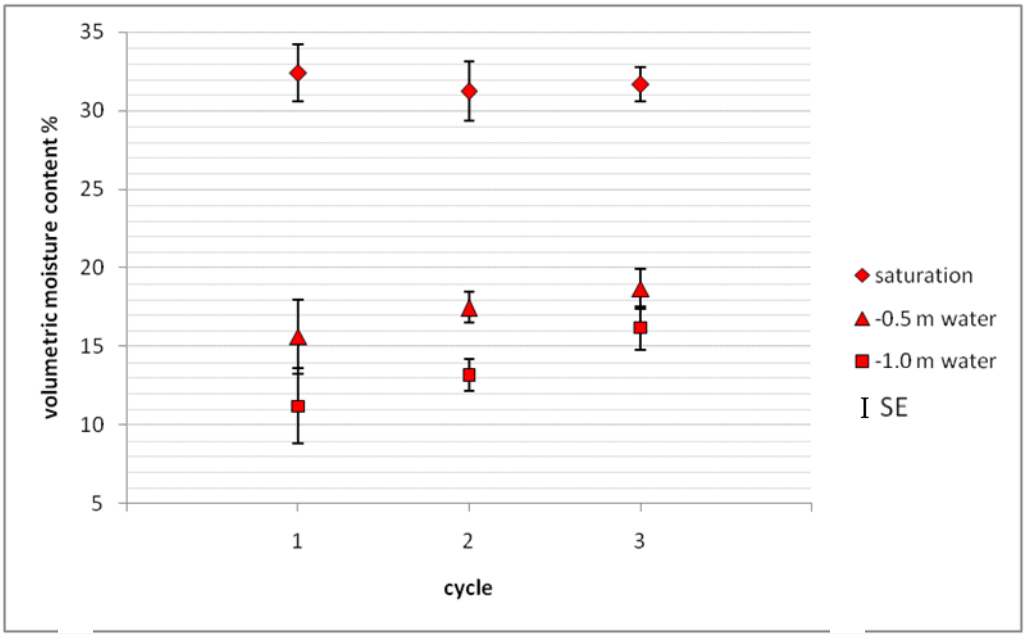

Figure 26. Changes in the volumetric moisture content of the plough layer of soil 1(PP/1).

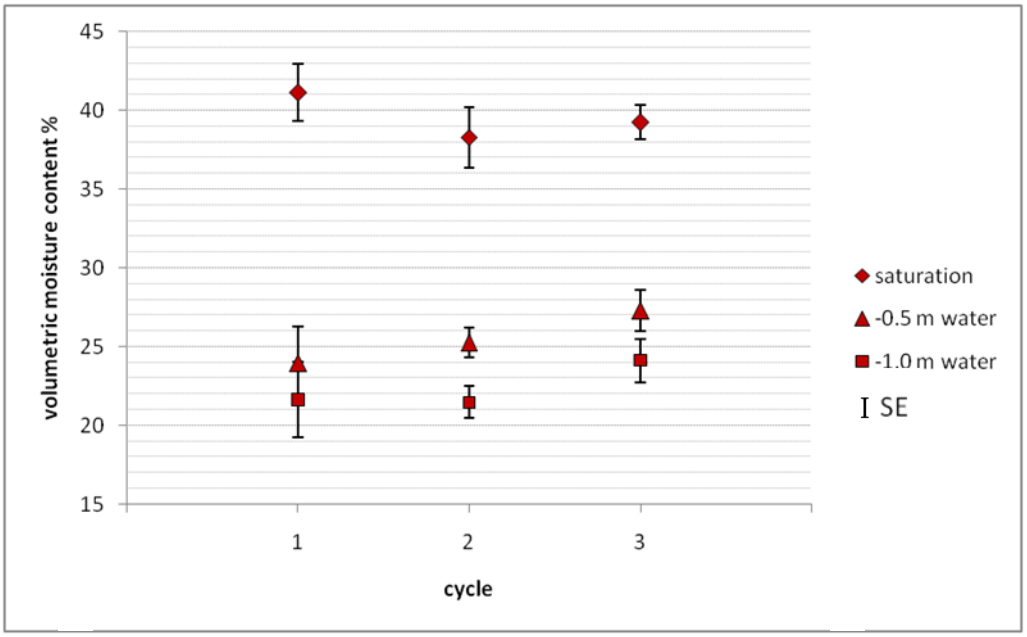

Figure 27. Changes in the volumetric moisture content of the subsoil of soil 1 (SS/1).

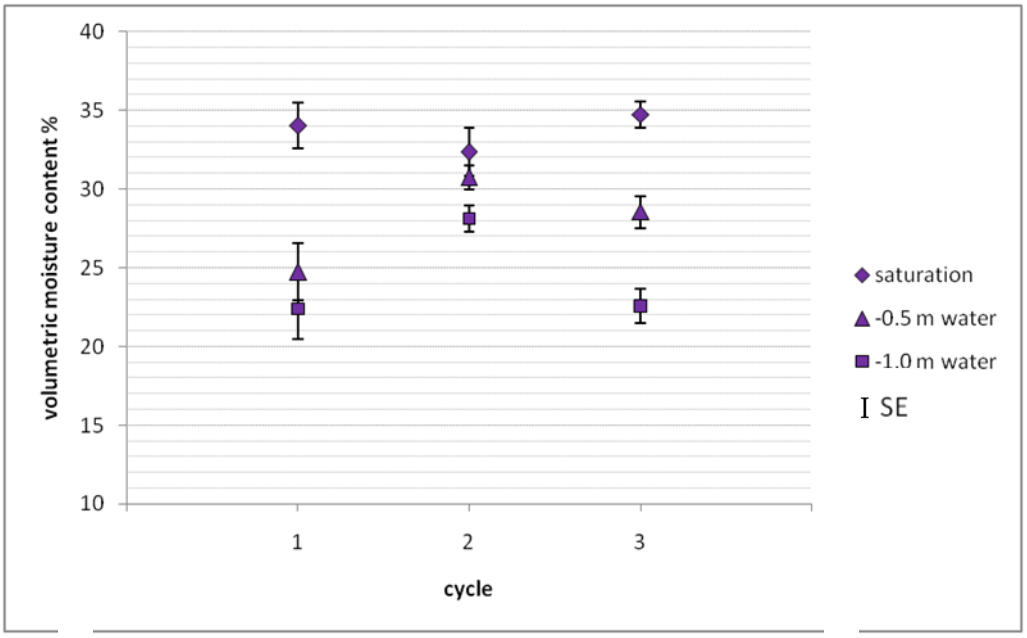

Figure 28. Changes in the volumetric moisture content of the plough layer of soil 5 (PP/5).

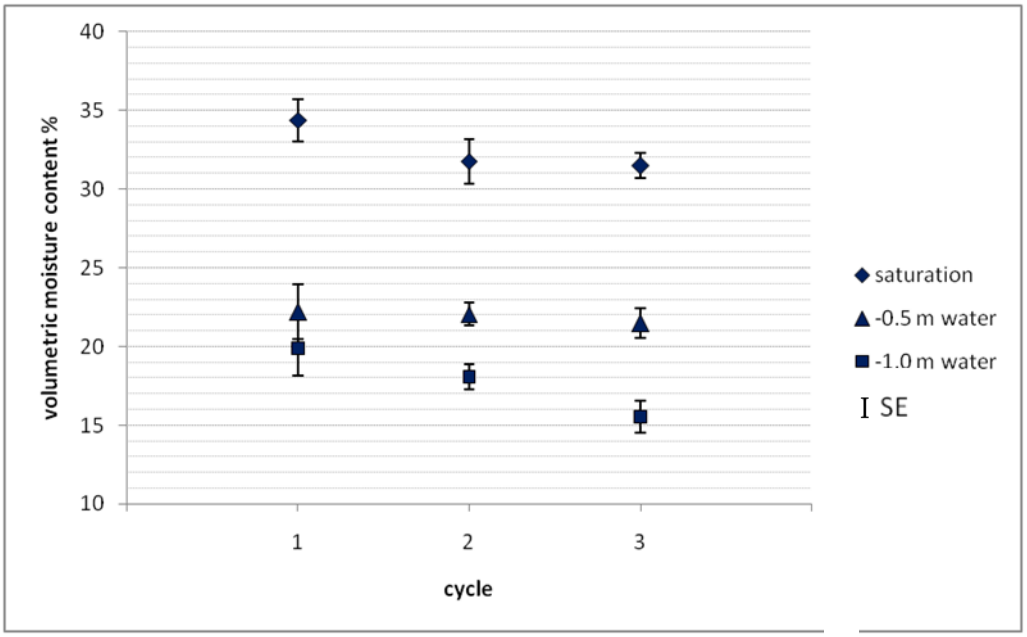

Figure 29. Changes in the volumetric moisture content of the subsoil of soil five (SS/5).

4.2.2 Changes in the volumetric moisture content at tension

The changes in the moisture content of the soils at tensions of - 0.5 m and at - 1.0 m of water were also considered. This was done in order to test the hypothesis that most of the changes in porosity would occur in the macro-pore range as a result of the soils cracking with wet/dry cycles. This is most clearly elucidated by considering the volumetric moisture content at these tensions (based on the total volume of soil and voids at saturation (Figure 20 to Figure 29) and by the proportion of these moisture contents relative to the saturated moisture content.

Apart from PP/4, all the soils retained an increasing volume of water at an applied pressure of - 0.5 m of water, with wet/dry cycles. This implies that the pores that were created by the wet/dry cycles were not merely those obviously visible as cracks and that the changes to the soil structure were more complex. If the increase in the total porosity of the samples was due purely to visible cracking, the additional porosity would be drained at very low tensions. This would result in the total volume of water remaining in the soil sample at a pressure of - 0.5 m of water being unchanged, whilst the total volume of soil and void had increased. This would mean that the volumetric moisture content of the soil at this tension would have decreased (although the gravimetric moisture content would remain the same). This was not the case here, however, which implies that the observed increases in porosity are attributable, at least in part, to other mechanisms such as aggregate formation or a change in bulk density of existing aggregates, or smaller scales of cracking.

Changes in the volumetric moisture content of soil two at an applied pressure of - 0.5 m and - 1.0 m of water reflect closely the changes in the saturated moisture content, although the difference in moisture content between - 0.5 m and - 1.0 m of water increased by wet/dry cycle three (Figure 20 and Figure 21). This suggests that the total water available for crop growth (the water held between field capacity and permanent wilting point) had increased, but not the aeration at field capacity (taking field capacity as - 1.0 m of water (Brady and Weil, 1999) as discussed in Chapter 3).

PP/3 (Figure 22), however, demonstrated a greater increase in saturated moisture content than at an applied pressure of - 0.5 m of water and almost no change in moisture content at - 1.0 m

of water. This suggests that a greater proportion of macro-pores were created and that aeration at field capacity increased more than the water available for crop growth. The changes between cycles 1 and 2 were less pronounced than the changes between cycles 2 and 3. Whilst the change in volumetric moisture content of SS/3 (Figure 23) at - 0.5 m of water was more pronounced between cycles 2 and t3 than between cycles 1 and 2, the change in the saturated moisture content was minimal between cycles 2 and 3. This appears to suggest that a few large pores were created between the first and the second cycle that subsequently broke down into smaller (if still macro) pores. This would occur if, during a cycle, large aggregates began to form which, during a subsequent cycle, experienced failure at a plane of weakness and broke down into smaller aggregates, as observed by Grant *et al.*, 1995. The total amount of space between the aggregates would have the potential to remain constant, but this porosity would be the result of the addition of several smaller pores, rather than one large pore.

PP/4 (Figure 24) displays a different pattern of changes again. Overall, there was a small increase in the saturated moisture content, no change in the moisture content at - 0.5 m of water and a decrease in the moisture content at - 1.0 m of water. This implies an increase in the macro-porosity and, therefore, the aeration at field capacity from approximately 5 % to 14 % of the total volume, but not the water available for crop growth. SS/4 (Figure 25) demonstrated similar behaviour with an increase in aeration at field capacity from approximately 5 % to 12 % of the total volume.

Although the previous paragraphs have discussed changes in aeration at an applied pressure of - 1.0 m of water, the figure quoted may not be an entirely accurate description of reality as the clayey soils demonstrated shrink/swell behaviour. This means that the pores that were not water filled may have been reduced in size relative to the saturated state. A soil that experienced completely normal shrinkage would, in effect, always be saturated. Without knowing the shape of the shrinkage curve, it is impossible to estimate aeration from moisture content alone. However, considering the moisture content relative to the minimum bulk density for that cycle still provided useful information regarding the changes to the water available for plant growth and the mechanisms of pore creation. It is also reasonable to assume that if the difference in moisture content increased between applied pressures of 0 and - 1.0 m of water then the capacity of air filled pore at an applied pressure of - 0.1 m of water also increased, if not to the same extent, as drying the soil caused the cracks to either expand or be created, thereby precluding the possibility of completely normal shrinkage and increasing aeration.

Similar to the clayey soils, the sandy soils demonstrated a change in pore size distribution with an increase in the moisture content at applied pressures of - 0.5 m and - 1.0 m of water, indicative of the collapse of the largest pores with wet/dry cycles. Changes in the moisture content of soil 1 appeared to be similar between cycles 1 and 2 and cycles 2 and 3 (Figure 26 and Figure 27). This would reduce the aeration at field capacity, but increase the water available for crop growth. Lipiec and Håkansson (2000) quoted 10 % air filled porosity as the critical limit for plant growth. As aeration is high and available water is low (compared to the clayey soils), a decrease in air filled porosity to closer to this critical value at low pressures

could be considered an improvement in the health of the soil, despite the increases in bulk density, at least where crop growth is the primary concern.

PP/5 (Figure 28) produced what appear to be cyclic results; an increase in moisture content under tension after cycle 1, followed by a decrease after cycle 2. This pattern was followed by all individual samples on all sand tables. This implies that some macro-pores collapsed during cycle 1, but reformed during cycle 3. The end result was that there was an appreciable change in neither bulk density, aeration at field capacity, nor the water available for crop growth. The decrease in moisture content of SS/5 (Figure 29) at an applied pressure of - 1.0 m of water mirrored the loss in saturated moisture content. This implies that the loss in porosity was not due to the collapse of the largest pores, but a reduction in the volume of pores that remained undrained at – 1.0 m of water, and that the water storage was reduced.

The change in moisture content with wet/dry cycles, the interaction between wet/dry cycles and the initial bulk density, and the interaction between changes with wet/dry cycles and the soil, were all significant at a probability in excess of 99 % (apart from the interaction between wet/dry cycles and soil at - 0.5 m which had a probability of 98.7 %) (Table 3). This means that the moisture content of the samples changed significantly with wet/dry cycles at all tensions. This is confirmed by looking at the raw data (not shown) in which the direction and magnitude of the changes demonstrated by all sets of replicates are remarkably consistent. Table 3 also shows that how the moisture content of the samples changed was effected, significantly, by both the soil and the initial bulk density of the individual samples.

4.2.3 Changes in saturated volumetric moisture content and the relation of these changes to soil parameters

The general linear model for repeated measures was again applied to the data set in order to determine the significance, or not, of the various measured soil parameters with regards to the changes in, initially, the saturated volumetric moisture content of the samples.

The results of this analysis were very dependent on what parameters were included in the model; not all the measured parameters could be considered by the model simultaneously. Sand, silt and clay contents could not be considered together because they add up to 100 %. Similarly, total sand could not be considered simultaneously with the three separate sand fractions. The plastic and liquid limits could not be included in the model with the Plasticity Index as the latter is a function of the former two parameters and the correlation between them would distort results. The degrees of freedom were also a limiting factor; there were insufficient degrees of freedom to consider all the predictors simultaneously.

The statistical analysis applied to the data set was, therefore, effectively a step-wise regression. The model was run with an initial set of predictor parameters. The parameters found to be insignificant were then removed from the model and replaced with parameters that were not included in the first run. After the second run of the model, insignificant parameters were removed and the model rerun. In an iteratively stepwise manner, the parameters most significant for predicting the changes to the moisture content of the soil samples (with wet/dry cycles) were identified.

Table 4. First run of the general linear model for repeated measures.

Cycle parameter interactions	p
Cycle	0.00027
Cycle*initial bulk density	0.00000
Cycle*clay	0.08929
Cycle*total sand	0.07343
Cycle*plastic limit	0.11593
Cycle*liquid limit	0.00347
Cycle*shrinkage limit	0.10491
Cycle*OM lost on ignition	0.00058
Cycle*oxidisable OM	0.00002
Cycle*cation exchange capacity	0.02881

The parameters shown in Table 4 were selected as they included the full range of physical and chemical soil characteristics i.e., the soil texture, the properties of the soil at different moisture contents, the behaviour of the soil upon drying, the organic matter content of the soil and the charge on the soil particles. The initial bulk density, the organic matter content (both lost on ignition and oxidisable) and the liquid limit of the soils most significant parameters in determining changes in saturated volumetric moisture content with wet/dry cycles.

Perhaps surprisingly, the clay content of the soils was only significant at the 90 % probability level, as was the total sand content, although Ball *et al.*, 2000, found that clay was only weakly correlated with compactibility, another soil behavioural characteristic which may have been presumed to be related to clay content, and was better predicted by liquid limit and

organic matter. However, soils with a similar clay content were differentiated by their organic matter contents (Figure 18). The prediction equation (Equation 28) produced by the model correlated well with the measured data (Figure 30).

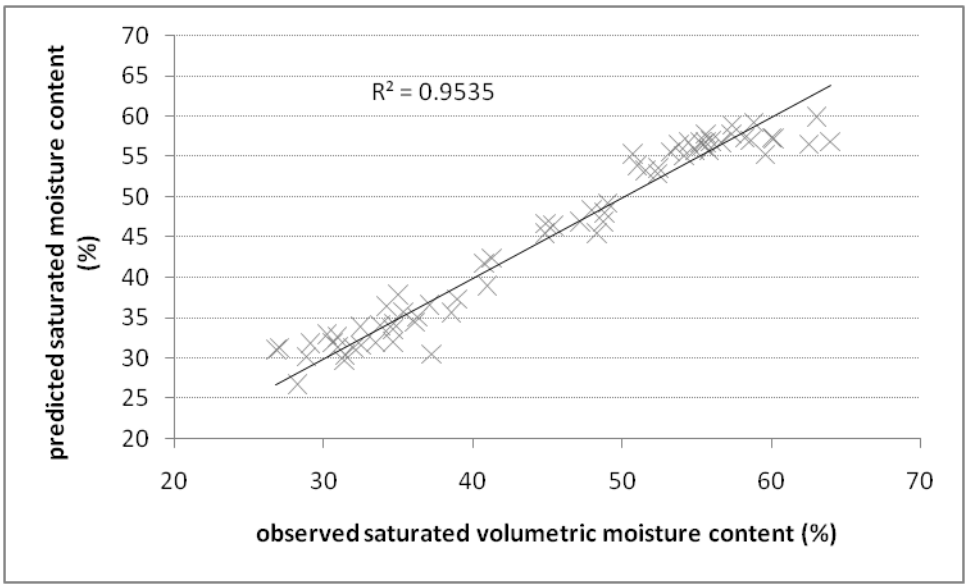

Figure 30. The observed and the predicted saturated volumetric moisture content of the samples at the third saturation, based on the first run of the general linear model for repeated measures.

$$mc = 139.90 - 33.68 \times BD + 0.10 \times C - 0.51 \times TS - 0.33 \times PL - 0.32 \times LL - 0.14 \times SL - 0.20 \times LOI + 2.71 \times OX - 0.10 \times CEC \quad (28)$$

Where: *mc = saturated volumetric moisture content at the third saturation (%)*

BD = initial bulk density (g cm^{-3})

C = clay content (%)

TS = total sand content (%)

PL = plastic limit (gravimetric moisture content in %)

LL = liquid limit (gravimetric moisture content in %)

SL = shrinkage limit (%)

LOI = organic matter content lost on ignition (%)

OX = oxidisable organic matter (%)

CEC = cation exchange capacity (meq 100 g^{-1}).

For the second run of the model, the plastic limit and the shrinkage limit were removed, the total sand content was replaced by the three different sand fractions and the Plasticity Index were included. The results of this analysis are shown in Table 5 and Figure 31. None of the three sand fractions were found to be significant, whereas in the previous run, total sand content had been significant at the 90 % level. The organic matter content (both oxidisable and that lost on ignition) were also not significant. Surprisingly, cycle, when considered alone, was not significant. However, the interaction between the cycle and other soil parameters remained significant, so the model was still detecting significant changes to the saturated volumetric moisture content of the soil samples. The clay fraction was significant at the 95 % probability level. The liquid limit and the cation exchange capacity remained significant. In Equation 29, the multipliers of initial bulk density, oxidisable organic matter and cation exchange capacity were similar to their multipliers in Equation 28. The clay fraction, liquid limit and organic matter lost on ignition, however, had different multipliers.

Table 5. Second run of the general linear model for repeated measures.

Cycle parameter interactions	p
Cycle	0.24977
Cycle*inital bulk density	0.00000
Cycle*clay	0.00734
Cycle*coarse sand	0.15436
Cycle*medium sand	0.15105
Cycle*fine sand	0.16984
Cycle*liquid limit	0.01244
Cycle*plasticity index	0.12304
Cycle*OM lost on ignition	0.32870
Cycle*oxidisable OM	0.47676
Cycle*cation exchange capacity	0.01995

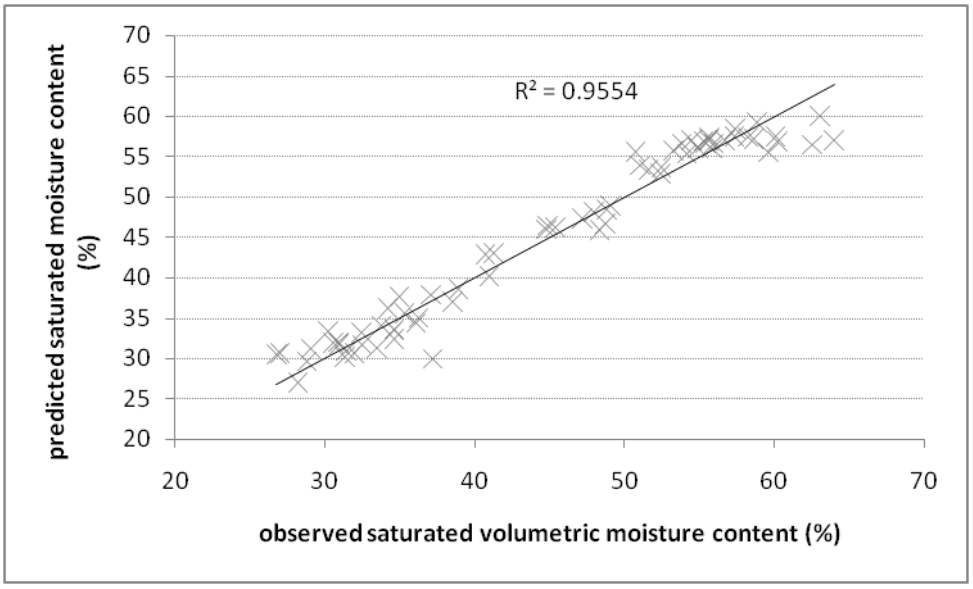

Figure 31. The observed and the predicted saturated volumetric moisture content of the samples at the third saturation, based on the second run of the general linear model for repeated measures.

$$mc = 76.62 - 32.25 \times BD + 0.43 \times C - 0.58 \times CS + 0.34 \times MS + 0.16 \times FS - 1.07 \times PI - 0.96 \times LL - 4.96 \times LOI - 2.36 \times OX - 0.12 \times CEC \quad (29)$$

Where: *mc = saturated volumetric moisture content at the third saturation (%)*

BD = initial bulk density (g cm^{-3}

C = clay content (%)

CS = coarse sand content (%)

MS = medium sand content (%)

FS = fine sand content (%)

PI = plasticity index

LL = liquid limit (gravimetric moisture content in %)

LOI = organic matter content lost on ignition (%)

OX = oxidisable organic matter (%)

CEC =cation exchange capacity (meq 100 g^{-1}).

Running the model for a third time with only the significant parameters from the second run included rendered the cation exchange capacity significant at only the 90 % probability level. The difference in moisture content between cycles regardless of other parameters such as the initial bulk density, however, became significant once again. The overall fit of the model was R^2 = 0.9322 (graph not shown). As so many of the potential predictor parameters had been removed from the model whilst retaining a reasonable goodness of fit of predicted against observed saturated volumetric moisture content, the model was run for a fourth time with

merely initial bulk density and the liquid limit as predictors. This was done as both the bulk density and the liquid limit are relatively uncomplicated parameters to measure in a laboratory from small volumes of soil and could, therefore, be useful, practical predictors of a soil's propensity to recover structure with wet/dry cycles.

The cycle, the initial bulk density and the liquid limit were all highly significant predictors (Table 6). The overall fit of the model, although marginally worse than the previous runs, was still good (R^2 = 0.9149, Figure 32). This suggests that the initial bulk density and the liquid limit alone would be adequate predictors of the change in saturated volumetric moisture content (and, therefore, the bulk density) that could be expected after a compaction event (assuming that sufficient drying of the soil had occurred between saturations). Equation 30 is a simple equation that would be easy to apply, once the necessary measurements of the soil parameters had been made. Based upon the research presented here, this would seem to be the most appropriate prediction equation to utilise.

Table 6. Fourth run of the general linear model for repeated measures.

Cycle parameter interactions	p
Cycle	0.000259
Cycle*initial bulk density	0.000223
Cycle*liquid limit	0.000001

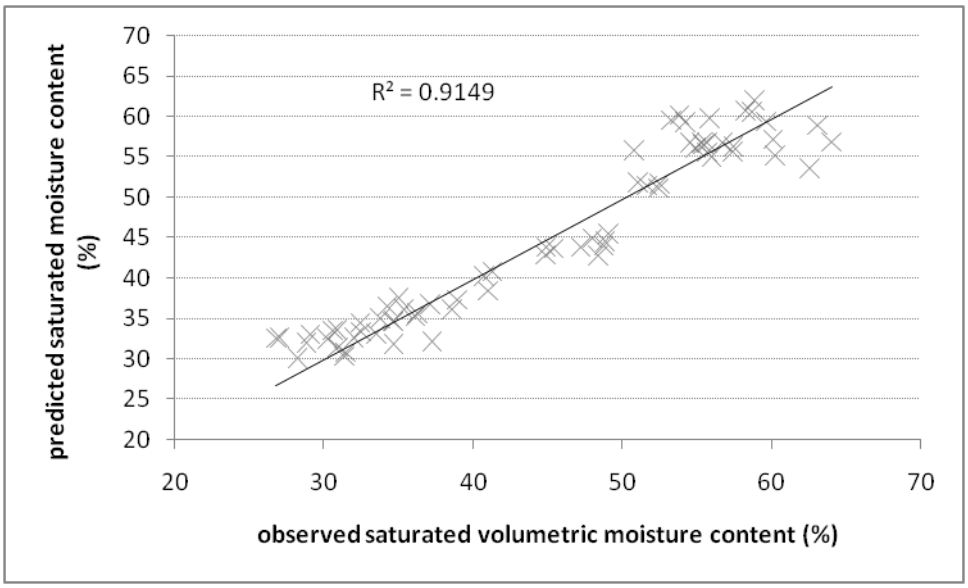

Figure 32. The observed and the predicted saturated volumetric moisture content of the samples at the third saturation, based on the fourth run of the general linear model for repeated measures.

$$mc = 63.65 - 22.56 \times BD + 0.38 \times LL \quad (30)$$

Where: *mc = saturated volumetric moisture content at the third saturation (%)*

BD = initial bulk density (g cm^{-3})

LL = liquid limit (gravimetric moisture content in %)

The equation produced by the model predicted changes in the saturated volumetric moisture content (Equation 30). As bulk density is a more easily accessible and comparable measure of soil structure, the data produced by the model were converted back to bulk densities and compared to the measured bulk densities of the samples at the third saturation (Figure 33).

The correlation between the observed and the predicted data was good (R^2 = 0.8926) and the relationship was close to 1:1. This suggests that the equation produced by the model could be a useful predictor of a soils propensity for structural change with wet/dry cycles.

The input parameters required by the model are: the initial bulk density and the liquid limit of the soil in question. The model then predicts the saturated volumetric moisture content at the third saturation. The equations used to convert volumetric moisture content to bulk density are shown in Chapter 3, Section 3.5.

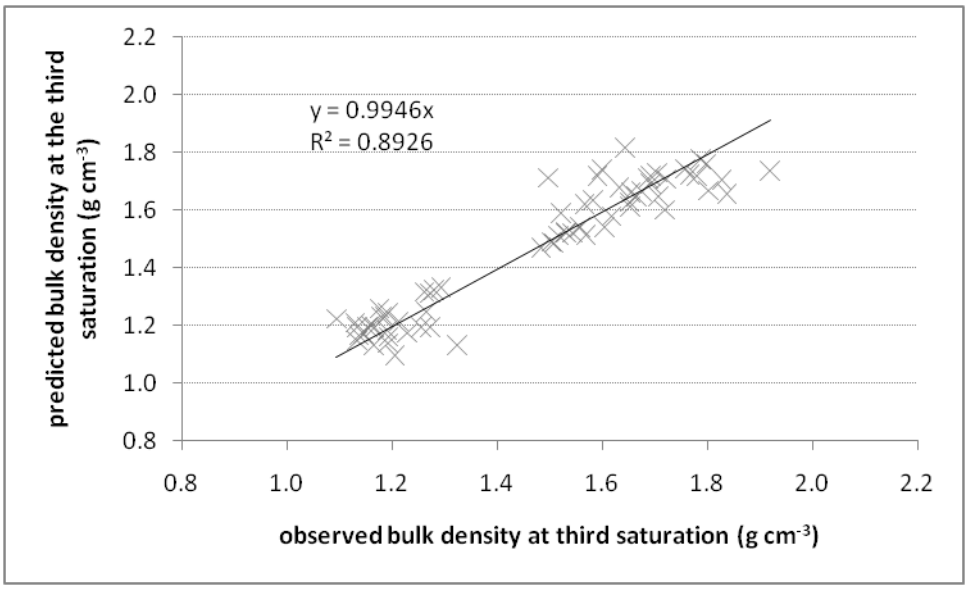

Figure 33. A comparison between the observed bulk density at the third saturation and that predicted by the model.

The model was also used to predict changes to the bulk density of the soil, assuming a greater range of initial bulk densities than were present in the original experiment (Figure 34 and Figure 35). The predictions indicate that the soils had an equilibrium bulk density to which

they would tend. This bulk density was different for all the soils and is shown on the graphs as the point at which the predicted bulk density intersects with the 1:1 line.

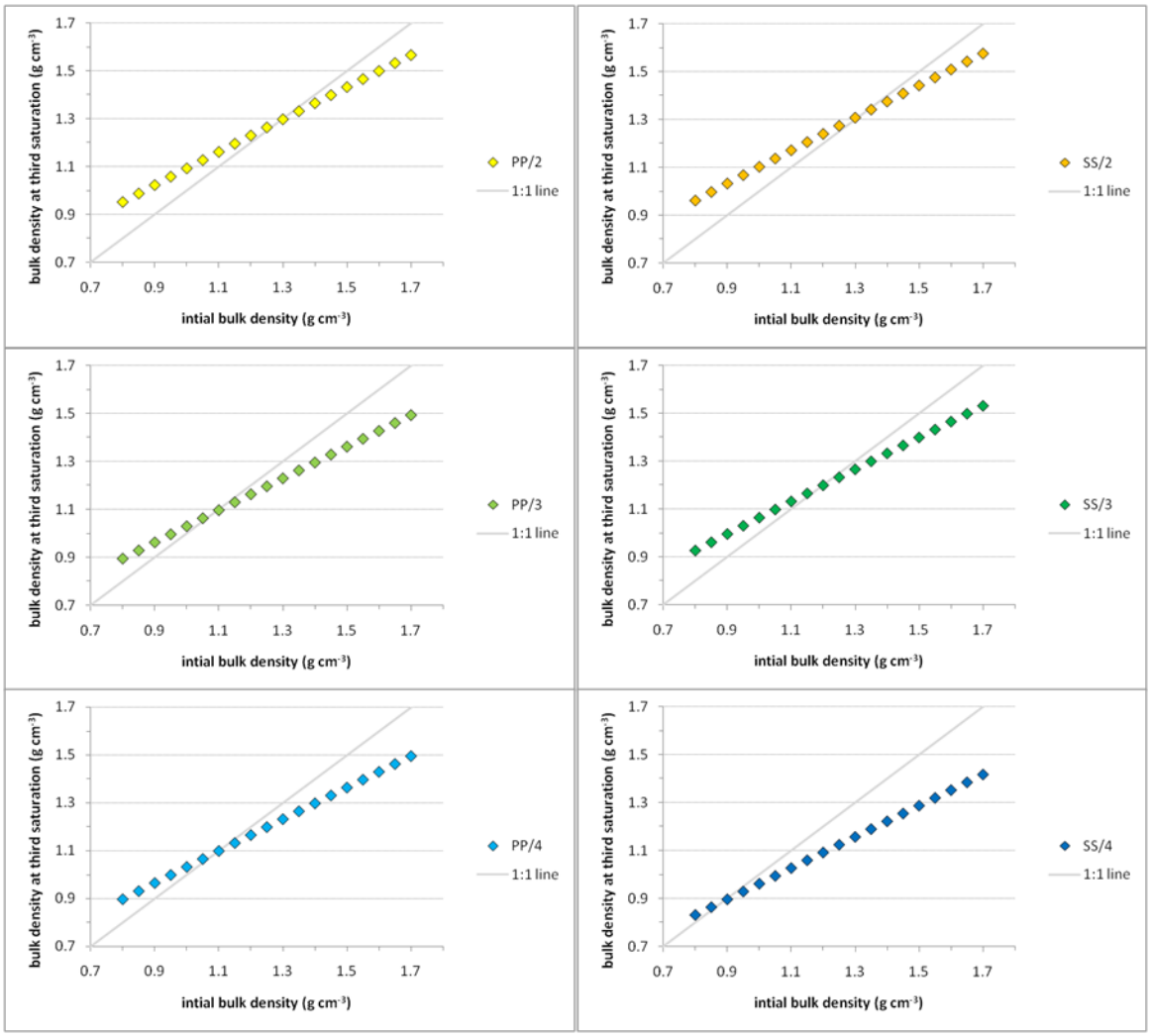

Figure 34. Predicted changes in the bulk density of the clayey soils, assuming a wide range of initial bulk densities.

For the clayey soils, this value ranged from approximately 0.8 (SS/4) to 1.3 g cm^{-3} (PP/2 and SS/2). When the initial bulk density was above these values, the bulk density would be reduced by wet/dry cycles, below this value, the bulk density would increase with wet/dry

cycles. The predicted equilibrium bulk density was much greater for the sandier soils than for the clayey soils and was always in excess of 1.6 g cm^3.

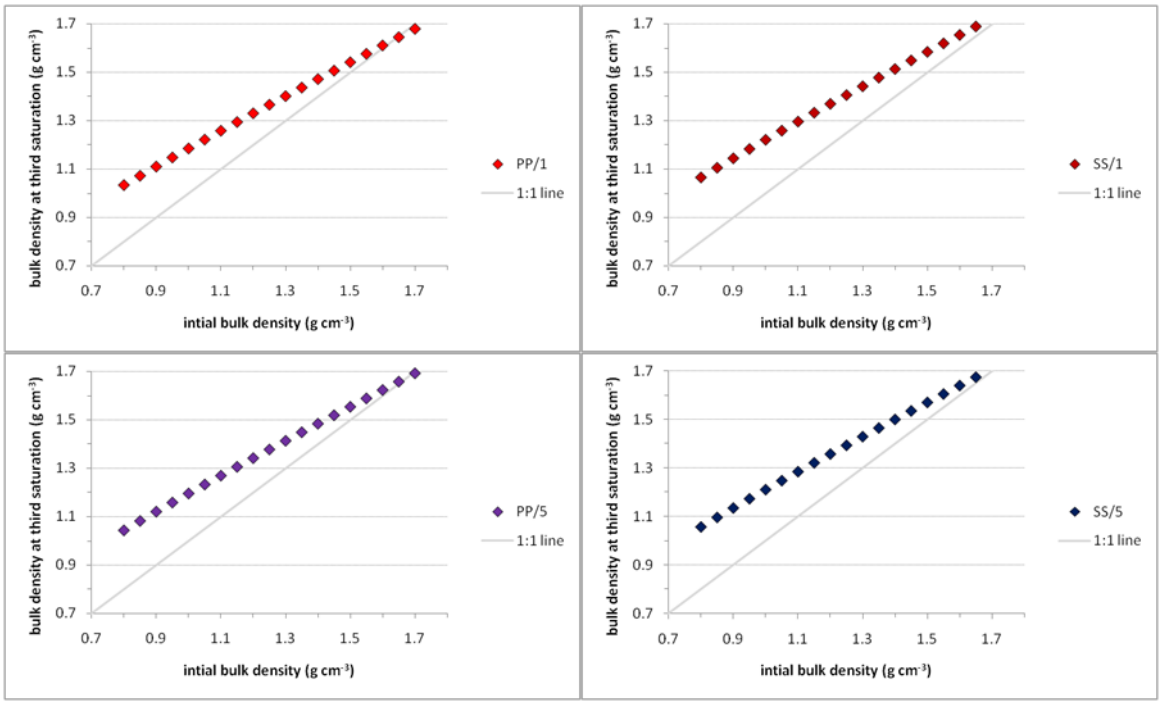

Figure 35. Predicted changes in the bulk density of the sandier soils, assuming a wide range of initial bulk densities.

Although the predicted and the measured values appeared to be strongly correlated over the range of measured values, the model needed to be verified over a wider range of initial bulk densities to ascertain whether the predicted equilibrium bulk densities were an accurate representation of reality. The three clayey subsoils, SS/2, SS/3 and SS/4 were selected for further investigation as the structure of subsoils is harder to engineer than the structure of shallower layers as tillage practices other than subsoiling are restricted to surface layers. The results of the experiments performed on these soils are described in the next section.

4.2.4 Conclusions on changes to bulk density and available water

Changes in the porosity of the soils investigated with wet/dry cycles were highly significant. The interaction between soil and wet/dry cycles and between initial bulk density and wet/dry cycles was also highly significant. The trend of the clayey soils was to decrease in bulk density. Whether this was realised as an increase in aeration at field capacity, an increase in the water available for crop growth, or both varied between soils, however. The trend of the sandy soils was to increase in bulk density, although the direction of the changes in pore size distribution varied between soils. This method has clearly demonstrated that wet/dry cycles affect the porosity of soils under laboratory conditions and that this is not restricted to soils with a high clay content. The model described by Equation 30 accurately predicted changes to the bulk density of the soils, over the range of initial bulk densities investigated, based on the initial bulk density of the soils and their liquid limit. Further verification of the accuracy of the model outside this range of initial bulk densities was, however, required.

4.3 Testing the predictive model against a range of initial bulk densities

The data gathered from the initial investigations was used to create a model, described by Equation 30, which predicted changes to the bulk density of the soils after three wet/dry cycles, as discussed above. This model will be referred to hereafter as the 'structural change model'. The structural change model predictions correlated well with the measured data, but

the soil samples used in the initial investigations had a limited range of bulk densities. Thus the structural change model needed testing with a data set containing a wider range of bulk densities.

Three soils from the original ten were, therefore, selected for further and more detailed investigation. Although it would have been ideal to conduct these experiments on all the soils, time was a limiting factor. By selecting three soils, it was expected that the model could be shown to be valid, opening up the possibility of extension and refinement at a later date. These soils were selected because as clayey soils, a reduction in bulk density of denser samples could be expected (based on the evidence gathered from the initial investigations) and an increase in the density of the loosest samples was predicted by the model. Subsoils were chosen as opposed to soils from the plough layer as the structure of subsoils is more difficult and more costly to engineer (due to greater draft force required to draw the subsoiler resulting in greater fuel consumption) than that of soils located closer to the soil surface and the changes that subsoils experience under natural mechanisms were, therefore, of greater interest.

Samples of the soils selected for further investigation were constructed in the laboratory so that wider a range of bulk densities than present in the initial study could be achieved. The ample rings (7.5 cm diameter by 5.0 cm deep) were positioned in a container that was then loosely filled with a known quantity of sieved soil. Pressure was then applied to the soil surface at a controlled rate and the soil compressed to bulk densities of 1.0, 1.3 and 1.6 g cm^{-3}, the responses to the applied pressure being shown in Appendix 2.

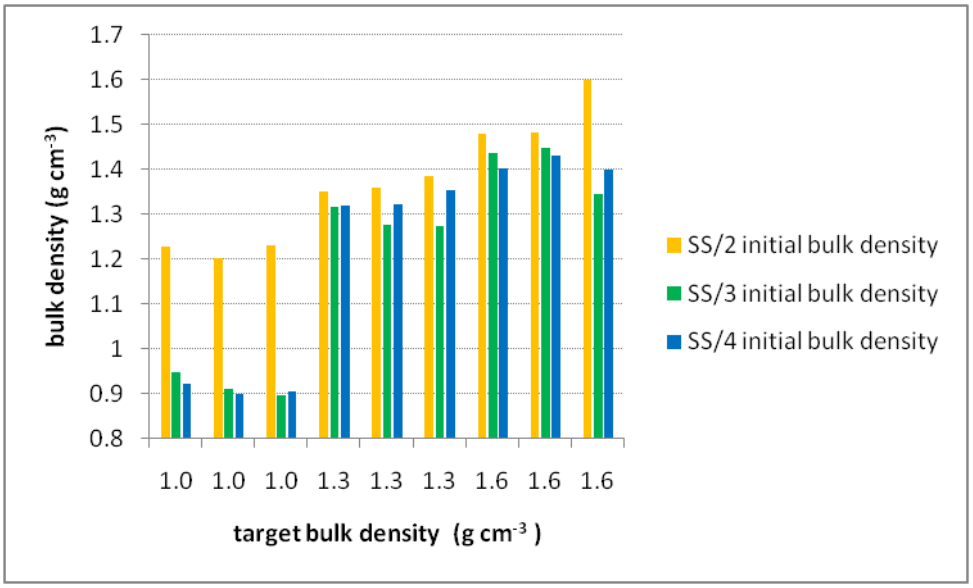

Figure 36. Initial bulk density of individual soil samples plotted against the bulk density to which the soil blocks from which they were taken were compressed.

Figure 36 shows the bulk density of the individual soil samples investigated in this phase of experimentation. The target bulk density was not achieved for all the individual soil samples, despite the overall bulk density of the soil block in the containers being accurately controlled. The disparity between the target bulk density and the achieved bulk density was probably due to the soil being unevenly distributed throughout the soil block from which the individual samples were taken, further compounded by friction within the system during the compaction process, causing compaction to be uneven throughout the soil block. Some rebound may also have occurred when the compressive forces were removed from the soil block. However, a wider range of bulk densities than were available in the initial investigations was attained, so it was possible to consider the effect of initial bulk density on changes to the soil structure

and density with wet/dry cycles in a more comprehensive manner than had been achieved during the initial investigations.

In a similar manner to the initial investigations, the soil samples were subjected to a series of wet/dry cycles. However, drying was achieved by applying a series of consecutively increasing air pressures to the surface of the soil samples and drainage with time was recorded during this process. The drainage data gathered were part of the multi-step outflow experiment described in Chapter 3. The hydraulic parameters estimated from this data are presented and discussed in Sections 4.5 and the full data set presented in Appendix 5.

4.3.1 Changes in bulk density with wet/dry cycles

The bulk density of the samples at their third saturation was estimated by measuring changes to the total volume of the samples. The data are shown in Figure 37. The general trend was a reduction in bulk density (shown by the points on the graph that lie below the 1:1 line), except for an increase where it was very low. This indicates that the soils had an equilibrium bulk density to which they tended as implied by the structural change model described by Equation 30.

The bulk density of SS/2 changed the least with wet/dry cycles, the majority of points being situated close to the 1:1 line (Figure 37). SS/3, which had a similar clay content to SS/2, but a

higher organic matter content (Figure 18), demonstrated a greater reduction in bulk density (over the same range of densities) than SS/2, but not as great as the reduction in bulk density demonstrated by SS/4, which had a higher clay content than the other two subsoils (Figure 17). However, SS/3 did experience a greater increase in bulk density of the loosest samples than SS/4, suggesting that its equilibrium bulk density could be higher than that of SS/4.

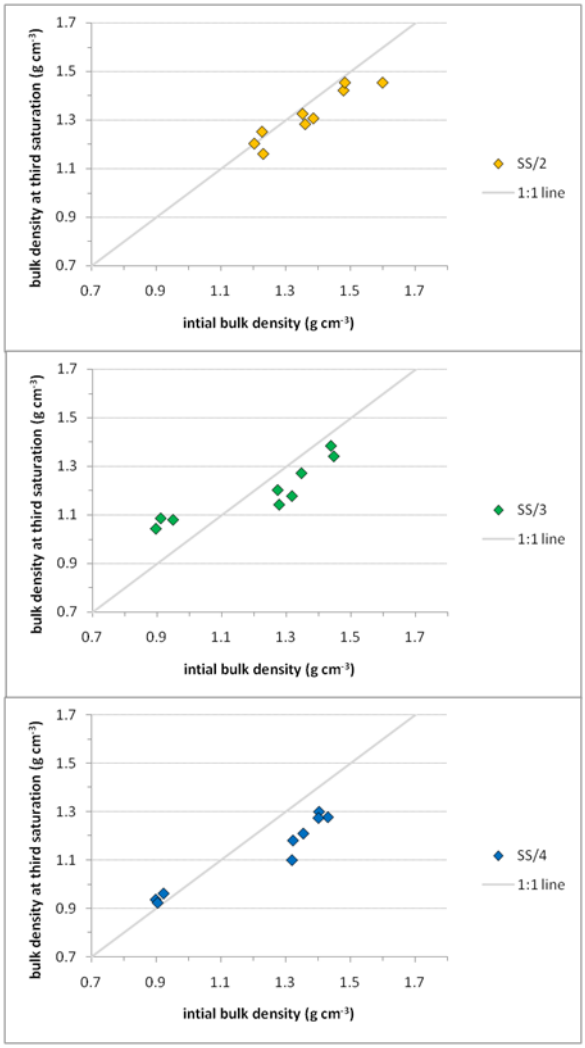

Figure 37. Changes in the bulk density of individual soil samples with wet/dry cycles.

As described in Section 4.2.3, saturated volumetric moisture content can be used as a proxy for investigating changes in bulk density. The general linear model for repeated measures was applied to the changes in the saturated volumetric moisture content (so that the initial bulk density of individual samples could be used as a predictor). Changes with wet/dry cycles were found to be significant at the 95 % level with a probability in excess of 99.9%. The interaction between wet/dry cycles and initial bulk density was also significant at the 95 % level, as was the interaction between soil and wet/dry cycles, implying that how the saturated moisture content changed with wet/dry cycles was dependent on both the soil and its initial bulk density. These findings reflected those of the initial investigations.

The data gathered were compared to the changes in bulk densities that were predicted by the model created using the sand table data (Figure 38). The graphs in the left hand column show the initial bulk density of the constructed samples against their density at the third saturation alongside the modelled data. The graphs in the right hand column show the correlation between the measured data and that predicted by the model. The trend lines have been constrained to run through the point 0,0. The modelled and the measured data appeared to be well correlated and to follow the trends predicted by the model; SS/2 had an R^2 value of 0.81, SS/3 an R^2 value of 0.80 and SS/4 an R^2 value of 0.93. These R^2 values compare well with the R^2 value of the original model (0.89), which supported the supposition that the model would be an appropriate tool to utilise when considering the likelihood and extent of structural change.

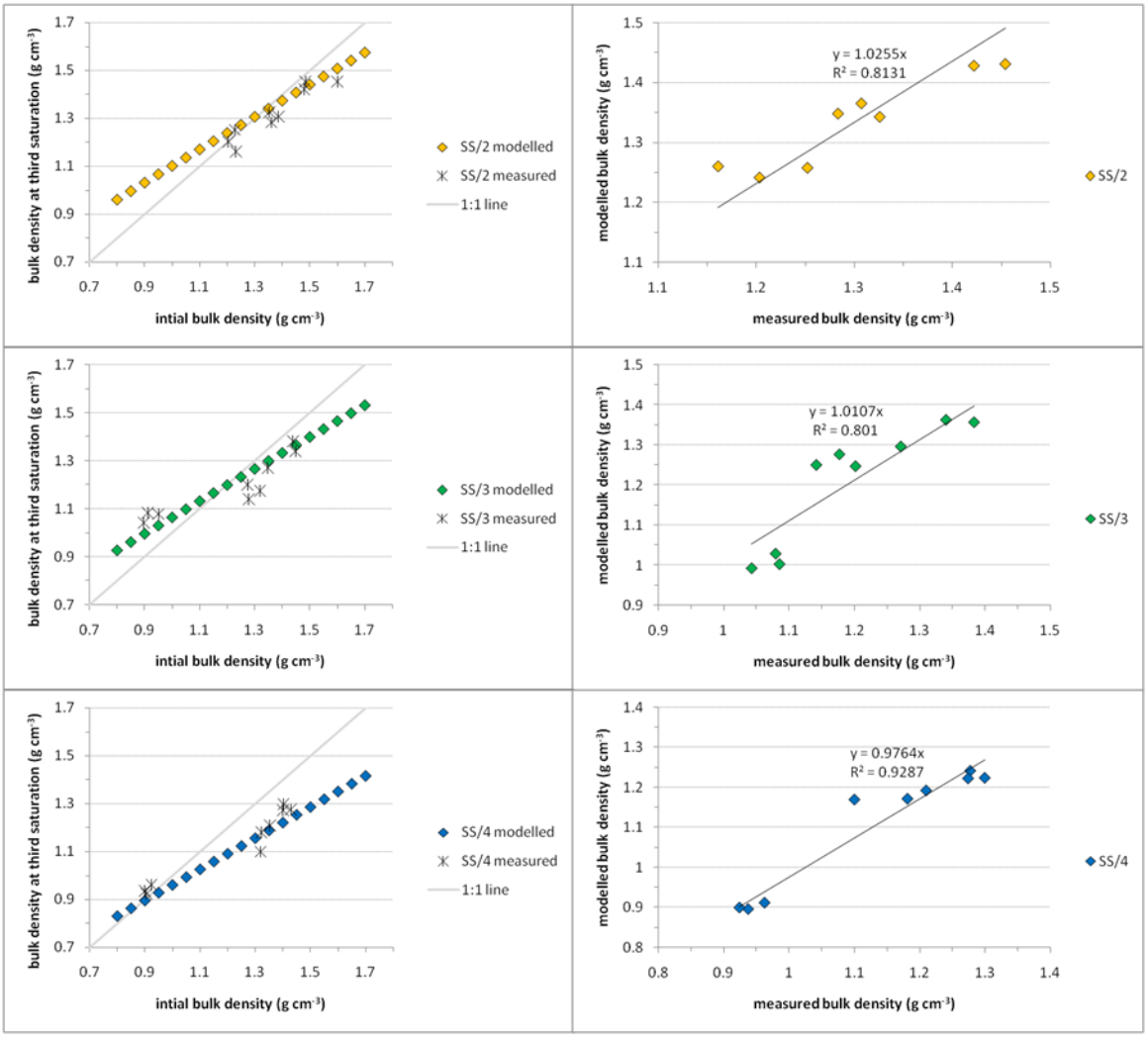

Figure 38. Comparisons between measured and modelled bulk density at the third saturation.

4.4 Equilibrium bulk density and 'D' value

Lipiec and Håkansson (2000) investigated a method of quantifying soil compaction that would be similar for different soil types. They assumed that the most critical factors to over

come, when considering the effects of compaction on plant growth, were aeration and penetration resistance. These factors were related to soil texture via the parameters of D-value and matric water potential. They found that increasing the degree of compactness of a soil (the bulk density as a proportion of the Proctor test at 200 kPa, or the D-value) decreased the volume of water conducting pores more than it decreased total macro-porosity. It also decreased pore connectivity (Lipiec and Håkansson, 2000).The D-value was linearly related to both penetration resistance and air filled porosity for a given moisture content for all soils, although the coefficient of variation varied between 27 and 58 %, depending on water tension, when considering the penetration resistance and between 3 and 28 % when considering air filled porosity.

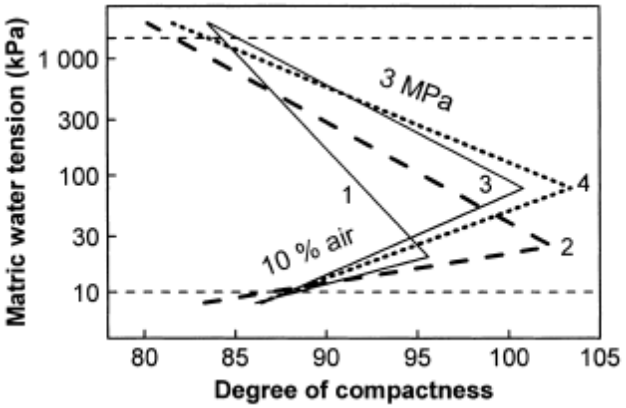

Figure 39. Critical limits for plant growth for 1 - loamy sand, 2 - light loam, 3 - silty loam, 4 - clay loam. Håkansson and Lipiec, 2000.

Emphasis was placed on whether an air filled porosity of 10 % (v/v) and a penetration resistance of 3 MPa (assumed critical limits of soil aeration and rootability) were similarly related to the D-value and matric water tension in the soils studied. When the critical limits for plant growth for the differing soil textures (loamy sand, light loam, silty loam and clay

loam) were plotted on a graph of D-value against matric water potential, they were found to be very similar envelopes (Figure 39). It reduced the maximal differences in intercepts between soils from 13 to 2 % (Håkansson and Lipiec, 2000).

Håkansson and Lipiec (2000) concluded that it would be more informative to site a D-value, rather than an absolute bulk density, when considering soil health in relation to agricultural production. The concept of a D-value does seem to have value as an assessment method as standard figures can be quoted and aimed for. It also informs management practices as it provided recommendations on the range of matric potentials at which crop growth will be optimised, for a given level of compaction and soil texture.

The model generated by the sand table data predicted that there would be an equilibrium bulk density at which no change would be experienced with wet/dry cycles. This equilibrium bulk density was approximately 1.3 g cm^{-3} for SS/2, 1.2 g cm^{-3} for SS/3 and 0.9 g cm^{-3} for SS/4. This prediction seems to have been upheld by the experimental data. Taking the bulk density achieved at 200 kPa from the compression data for SS/2, SS/3 and SS/4 (shown in Appendix 2), a D value of 85 can be estimated. The estimated optimum bulk densities were: SS/2, 1.3 g cm^{-3}; SS/3, 1.2 g cm^{-3}; SS/4, 1.1 g cm^{-3}. These values are close to the equilibrium bulk densities predicted by the model, suggesting that the natural reduction in the bulk density of a soil with wet/dry cycles would result in the soil achieving the optimum bulk density for crop growth for that soil. (However, only the clayey soils had compression data available and the sandier soils, therefore, may not follow the same pattern).

4.5 Changes in saturated hydraulic conductivity with wet/dry cycles

The saturated hydraulic conductivity (K_s) of all the subsoil samples constructed to have a range of initial bulk densities was measured at the beginning of drying cycles one and three for inclusion in the multi-step outflow method and at the end of cycle three for purposes of comparison. Changes in the measured K_s were significant (95 %) between cycles and between initial bulk densities. The direction and magnitude of changes between cycles was also significantly influenced by the initial bulk density of the samples and the soil. There was not, however, any significant difference between how the different soils changed between cycles. Figure 40 shows the mean changes in measured K_s between cycles with bulk density groups (as opposed to measured bulk density). Soil samples of similar bulk density were grouped together into three categories (namely 1.0, 1.3 and 1.6 g cm^{-3}) based on their target bulk densities so that means, and significant differences, could be calculated and clearly displayed and interpreted.

The general trend of the soil samples was to increase in K_s with wet/dry cycles. This trend was not, however, linear. For the least dense soil samples, the increase in K_s was much greater between the third and the fourth saturation than it was between the first and the third saturation. This pattern was also demonstrated by the soil samples in the bulk density group 1.3 g cm^{-3}, although changes experienced by this group were less pronounced. The pattern was not followed by the bulk density group 1.6 g cm^{-3}, however, which demonstrated only a marginal increase in K_s with wet/dry cycles and no appreciable difference in conductivity between the third and fourth saturation.

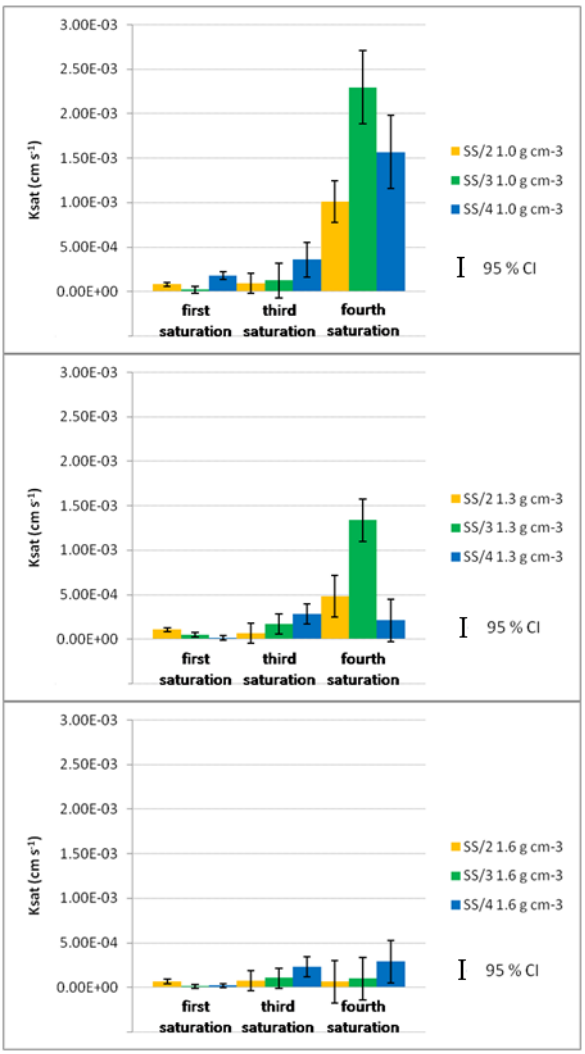

Figure 40. Changes in saturated hydraulic conductivity with time, grouped by initial bulk density.

The soil which demonstrated the greatest increase in K_s was SS/3. This was significant only between the third and the fourth saturation of the two lower bulk density groups and most significant for the least dense bulk density group. SS/2, which had a similar clay content, but

less organic matter than SS/3, also demonstrated a significant increase in K_s between the third and the fourth saturation, but to a lesser degree than SS/3. Again, this increase was most significant for the bulk density group 1.0 g cm^{-3} and not significant for the bulk density group 1.6 g cm^{-3}. SS/4, which had a higher clay content than the other two soils, only experienced a significant increase in K_s in bulk density group 1.0 g cm^{-3}, although the increase within this class was greater than that demonstrated by SS/2.

The greatest increase in K_s was experienced by the least dense samples, despite the fact that the density of these samples increased with wet/dry cycles; there was no linear correlation between bulk density changes and K_s changes for these initially homogenous samples. It would be natural to assume that the increase in K_s of samples that had increased in density would be attributable to preferential flow around the sides of the samples. However, the samples were checked and rechecked for this phenomenon and any potential routes for preferential flow were sealed. The increase in K_s was, therefore, better explained by the fact that the samples had little or no structure at the beginning of the experiment. As the samples dried and the soil particles were drawn together, aggregates may have been formed which, while increasing the overall density, would have created larger pores between the aggregates than had previously existed. This could explain why the saturated hydraulic conductivity of the soils increased, despite the density of the samples also increasing. This is corroborated by the analysis of crack emergence, reported and discussed in detail in Section 4.8, which showed that even the least dense samples developed surface cracks during the wetting and drying process.

The soil samples in the medium bulk density group experienced a reduction in bulk density and increased K_s with wet/dry cycles. This could be explained by the cracking of the soil samples that occurred during both the wetting and the drying processes. These cracks, which remained apparent at saturation, provided routes for faster flow through the soil samples. (Surface cracking during the wetting and drying process is discussed in Section 4.8).

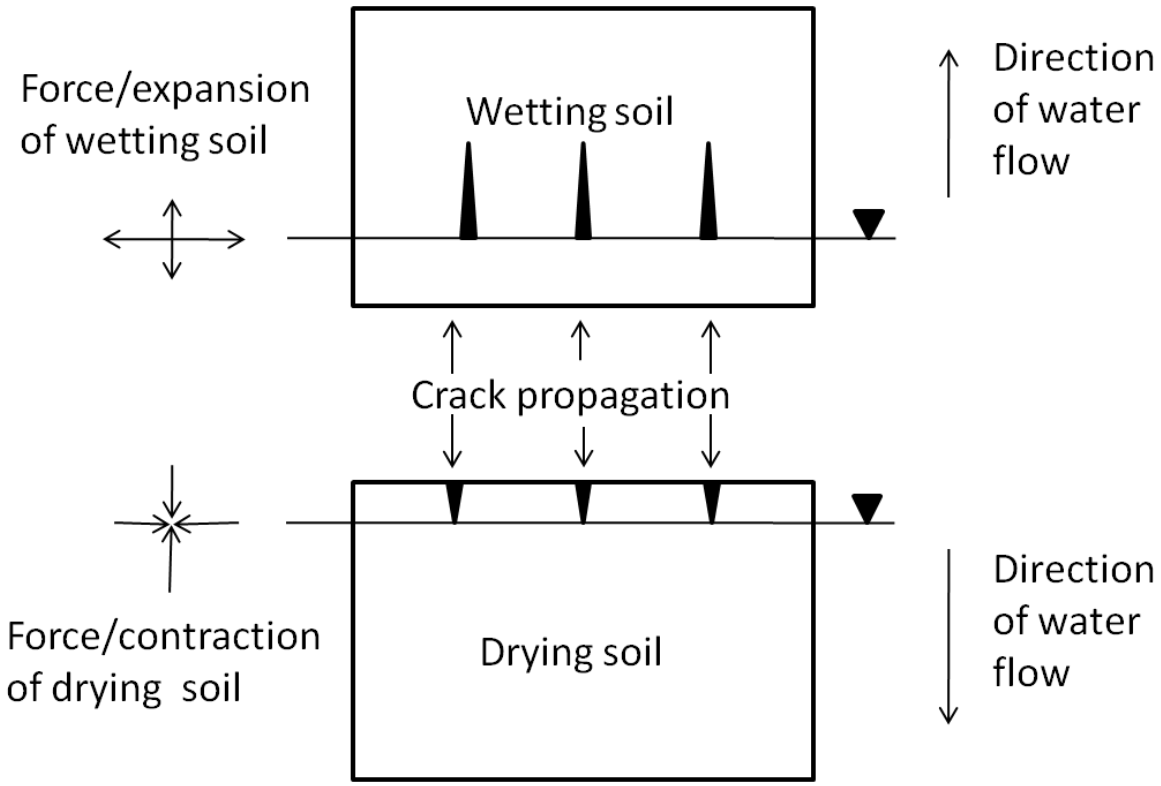

Figure 41. Diagram showing the direction of crack propagation during both the wetting and the drying phase.

The increase in K_s for the medium density group was less than for the loosest samples. This could have been because the density of these samples at the fourth saturation was still greater than that of the equilibrium bulk density, hence it is likely that the soil aggregates were

tending to increase in volume, concomitantly decreasing the volume of the pores between them. This would also be true of the densest samples, but to a greater extent, hence the smaller changes to the saturated hydraulic conductivity with wet/dry cycles. The densest samples were closer to their theoretical maximum bulk density than the other samples and, therefore, did not shrink to the same extent during the drying phase as the other, more loosely packed samples and the potential for crack generation during this phase was less.

There was a difference in the magnitude of changes in K_s between wet/dry cycles, the increase over a wet/dry cycle being greater between saturation 3 and 4 than between saturation 1 and 3. Figure 41 shows how cracking may occur during the wetting and the drying phases of a cycle. During the wetting phase, the rapidly expanding soil is causing the still dry soil to crack, due to the disparity in volume between the wet and dry soil. Some shear failure could also occur at the wet/dry interface if wetting were sufficiently rapid. During the drying phase, the contracting soil is cracking, again due to the disparity in volume between the wet and dry soil. Some shear failure could occur at the interface if drying were sufficiently rapid. It may have been the case that, between saturations 1 and 3, the cracks that were generated did not extend to the full depth of the soil profile. Between saturations 3 and 4, cracks that had been generated during previous wet/dry cycles became connected, causing the greater increase in K_s than had already been recorded. Another explanation for the more rapid increase in K_s between saturations 3 and 4 than during previous cycles is that as the overall density of the samples decreased, the potential for cracking during the drying phase increased, hence increasing the network of cracks.

4.6 Changes to the water retention and hydraulic conductivity functions

The results described in the following section are those obtained from the multi-step outflow experiments (see Chapter 3) that simultaneously optimised the parameters of the moisture release and hydraulic conductivity curves, estimated from transient outflow data. During the drying phase of the wet/dry cycles, the soil samples were dried by incrementally applying controlled air pressures to the surface of the samples, followed by a period of air drying. Cumulative outflow from the samples was logged with time and applied pressure. The consecutive outflows with time were then input into the HYDRUS-1D model. This model used the outflow data to estimate the parameters of the van Genuchten-Mualem Equation (Equation 12) by minimising the objective function between measured outflow data and that predicted by Richards' Equation (Equation 5).

HYDRUS-1D returned the individual parameters of the van Genuchten-Mualem Equation (Equation 12), with 95 % confidence intervals based on the difference between the unknown 'true' value and the results of the Levenberg-Marquard non-linear minimisation method (Equation 26) (Šimůnek *et al.,* 2005). These were used to compare the parameters between cycles. Comparisons between the parameters estimated during the first and the third drying phase of the wet/dry cycles and, therefore, changes to the pore size distribution and the hydraulic conductivity of the soils, are made in the following sections, followed by a more general discussion of the statistical relationships between the parameters of the van Genuchten-Mualem Equation (Equation 12) and other measured soil properties. The behaviour of each subsoil will be described separately, using one sample of each an example.

Three replicates of three subsoils of three bulk densities, totalling 27 samples in all, were analysed, however a small number of samples were subject to experimental problems such as blocking of the semi-permeable membranes; eight samples of SS/2, seven samples of SS/3 and eight samples of SS/4 were successful. The full set of graphs and tables describing these samples is shown in Appendix 5.

4.6.1 SS/2

Sample 3 of SS/2 is shown as an example of SS/2 in Figure 42. This sample had an initial bulk density of 1.23 g cm^{-3}, which decreased to 1.16 g cm^{-3} with wet/dry cycles. There was a shift to the left in the pore size distribution with wet/dry cycles and an increase in the hydraulic conductivity at all applied pressures, reflected in the more rapid draining demonstrated during cycle 3. All eight of the samples of SS/2 drained more rapidly during cycle 3 than cycle 1, regardless of whether they experienced an increase or a decrease in bulk density. The majority of the SS/2 samples experienced a significant change to their hydraulic conductivity. The nature of this change, however, varied between samples. The samples with initial bulk densities of less than approximately 1.23 g cm^{-3}, and the sample with the highest initial bulk density, increased in hydraulic conductivity at low tensions and decreased at higher tensions; the hydraulic conductivity of samples with more moderate initial bulk densities (between approximately 1.39 to 1.48 g cm^{-3}) changed very little at low tensions but

increased at higher tensions. Changes to the hydraulic conductivity did not appear to be purely attributable to changes to the volume of pores conducting water.

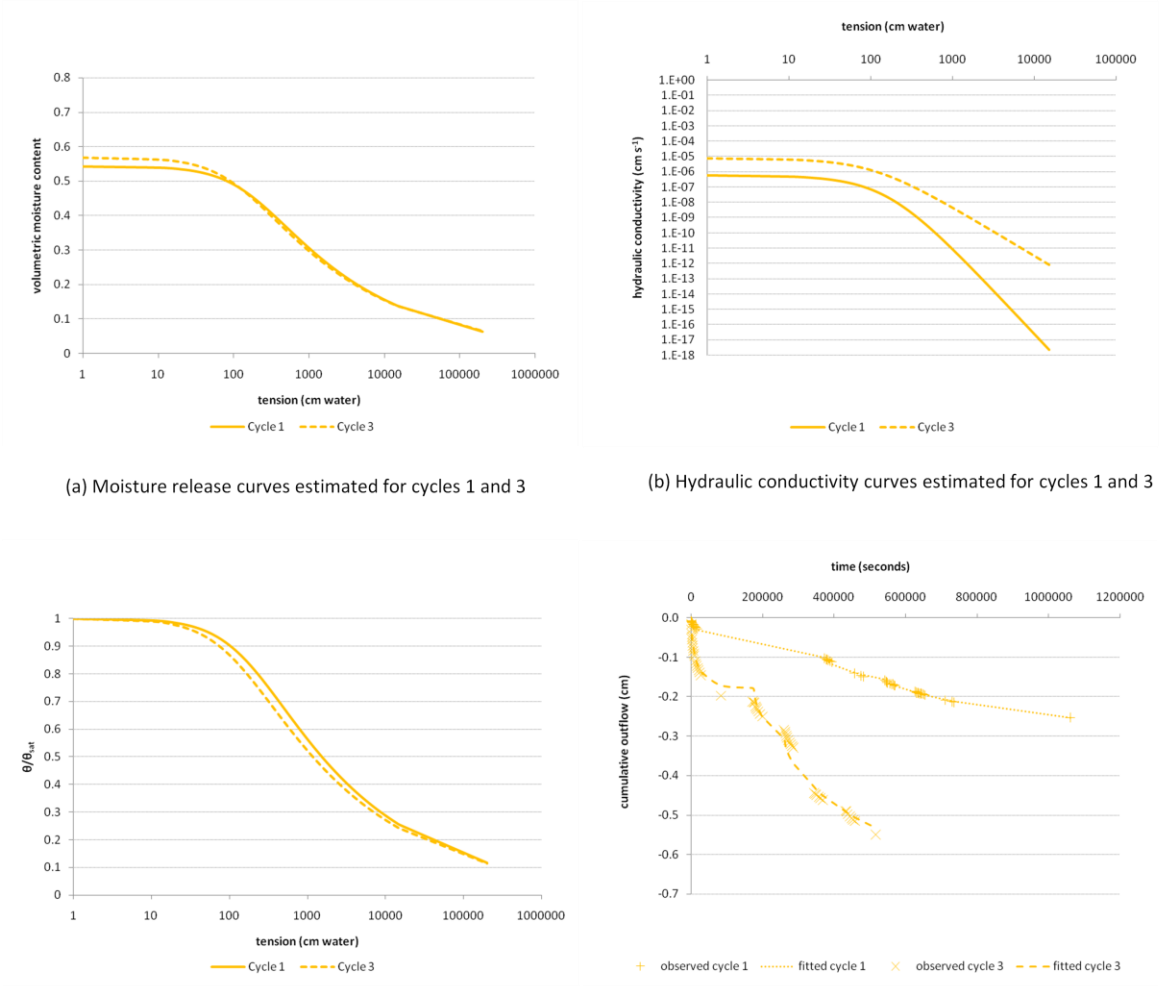

(a) Moisture release curves estimated for cycles 1 and 3

(b) Hydraulic conductivity curves estimated for cycles 1 and 3

(c) Relative moisture release curves estimated for cycles 1 and 3

(d) Measured drainage data for cycles 1 and 3

Figure 42. Hydraulic properties of sample 3 of SS/2 (initial bulk density 1.23 g cm^{-3}) estimated with HYDRUS-1D.

An example of this can be seen in Figure 42 (the other eight samples are described in Appendix 5). Graph (a) shows that the proportion of pores that were water filled at tensions greater than 1 m of water decreased with wet/dry cycles, while graph (b) shows that the conductivity of these pores increased. It was surmised that increases in the connectivity of the pore network were at least partially responsible for increases to the hydraulic conductivity; decreases in hydraulic conductivity demonstrated by some of the other samples (shown in Appendix 5) were attributed to particles released into solution during the wetting phase blocking or partially blocking smaller pores. In the majority of cases, the parameters K_s and l were modelled to have significantly increased with wet/dry cycles.

Another interesting observation that was made regarding the changes to the porosity of the soil samples as that there appeared to be changes to the total volume of pores of all effective diameters, not just those that were visible as surface cracks. The dynamics of these changes, however, varied between samples in an irregular manner. Those samples that increased in bulk density had proportionally less macro-pores during cycle 3 than cycle 1, those that decreased in bulk density increased their proportion of macro-pores. However, there was no clear pattern in the changes to the proportions of meso- and micro-pores. The changes to the total volume of pores of the sample described by Figure 42 are shown in Figure 43. This figure shows that there was a reduction in the total volume of water filled pores at tensions greater than 1 m of water. This suggests that some of the smaller pores may have expanded to increase the volume of larger pores.

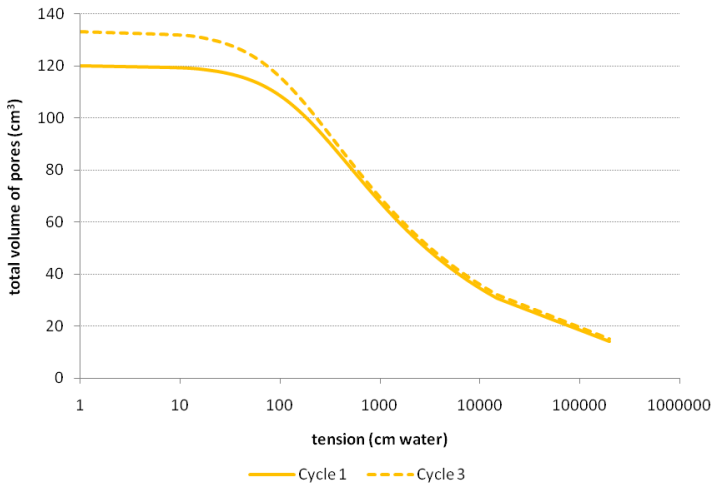

Figure 43. Total volume of water filled pores of sample 3 of SS/2 during cycles 1 and 3.

4.6.2 SS/3

Changes to the samples of SS/3 were very similar to those demonstrated by SS/2, but tended to be an exaggerated reflection (all the samples of SS/3 are shown in Appendix 5). The first sample of SS/3, for example, had a low initial bulk density (0.90 g cm^{-3}) and increased substantially in bulk density with wet/dry cycles (1.04 g cm^{-3}). The only parameter change modelled as significant was the value of *n*. Figure 44 indicates that there was no change to the pore size distribution of the sample. This is further illustrated by Figure 45, which shows that pores of all sizes were lost.

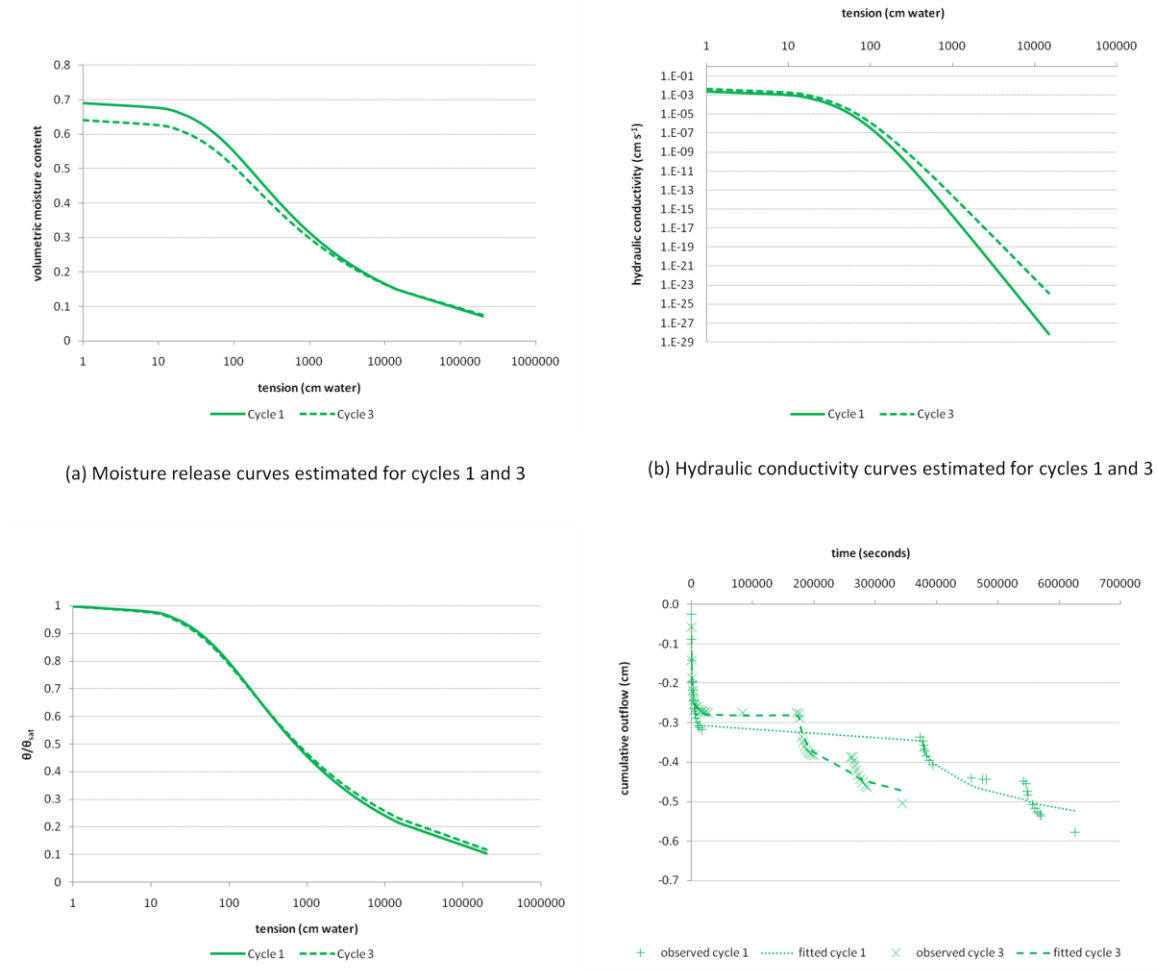

(a) Moisture release curves estimated for cycles 1 and 3

(b) Hydraulic conductivity curves estimated for cycles 1 and 3

(c) Relative moisture release curves estimated for cycles 1 and 3

(d) Measured drainage data for cycles 1 and 3

Figure 44. Hydraulic properties of sample 1 of SS/3 (initial bulk density 0.90 g cm^{-3}) estimated with HYDRUS-1D.

This is perhaps surprising as it might have been assumed that it would be the largest pores alone that would collapse and in so doing, increase the proportion of smaller pores. This does not appear, however, to have been the case. Smaller pores may have been lost through blocking by particles released into solution during the wetting phase. They may also have been lost as the surface tension of the water drew soil particles together during the drying

phase, closing small pores and forming denser soil aggregates. The soil particles within these newly formed aggregates could have bonded via electrostatic forces and by the glues released by soil micro-organisms. These aggregates would then have remained in tact during the subsequent wetting phases, resulting in an overall decrease in total porosity, but little change to the pore size distribution.

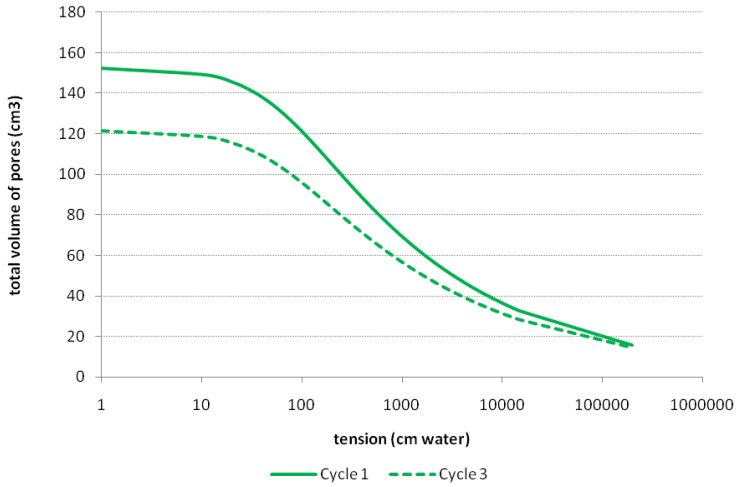

Figure 45. Total volume of water filled pores of sample 1 of SS/3 during cycles 1 and 3.

Not all the samples of SS/3, SS/2, or SS/4 (4.6.3) that increased in bulk density retained their original pore size distributions, however (see Appendix 5). Figure 46 is a simplified hypothetical visualisation of how the pore structure may have changed during the wetting and drying process. In scenario 1, the loss of porosity relative to the initial state is explained by

the complete collapse of a number of the largest pores, whilst the remaining pores are unchanged. The dark circles represent pores of various sizes. The lighter circles represent porosity that has been lost as the soil sample became more dense with wet/dry cycles. In both scenario 1 and scenario 2, the total volume of larger pores has been reduced and this has altered the pore size distribution so that there are a greater proportion of smaller pores. In scenario 1 this effect has been realised as the loss of just a percentage of the larger pores. In scenario 2, pores of a wider variety of sizes have collapsed or partially collapsed, resulting in the same apparent changes to the total volume of the larger pores and the same changes to the pore size distribution. This seems unlikely, as samples lost pores of all effective diameters during the wetting and drying process. It is also hard to explain why some pores should be so susceptible to change and others not at all. Scenario 2 illustrates a slightly different course of events; rather than the complete collapse of pores, a greater number of pores have partially collapsed. Some of the smallest pores have collapsed sufficiently to have a negligible diameter. These pores have been replaced by the partial collapse of larger pores. This has led to the total volume of smaller pores remaining unchanged overall, whist the total volume of larger pores has been reduced. This seems the more likely scenario as this behaviour better reflects the behaviour of the samples.

The changes to the hydraulic conductivity of the example of SS/3 described here, implied by Figure 44, were concentrated at higher tensions where conductivity increased with cycles. This suggests that, although there was no increase in the proportion of conducting pores, pore connectivity was increased. This is supported by the drainage data which shows more rapid drainage after the first drainage step (Figure 44). This could be explained by larger pores,

rather than collapsing completely, reducing in effective diameter and therefore creating a more extensive pore network of smaller pores. If the very largest pores present at the beginning of the first wet/dry cycle were connected to each other by smaller pores, their reduction in effective diameter would have little effect on the saturated hydraulic conductivity, but would increase the unsaturated hydraulic conductivity (Figure 47).

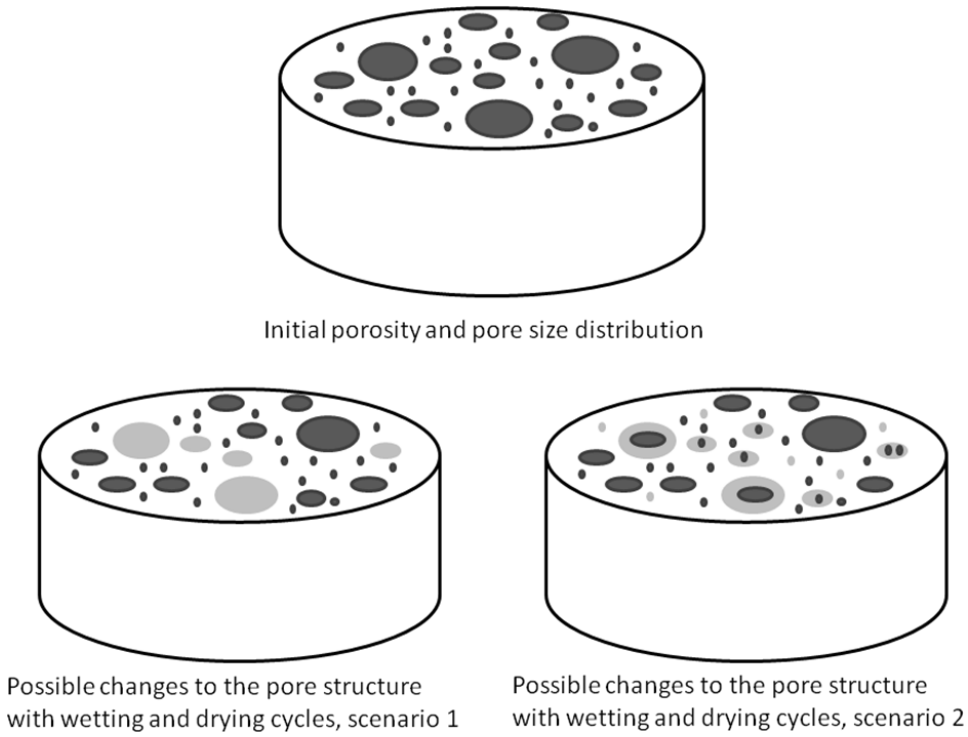

Figure 46. A simplified model of soil structure.

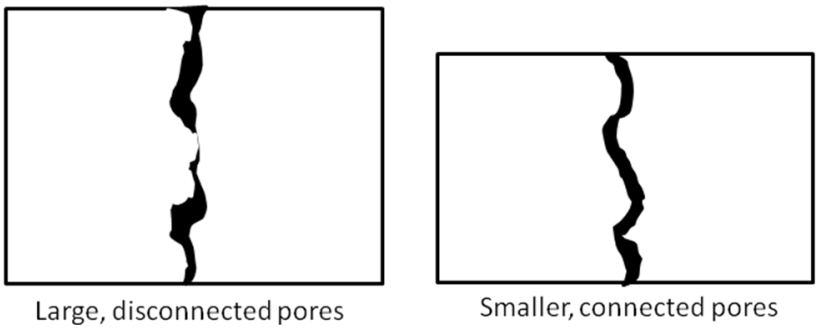

Figure 47. A simplification of the possible changes to the pore network that would result in a loss of total porosity but an increase in hydraulic conductivity.

The diagram on the left of Figure 47 shows a hypothetical soil sample before experiencing wet/dry cycles. It has low density and large pores. However, these pores are not well connected. The diagram on the right of Figure 47 shows the same hypothetical soil sample after experiencing wet/dry cycles. It has increased in density/reduced in total porosity. However, the remaining pores are better connected and, therefore, hydraulic conductivity is increased.

All the samples of SS/3 exhibited some degree of change in the measured bulk density and in the measured drainage rates. Changes to the pore size distribution tended to be less pronounced than changes to the total volume of water filled pores at any applied pressure. This may imply that at least some of the observed changes at pressure were due to normal shrinkage, i.e. that the same pores were modelled as being water filled at a range of applied pressures as the effective diameter of the pores was reduced with water loss. The parameter α was modelled to have significantly increased for approximately half the samples, but changes

in the parameter *n* were rarely modelled to be significant. The soil samples also experienced alterations to their modelled hydraulic conductivity over a range of applied pressures; the majority of samples were modelled to have increased significantly their values of K_s, similarly to SS/2. These changes could not be explained purely by changes to the porosity or the pore size distribution, but implied changes to the pore connectivity and/or tortuosity, although changes to the parameter *l* were only modelled to be significant in three cases.

4.6.3 SS/4

An initially dense example of SS/4 that experienced a decrease in bulk density with wet/dry cycles is shown in Figure 48 (initial bulk density 1.43 g cm^{-3}). Although the total volume of water filled pores of all effective diameters increased, the pore size distribution was altered resulting in a greater proportion of macro-pores. This change in the pore size distribution was reflected in the changes to the hydraulic conductivity of the sample, although the changes were exaggerated; where there was a small reduction in the proportion of pores that conducted water at tensions greater than 1 m of water, there was a large decrease in the rate of conductivity. This may have been the result of a number of processes: the release of particles into solution during the wetting phase blocking smaller pores, thereby making them discontinuous; larger, newly created pores may have bisected smaller pores and hence interrupted their continuity; newly created smaller pores had not formed a continuous network.

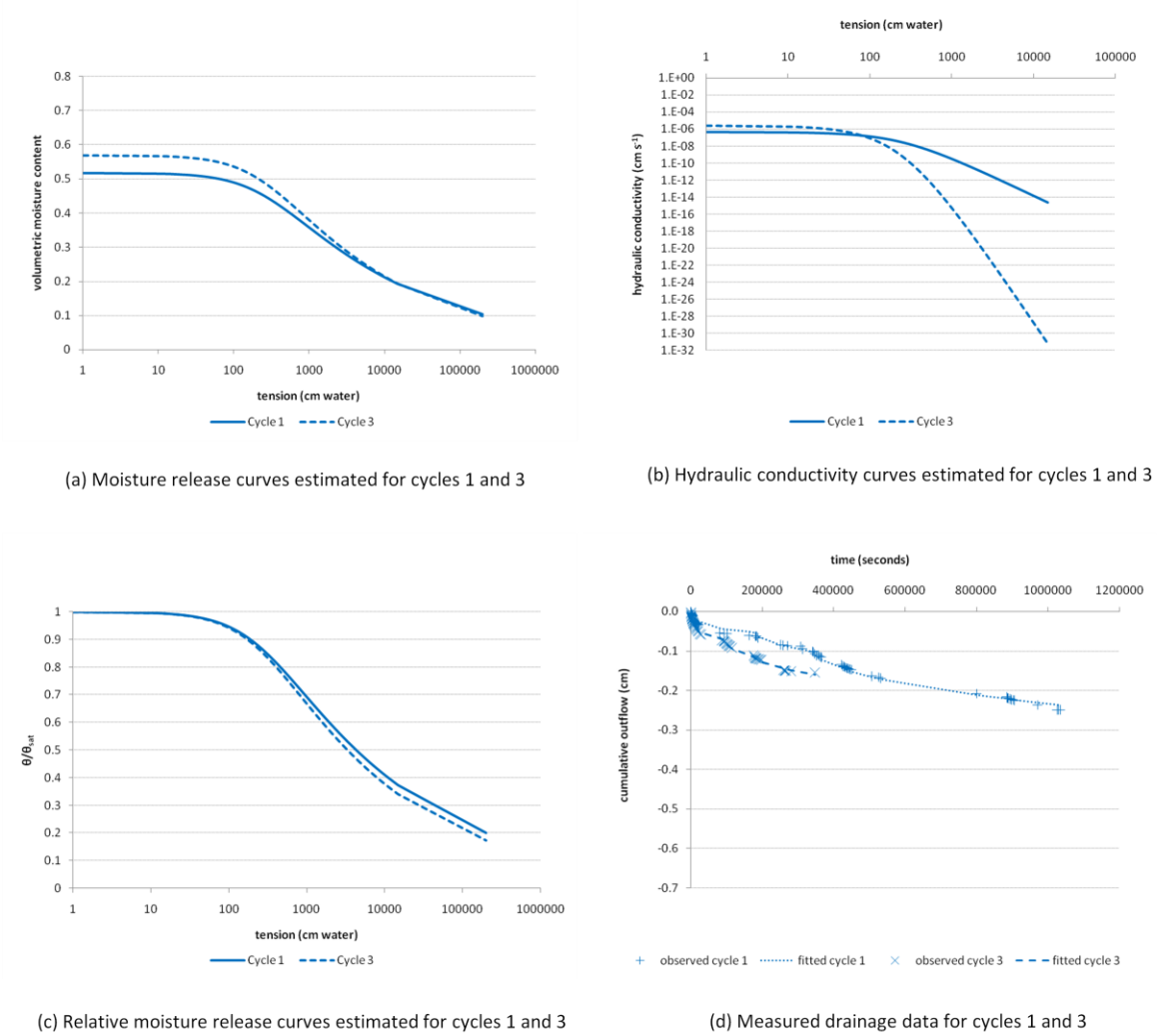

(a) Moisture release curves estimated for cycles 1 and 3

(b) Hydraulic conductivity curves estimated for cycles 1 and 3

(c) Relative moisture release curves estimated for cycles 1 and 3

(d) Measured drainage data for cycles 1 and 3

Figure 48. Hydraulic properties of sample 8 of SS/4 (initial bulk density 1.43 g cm^{-3}) estimated with HYDRUS-1D.

Unlike SS/2 or SS/3, changes to the all the parameters of the majority of the samples of SS/4 were modelled to have increased significantly with wet/dry cycles, apart from α which was modelled to have been significantly reduced with wet/dry cycles (see Appendix 5). However, changes to the porosity, pore size distribution and hydraulic conductivity followed very similar patterns.

In general, these experiments have demonstrated that changes to the structure of the soils studied were not confined to changes in macro-porosity visible as cracks, but extended to changes in the whole pore network. These experiments also implied that changes to the hydraulic conductivity of the soils at all tensions was more pronounced than changes to the volume of conducting pores and not necessarily reflected by changes to the total volume of conducting pores, tending to increase regardless of changes to porosity. This is similar to the findings of the saturated hydraulic conductivity experiments, described and discussed in Section 4.5, which also showed that saturated hydraulic conductivity increased, even when porosity decreased.

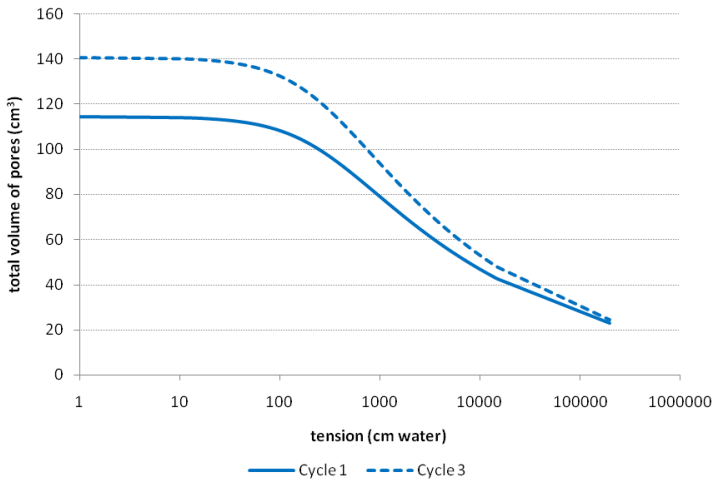

Figure 49. Total volume of water filled pores of sample 8 of SS/4 during cycles 1 and 3.

4.6.4 General statistical trends in changes to the parameters of the van Genuchten-Mualem Equation with wet/dry cycles

The following section discusses the changes in α and n of the van Genuchten-Mualem Equation (Equation 12) experienced by the three subsoils with wet/dry cycles estimated by HYDRUS-1D, and looks at statistical relationships that were found between these parameters, how they changed with wet/dry cycles, and measured soil properties. Changes to the modelled saturated hydraulic conductivity (K_s) are not discussed here as this parameter was measured separately and reported and discussed in Section 4.5. The parameter l was compared to the area of surface cracks at various stages of the wetting and drying process as it was thought that the flow of water through the soil samples would relate to surface cracking. Statistical analysis of the parameter l is therefore reported and discussed in Section 4.8.5.

The results of the analysis of α and n were very varied. The parameter α was higher during cycle 3 than cycle 1 for SS/2, where the difference was estimated to be significant by HYDRUS-1D. (Two samples from the densest group of samples and one sample from each of the other density groups had significantly different values of α). There was no obvious pattern to the changes in the value of α of the SS/3 samples, but more of the samples changed significantly. Only one of the loosest samples of SS/4 changed its value of α significantly. However, all of the mid-density samples did, although two out of the three replicates exhibited reduced values of α. The trend of the densest samples was to increase their value of α, but this was only significant in one case.

Linear models for repeated measures were used to investigate the data set. Statistically, bulk density was not significant in determining how α changed with wet/dry cycles, although bulk density was significant in determining the value of α i.e., α did tend to be lower when bulk density was higher when each data set was considered separately, but the changes in the bulk density were not reflected by the changes in α. These results are surprising as a reduction in bulk density implies a concomitant reduction in the air entry pressure (and, therefore, an increase in α) and an increase in K_s. However, the measured increases in K_s between the beginnings of drying cycles 1 and 3 were not significant in many cases (Section 4.5). The data gathered from the initial experiments also showed that, while the saturated volumetric moisture content increased, so did the moisture content at 0.5 and 1.0 m of water, implying that the increase in porosity was not exclusively in the macro-pore range. This phenomenon would explain why the air entry pressure was not necessarily reduced when the bulk density was reduced.

The parameter α was also compared to the other soil parameters with the general linear model for repeated measures. The initial bulk density and one other parameter were included in each run of the model as there were insufficient degrees of freedom to consider all the parameters simultaneously. Coarse sand was found not to be significant in determining the value of α, but was significant at the 90 % probability level in determining the changes in α with wet/dry cycles. Medium texture sand was not significant in determining α, but was significant at the 95 % probability level when considering changes with wet/dry cycles. Fine sand was significant in determining changes with wet/dry cycles at the 90 % probability level, as was

the total sand content. Silt content was not significant. Clay content was found to be highly significant in dictating how the value of α changed with wet/dry cycles, but not the value of α. The liquid limit and the plasticity index were found to be significant at the 90 % probability level in determining the changes to α with wet/dry cycles, but not the plastic limit, nor the shrinkage limit. The oxidisable organic matter was significant at the 90 % probability level in determining the changes in the value of α with wet/dry cycles, but not the organic matter lost on ignition, nor the CEC. The most significant factors in determining the changes in the value of α with wet/dry cycles were clay, closely followed by the medium texture sand. As SS/4 appeared to experience the greatest change in α, it can be concluded that a higher clay content will result in a greater change in α with wet/dry cycles. Only bulk density was significant in determining the value of α.

As n increases, so does the slope of the van Genuchten-Mualem curve (although α also affects the slope of the graph; as α increases, the gradient of the slope decreases). The parameter n is, therefore, thought to relate to the pore size distribution of the soil. For two samples with the same value of α, the graph with the steepest slope (higher value of n) is retaining more water at low matric potential and, therefore, has a greater concentration of smaller pores. However, if the soil with the higher value of n also had a much higher value of α, it would drain more readily and retain less water at low matric potentials.

The parameter n was not significantly different for any of the samples of SS/2 and the values for both cycles were mostly identical. The trend for SS/3 was a decreased value of n for the third cycle of the loosest samples and an increase in n between cycle one and three for the

other two density groups, although this was only predicted as significant by HYDRUS-1D for two of the loosest samples and one sample from each of the other two density classes. SS/4 followed a similar pattern, significant for none of the loosest samples, all of the mid density samples and one of the densest samples.

These trends suggest an increase in the volume of smaller pores for the denser samples and a decrease in the volume of small pores of the loosest samples. The trend in the denser samples is reflected by the data gathered from the initial investigations that showed that the increase in porosity was not purely in the macro-pore range. The trend in the loosest samples could be caused by water menisci drawing the soil particles together to form aggregates as the soil dried. If these aggregates remained in tact when the soil was rewetted, larger, coarser pores would have been formed between the aggregates. This would result in less water being retained by the soil at low matric potentials and, therefore, a decrease in *n*.

All the soil particle size fractions (apart from coarse sand) were found to be highly significant (95 %) by the general linear model for repeated measures in determining the changes in *n* with wet/dry cycles. The most significant particle size was fine sand, closely followed by the total sand fraction. These particle sizes were also significant in determining the value of *n*, as was the silt fraction, but not the clay fraction. The plastic limit, liquid limit, plasticity index and shrinkage limits were all highly significant in determining both the value of *n* and the way it changed with wet/dry cycles. Neither the organic matter lost on ignition, the oxidisable organic matter, nor the cation exchange capacity were significant in determining the changes with *n* with wet/dry cycles, but the cation exchange capacity and the organic matter lost on

ignition were significant in determining the value of *n*. Overall, subsoil two experienced the least change in *n* and subsoil four the most (except for the loosest samples where subsoil three changed the most). Subsoil four was the soil with the highest values of the significant parameters.

4.6.5 Conclusions on the results of the transient outflow experiments

All three soils experienced an increase in bulk density when the initial bulk density was low and a decrease in bulk density when the initial bulk density was higher, although the turning point for this varied between soils, as already discussed in the sand table results. The initial investigations also suggested that is was not merely the saturated porosity that was affected by wet/dry cycles, but the water filled porosity at tension. This has been reflected in the modelled results which suggested that there were pores created, or lost, of all effective diameters. Whether the changes to the parameters α and *n* were deemed significant by the model run through HYDRUS-1D varied considerable between samples and no obvious patterns were evident. However, the change in bulk density of the samples dictated that these parameters must have changed. Modelled changes generally suggested that when bulk density increased, a greater proportion of macro-pores were lost than meso- or micro-pores, changing the pore size distribution; when bulk density decreased, a greater proportion of macro-pores were created than micro-pores. Some of the micro-porosity may even have been lost. This was thought to be due to the expansion in the effective diameter of existing pores.

Horn and Dexter (1989) similarly found that wetting and drying of a soil changed its pore size distribution. After two years, they found that their irrigated loess retained more water in the macro and micro-pores. The soils considered by this study, however, tended not to retain more water in their micro-pores. They behaved more like the soil with 48 % clay content studied by Pires *et al.* (2005) that tended to increase in macro-porosity with wet/dry cycles. The other soils studies by these authors, however, increased in the proportion of water filled pores at tensions above 1 m for the soil with 28 % clay and 15 m for the soil with 43 % clay.

A factor which complicates the interpretation of the data presented so far is the affect that the shrinkage behaviour of the soils has on their pore size distributions. The soils explored here are shrink swell soils; as the soils dry out they shrink, as the wet up they swell. The relationship between the moisture content and shrinkage of these soils is not known. If the soils shrank completely normally, the decrease in their total volume would be exactly equal to the volume of water lost. If soil shrinkage was not completely normal, the reduction in porosity would be normal at high moisture contents and would then pass through a phase where the reduction in total volume was proportional to, but less than, the volume of water lost. This means that the porosities shown in the previously explored moisture release curves were only true for any one moisture content i.e., for any given moisture content shown, the water filled porosity is correct, but the air filled porosity is over estimated. It also implies that the creation of a single pore that was shown as in increase in the saturated porosity may also have been evident as an increase in the porosity at higher tensions as the pore shrank with loss of water.

It is also the case that the volumetric moisture contents were calculated based on the volume of the samples at saturation. This could be considered erroneous. However, in a field situation, this effect is reduced because the lateral shrinkage of the soil will not alter the total volume of the soil-plant root system, it merely alters the porosity of the system as the lateral shrinkage is realised as cracks, or, indeed, macro-pores. Vertical shrinkage will, however, reduce the total volume of the soil system and vertical swelling will be the only means by which the volume of the soil will increase as the soil is effectively confined in the lateral direction by the surrounding soil. Subsoils will be also confined in the vertical direction, the magnitude of these confining forces being dependent upon the depth of the soil considered, or the overburden pressure. Counteracting the overburden pressure is the swelling pressure. The swelling pressures of these soils are in need of further investigation in order to relate these findings to the field situation at different depths with greater accuracy. However, these findings are still indicative of the soils' potential for natural restructuring after a disturbance event.

Changes to the hydraulic conductivity of the soils were more varied and did not consistently reflect the changes in the pore size distribution. The disparity in the modelled changes to the pore size distribution and the hydraulic conductivity suggest the wetting and drying process had a large influence on the connectivity/tortuosity of the pore network. It was thought that wetting the samples may also have released some particles into solution which then became trapped in smaller pores, blocking them and, therefore, reducing conductivity even when the proportion of pores of the relevant sizes increased. Conversely, wetting and drying may have

increased the connectivity of the pore network in some instances, increasing the conductivity even when there was no increase in the proportion of relevant pores.

Considering purely the measured drainage data, SS/2 consistently drained faster during the third drying cycle than the first and this was generally more pronounced at lower applied pressures. Where samples of SS/3 increased in bulk density, the rate of drainage decreased; where a reduction in bulk density occurred, the rate of drainage, especially at low pressure, increased. A similar pattern of behaviour was observed in SS/4, although in some cases, drainage continued at a faster rate for longer during the third drainage than during the first drainage cycle before tailing off, rather than the initial rate itself increasing. It would be reasonable to assume that an increase in drainage rate would equate to a concomitant increase in infiltration rate. Sarmah *et al.* (1996) observed an increase in the infiltration rate of a compacted Vertisol with wet/dry cycles. An increase in infiltration rate of snig tracks on various soil types was also observed by Croke *et al*. (2001), but this was not found to be the case in the areas where *Eucalyptus* had been generally harvested.

The results of this and other studies do seem to support the proposition, however, that reduced infiltration rate (a negative consequence of a degraded soil structure) will be alleviated by wet/dry cycles. They also suggest that wet/dry cycles will increase the proportion of macro-pores in a soil, thereby increasing the water available for crop growth. It has been shown that it is possible to estimate the parameters of the van Genuchten-Mualem Equation (Equation 12) relatively rapidly from transient outflow experiments. The ideas resented here could, therefore, be extended to include a wider range of soils. A modelling

exercise, similar to that applied to the changes in bulk density, could then be executed, relating measurable soil parameters to changes in measures of structure such as the slope of the of the moisture release curve at the inflections point, suggested by Dexter (2004) to be an informative quantifier of soil structure.

4.7 Dexter's index of soil physical quality

Dexter (2004) suggested a method for assessing the quality of a soil's structure, based on the slope of the soil's moisture release curve (Equation 31). A critical, minimum value of 0.035 was suggested for the modulus of the slope of the curve at the inflection point, based on a graph of gravimetric moisture content against the natural log of the soil water tension, and referred to as *S*.

$$S = \left| -n(\theta_s - \theta_r).\left[\frac{2n-1}{n-1}\right]^{\left[\frac{1}{n}-2\right]} \right| \qquad (31)$$

Where: S = *Dexter's S value*

θ_s = *the saturated gravimetric moisture content*

θ_r = *the residual gravitational moisture content*

n = *the parameter from the van Genuchten-Mualem Equation.*

Dexter said that the value of *S* was a measure of a soil's microstructure and that this controls many key soil physical properties such as the ability of roots to penetrate the soil. The critical minimum value of *S* was proposed based on comparisons of clay content, bulk density and the presence of roots made by Jones, 1983, in a review of root growth in soils at a water potential of -330hPa (Dexter, 2004). Soils predicted by Jones (1983) to have 'many roots' were calculated by Dexter (2004) to have an *S* value in excess of 0.03, based on pedo-transfer functions.

The moisture release curves estimated by HYDRUS-1D based on volumetric moisture contents were converted to gravimetric moisture contents and the *S* value was calculated for all the samples (Figure 50). SS/2 is shown in yellow, SS/3 in green and SS/4 in blue. The solid bars denote cycle 1 and the hashed bars denote cycle 3. SS/4 experienced the greatest increase in the value of *S* of the moderately dense samples and a similar change in the value of *S* to SS/3 of the most dense samples. SS/2 displayed very little change in the value of *S* of any of the density classes.

Dexter (2004) makes no mention of an upper critical value for *S*. However, logic suggests that there must be one. A soil with a very high value of *S* would have a very low moisture content at low soil water tensions and would, therefore, dry out quickly and store very little water for use by a crop. The trend exhibited by the loosest samples in this study was to decrease their value of *S*. This effect was greatest for SS/3, which contained less clay than SS/4, but which had a higher organic matter content.

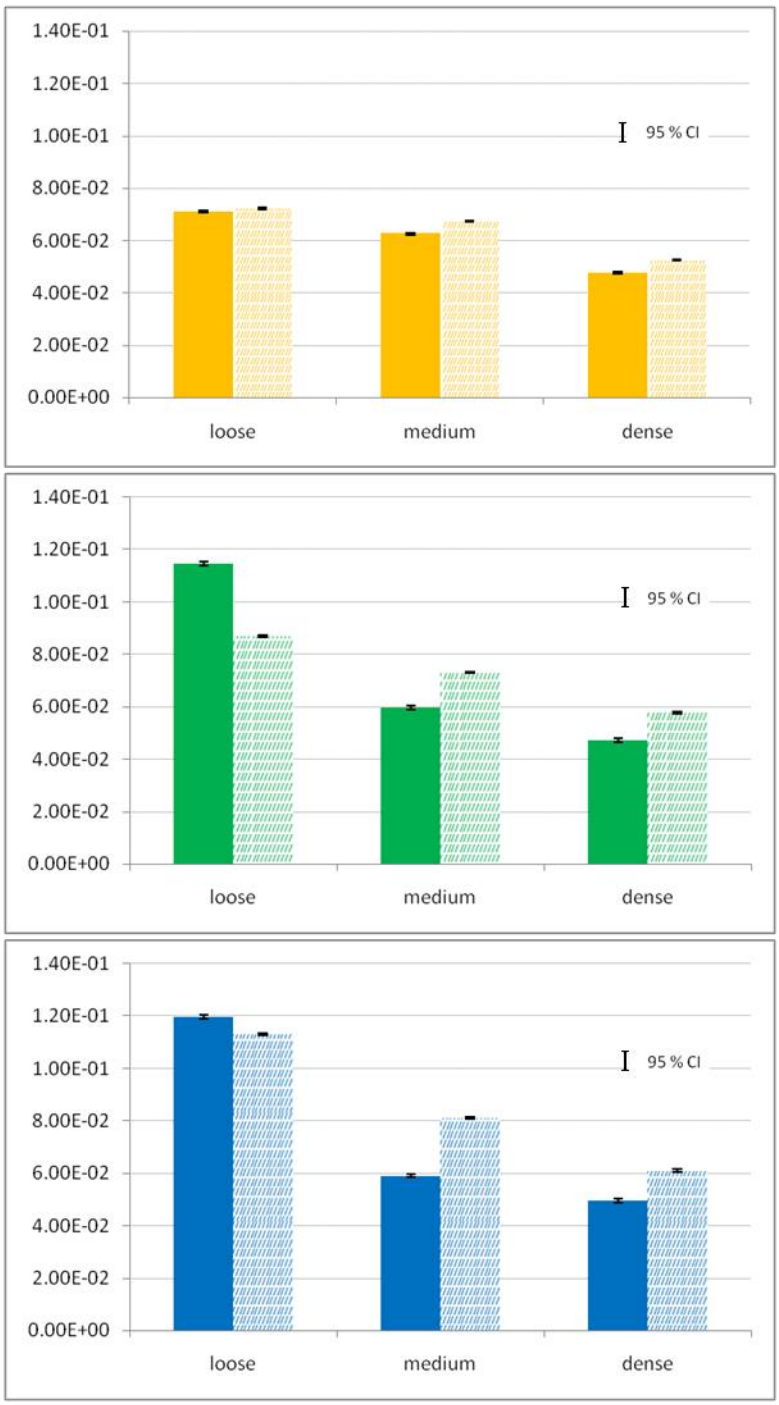

Figure 50. Changes in Dexter's Soil Quality Index between cycles 1 and 3.

Perhaps surprisingly, all the samples returned a value that was greater than Dexter's suggested critical value (Figure 50) and closer to those he predicted for sandy loam soils, based on pedo-transfer functions. However, Dexter also discussed the effect of organic matter on the value of *S*. When the *S* value was plotted against organic matter content of soils from an experimental site at Rothamstead (clay content 25 %, sand content 10 %) a positive, linear relationship was found (Dexter, 2004); as the organic matter increased, so did the value of *S*. When the levels of organic matter exceeded 4 %, the value of *S* exceeded 0.035. SS/2 had close to 4 % organic matter and SS/3 and SS/4 had approximately 5.5 and 5 % organic matter content respectively. This could explain some of the discrepancy between the values predicted by Dexter and those calculated for the samples in this study. Dexter also correlated *S* with the organic matter content of a sandy loam soil from Poland and found that the organic matter content had a greater effect on the value of *S* for this soil. The critical organic matter content for this soil (4 % clay, 71 % sand) was 1.2 % (Dexter, 2004). As the soils in this study had a higher sand content than those from Rothamstead, it could be that their organic matter content was sufficient to raise the value of *S* above the critical value.

4.8 Surface crack generation with wet/dry cycles

During the process of wetting and drying the soil samples, the surface of the samples were photographed with a digital camera. This was done when the soil samples had equilibrated at an applied pressure of 0.1 m of water and after they had been air drying for five days at the end of the drying cycle. These images were then analysed for the total percentage of the

surface area that was crack using the imageJ programme. The method is described in detail in Chapter 3. The full set of thresholded images can be seen in Appendix 6. The area of surface cracks, along with visual inspection of the photographs, provided an indication of the propensity of the soils to crack, when this cracking was occurring (during the wetting or the drying phases, or both) and the cracking pattern (whether it was a few large cracks, or many small cracks). The following section will explore this information and attempt to relate it to the changes in the hydrology and the bulk density of the soil samples.

4.8.1 The cracking of SS/2

A photograph showing an example of SS/2 is shown in Figure 51. The top row, going from left to right, are 0.10 m tension events 1, 2 and 3. The bottom row are the air dry events 1, 2 and 3. The full set of thresholded images is shown in Appendix 6. SS/2 exhibited a clear trend of an increasing area of cracks with wet/dry cycles (Figure 52) which was shown to be highly significant by the statistical analysis (Section 4.8.5). All three density classes followed this trend. All the samples were smooth when initially created. They were then saturated, had their saturated hydraulic conductivity measured, followed by being equilibrated at an applied pressure of 0.1 m of water. At this stage, the first photographs were taken. Figure 52 shows that this in itself was enough to produce some cracking in all the samples, although the extent of this was less for the densest samples.

Figure 51. An example of one of the samples of SS/2 (initial bulk density 1.48 g cm^{-3}).

This suggests that the wetting phase of the first cycle caused some cracking to occur. The samples were wetted rapidly from the bottom up. Soil swelling occurs when water is attracted to and enters the inter-layer space of 2:1 type clays, which are held weakly together by oxygen to oxygen and cation to oxygen bonds, forcing the layers apart (Brady and Weil, 1999).The disparity between the density of the portion of the soil sample that had adsorbed water molecules and that which had not as the water level rose up the soil profile may have caused the soil to rupture along planes of weakness, resulting in cracking that was visible on

the surface of the soil samples. This process has been illustrated diagrammatically in Figure 41, Section 4.5.

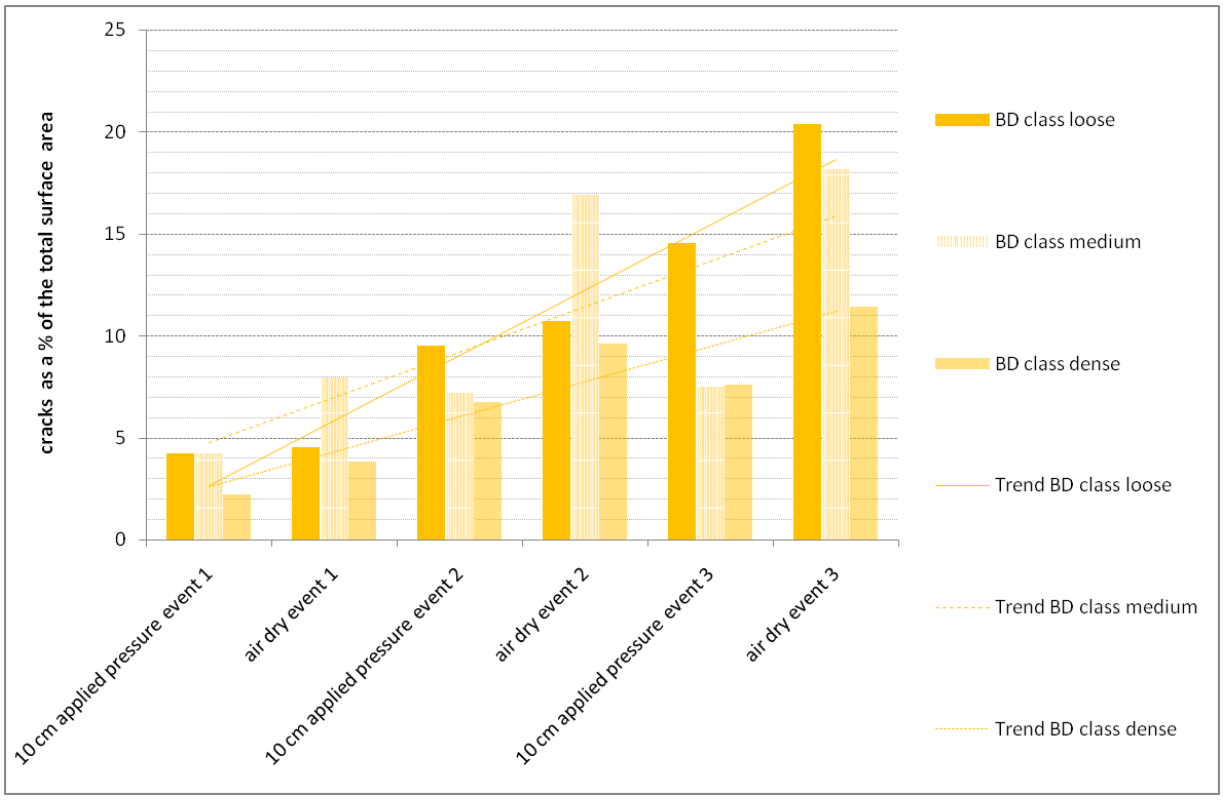

Figure 52. The total area of crack on the surface of the samples of SS/2, averaged for the initial bulk density class.

After this first wetting event, the different behaviour of the bulk density classes became more apparent. At the first air dry event, the bulk density class that exhibited the smallest increase in the area of surface cracks was the loose class. The total area of cracks was marginally greater, however, than that of the densest samples, but much less than the medium bulk density class, both of which experienced an increase in the total area of surface cracks.

At the second wet photographing event, the total area of cracking had increased relative to the area of cracks on the surface of the first air dried event of the loosest and the densest samples, but the medium density class samples displayed a marginal decrease in the area of cracks relative to their air dry state. However, the areas of cracks on the surface of the medium density samples were still greater at air dry event 2 than 1.

This suggests that the second wetting phase resulted in additional cracks emerging in the loosest and the densest samples, but not necessarily in the medium density group. This could be because the moderately dense samples had developed a pore structure closer to the equilibrium state predicted by the initial investigations than the looser or the denser samples and were, therefore, demonstrating behaviour closer to a stable and repeated pattern of cracking along well defined planes of weakness on drying and those cracks closing up upon wetting/swelling.

In contrast, the soil samples in the medium density class exhibited the greatest total area of surface cracks, and the greatest increase in said, at the second air dry event. All the samples, however, experienced some increase in the area of surface cracks. The total area of cracks of the loosest samples was greater than the densest samples, but the increase in cracks relative to the previous wetting event was less. The increase in the area of cracks from the previous drying event was very similar for all three density classes.

The area of cracks apparent on the surface of the medium and the dense classes dropped back to that of second wet event at the third wet event. The area of cracks of the loosest samples, however, increased relative to all previous measuring events. This implies that the wetting phase was still causing rupturing of the loosest samples, possibly because the bonds formed between the soil particles were weaker in the loosest samples and, therefore, posed less resistance to the rising water table and were more easily forced apart. An analogy with a muffin baking in the oven could possibly be drawn here. As the muffin cooks, the air within the muffin expands, causing the muffin to rise and the surface of the muffin to crack. As the water level rose in the soil sample, the sample expanded (but due to water adsorption rather than air expansion) and the tenuous bonds at the soil sample surface broke and cracks appeared. An explanation for why the medium and the dense samples did not behave in the same way as the loosest samples is the confining nature of the rings in which the samples had been formed. As the samples swelled, they made contact with the sides of their receptacles at a lesser moisture content than the loosest samples. The continued swelling of the samples beyond this point would have forced the cracks closed, despite the samples being unconfined in the vertical direction.

The third air drying event caused the samples in all the density classes to crack more than all previous events. The loosest samples cracked the most, the densest samples the least. An explanation for this would be the proximity of the density of individual soil aggregates to the maximum density achievable for that soil. If the loosest soil samples still had loose aggregates, these aggregates could have been drawn together by the surface tension of the water menisci, creating denser aggregates with large spaces, or cracks, in between. In

contrast, the denser soil samples would have denser soil aggregates that would experience a lesser increase in density with drying. The gaps that appeared between these aggregates (the cracks) would, therefore, have been smaller than for the loosest soil samples.

In general, Figure 52 appears to suggest that for SS/2 at least, the wetting phase of the wet/dry cycle is important for crack generation, and that this phenomenon is more pronounced the less structure the soil has and the looser it is. The greatest area of surface cracks was observed in the loosest samples, least in the densest samples, although when the samples were wet, the area of surface cracks was very similar between the densest samples and those of medium density. At the third dry event, the loosest samples had an average area of surface cracks of approximately 20 %, the medium density samples approximately 18 % and the densest samples approximately 11 %.

4.8.2 The cracking of SS/3

An example of the photographs taken of SS/3 is shown in Figure 53 (the top row, going from left to right, are 0.10 m tension events 1, 2 and 3; the bottom row are the air dry events 1, 2 and 3) and the full set of thresholded images is shown in Appendix 6. Similarly to SS/2, SS/3 demonstrated a clear and significant trend of an increasing area of surface cracks with wet/dry cycles (Figure 54). Unlike SS/2, however, the changes were less evenly spread across

cycles; there was a greater increase in the area of surface cracks between cycles 1 and 2 than between cycles 2 and 3.

Figure 53. An example of SS/3 (initial bulk density 1.44 g cm^{-3}).

Also similarly to SS/2, the first wetting event caused some cracking to occur. This was most pronounced, however, in the soil samples of medium density, rather than the loosest samples. The first air drying event resulted in no increase in the area of cracks for the loose and the dense samples and only a marginal increase in the area of cracks of the moderately dense samples. All the classes, however, experienced an increase in surface cracks at the second wetting event, relative to the first drying event. The medium density soil samples experienced

the greatest increase in the area of surface cracks, followed by the loosest samples and the densest samples cracked the least.

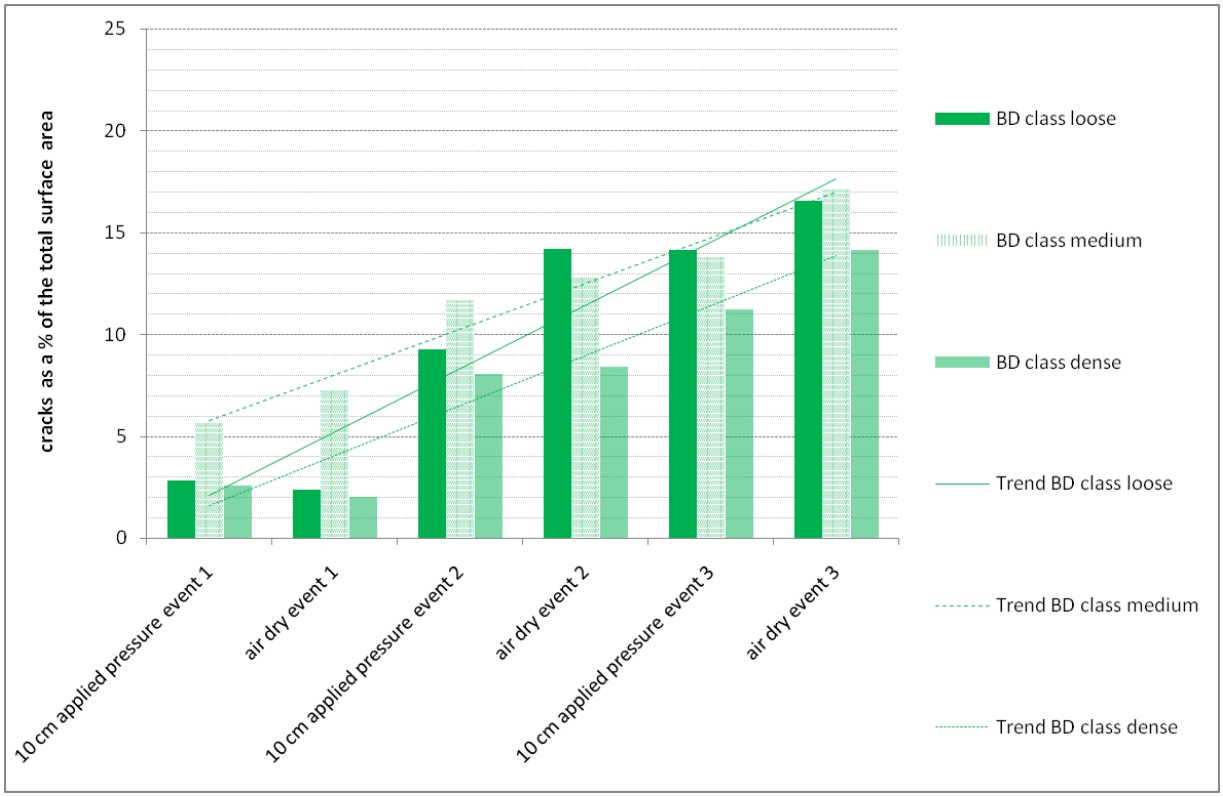

Figure 54. The total area of crack on the surface of the samples of SS/3, averaged for the initial bulk density class.

The second air drying event resulted in another increase in the area of cracks, although this was negligible for the densest soils. The loosest samples experienced the most cracking and the biggest increase in crack area. Conversely, the loosest samples were the least reactive to the third wetting event, changes to the area of surface cracks of the medium density samples marginal and the densest samples displayed the greatest increase in the area of cracks, although the loosest samples still had the greatest area of cracks overall. Drying the soil

samples for the third time resulted in an increase in the total area of surface cracks across all density classes. This increase (relative to their crack area at the second dry event), however, was less than the increase between the first and the second drying event.

The biggest increase in the total area of surface cracks was experienced by SS/3 between the first drying event and the second *wetting* event. The wetting phase of the wet/dry cycles does seem to have a considerable role to play in the generation of surface cracks. At the third and final drying event the loosest samples had an average area of surface cracks of approximately 17 %, the medium density samples approximately 17 % and the densest samples approximately 14 %. Although the greatest average area of surface cracks was marginally less than that achieved by SS/2, the difference between the different density classes was less

4.8.3 The cracking of SS/4

An example of the photographs taken of SS/4 is shown in Figure 55 (the top row, going from left to right, are 0.10 m tension events 1, 2 and 3; the bottom row are the air dry events 1, 2 and 3) and the full set of thresholded images is shown in Appendix 6. SS/4 behaved in a very similar manner to SS/2 and SS/3; there was a clear and significant trend of increased cracking, the initial wetting event produced some surface cracking and the wetting phase of the wet/dry cycles appeared to play an important part in the generation of surface cracks (Figure 56). The loosest samples had the most surface cracks at wet event one, the medium

and the dense samples had slightly less. At dry event one, the loosest and the moderately dense samples had experienced an increase in their area of surface cracks, but the densest samples had not.

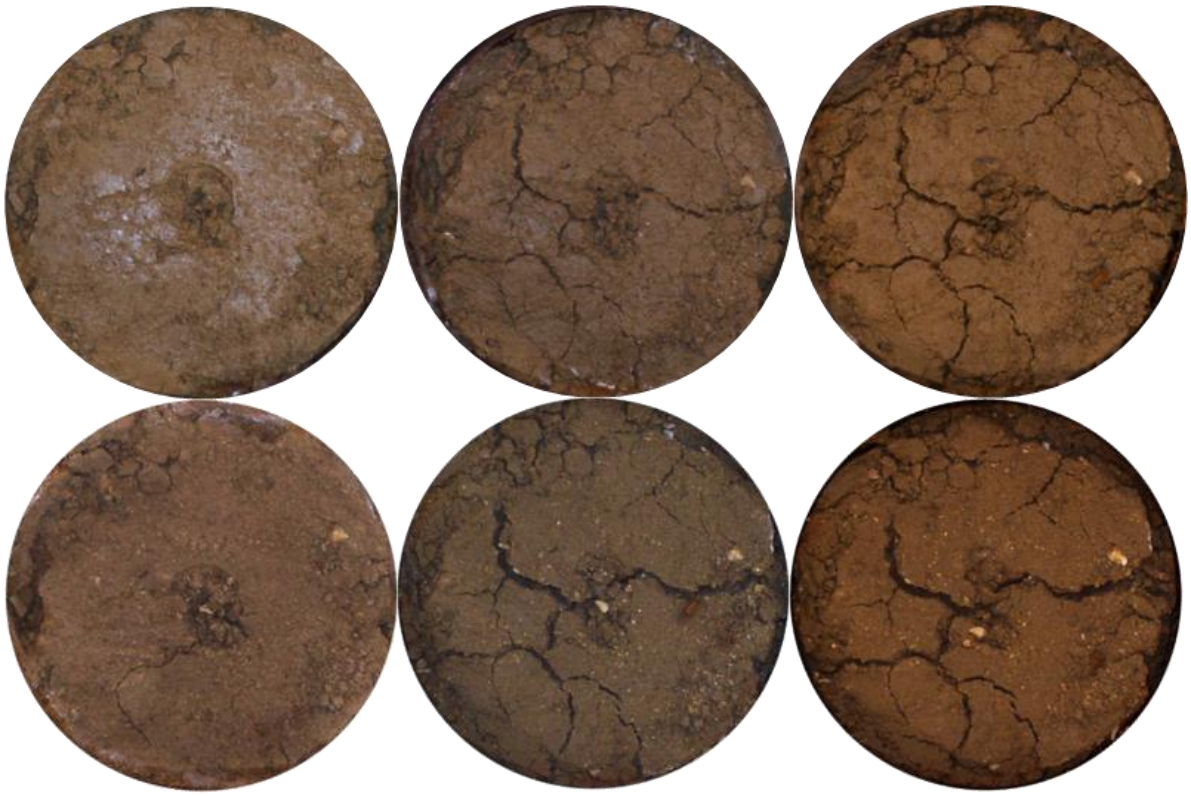

Figure 55. An example of SS/4 (initial bulk density 1.40 g cm^{-3}).

The second wet photographing event showed that all the bulk density classes had an increased area of cracks relative to all previous events. All the bulk density classes had very similar areas of cracks, but the densest samples displayed the greatest increase. The greatest increase in crack area at the second air dry event was demonstrated by the medium density

samples. The loosest samples also showed an increase in the area of cracks, but the densest samples did not experience additional cracking during the drying phase.

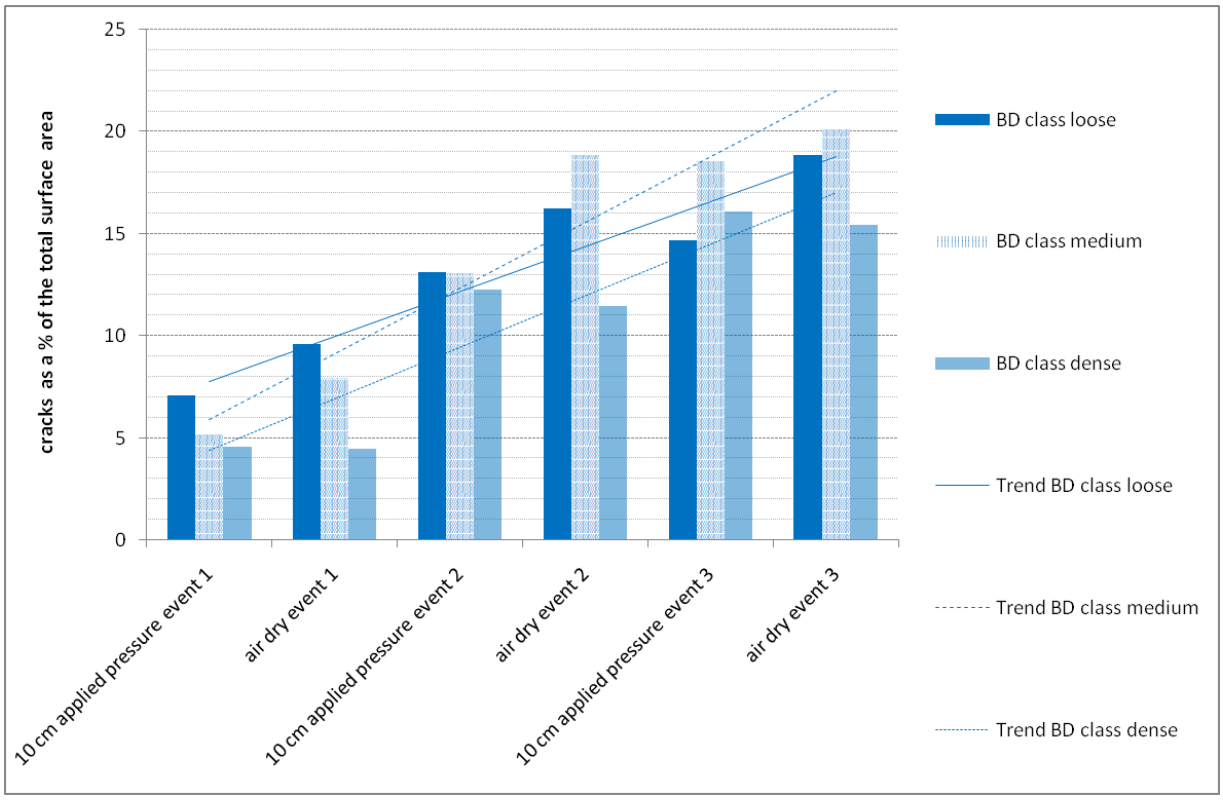

Figure 56. The total area of crack on the surface of the samples of SS/4, averaged for the initial bulk density class.

At the third wet photographing event, the loose and the medium density samples exhibited a marginal decrease in their area of surface cracks relative to the previous drying event, but had a greater area of cracks relative to the previous wet photographing event (Figure 56). The dense samples, however, experienced an increase in the area of cracks relative to all previous events. At the third and final air dry photographing event the loose and the medium density

samples displayed an increase in the area of surface cracks relative to all previous events, but the effect of wetting and drying on the area of cracks appeared to have diminished. The dense samples showed a marginal decrease in the area of cracks relative to the previous wet photographing event, but an increase relative to the previous air dry photographing event. Overall, the loose samples had an average area of surface cracks of approximately 19 %, the medium density samples approximately 20 % and the dense samples 15 %. These figures were very similar to the other soils.

This evidence again supports the supposition that the wetting phase of the wet/dry cycles is important in the generation of surface cracks. This was especially true of the densest samples. This phenomenon is more pronounced for SS/4 then for the other soils investigated. The other proposition suggested by this data is that the initial wetting and drying phases have a greater effect on the generation of surface cracks than later cycles. However, what can not be seen is the effect that these later cycles have on the cracks/pore structure below the surface, which may have a more pronounced effect on the bulk density and the hydrology of the soils.

4.8.4 Correlations between the area of surface cracks and other soil characteristics

In Section 4.3.1, it was shown that the greatest reduction in bulk density would be experienced by the densest samples and yet here it has been shown that these samples had the smallest area of surface cracks. Figure 57 shows the correlations between the final area of

surface cracks and the changes in bulk density, the initial bulk density and the final bulk density. It also shows the correlation between the area of surface cracks when wet and the saturated hydraulic conductivity at the first and the third wet event. The area of surface cracks is that at the third air dry event on the bulk density graphs and at the corresponding wet event on the saturated hydraulic conductivity graphs. The changes in bulk density are displayed as a percentage of the initial bulk density. Graphs shown in yellow represent SS/2, in green SS/3 and in blue SS/4. Graphs show individual data points rather than averages.

Perhaps surprisingly, all these correlations were apparently poor. It might have been expected that the soil samples that cracked the most also experienced the greatest reduction in bulk density and the greatest increase in saturated hydraulic conductivity. However, the relationship between the area of surface cracks and these factors appeared to be more complex than a direct, linear relationship; no clear trend was apparent.

The lack of a direct, linear correlation between the area of surface cracks and changes in bulk density and saturated hydraulic conductivity could be because what happened at the surface of the samples was not representative of what was happening at depth. Returning to the previous analogy with a muffin, the cracks that appear on the surface of the muffin do not extend to the bottom of the muffin. If this was also true of the soil samples then the area of surface cracks would have very little immediate effect on the saturated hydraulic conductivity. It may also be the case that surface cracking was not linearly related to the overall bulk density of the samples because as the soil dries, drawing some soil particles together and breaking the bonds between others, the soil will experience localised areas of

densification and increasing porosity. The overall effect on bulk density, therefore, would be harder to predict. To gain a better understanding of how the cracking of the soils with wet/dry cycles relates to changes in bulk density, saturated hydraulic conductivity and other soil structure properties would require more complex experimental techniques. A possible option would be utilising x-rays and computed tomography as this is a non destructive technique that allows the entire depth of soil to be analysed.

The issue of activity at depth also raises the question, how deep must a crack be for it to count as a crack, rather than surface roughness? Referring to Appendix 6, which shows the thresholded photographs used in the image analysis, the problem of distinguishing cracks from surface roughness becomes more apparent. In general, the looser the samples, the more surface roughness/small, shallow cracks are visible; the denser the samples, the fewer, wider and deeper the cracks appear. The method of analysis chosen was informative but simplistic and made no allowance for the quantifying of this phenomenon.

However, what can be clearly seen is that there were very obvious cracks visible when the samples were wet as well as when they were dry. It can also be clearly seen that cracks were emerging during the wetting phase of the cycle and not exclusively in the drying phase. This is valuable information as it implies that changes to the structure of field soils could potentially be achieved with rapid wetting from the bottom up, via flooding of field drains or ditches. This would mean that changes to the soil structure could possibly be accelerated beyond that achievable under purely natural conditions. As the wetting phase of the cycle is quicker than the drying phase, it may be possible to allow only a minimal drying time

followed by rapid wetting. This cycle could be repeated many times over a season as an alternative to mechanical loosening.

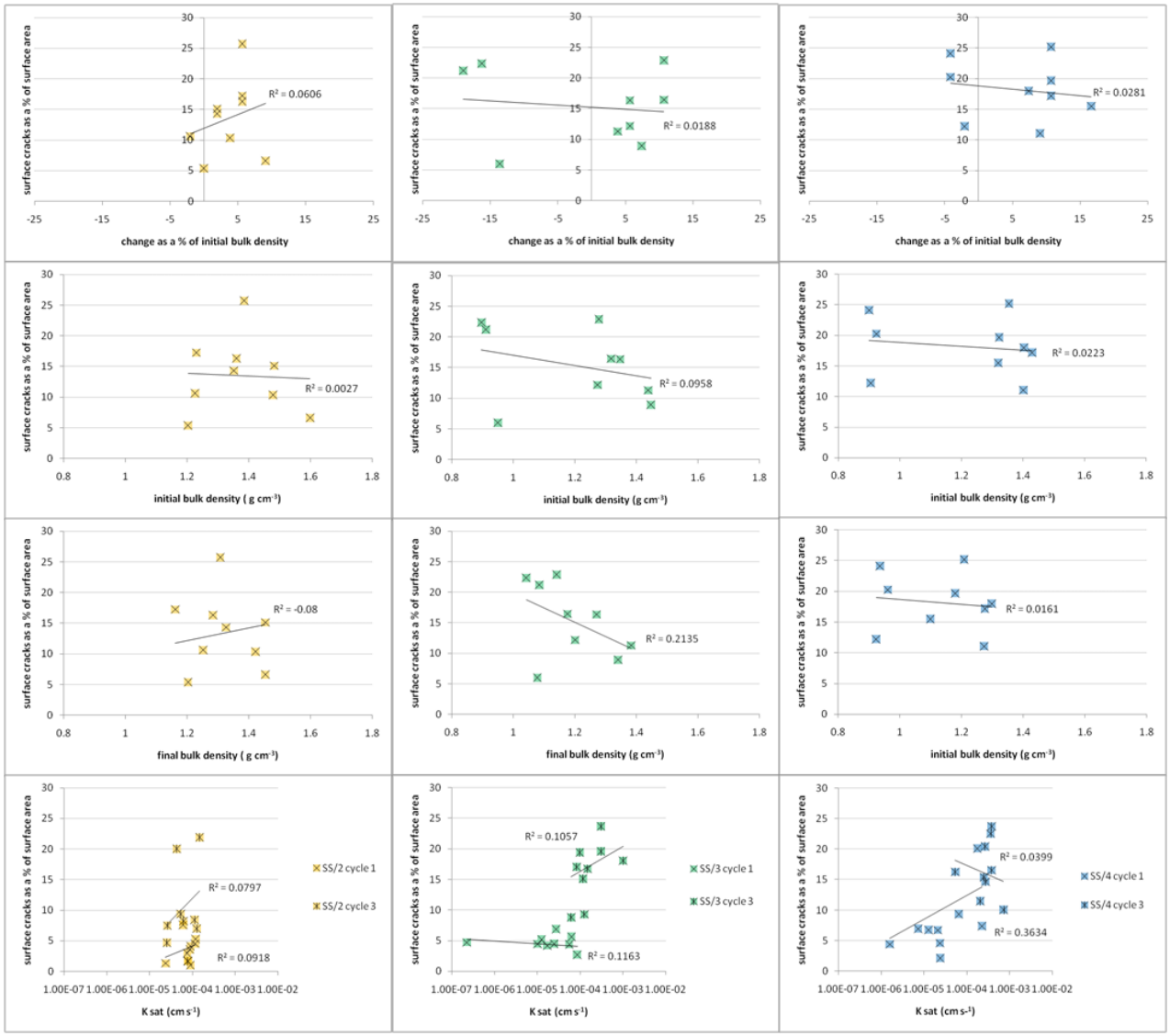

Figure 57. Correlations between surface crack area and bulk density, changes in bulk density and saturated hydraulic conductivity.

4.8.5 Statistical analysis of surface cracks

The data gathered on the generation of surface cracks was analysed statistically using Statistica 8.0 to generate a general linear model for repeated measures. This analysis was conducted on both the total data set and on a data set selected from those samples whose surface cracks were able to be more clearly distinguished from the surface roughness. These samples were: 5-ss/2, 7-ss/2, 8-ss/2, 9-ss/2; 7-ss/3, 8-ss/3, 9-ss/3; 4-ss/4, 5-ss/4, 6-ss/4, 7-ss/4, 8-ss/4 and 9-ss/4.

Table 7. The interactions between the cycle and the area of surface cracks when considering the value of α of the selected data set.

parameter cycle interaction	p
cycle	0.989144
cycle*initial bulk density	0.969943
cycle*1st 0.1 m tension cracks	0.895135
cycle*1st air dry tension cracks	0.853494
cycle*2nd 0.1 m tension cracks	0.209411
cycle*2nd air dry tension cracks	**0.069603**
cycle*3rd 0.1 m tension cracks	0.667021
cycle*3rd air dry tension cracks	**0.062265**
cycle*soil	0.499889

The area of surface cracks of the soil samples was significantly different between soils and cycles with a probability in excess of 99 %. Changes in the percentage area of surface cracks between cycles did not differ significantly, however, between soils. The first parameter to be considered in relation to the area of surface cracks was α. When the whole data set was

considered, the area of cracks was not found to have a significant effect on the value of α, nor how it changed with wet/dry cycles. When the selected data set was considered, however, the interaction between the cycle and the area of surface cracks visible at the second and third air dry events was found to be significant at the 90 % probability level. This suggests that a soil's propensity for cracking is an indication of how its value of α will change with wet/dry cycles, but that the cracks themselves do not directly affect the value of α.

Table 8 shows how the area of cracks affected the value of *n* for the whole data set. Not surprisingly, the value of *n* was significantly affected by the initial bulk density and the soil (probabilities shown in red). Although not significant at the 95 % probability level, the area of cracks after the first air drying event seem to have had an effect on the value of *n* at a probability level of approximately 89 %.

This finding supports the earlier proposition that it may take time and wet/dry cycles for cracks to propagate and travel down the soil profile. For the cracks to have an effect on the value of *n*, they would have to represent what was happening at depth. The cracks that appeared early on in the wetting and drying process are more likely to have had an effect on the value of *n*, especially during the third drying phase, as they would have had the opportunity to travel through the soil profile by the third drying phase. However, the statistics implied that the area of cracks visible after the first wetting event were not significant in determining the value of *n*. The area of cracks were also calculated to be insignificant in determining how the value of *n* changed with wet/dry cycles, despite these changes being calculated to be significant and significantly different between soils (table not

shown). This would suggest that the drying phase was more important in determining the value of *n* than the wetting phase.

Table 8. The statistical dependence of *n* on surface cracks.

parameter	p
initial bulk density	**0.003105**
1st 0.1 m tension cracks	0.911470
1st air dry tension cracks	0.114342
2nd 0.1 m tension cracks	0.133860
2nd air dry tension cracks	0.284635
3rd 0.1 m tension cracks	0.320585
3rd air dry tension cracks	0.855497
soil	**0.000011**

The story is different, however, when the limited data set is considered (Table 9). The only parameters found to be significant were the interaction between the cycle and the surface cracks visible at the second and third air drying event (at a probability level greater than 90 %). This would suggest that it was cracks that were spreading for the bottom of the sample up, rather than from the surface of the samples down, that were most influential in determining how *n* changed between wet/dry cycles one and three, as these cracks could have been present at depth earlier in the cycles, but not visible on the surface.

The next parameter to be considered was *l*. Only when the entire data set was considered were any parameters found to be significant in determining the value of *l* (Table 10). None of the parameters considered were found to be significant in determining how *l* changed with

wet/dry cycles. The area of surface cracks visible at the second air dry event and the third wet event were significant in determining the value of *l*, but not how it changed with wet/dry cycles. This suggests that the propensity of a soil to crack is perhaps more important in determining *l* than the actual area of cracks, although if this were the case, the final area of surface cracks measured should have been the most significant event.

Table 9. The interaction between cycle and the area of surface cracks in determining *n* for the selected data set.

parameter cycle interaction	p
cycle	0.793730
cycle*initial bulk density	0.763692
cycle*1st 0.1 m tension cracks	0.234239
cycle*1st air dry tension cracks	0.301615
cycle*2nd 0.1 m tension cracks	0.182232
cycle*2nd air dry tension cracks	**0.078603**
cycle*3rd 0.1 m tension cracks	0.480515
cycle*3rd air dry tension cracks	**0.057430**
cycle*soil	0.734013

Table 10. The statistical dependence of *l* on surface cracks.

parameter	p
initial bulk density	**0.096782**
1st 0.1 m tension cracks	0.434281
1st air dry tension cracks	0.428089
2nd 0.1 m tension cracks	0.154625
2nd air dry tension cracks	**0.073393**
3rd 0.1 m tension cracks	**0.070897**
3rd air dry tension cracks	0.630444
soil	0.228029

Table 11. The interaction between cycle and the area of surface cracks in determining *l* for the whole data set.

parameter cycle interaction	p
cycle	0.154991
cycle*initial bulk density	**0.085846**
cycle*1st 0.1 m tension cracks	0.551757
cycle*1st air dry tension cracks	**0.020424**
cycle*2nd 0.1 m tension cracks	0.134025
cycle*2nd air dry tension cracks	0.205433
cycle*3rd 0.1 m tension cracks	0.374040
cycle*3rd air dry tension cracks	0.917553
cycle*soil	0.628644

Despite the poor correlation when the area of surface cracks was compared directly to the saturated hydraulic conductivity, statistical analysis suggested that the area of surface cracks was significant in determining the saturated hydraulic conductivity (Table 12) and how this changed with wet/dry cycles (

Table 11). Both the value of the saturated hydraulic conductivity and how this changed with wet/dry cycles seem to have been affected more by the cracks that were visible early in the wetting and drying process, rather than those visible nearer the end of the wetting and drying process. This suggests that cracks that were visible at the first air dry event propagated through the soil profile and became active in the transport of water with wet/dry cycles. This is similar to the behaviour exhibited by *n*.

Table 12. The statistical dependence of K_{sat} of the whole data set on surface cracks.

parameter	p
initial bulk density	**0.001986**
1st 0.1 m tension cracks	0.861410
1st air dry tension cracks	**0.071289**
2nd 0.1 m tension cracks	0.252592
2nd air dry tension cracks	0.515525
3rd 0.1 m tension cracks	0.299142
3rd air dry tension cracks	0.572901
soil	0.423288

Table 13. The interaction between cycle and the area of surface cracks in determining K_s for the selected data set.

parameter cycle interaction	p
cycle	**0.068136**
cycle*initial bulk density	**0.085082**
cycle*1st 0.1 m tension cracks	**0.088970**
cycle*1st air dry tension cracks	0.728057
cycle*2nd 0.1 m tension cracks	0.280639
cycle*2nd air dry tension cracks	0.189748
cycle*3rd 0.1 m tension cracks	0.724008
cycle*3rd air dry tension cracks	0.622547
cycle*soil	0.321003

A similar pattern was also displayed by the selected data set, although not the same (Table 13). Cracks that appeared early in the wetting and drying process were significant at the 90 % probability level in determining how the saturated hydraulic conductivity changed with wet/dry cycles. They were not, however, significant in determining the value of the saturated hydraulic conductivity. The other difference between the two data sets was that it was the cracks that appeared at the first wetting event, rather than the first drying event, that were significant.

Table 14. The effect of surface cracks in determining Dexter's S value and how it changed with wet/dry cycles, for the whole data set.

parameter	p
initial bulk density	**0.000000**
1st 0.1 m tension cracks	0.489357
1st air dry tension cracks	0.418268
2nd 0.1 m tension cracks	**0.081068**
2nd air dry tension cracks	0.531074
3rd 0.1 m tension cracks	**0.044854**
3rd air dry tension cracks	0.624271
soil	**0.091064**

parameter cycle interaction	p
cycle	**0.000048**
cycle*initial bulk density	**0.000007**
cycle*1st 0.1 m tension cracks	0.980547
cycle*1st air dry tension cracks	**0.051335**
cycle*2nd 0.1 m tension cracks	**0.092314**
cycle*2nd air dry tension cracks	0.829435
cycle*3rd 0.1 m tension cracks	0.630348
cycle*3rd air dry tension cracks	0.437623
cycle*soil	0.268625

Dexter's *S* value was the last parameter to be considered (Table 14). The cracks visible at the second and third wetting event were significant in determining the value of *S*, the first dry event and second wet event in determining how the value of *S* changed with cycles. When the selected data set was considered, however, the area of surface cracks only had a significant effect on how the value of *S* changed with wet/dry cycles, but not on the actual value of *S*. What also differed between the two data sets was that for the selected data set, it was that cracks that appeared during the second and third cycles, rather than the first cycle, which were significant.

Table 15. The interaction between parameters and cycle in determining the value of S of the selected data set.

parameter cycle interaction	p
cycle	0.826272
cycle*initial bulk density	0.854157
cycle*1st 0.1 m tension cracks	0.397432
cycle*1st air dry tension cracks	0.440430
cycle*2nd 0.1 m tension cracks	**0.054048**
cycle*2nd air dry tension cracks	**0.039390**
cycle*3rd 0.1 m tension cracks	0.100697
cycle*3rd air dry tension cracks	**0.040166**
cycle*soil	0.182405

In general, there does seem to be some statistical indication that the area of surface cracks of the soil samples related to the van Genuchten-Mualem parameters *n* and *l*, to the measured saturated hydraulic conductivity (the modelled conductivity was not considered) and to

Dexter's *S* value and how these values changed with wet/dry cycles. However, as has already been discussed, assumptions based on the whole of the set of thresholded images should be treated with caution, due to lack of clear distinction between surface cracks and surface roughness.

For this reason, the analysis was repeated on a set of images selected specifically because they showed more definitively the area of cracks. These results also indicated that the area of surface cracks was related to the other soil parameters to some degree, but as the data set was a limited one, these findings should also be treated as indicative, rather than conclusive. However, despite the results of the analysis being indicative, rather than conclusive, there were strong indications that surface cracking can be related to soil structural properties, particularly those that relate to the movement of water through the soil. This suggests that if Vogel *et al.*'s (2005) model could be extended into three dimensions as they proposed, it could indeed be used to predict changes to saturated and unsaturated hydraulic conductivity.

5 Summary of Results and Discussions and Directions of Further Research

The aims of this study were to assess the changes in bulk density and hydrological parameters of a range of soils, varying in texture and other physical and chemical properties, with wet/dry cycles and to explore the relationships between any measured changes in structure and the measured soil properties. The following sections summarise the results reported and discussed in Chapter 4 and discuss possible directions in which the results presented here could be built upon.

5.1 Summary of results and discussions

Fifty undisturbed soil samples, taken from ten different soils ranging in texture from loamy sand to clay (approximately 7 – 53 % clay contents) and varying in other soil physical and chemical parameters, were repeatedly wetted and dried in the laboratory, three complete cycles in total. During this process, changes to the bulk density at saturation were monitored and compared statistically to the various measured soil parameters (particle size fractions; oxidisable organic matter and that lost on ignition; plastic, liquid and shrinkage limits; and cation exchange capacity). Changes to the bulk density of the soils after three wet/dry cycles were found to be significant (at the 95 % probability level), and to be significantly different

between soils and between initial bulk densities. Of the soil parameters measured, those found to be most significant in predicting changes to the bulk density were the liquid limit and the oxidisable organic matter and that lost on ignition. An equation was developed, which predicted changes to bulk density with wet/dry cycles from the initial bulk density and the liquid limit of the soils alone (Equation 30, Chapter 4, Section 4.2.3).

These were the same two parameters, found by Ball *et al.* (2000), that were also able to predict the compactibility of soils. Zang *et al.* (2005) also found organic matter content to be influential in determining the mechanical resilience of soils and Wagner *et al.* (2007) found that the meanweight diameter of aggregates produced by wet/dry cycles was affected by organic matter content. Correlations were also found between the meanweight diameter of soil aggregated produced by wet/dry cycles and the liquid limit of the soils investigated by Grant *et al.* (1995). The results of this study support the theory that organic matter plays a significant part in influencing structural change as these factors were also influential in determining the observed changes in bulk density with wet/dry cycles. Further analysis, however, showed that approximately 90 % of the variation in the data set could be accounted for by the initial bulk density and the liquid limit alone. This was an important finding as the liquid limit of a soil is a relatively simple parameter to measure. The implication of this finding is that it would be possible to predict changes to the bulk density of field soils if the liquid limit of the soil (and the initial bulk density) was known although including other factors, such as the rate and extent of the wetting and drying experienced in the field, would be likely to improve predictions, as they have been shown by van de Graff (1978), Grant and Dexter (1986), Horn and Dexter (1989), Sarmah *et al.*, (1996) and Hussein and Adey (1998)

to also be influential in dictating the extent of structural changes. This is particularly true of subsoils as changes to their moisture content are likely to be less pronounced than changes to the moisture content of surface soils. However, the potential is there to include rates of wetting and drying in the model and/or to manipulate these rates in the field via drainage and irrigation, as suggested by van de Graff (1978).

The other important prediction made by the equation is the equilibrium bulk density to which the soils would tend. When a soil's initial bulk density was below the predicted equilibrium bulk density, the density of that soil would increase with wet/dry cycles; when a soil's initial bulk density is greater than the equilibrium bulk density, the density of that soil would decrease with wet/dry cycles. For soils with a similar clay content, the soils with higher organic matter contents had a lower predicted equilibrium bulk density; the lowest equilibrium bulk density, however, was predicted for the soil with the highest clay content. The highest equilibrium bulk density was predicted for the sandier soils. In general, the higher the liquid limit of the soil, the lower the predicted equilibrium bulk density. The validity of this prediction was explored by monitoring changes in bulk density of samples of the clay subsoils that had been created with a range of initial bulk densities and comparing these to those predicted by the model. Correlations between the measured and predicted results were reasonably good (R^2 greater than 0.8 for all three soils). These equilibrium values were also compared with the D values suggested by Håkansson and Lipiec (2000) and found to be the same. This implies that the liquid limit of soils may also be able to predict their D value, as well their compactibility and their swelling potential. The model was developed based on the behaviour of ten soils of varying texture, initial bulk density and

other parameters and validated with data gathered from three clay soils with a wider range of initial bulk densities. This provides the basis for further research, testing the model against other soils with properties different to those explored here.

The principal upon which the prediction model developed in this thesis is based is strongly supported by the literature, implying that changes to the bulk density of soils with wet/dry cycles will be some function of their initial bulk density and liquid limit. The practical implication of this finding for agriculture is that it may be possible to calculate the economic benefit of removing a compacted field from production to allow wet/dry cycles to ameliorate a degraded structure, rather than engaging in practices such as subsoiling, as subsoiling can be expensive in fuel consumption and has been shown to leave the soil vulnerable to recompaction (Horn *et al.,* 1995; Motovalli *et al.,* 2003) and can cause significant reductions in saturated hydraulic conductivity (Dexter *et al.,* 2004).

The same samples that were used to test the predictive model were also used to explore changes to soil hydraulic parameters with wet/dry cycles in detail. The saturated hydraulic conductivity was measured at the first, third and fourth saturation. Whereas changes to this parameter have been hard to detect in the field by some authors, due to infield heterogeneity (Alakukku, 1996[a]; Alakukku, 1996[b]; Alakukku *et al*., 2003; and Chamen *et al*., 2003), others have found it to be a more sensitive measure of structural recovery than bulk density (Croke *et al.,* 2001; Halvorson *et al.,* 2003; Rab, 2004). Perhaps the most interesting finding of this particular experiment was that a much greater increase in saturated hydraulic conductivity occurred between the third and fourth saturation than between the first and the third

saturation for all soils and densities. It was suggested that this could be explained by the continued propagation of vertical cracks with every wet/dry cycle, those cracks only extending through the whole length of the soil profile during the third drying phase and/or the fourth wetting phase. This implies that there may be a critical number of cycles required to achieve continuity in the emerging crack network of a completely homogenised soil, regardless of the initial bulk density or the extent, or direction of changes to the bulk density (the loosest samples demonstrated an increase in bulk density, but also the greatest increase in saturated hydraulic conductivity, with wet/dry cycles).

Changes to the clayey subsoils moisture release curves were estimated from transient outflow data. Examination of the moisture release curves suggested that the porosity gained or lost or gained during wet/dry cycles was not confined to the macro-pore region visible as cracks, but included changes to pores that were undrained at pressures up to and including 1000 m of water, although how this was realised in the pore size distribution varied between soils. This phenomenon was also implied from the results gained from the simpler experiments conducted on all ten soils. This is similar to the results of Horn and Dexter (1989) who found that pores were created in both the macro- and micro-pore regions of a loess with wet/dry cycles. Changes in the pore size distribution of the three soils studied by Pires *et al.* (2005) varied considerably between soils and did not appear to be correlated with clay content. The results of this study and the studies of Horn and Dexter (1989) and Pires *et al.* (2005) implied that changes in the porosity, and, more specifically, the pore size distribution, cannot be accounted for purely by additions to macro-porosity and further, that differences in soil

texture and other factors, such as the mineralogy and the organic matter content, are influential in determining changes to the pore size distribution of soils with wet/dry cycles.

Values of the van Genuchten-Mualem parameters α and n were compared to the measured soil properties. The most significant factor in determining how the value of α changed with wet/dry cycles was the clay content; the most significant soil property in determining changes in the value of n with wet/dry cycles was the proportion of sand. The organic matter content and the Atterberg limits were also found to be highly significant in determining changes, however. This evidence further corroborates the proposition that soil properties other than soil texture are influential in determining changes to the pore size distribution.

The index of soil physical quality, *S*, (the modulus of the slope of the moisture release curve at the inflection point) proposed by Dexter (2004) was calculated for all the soil samples from the curves generated during the first and the third drainage cycle. Although significant differences were found between cycles, no value was found to be less than the critical minimum for crop growth suggested by Dexter (0.035), despite the samples being initially compact and/or homogenised. Dexter (2004) did also state, however, that there appears to be a linear relationship between the value of *S* and organic matter content and that when organic mater exceeded 4 %, the value of *S* exceeded its critical minimum value. This could imply two things; either compaction is not an issue for soils with organic matter contents in excess of 4 %, or that the critical value needs to be revised based on soil properties. The first proposition seems unlikely as Arvidsson and Håkansson (1996) reported yield losses after compacting soils with more than twice this organic matter content. It would seem, therefore,

that although the concept of Dexter's *S* value could be a useful tool in assessing the structure of soils with reference to their utility as a medium for crop production, it needs to be refined to take account of the effect of organic matter on soil structure (further corroborating the theory that changes in pore size distribution are effected by soil properties other than texture.) It may also be appropriate to include a maximum value in the model as, theoretically, too steep a slope on the moisture release curve of a soil would result in the soil drying out too quickly and retaining very little water for crop growth at soil matric potentials exceeding field capacity.

The hydraulic conductivity curves of the subsoil samples were modelled simultaneously with their moisture release curves, and curves produced from the first drying phase were similarly compared with those produced during the third drying phase. Changes in the hydraulic conductivity at any given tension of the soil samples did not necessarily appear to be directly equated with changes to the water filled porosity at that tension. This was a reflection of the independently measured changes to the saturated hydraulic conductivity; the samples that increased in bulk density and a proportion of their macro-porosity (the loosest samples) also increased the most in their saturated hydraulic conductivity. This implies that the process of wetting and drying the samples affected their pore continuity/tortuosity as well as their porosity and pore size distribution. This would explain why some authors detected no change in the bulk density of the soils that they were studying, but did detect changes in saturated hydraulic conductivity or infiltration rates (Croke *et al.,* 2001; Halvorson *et al.,* 2003). In general, the subsoil with a smaller proportion of clay than one of the other subsoils and a lower organic matter content than the other (the subsoil with the lowest liquid limit) increased

in hydraulic conductivity at all tensions with wet/dry cycles, but this was more pronounced at higher tensions for the samples that decreased in density. The changes experienced by the subsoil with the greatest organic matter content (the subsoil with a liquid limit lying between that of the other two soils) with wet/dry cycles were more varied. The hydraulic conductivity of the samples that increased in bulk density was largely unchanged at low tensions, but increased at higher tensions; the hydraulic conductivity if the samples the reduced in bulk density tended to increase at low tensions, but decreased at higher tensions. The behaviour of the subsoil with the highest clay content (and greatest liquid limit) was different again. The hydraulic conductivity of the samples at low tensions tended to remain largely unchanged, while the hydraulic conductivity at higher tensions was reduced. These results suggest that changes to the hydraulic conductivity of soils are more complex than changes to their bulk density or pore size distributions.

This implies that in a field situation, wet/dry cycles alone would be insufficient to necessarily improve infiltration rates or the flow of water through the soil profile at moisture contents less than saturation. The establishment of a continuous macro-pore network may be better achieved by the implementation of appropriate cropping regimes. Bushamuka and Zobel (1998) and Williams and Weil (2004), for example, found that strong rooted plants created a pore network that was utilised by successive crops. Pillai and McGarry (1999) also found that the inclusion of crops increased the positive effect that wet/dry cycles had on the porosity if the soil they studied. It seems likely that to repair the structure of a severely compacted soil, some initial wet/dry cycles may be necessary in order to reduce bulk density (implying a reduction in the resistance to penetration by roots) sufficiently for the establishment of a

recovery crop that would penetrate compacted subsoils, both establishing a macro-pore network and accelerating and accentuating the wetting and drying process to further improve porosity and saturated hydraulic conductivity from the initial, compacted and/or homogenised state.

Development of structure within the subsoil samples was further investigated by monitoring the area of surface cracks that were visible at various stages in the wetting and drying process. Analysis of the surface crack emergence of the soil samples produced some interesting results. The first of these was that the cracks did not close up entirely when the samples were saturated. This is similar to the findings of Yesiller *et al.* (2000), who found that by the third wetting of their compacted clay soils, wetting merely reduced the area of cracks visible, rather than reducing it virtually zero as it had done on the second wetting event. However, the surface cracks apparent on the soils in this study never completely closed up. In fact, there were many instances where wetting increased the area of surface cracks, relative to the preceding dry event, which was probably due to rapid wetting causing uneven swelling through the soil profile that resulted in rupturing of the soil before the wetting front. This phenomenon would explain the findings of Sarmah *et al.* (1996) and Hussein and Adey (1998) who found that rapid wetting of the soil produced more pronounced structural changes than slower methods of wetting. Grant and Dexter (1986) found a critical wetting rate for their soil to experience structural change. This evidence implies that wetting (and the rate of wetting) is as important as drying in the formation of soil structure.

Velde (2001) suggested that when water stable aggregates are not present, surface cracking will be the predominant pore forming mechanism. Vogel *et al*. (2005) developed a model of crack emergence that they proposed could be extended and coupled with transport models to simulate preferential flow along macro-pores. This suggests that there may be some correlation between the emergence of surface cracks and changes in other measureable parameters, such as bulk density, or saturated hydraulic conductivity, especially as cracks were visible on the surface of the soils investigated in this study close to saturation, implying that they would be active in the transport of water at saturation. However, no immediate, obvious relationships were observed, which suggested that what was happening at the surface of the samples was not directly representative of what was happening at depth. This was demonstrated by the behaviour of the loosest soil samples. These samples experienced cracking that was comparable with the other, denser samples, despite the fact that the loose samples experienced an increase in bulk density and the other samples a decrease. It does not seem, therefore, that the area of surface cracking can be related to changes in bulk density directly. This is expected since cracking is caused by water leaving the clay matrix, drawing some soil particles together and breaking bonds between other along planes of weakness. This implies that there is both localised densification and areas that experience increases in their volume of voids. Being able to predict overall changes in bulk density directly from areas of surface cracking alone seems unlikely.

The area of surface cracks was also compared with the parameters of the van Genuchten-Mualem Equation α, n and l. When the whole data set was considered, no correlation was found between the area of surface cracks and either the value of α or how it changed with

wet/dry cycles. Similar results were found for *n*. This implies that the area of surface cracks has very little effect on the pore size distribution of the soil, or its development. The problem of differentiating between surface cracking and surface roughness was raised. To eliminate the possibility of confusing surface roughness with surface cracking, a limited set of soils were selected, based on visual inspection, whose surface cracking was clearly differentiated from the rest of the soil surface. When this limited data set was considered statistically, how α changed with wet/dry cycles was found to be significantly affected by the area of surface cracks visible at the second and third drying events (at the 90 % probability level). Similarly, when the limited data set was considered, how *n* changed with wet/dry cycles was affected by the surface cracks visible at the second and third air dry event (significant at the 90 % probability level).

The contribution of the van Genuchten-Mualem parameters α and *n* to the pore size distribution may be combined by considering Dexter's *S* value as this is a direct measurement of the slope of the moisture release curve. Comparing Dexter's *S* value to the area of surface cracks suggested that how this value changed with wet/dry cycles was statistically related to area of surface cracks visible at the first dry event and the second wet event at the 90 % probability level. When the limited data set was considered, the areas of cracks visible at the second and third dry events were significant at the 95 % probability level. Perhaps unsurprisingly, these results reflect those of the comparisons with α and *n*, parameters which describe the slope of the moisture release curve.

The area of surface cracks was also compared to the hydrological parameters of the soils. A correlation was found between the area of cracks at the second dry event and the third wet event and the value of *l*, but not how this value changed with wet/dry cycles, based on the whole data set (significant a the 90 % probability level). However, when the limited data set was considered, no significant correlations were found. It may well be that the area of surface cracks does not in fact relate well to change in the pore size distribution described by the parameters α and *n* as significant relationships were only found when the limited data set was considered. The parameter *l* however, is a parameter of the hydraulic conductivity curve. The relation of cracks to hydraulic conductivity, especially at saturation, is a more easily explained one, provided that sufficient cracking has occurred to create a continuous network of cracks through the soil profile. Micro-cracks would contribute to hydraulic conductivity at less than saturation (dependent again on the continuity of the network) but these cracks, if indeed visible at all without magnification, would be harder to distinguish from surface roughness. On the other hand, if only large, obvious cracks are present (as in the limited data set) these would be highly unlikely to contribute to hydraulic conductivity at less than saturation as they would be drained at very low tensions. This would explain why there was some correlation found between cracking and the value of *l* when the whole data set was considered, but not the selected data set.

The measured saturated hydraulic conductivity was also compared to the area of surface cracks. Stronger correlations were found between the two parameters. The area of cracks at the first air dry event was correlated with the saturated hydraulic conductivity at a probability level of 90 % and with how the saturated hydraulic conductivity changed with wet/dry cycles

at a probability level of 95 %. The probability that it was the cracks that appeared early on in the wetting drying process that affected the saturated hydraulic conductivity suggests that with successive wet/dry cycles, cracks propagated through the soil profile, becoming more connected with each cycle. The cracks that appeared on the surface of the samples later in the wetting and drying process probably did not extend so far through the profile and hence did not contribute to the saturated hydraulic conductivity. It could have been expected that when the selected data set was considered, the significance of the contribution of the area of surface cracks to saturated hydraulic conductivity would be greater than when the full data set was considered. However, this was not the case, although the relationship between the area of surface cracks and changes to the saturated hydraulic conductivity was still significant at the 90 % probability level. It was also the area of cracks that were visible at the first wet event, rather than the first dry event, that were significant although there is some logic to this as cracks would have to be open under saturated conditions in order to contribute to conductivity.

A factor which may have confused the results is the fact that only total crack area was considered, rather than crack width and tortuosity. When considering two soils with the same area of cracks, the soil with fewer, larger cracks would be expected to have a higher saturated hydraulic conductivity than the soil with more but narrower, more tortuous cracks, due to the friction between the water and the walls of the cracks. Clearer, more definitive results may have been achieved if crack width had been included in the analysis. Nevertheless, there does seem to be a relationship between surface cracking and hydraulic conductivity. The more detailed model proposed by Vogel *et al.* (2005) would be able to account for the finer detail

in cracking patterns. If these cracking patterns could be predicted from parameters such as soil activity (related to soil mineralogy) it may be possible to hence predict changes in saturated hydraulic conductivity.

This analysis did imply that it may be possible to relate the emergence of surface cracks with the behaviour of soil at depth regarding changes to its pore size distribution and hydraulic conductivity. However, the results reported here should be treated with caution. It would necessary to repeat the experiments with a more sophisticated technique of separating surface roughness from surface cracks to make more definitive conclusions on the relationship between surface cracking and changes in pore size distribution and hydraulic conductivity. Using a more sophisticated technique that included measures of crack width as well as total area to quantify surface cracking patterns would also be likely to improve correlations between cracking and changes to the soil structure. Despite its limitations however, the data set presented in this study does suggest that there is a relationship between cracking and structural change can be successfully modelled.

5.2 Further research

The model predicting changes in bulk density with wet/dry cycles needs to be tested against other soils that were not used in its development. However, as already stated, the principal is strongly supported by the literature, implying that changes to the bulk density of soils with

wet/dry cycles will be some function of their initial bulk density and liquid limit. The functions predicted here would be refined by including a range of soils with a more silty texture in the statistical analysis. A reliable model that predicted changes in bulk density under various water management regimes would have value, especially to the farming community, as subsoiling has been shown to leave the soil vulnerable to recompaction (Horn *et al.,* 1995; Motovalli *et al.,* 2003) and can cause significant reductions in saturated hydraulic conductivity (Dexter *et al.,* 2004).

Changes to saturated hydraulic conductivity also merit further investigation. Repeating experiments with longer soil columns would demonstrate whether the number of cycles required to develop a continuous pore network varied with depth, or whether factors such as the extent to which the soil dried were more important. Repeating the experiment with a greater range of soils, varying in texture and other physical/chemical parameters, could also lead to a model similar to that used to predict bulk density changes. Changes to the saturated hydraulic conductivity of soils, however, is likely to be more complex and harder to predict than changes to bulk density; changes to the bulk density of soils are dependent purely on changes in overall porosity, whereas changes to the saturated hydraulic conductivity are dependent on changes specifically to the macro-porosity of the soil (a decrease in overall porosity may still be concomitant with an increase in saturated hydraulic conductivity) and to changes in the connectivity/tortuosity of the pore network. However, changes in the saturated hydraulic conductivity of a soil are more informative than changes to bulk density when considering improvements to the soil as a medium for crop growth and as an environmental resource. Increased saturated hydraulic conductivity implies an increased macro-pore

network that can be utilised by crops and increased aeration. It also implies an increased infiltration rate which will reduce runoff and hence soil erosion and the pollution of surface waters. Being able to predict changes to saturated hydraulic conductivity of a soil would, therefore, improve the predictions of the economic benefit of allowing natural processes to ameliorate a degraded soil structure.

An even more informative model would be one that predicted changes to the moisture release curve. The results presented in this study do appear to suggest that it may be possible, with further research, to extend the model that predicted changes in bulk density to predict changes to the parameters α and n of the van Genuchten-Mualem Equation that describe the moisture release curve. The parameter saturated moisture content is already predicted by the bulk density model developed by this study and the residual moisture content can be reasonably set to zero as the residual moisture content of a soil is the moisture content at infinite tension which must, logically, be zero. Additionally, the air dry moisture content of the soils was found not to change with wet/dry cycles and would, therefore, provide a fixed point the moisture release curve. Such a model would be highly valuable to the farming community (and, potentially, civil engineers) as it could be used to design irrigation and drainage regimes that would result in optimal growing conditions. This would, however, require more raw data upon which to base the model, collected in similar manner to that described in this study.

Complicating the interpretation of pore size distributions and their changes, however, is soil shrinkage. At moisture contents where soils shrinkage is normal (i.e. the reduction in the

volume of the soil is equal to the volume of water lost) the same pores may displayed as additional porosity at a range of tensions. This problem has been described by Kim *et al.* (1999) with reference to the parameters of the van Genuchten equation, Baumgartl (2002), with reference to critical state soil mechanics and the parameters of the van-Genuchten equation, Chertkov (2004 and 2005) with reference to changes in the shrinkage geometry factor with moisture content and the effect of cracks and Peng and Horn (2005 and 2006) who modelled shrinkage curves with the parameters of the van Genuchten equation. What does not appear to have yet been developed is a method of predicting changes to the shrinkage curve with wet/dry cycles, based on physical soil parameters, although these authors did note differences between different initial structural states (Chertkov 2005) and levels of soil organic matter (Peng and Horn, 2006) and the soils' history of mechanical and hydrological stress was compared to the preconsolidation stress described in critical state soil mechanics (Baumgartl, 2002). There is the potential to combine the kind of data described in this study with the above models to create a comprehensive model of soil dynamics that predict changes to moisture retention and hydraulic conductivity curves, aeration status and available moisture content, possibly including factors such as swelling pressure and overburden pressure, and based on mapped parameters, such as soil texture, and relatively easily measureable soil parameters such as liquid limit and organic matter and, it seems, some function of structure as could potentially be described by saturated hydraulic conductivity measurements.

A model of such detail and complexity would be advantageous when making long term predictions of climate change as soils store large proportions of the total carbon pool (Batjes,

1996) and carbon losses from UK soils are comparable with emissions from industry (Bellamy *et al.,* 2005), a factor which has been found to be effected by soil structure (Brevick *et al.,* 2002). Soil structure has also been found to have an impact on fluxes of other greenhouse gasses, such as CH_4 (Teepe *et al.,* 2004). Including models of soil structural dynamics in climate change predictions could, therefore, have a substantial impact on the accuracy of climate change models.

Environmentalists and town planners may also be interested in the envisaged model as it could be used to predict infiltration rate and hence the time to peak flow after a rainfall event and the total volumes of runoff. This information would have implications for flood management and the prevention of pollution of surface waters from runoff from agriculture. Such a model may also be of interest to engineers as swelling soils can disturb the foundations of structures. Slope stability of newly constructed embankments and the establishment of plant cover intended to improve slope stability would also be influenced by the structure of the soil in question and changes to it. The structure and hydraulic functions of sports pitches affect their performance. Predicting how these change and how to maintain optimal conditions with water management strategies would improve sport pitch maintenance. Further research is required, therefore, that refines the model of bulk density changes with wet/dry cycles presented here against data gathered from other soils and incorporates predictions of changes to the saturated hydraulic conductivity and the parameters of the van Genuchten-Mualem Equation that the results presented in this study implied could be similarly related to soil properties such as the liquid limit.

6 Conclusion

The aims of this study were to assess the changes in bulk density and hydrological parameters of a range of soils varying in texture and other physical and chemical properties with wet/dry cycle cycles and to explore the relationships between any measured changes and the measured soil properties.

Overall, this study has lent considerable weight to the argument that changes to the bulk density of soils can be predicted from the relatively easily measurable soil property, liquid limit, a parameter which relates not only to the clay content of a soil, but also its clay mineralogy; analysis showed that approximately 90 % of the variation in the data set could be accounted for by the initial bulk density and the liquid limit alone. In general, the higher the liquid limit of the soil, the greater the effect of wet/dry cycle cycles on the bulk density.

This study has also presented evidence that suggests that there is an equilibrium bulk density to which soils will tend that can also be predicted from their liquid limit and that this bulk density may well be the optimum for crop growth predicted by Håkansson and Lipiec (2000). In general, the higher the liquid limit of the soil, the lower the predicted equilibrium bulk density.

Changes in porosity resulting from wet/dry cycle cycles were not limited to changes in macro-porosity and were evident across pores of all effective diameters. However, increases

in the proportion of pores in any size class were not necessarily concomitant with an increase in the hydraulic conductivity at equivalent tensions. This implies that the process of wet/dry cycle the samples affected their pore continuity/tortuosity as well as their porosity and pore size distribution. These results suggest that changes to the hydraulic conductivity of soils are more complex than changes to their bulk density or pore size distributions. This leads to the conclusion that in a field situation, wet/dry cycle cycles alone could be insufficient to necessarily improve infiltration rates or the flow of water through the soil profile at moisture contents less than saturation. The establishment of a continuous macro-pore network may be better achieved by the implementation of appropriate cropping regimes.

Evidence presented in the literature review suggested that the time scales involved in the recovery of soil structure after a compaction event in the field were extremely variable. The laboratory studies and the results presented here, however, have shown that there is the potential for the recovery of soil structure with wet/dry cycle cycles to be achievable within shorter time scales. The controlling factor appears to be the rapidity and extent at which repeated wet/dry cycle of the soil occur.

The wetting phase of wet/dry cycle cycles was also shown to be important, both by the results of this study and the literature. It was proposed that rapid wetting causes uneven swelling through the soil profile, resulting in rupturing of the soil before the wetting front. This evidence implies that wetting (and the rate of wetting) is as important as drying in the formation of soil structure. Rates and degrees of wetting can be manipulated in the field by

irrigation regimes. Drainage of a soil can be accelerated by the presence of a cover crop that has roots strong enough to penetrate compacted layers (Pillai and McGarry, 1999).

It seems likely that to repair the structure of a severely compacted soil, some initial wet/dry cycle cycles may be necessary in order to reduce bulk density (implying a reduction in the resistance to penetration by roots) sufficiently for the establishment of a recovery crop that would penetrate compacted subsoils, both establishing a macro-pore network and accelerating and accentuating the wet/dry cycle process to further improve porosity and saturated hydraulic conductivity from the initial, compacted and/or homogenised state.

The practical implication of these findings for agriculture is that it may be possible to calculate the economic benefit of removing a compacted field from production to allow wet/dry cycle cycles, aided by appropriate crop cover, to ameliorate a degraded structure, rather than engaging in practices such as subsoiling, as subsoiling can be expensive in fuel consumption and has been shown to leave the soil vulnerable to recompaction (Horn *et al.*, 1995; Motovalli *et al.*, 2003) and can cause significant reductions in saturated hydraulic conductivity (Dexter *et al.*, 2004).

References

Abu-Hamdeh, N. H. and Reeder, R. C. (2003). Measuring and predicting stress distribution under tractive devices in undisturbed soils. *Biosystems Engineering* **85**, 493-502.

Abu-Hamdeh, N. H. (2003). Compaction and Subsoiling Effects on Corn Growth and Soil Bulk Density. *Soil Sci. Soc. Am. J.* **67**, 1213-1219.

Alakukku, L. (1996a). Persistence of soil compaction due to high axle load traffic .1. Short-term effects on the properties of clay and organic soils. *Soil & Tillage Research* **37**, 211-222.

Alakukku, L. (1996b). Persistence of soil compaction due to high axle load traffic .2. Long-term effects on the properties of fine-textured and organic soils. *Soil & Tillage Research* **37**, 223-238.

Alakukku, L. (1998). Properties of compacted fine-textured soils as affected by crop rotation and reduced tillage. *Soil & Tillage Research* **47**, 83-89.

Alakukku, L., Weisskopf, P., Chamen, W. C. T., Tijink, F. G. J., van der Linden, J. P., Pires, S., Sommer, C., and Spoor, G. (2003). Prevention strategies for field traffic-induced subsoil compaction: a review Part 1. Machine/soil interactions. *Soil & Tillage Research* **73**, 145-160.

Arvidsson, J., and Hakansson, I. (1996). Do effects of soil compaction persist after ploughing? Results from 21 long-term field experiments in Sweden. *Soil & Tillage Research* **39**, 175-197.

Arvidsson, J., and Ristic, S. (1996). Soil stress and compaction effects for four tractor tyres. *Journal of Terramechanics* **33**, 223-232.

Avery, B. W. and Bascomb, C. L., (eds), 1982. Soil Survey Laboratory Methods. *Soil Survey Technical Monograph* **6**., Harpenden, UK.

Ball, B. C., Campbell, D. J., and Hunter, E. A. (2000). Soil compactibility in relation to physical and organic properties at 156 sites in UK. *Soil & Tillage Research* **57**, 83-91.

Batjes, N. H., (1996). Total carbon and nitrogen in the soils of the world. *European Journal of Soil Science* **47**, 15 1 – 163.

Baumgartl, T., 2002. The dynamic of water retention curves caused by soil deformation. Oral Presentation, World Congress Of Soil Science, Thailand.

Baveye, P., Boast, C. W., Ogawa, S., Parlange, J-Y. and Steenhuis, T., (1998). Influence of image resolution and thresholding on the apparent mass fractal charactistics of preferential flow patterns in field soils. *Water Resources Research*, **34**, 2783-2796.

Bellamy, P. H., Loveland, P. J., Bradley, R. I., Lark, R. M., and Kirk, G. J. D., (2005). Carbon losses from all soils across England and Wales 1978–2003. *Nature* **437**, 245 – 248.

Blackwell, P. S., Ward, M. A., Lefevre, R. N., and Cowan, D. J. (1985). Compaction of a Swelling Clay Soil by Agricultural Traffic - Effects Upon Conditions for Growth of Winter Cereals and Evidence for Some Recovery of Structure. *Journal of Soil Science* **36**, 633-650.

Borcher, C. A., Skopp, J., Watts, D. and Schepers, J., (1987). Unsaturated hydraulic conductivity determination by one-step outflow for fine-textured soils. *Transactions of the American Society of Agricultural Engineers*, **30**, 1038-1042.

Botta, G. F., Jorajuria, D., and Draghi, L. M. (2002). Influence of the axle load, tyre size and configuration on the compaction of a freshly tilled clayey soil. *Journal of Terramechanics* **39**, 47-54.

Brady, N., and Weil, R., (1999) The Nature and Properties of Soils. *Pentice-Hall Inc.*, US.

Brevik, E., Fenton, T. and Moran, L., (2002). Effect of soil compaction on organic carbon amounts and distribution, South-Central Iowa. *Environmental Pollution* **116**, 137-141.

BS1377:Part 2: 1990. Methods of test for soils for civil engineering purposes. Classification tests.

BS1377: Part 3: 1990. Methods of test for soils for civil engineering purposes. Chemical and electro-chemical tests.

Bushamuka, V., and Zobel, R. (1998). Differential genotypic and root type penetration of compacted soil layers. *Crop Sci.* **38**, 776-781.

Çarman, K. (2002). Compaction characteristics of towed wheels on clay loam in a soil bin. *Soil & Tillage Research* **65**, 37-43.

Chamen, T., Alakukku, L., Pires, S., Sommer, C., Spoor, G., Tijink, F., and Weisskopf, P. (2003). Prevention strategies for field traffic-induced subsoil compaction: a review Part 2. Equipment and field practices. *Soil & Tillage Research* **73**, 161-174.

Chen, C. Y. and Martin G. R., 2002. Soil–structure interaction for landslide stabilizing piles. *Computers and Geotechnics*, **29**, 363-386.

Chertkov, V. Y., Ravina, I. and Zadoenko, V., 2004. An approach for estimating the shrinkage geometry factor at a moisture content. *Soil Sci. Soc. Am. J* **68**, 1807-1817.

Chertkov, V. Y., 2005. The shrinkage geometry factor of a soil layer. *Soil Sci. Soc. Am. J* ***69****, 1671-1683.*

Crescimanno, G. and Iovino, M., (1995). Parameter estimation by inverse method based on one-step and multi-step outflow experiments. *Geoderma*, **68**, 257-277.

Croke, J., Hairsine, P., and Fogarty, P. (2001). Soil recovery from track construction and harvesting changes in surface infiltration, erosion and delivery rates with time. *Forest Ecology and Management* **143**, 3-12.

Dexter, A. (1988). Advances in Characterization of Soil Structure. *Soil & Tillage Research* **11**, 199-238.

Dexter, A. (2004). Soil physical quality part I. Theory, effects of soil texture, density, and organic matter, and effects on root growth. *Geoderma* **120**, 201-214.

Dexter, A. R., Czyź , E. A. and Gaţe O. P., (2004). Soil structure and the saturated hydraulic conductivity of subsoils. *Soil & Tillage Research* **79**, 185-189.

Doering, E.J., (1965). Soil water diffusivity by the one-step method. *Soil Science*, **99**, 322-326.

Drewry, J. J., (2006). Natural recovery of soil physical properties from treading damage of pastoral soils in New Zealand and Australia: A review. *Agriculture, Ecosystems and Environment*, **114**, 159-169.

Echings, S. O. and Hopmans, J. W., (1993). Optimization of hydraulic functions from transient outflow and soil water pressure data. *Soil Sci. Soc. Am. J.* **57**, 1167-1175.

Eching, S. O., Hopmans, J. W. and Wendroth, O., (1994). Unsaturated hydraulic conductivity from transient multistep outflow and soil water pressure data. *Soil Sci. Soc. Am. J.*, **58**, 687-695.

Etana, A., and Hakansson, I. (1994). Swedish Experiments on the Persistence of Subsoil Compaction Caused by Vehicles with High Axle Load. *Soil & Tillage Research* **29**, 167-172.

Finsterle, S. and Faybishenko, B., (1999). Inverse modeling of a radical multistep outflow experiment for determining unsaturated hydraulic properties. *Advances in Water Resources* **22**, 431-444.

Fujimaki, H. and Inoue M. (2003). Reevaluation of the multistep outflow method for determining unsaturated hydraulic conductivity. *Vadose Zone Journal* **2**, 409-415.

Grant, C. D. and Dexter, A. R., 1986. Soil structure generation by wetting and drying cycles. *Proc. 13th Cong. Inf. Soc. Sci., Hamburg*, II, 60-62.

Grant, C. D., Watts, C. W., Dexter, A. R., and Frahn, B. S. (1995). An Analysis of the Fragmentation of Remolded Soils, with Regard to Self-Mulching Behavior. *Australian Journal of Soil Research* **33**, 569-583.

Green, T. W., Paydar, Z., Cresswell, H. P. and Drinkwater, R. J., (1998). Laboratory outflow technique for measurement of soil diffusivity and hydraulic conductivity. *CSIRO*, Australia. Technical Report No. **12/98**.

Gregory, A. S., Watts, C. W., Whalley, W. R., Kuan, H. L., Griffiths, B. S., Hallet, P. D. and Whitmore, A. P., (2007). Physical resilience of soil to field compaction and the interactions with plant growth and microbial community structure. *European Journal of Soil Science* **58**, 1221 – 1232.

Gupta, S., Schneider, E., Larson, W., and Hadas, A. (1987). Influence of Corn Residue on Compression and Compaction Behaviour of Soils. *Soil Science Society of America Journal* **51**, 207-212.

Gupta, S. C., Farrell, D. A. and Larson W. E., (1974). Determining effective soil water diffusivities from one-step outflow experiements. *Soil Sci. Soc. Am. J.*, **38**, 710-716.

Håkansson, I., and Lipiec, J. (2000). A review of the usefulness of relative bulk density values in studies of soil structure and compaction. *Soil & Tillage Research* **53**, 71-85.

Håkansson, I., and Reeder, R. C. (1994). Subsoil Compaction by Vehicles with High Axle Load Extent, Persistence and Crop Response. *Soil & Tillage Research* **29**, 277-304.

Halvorson, J. J., Gatto, L. W., and McCool, D. K. (2003). Overwinter changes to near-surface bulk density, penetration resistance and infiltration rates in compacted soil. *Journal of Terramechanics* **40**, 1-24.

Hamza, M. A., and Anderson, W. K. (2003). Responses of soil properties and grain yields to deep ripping and gypsum application in a compacted loamy sand soil contrasted with a sandy clay loam soil in Western Australia. *Australian Journal of Agricultural Research* **54**, 273-282.

Hamza, M. A., and Anderson, W. K., (2005). Soil compaction in cropping systems - A review of the nature, causes and possible solutions. *Soil & Tillage Research* **82**, 121-145.

Hopmans, J. W., Vogel, T. and Koblik P.D., 1992. X-ray Tomography of Soil Water Distribution in One-Step Outflow Experiments. *Soil Sci Soc Am J* **56**, 355-362.

Horn, R. and Dexter, A. R., (1989). Dynamics of soil aggregation in an irrigated desert loess. *Soil & Tillage Research* **13**, 253-266.

Horn, R., Domżał, H., Słowińska-Jurkiewicz, A. and van Ouwerkerk, C., (1995). Soil compaction processes and their effects on the structure of arable soils and their environment. *Soil & Tillage Research* **35**, 23-36.

Horn, R., Way, T. and Rostek, J., (2003). Effect of repeated tractor wheeling on stress/strain properties and consequences on physical properties in structured arable soils. *Soil and Tillage Research* **73**, 291 – 299.

Hussein, J., and Adey, M. A., (1998). Changes in microstructure, voids and b-fabric of surface samples of a Vertisol caused by wet/dry cycles. *Geoderma* **85**, 63-82.

Hwang, S. I. and Powers, S. E., (2003). Estimating unique soil hydraulic parameters for sandy media from multi-step outflow experiments. *Advances in Water Resources* **26**, 445-456.

Ippisch, H. J. Vogel and P. Bastian, 2006. Validity limits for the van Genuchten–Mualem model and implications for parameter estimation and numerical simulation. *Advances in Water Resources* **29**, 1780-1789.

Jaynes, D. B. and Tyler, E. J., (1980). Comparison of one-step outflow laboratory method to an in situ method for measuring hydraulic conductivity. *Soil Sci. Soc. Am. J.* **44**, 903-907.

John Deere, 2010, http://www.deere.com/en_US/cfd/forestry/deere_forestry/media/pdfs/skidders/hskidders_DKA648H.pdf (accessed 04-2010).

Jones, R. J. A., Spoor, G., and Thomasson, A. J. (2003). Vulnerability of subsoils in Europe to compaction: a preliminary analysis. *Soil & Tillage Research* **73**, 131-143.

Jorgeson, J. and Julien,P., 2005. Peak flow forecasting with radar precipitation and the distributed model CASC2D. *Water International*, **30**, 40–49.

Kim, D., J., Angulo Jaramillo, R., Vauclin, M., Feyen, J. and Choi. S. I., 1999. Modeling of soil deformation and water flow in a swelling soil. *Geoderma* **92**, 217-238.

Keller, T., and Arvidsson, J. (2004). Technical solutions to reduce the risk of subsoil compaction: effects of dual wheels, tandem wheels and tyre inflation pressure on stress propagation in soil. *Soil & Tillage Research* **79**, 191-205.

Kool, J. B., Parker, J. C. and van Genuchten, M. TH., (1985). Determining soil hydraulic properties from one-step outflow experiments by parameter estimation: 1. Theory and numerical studies. *Soil Sci. Soc. Am. J,* **49**, 1348-1354.

Kool, J. B., Parker, J. C. and van Genuchten, M. TH., (1985). Determining soil hydraulic properties from one-step outflow experiments by parameter estimation: II Experimental studies. *Soil Sci. Soc. Am. J.* **49**, 1354-1359.

Kool, J. B., Parker, J. C. and van Genuchten, M. TH., (1987). Parameter estimation for unsaturated flow and transport models – a review. *Journal of Hydrology* **91**, 255-293.

Lambe, T., and Whitman, R., (1969). Soil Mechanics. *John Wiley & Sons, Inc.*, US.

Larink, O., Werner, D., Langmaack, M. and Schrader, S., (2001). Regeneration of compacted soil aggregates by earthworm activity. *Biol Fertil Soils* **33**, 395-401.

Leeson, J., and Campbell, D. J. (1983). The variation of soil critical state parameters with water content and its relevance to the compaction of two agricultural soils. *Journal of Soil Science* **34**, 33-44.

Lesley Dampier & Distance Education and Technology Continuing Studies, The University of British Columbia. http://www.landfood.ubc.ca/soil200/interaction/structure.htm

Lipiec, J., and Hakansson, I. (2000). Influences of degree of compactness and matric water tension on some important plant growth factors. *Soil & Tillage Research* **53**, 87-94.

Lister, T. W., Burger, J. A., and Patterson, S. C. (2004). Role of vegetation in mitigating soil quality impacted by forest harvesting. *Soil Science Society of America Journal* **68**, 263-271.

Liu, Y. P., Hopmans, J. W., Grismer. M. E. and Chen. J. Y., (1998). Direct estimation of air-oil and oil-water capillary pressure and permeability relations from multi-step outflow experiments. *Journal of Contaminant Hydrology* **32**, 223-245.

Marcelino, V., Cnudde, V., Vansteelandt S. and Carò, F., (2006). An evaluation of 2D-image analysis techniques for measuring soil microporosity. *European Journal of Soil Science* **58**, 133-140.

McGovern, H. (2002). The Influence of Micro-organisms on Structural Generation in Direct Drilled and Ploughed Soils. *PhD, Cranfield University at Silsoe*.

Mohanty, B. P. 1999. Scaling hydraulic properties of a microporous soil. *Water Resources Research* **35**, 1927-1931.

Mohanty, B. P., Shouse, P. J., Miller, D. A. and van Genuchten, M. TH., (2002). Soil properties database: Southern Great Plains 1997 hydrology experiment. *Water Resources Research* **38**, 1-7.

Motavalli, P. P., Stevens, W. E., and Hartwig, G. (2003). Remediation of subsoil compaction and compaction effects on corn N availability by deep tillage and application of poultry manure in a sandy-textured soil. *Soil & Tillage Research* **71**, 121-131.

Munkholm, L. J., and Schjonning, P. (2004). Structural vulnerability of a sandy loam exposed to intensive tillage and traffic in wet conditions. *Soil & Tillage Research* **79**, 79-85.

Nigg, B. M., 1990. The validity and relevance of tests used for the assessment of sports surfaces. *Medicine and Science in Sports And Exercise*, **22**, 131-139.

O'Sullivan, M. F., Henshall, J. K. and Dickson, J. W., (1999). A simplified method for estimating soil compaction. *Soil & Tillage Research* **49**, 325-335.

Parker, J. C., Kool, J. B. and van Genuchten, M. Th., (1985). Determining soil hydraulic properties from one-step outflow experiments by parameter estimation: II. Experimental studies. *Soil Science Society of America Journal* **49**, 1354 – 1359.

Pillai, U. P., and McGarry, D. (1999). Structure repair of a compacted vertisol with wet-dry cycles and crops. *Soil Science Society of America Journal* **63**, 201-210.

Peng, X., Horn, R., (2005). Modeling soil shrinkage curve across a wide range of soil Types. *Soil Science Society of America Journal* **69**, 584-592.

Peng, X., Horn, R., (2006). Anisotropic shrinkage and swelling of some organic and inorganic soils. *European Journal of Soil Science* **58,** 98-107.

Peng, X., Horn, R., Peth, S. and Smucker, A., (2006). Quantification of soil shrinkage in 2D digital image processing of soil surface. *Soil & Tillage Research* **91**, 173-180.

Pengthamkeerati, P., Motavalli, P. P., Kemer, R. J. and Anderson, S. H., (2005). Soil

carbon dioxide efflux from a claypan soil affected by surface compaction and applications of poultry litter. *Agriculture Ecosystems and Environment* **109**, 75-86.

Pillai, U. P., and McGarry, D. (1999). Structure repair of a compacted vertisol with wet-dry cycles and crops. *Soil Science Society of America Journal* **63**, 201-210.

Pires, L. P., Bacchi, O. O. S. and Reichardt, K., (2005). Gammer ray computed tomography to evaluate wetting/drying soil structure changes. *Nuclear Instruments and Methods in Physics Research B* **229**, 443-456.

Poodt, M. P., Koolen, A. J., and van der Linden, J. P., (2003). FEM analysis of subsoil reaction on heavy wheel loads with emphasis on soil preconsolidation stress and cohesion. *Soil & Tillage Research* **73**, 67-76.

Preston, S., Griffiths, B. S. and Young I. M., (1997). An investigation into sources of soil crack heterogeneity using fractal geometry. *European Journal of Soil Science* **48**, 31-37.

Preston, S., Wirth, S., Ritz, K., Griffiths, B. S. and Young, I. M., (2001). The role played by microorganisms in the biogenesis of soil cracks: importance of substrate quantity and quality. *Soil Biology and Biochemistry* **33**, 1851-1858.

Rab, M. A. (2004). Recovery of soil physical properties from compaction and soil profile disturbance caused by logging of native forest in Victorian Central Highlands, Australia. *Forest Ecology and Management* **191**, 329-340.

Radford, B. J., Yule, D. F., McGarry, D. and Playford, C., (2007). Amelioration of soil compaction can take 5 years on a Vertisol under no till in the semi-arid subtropics. *Soil & Tillage Research* **97**, 249-255

Reeve, M. J., and Earl, R. (1989). The Effect of Soil Strength on Agricultural and Civil Engineering Field Operations, Rep. No. 3806. *Soil Survey and Land Research Centre*, Silsoe.

Reeve, M. J., and Hall, D. G. M. (1978). Shrinkage in clayey subsoils of contrasting structure. *Journal of Soil Science* **29**, 315-323.

Richards, L. A., (1931). Capillary conduction of liquids through porous mediums. *Physics* **1**, 318 – 333.

Ringrose-Voase, A., J. (1996). Measurement of soil micropore geometry by image analysis of sections through impregnated soil. Plant and Soil 183, pages 27-47.

Sarmah, A. K., Pillai, U., and McGarry, D. (1996). Repair of the structure of a compacted Vertisol via wet/dry cycles. *Soil & Tillage Research* **38**, 17-33.

Schaap M G. and van Genuchten, M. Th., 2005. A Modified Mualem–van Genuchten Formulation for Improved Description of the Hydraulic Conductivity Near Saturation. *Vadose Zone Journal.* **5**, 27-34

Schulze, E. D., and Freibauer, A., (2005). Carbon unlocked from soils. *Nature* **437**, 205 – 206.

Sharifi, A. (2004). Development of a Soil Compaction Profile Sensor. *Doctoral Thesis presented to Cranfield University at Silsoe*.

Shestak, C. J., and Busse, M. D. (2005). Compaction Alters Physical but Not Biological Indices of Soil Health. *Soil Sci. Soc. Am. J.* **69**, 236-246.

Šimůnek, J., van Genuchten, M. Th. and Šejna M., 2005. The HYDRUS-1D Software Package for Simulating the One-Dimensional Movement of Water, Heat, and Multiple Solutes in Variably-Saturated Media. Department of Environmental Sciences, University of California Riverside, Riverside, California.

Slatyer, R. O. (1967). *Plant-water Relationships.* London: Academic Press.

Smith, R., Ellies, A., and Horn, R. (2000). Modified Boussinesq's equations for nonuniform tire loading. *Journal of Terramechanics* **37**, 207-222.

Soehne, W. (1958). Pressure Distribution and Soil Compaction Under Tractor Tires. *Agricultural Engineering*.

Spoor, G., Godwin, R. J., and Taylor, J. C. (1977). "Effects of Autumn and Spring Tillage Practices on Fine Textured Soils," Rep. No. AG 63/113. National College of Agricultural Engineering.

Sridharan, A., and Gurtug, Y., (2004) Swelling behaviour of compacted fine-grained soils. *Engineering Geology* **72**, 9-18.

Sridharan, A. and H. B. Nagaraj, H. B., (2005). Plastic limit and compaction characteristics of finegrained soils. *Ground Improvement* **9**, 17–22.

Stiles, V. H., James, I. T., Dixon, S. J. and Guisasola, I. N., 2009. Natural turf surfaces: The case for continued research. *Sports Medicine*, **39**, 65-84.

Taylor, R. (2003). Weekly Crop Update. Vol. 2005. University of Deleware.

Teepe, R., Brumme, R., Beese, F., and Ludwig, B. (2004). Nitrous Oxide Emission and Methane Consumption Following Compaction of Forest Soils. *Soil Sci. Soc. Am. J.* **68**, 605-611.

Thompson, L.M. and Troeh, F.R., 1993 (Fifth edition). *Soils and Soil Fertility*. Oxford University Press, New York.

Tyrrel, S. F., Leeds-Harrison, P. B. And Harrison, K. S., (2002). Removal of ammoniacal nitrogen from landfill leachate by irrigation onto vegetated treatment planes. *Water Research* **36**, 291 – 299.

van Dam, J. C., Stricker, J. N. M. and Droogers, P., (1992). Inverse method for determining soil hydraulic functions from one-step outflow experiments. *Soil Sci. Soc. Am. J*. **56**, 1042-1050.

van Dam, J. C., Stricker, J. N. M. and Droogers, P., (1994). Inverse method to determine soil hydraulic functions from multistep outflow experiments. *Soil Science Society of America Journal*. **58**, 647-652.

van de Graaff, R. H. M. (1978). Size of Subsoil Blocky Peds in Relation to Textural Parameters, Depth and Drainage. *In* "Modification of Soil Structure" (W. W. Emerson, R. D. Bond and A. Dexter, eds.), pp. 87-96. John Wiley and Sons.

van den Akker, J. J. H. (2004). SOCOMO: a soil compaction model to calculate soil stresses and the subsoil carrying capacity. *Soil & Tillage Research* **79**, 113-127.

van den Akker, J. J. H., Arvidsson, J., and Horn, R. (2003). Introduction to the special issue on experiences with the impact and prevention of subsoil compaction in the European Union. *Soil & Tillage Research* **73**, 1-8.

van Genuchten, M. Th., (1980). A closed-form equation for predicting the hydraulic conductivity of unsaturated soils. *Soil Science Society of America Journal* **44**, 892 – 898.

van Genuchten, M. Th., (1982). A Comparison of Numerical Solutions of the One-Dimensional Unsaturated Flow and Mass Transport Equations. *Advances in Water Resources* **5**, 47 – 55.

Vanderborght, J., Kasteel, R., Herbst, M., Javaux, M., Thiéry, D., Vanclooster, M., Mouvet, C. and Vereecken, H., (2005). A set of analytical benchmarks to test numerical models of flow and transport in soils. *Vadose Zone Journal* **4**, 206-221.

Velde, B. (1999). Structure of surface cracks in soils and muds. *Geoderma* **93**, 101-124.

Velde, B. (2001). Surface cracking and aggregate formation observed in a Rendzina soil, La Touche (Vienne) France. *Geoderma* **99**, 261-276.

Vereecken, H., Kaiser, R., Dust, M. and Pütz, T., (1997). Evaluation of the multistep outflow method for the determination of unsaturated hydraulic properties of soils. *Soil Science* **162**, 618 – 631.

Verheijen, F. (2005). A Reveiw of SOM, it's Controls and Fractions, and the Impact on Farming, *Cranfield University at Silsoe*.

Vogel, H.-J., Hoffmann, H. and Roth, K., (2005). Studies of crack dynamics in clay soil I. Experimental methods, results, and morphological quantification. *Geoderma* **125**, 203-211.

Vogel, H.-J., Hoffmann, H., Leopold, A. and Roth, K., (2005). Studies of crack dynamics in clay soil II. A physically based model for crack formation. *Geoderma* **125**, 213-223.

Vrugt, J. A., Bouten, W., and Weerts, A. H., (2001). Information content of data for identifying soil hydraulic parameters from outflow experiments. *Soil Sci. Soc. Am. J.* **65**, 19-27.

Wagner, S., Cattle, S. R. and Scholten, T., 2007. Soil-aggregate formation as influenced by clay content and organic-matter amendment. *Journal of Plant Nutrition and Soil Science* **170**, 173 – 180.

Werner, D., and Werner, B. (2001). Compaction and recovery of soil structure in a silty clay soil (Chernozem): physical, computer tomographic, and scanning electron microscopic investigations. *Journal of Plant Nutrition and Soil Science-Zeitschrift Fur Pflanzenernahrung Und Bodenkunde* **164**, 79-90.

Whalley, W. R., Riseley, B., Leeds-Harrison, P. B., Bird, N. R. A., and Leech, P. K. (2005). Structural differences between bulk and rhizophere soil. *European Journal of Soil Science* **56**, 353-360.

Whitlow, R. (2001). "Basic Soil Mechanics," 4th/Ed. Pearson Education Ltd.

Wiermann, C., Werner, D., Horn, R., Rostek, J., and Werner, B. (2000). Stress/strain processes in a structured unsaturated silty loam Luvisol under different tillage treatments in Germany. *Soil & Tillage Research* **53**, 117-128.

Williams, S. M., and Weil, R. R. (2004). Crop Cover Root Channels May Alleviate Soil Compaction Effects on Soybean Crop. *Soil Sci. Soc. Am. J.* **68**, 1403-1409.

Wolharn, S., (2001). The practical application of precision farming techniques. MPhil (Tec), Cranfield University.

Yesiller, N., Miller, C. J., Inci, G. and Yaldo, K., (2000). Desiccation and cracking behaviour of three compacted landfill liner soils. *Engineering Geology* **57**, 105-121.

Zhang, B., Horn, R., and Hallett, P. D. (2005). Mechanical resilience of degraded soil amended with organic matter. *Soil Science Society of America Journal* **69**, 864-871.

Appendix 1

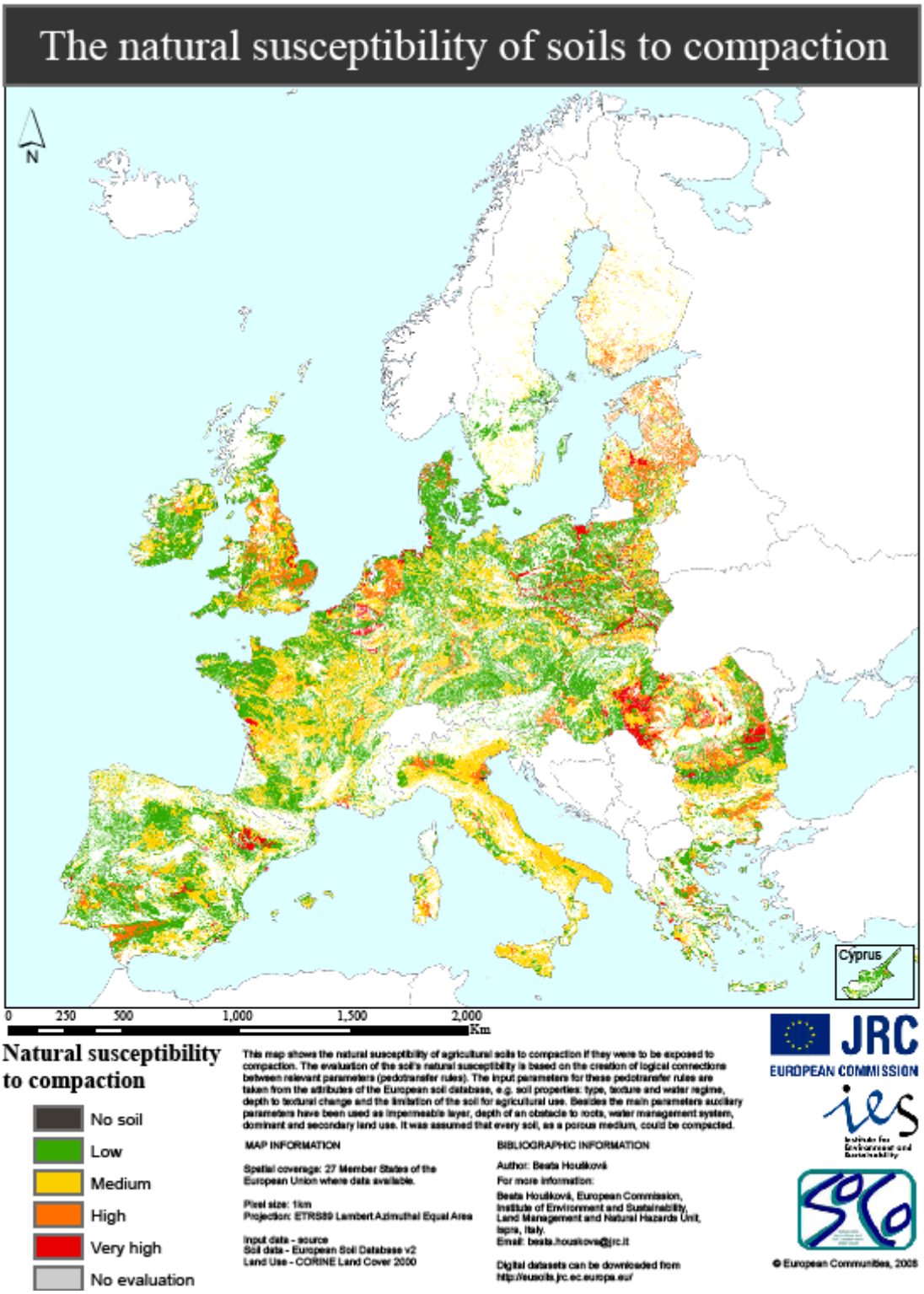
The natural susceptibility of soils to compaction
N
Cyprus
0 250 500 1,000 1,500 2,000
Km
Natural susceptibility to compaction
No soil
Low
Medium
High
Very high
No evaluation
This map shows the natural susceptibility of agricultural soils to compaction if they were to be exposed to compaction. The evaluation of the soil's natural susceptibility is based on the creation of logical connections between relevant parameters (pedotransfer rules). The input parameters for these pedotransfer rules are taken from the attributes of the European soil database, e.g. soil properties: type, texture and water regime, depth to textural change and the limitation of the soil for agricultural use. Besides the main parameters auxiliary parameters have been used as impermeable layer, depth of an obstacle to roots, water management system, dominant and secondary land use. It was assumed that every soil, as a porous medium, could be compacted.
MAP INFORMATION
Spatial coverage: 27 Member States of the European Union where data available.
Pixel size: 1km
Projection: ETRS89 Lambert Azimuthal Equal Area
Input data - source
Soil data - European Soil Database v2
Land Use - CORINE Land Cover 2000
BIBLIOGRAPHIC INFORMATION
Author: Beata Houšková
For more information:
Beata Houšková, European Commission, Institute of Environment and Sustainability, Land Management and Natural Hazards Unit, Ispra, Italy.
Email: beata.houskova@jrc.it
Digital datasets can be downloaded from http://eusoils.jrc.ec.europa.eu/
JRC
EUROPEAN COMMISSION
© European Communities, 2008

The text on the above map reads:

This map shows the natural susceptibility of agricultural soils to compaction if they were to be exposed to compaction. The evaluation of the soil's natural susceptibility is based on the creation of logical connections between relevant parameters (pedotransfer rules). The input parameters for these pedotransfer rules are taken from the attributes of the European soil database, e.g. soil properties: type, texture and water regime, depth to textural change and the limitation of the soil for agricultural use. Besides the main parameters auxiliary parameters have been used as impermeable layer, depth of an obstacle to roots, water management system, dominant and secondary land use. It was assumed that every soil, as a porous medium, could be compacted.

MAP INFORMATION

Spatial coverage: 27 Member States of the European Union where data available.

Pixel size: 1km

Projection: ETRS89 Lambert Azimuthal Equal Area

Input data - source

Soil data - European Soil Database v2

Land Use - CORINE Land Cover 2000

BIBLIOGRAPHIC INFORMATION

Author: Beata Houšková. For more information: Beata Houšková, European Commission, Institute of Environment and Sustainability, Land Management and Natural Hazards Unit,

Ispra, Italy. Email: beata.houskova@jrc.it Digital datasets can be downloaded from http://eusoils.jrc.ec.europa.eu/ .

Appendix 2

During the process of compressing the soil samples, data regarding the force required to compress the samples was gathered. An example of this data is shown in Figure 58, one compression curve for each soil (full data set shown in Figure 59). Preconsolidation stresses between different compression events create noise at low pressures when the entire data set is considered simultaneously. When pressures exceeded the preconsolidation stress, however, results were very consistent. The pressure shown was calculated from the force that was applied to the top of the sample during compression and the area of the compression plate. The void ratio, e (the volume voids divided by the volume of solid), was estimated from the displacement of the compression plate, assuming a particle density of 2.65 g cm^{-3}.

Figure 58 clearly shows the different reaction of the soils to compressive forces. Subsoil two (SS/2) compacted more readily than the other two soils when compressed. Subsoil three (SS/3) required a greater force to achieve the same level of compaction at values of e (void ratio) less than 2.0. Subsoil four (SS/4) required the most compactive effort to achieve higher densities. These results show that, of the two soils with similar clay content (subsoils two and three), the soil with the higher organic matter content (subsoil three) was less vulnerable to compaction. However, the soil with the highest clay content (subsoil four) was the least vulnerable to compaction at the gravitational moisture content investigated (25 %, which is within approximately 5 % of the plastic limit of all three soils).

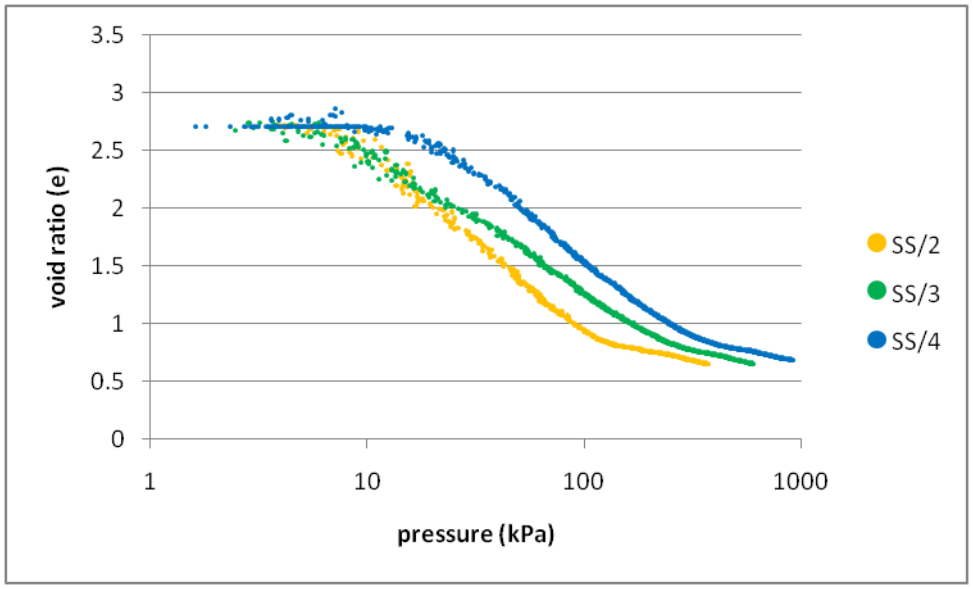

Figure 58. An example of the compression data gathered for sub-soils two, three and four. [6]

Assuming that the particle density was the same for all the soils may have skewed the results somewhat; differences in the particle size distribution and the organic matter content would have an effect on the particle density. However, the differences in the force required to achieve the same bulk density was preserved. The differences apparent between the behaviour of the soils to compressive forces shown in Figure 58 are, therefore, informative.

Compressing the soils at the same moisture content may also have distorted the results. It could be argued that compression should have been conducted at the moisture content at which the individual soils were most compressible. However, it was found by Sridharan and Nagaraj (2005) that soils were most compressible at their approximate plastic limits. As the soils were compressed at moisture contents that were within 5 % of their plastic limits, the

[6] The void ratio (volume of voids divided by the volume of solids) was estimated assuming a particle density of 2.65 g cm-3 for all three soils.

influence of moisture content on the differences in the final results is assumed to have been minimal.

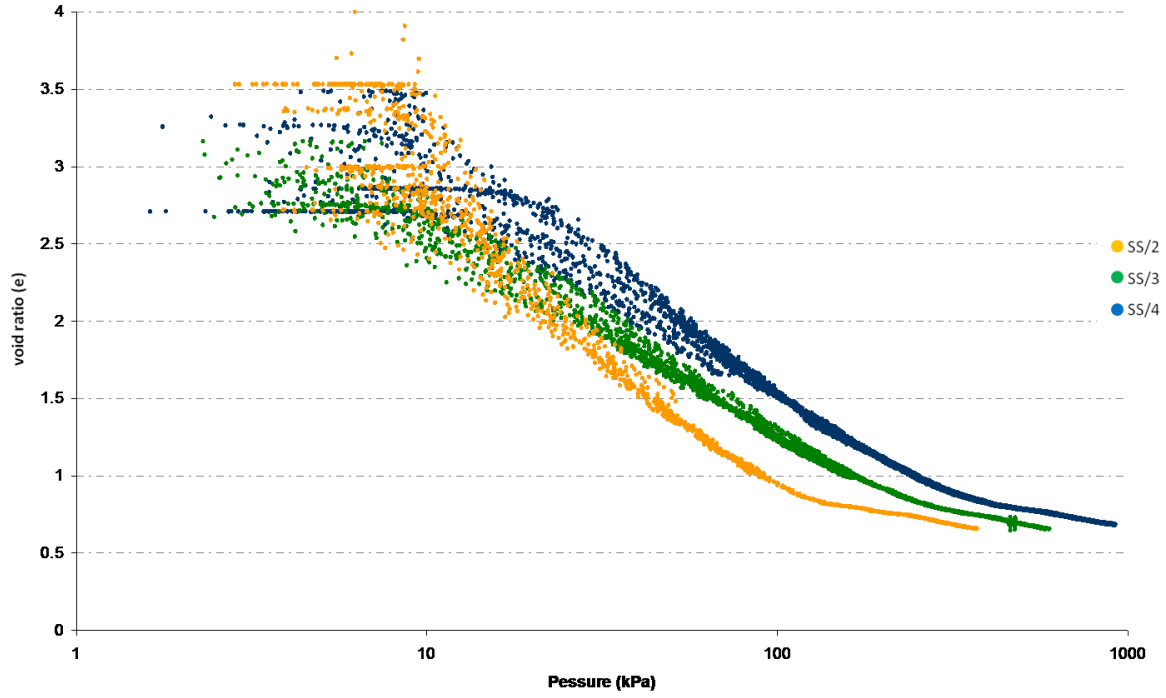

Figure 59. Graph showing all data obtained from compressing six samples of each soil, assuming a particle density of 2.65 g cm^{-3}.

Appendix 3

WatsonSmith

MANOSTAT PRECISION PRESSURE REGULATOR SERIES MANUALLY OPERATED

FEATURES

- Reliable, durable
- Precise regulation
- Excellent setting sensitivity
- High relief capability
- Versatile design for varied applications

GENERAL DESCRIPTION

The manostat precision pressure regulator series are designed for critical pressure control applications and have demonstrated outstanding reliability and durability in many thousands of applications worldwide. It is suitable for dead-end (closed load) conditions and can be supplied on its own or with a visual display dial.
Other versions include; plunger, lever operated and volume boosting air relay (see separate datasheet).

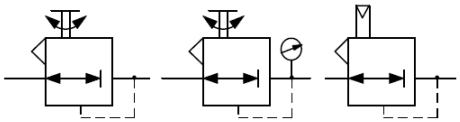

Functional Symbols

TECHNICAL DATA

PNEUMATIC

•Output Signal	See ordering information. Pressure range can be limited by resetting the locknuts provided
•Air Supply	Oil free, dry air or other dry gases, filtered to better than 25 microns; at least 0.2bar (3psig) above output pressure to a maximum of 10bar (150psig, 1000kPa)
•Flow Capacity	Up to 300Nl/min (10scfm). High relief version available (applications requiring rapid exhaust)
•Air Consumption	0.2 l/min (0.006scfm) at 1bar (15psig); 0.3 l/min (0.01scfm) at 1.7bar (25psig); 0.6 l/min (0.02scfm) at 4bar (60psig); 1.2 l/min (0.04scfm) at 8bar (120psig) (typical values at maximum supply pressure)
•Response Time	less than 0.2 seconds for 50% load change
•Regulation Accuracy	% output change for 1bar/15psi supply pressure change at mid-range output: 0.1% (0.14bar/2-25psi), 0.05% (0.14-4bar/2-60psi), 0.02% (0.14-8bar/2-120psi)
•Sensitivity	Better than 0.3mbar (0.005psi)
•Hysteresis and Repeatability	Typically less than 0.05% setting at mid-range
•Temperature Effect	Typically better then ±1% change of full span between -20°C and +70°C
•Connections	1/4" NPT female standard (plus two integral 1/4" NPT gauge ports); others on request

MODEL TYPES

•Handwheel:	Basic manostat unit with pressure adjusting handwheel; mounting in any attitude, integral mounting nut supplied
•Dial manostat:	Manual pressure loading unit combining a manostat regulator with a 4" diameter gauge
•DIN manostat:	As above but with a DIN standard pressure gauge
•DMW:	Weatherproof version of dial manostat with 100mm diameter gauge; pneumatic connections taken to lower face of casing; surface or post mounting (yoke supplied suitable for a 50mm/2" diameter post); casing is polycarbonate, grey finish to IP55
•Volume Boosting Air Relay (manual bias):	Remote control of regulated pressures is possible with minimal air usage; positive or negative bias between pilot signal and regulated pressure can be set up of up to 2bar/30psig

PHYSICAL

•Operating Temperature	-20°C to +70°C
•I.P. Rating	IP65
•Vibration	The unit is unaffected by moderate vibration
•Material of Construction	Zinc diecasting passivated and epoxy painted, Beryllium copper capsule; Nitrile diaphragms

Note: a small pressure (<2psig, 0.14bar) will show at the lower end of dial manostats gauge scale (due to regulator servo operation)

HANDWHEEL MANOSTAT DIAGRAMS

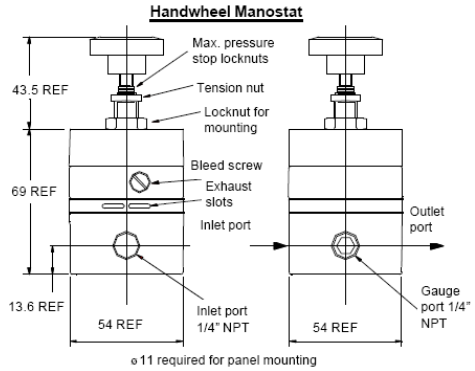

CHARACTERISTIC GRAPHS

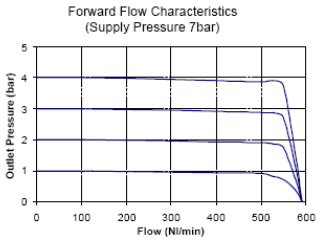

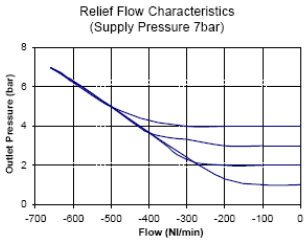

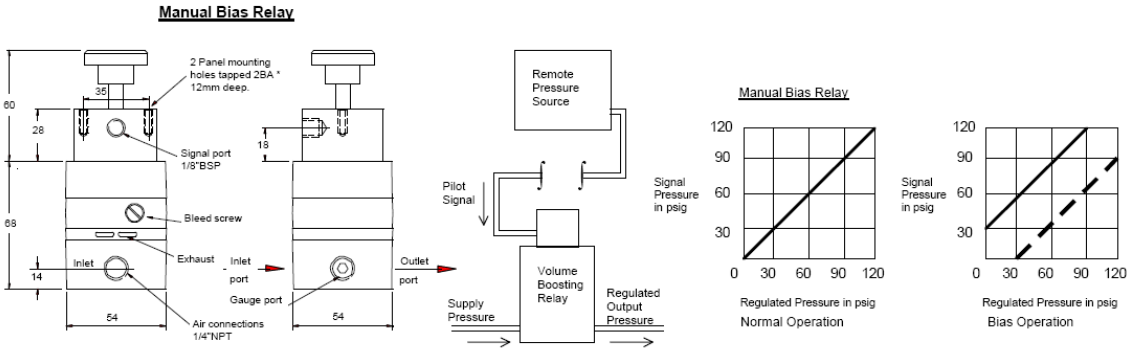

ORDERING INFORMATION

Handwheel manostats		
Output pressure		Order code
0.14-1.7bar, 2-25psig	Standard	53100200R
	High Relief	53120200R
0.14-4bar, 2-60psig	Standard	53100300R
	High Relief	53120300R
0.14-8bar, 2-120psig	Standard	53100400R
	High Relief	53120400R

Manual bias relay		
Output pressure		Order code
0.2-1bar, 3-15psig	Standard	53220100R
	High Relief	53230100R
0.14-8bar, 2-120psig	High Relief	53220400R
	Standard	53230400R

Options to special order: Captured bleed version of handwheel manostat suitable for natural gas applications available. Factory fitting of a reduction gearbox to handwheel manostat (change "00R" to "96R"). Yoke mounting for Weatherproof Manostat (change "00R" to "10R"). Alternative pneumatic connections. Low pressure versions of standard models.

WatsonSmith

DIAL / DIN MANOSTAT DIAGRAMS

Dial Manostat

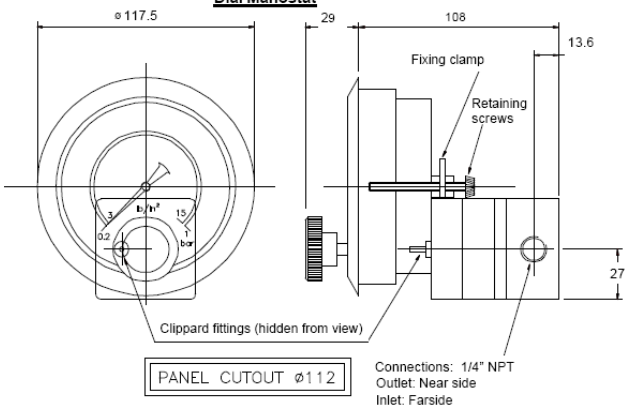

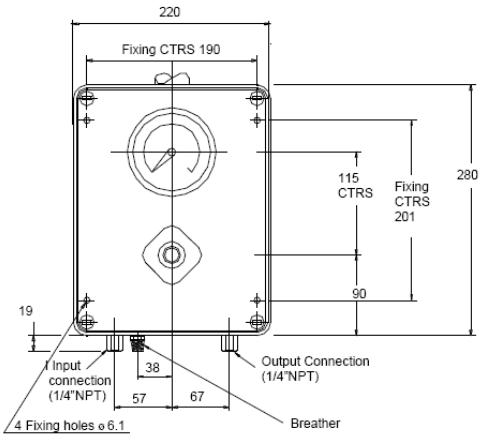

DIN Manostat

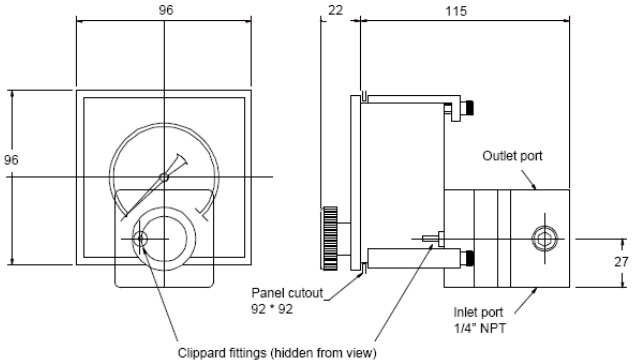

Weatherproof Dial Manostat

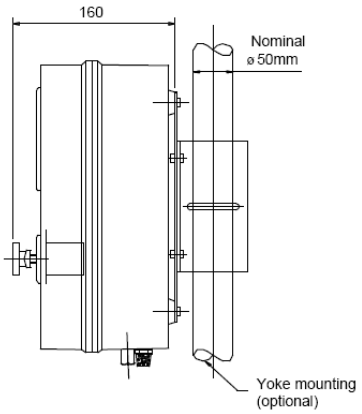

ORDERING INFORMATION

DIN / Dial manostats				
Pressure range	Scale	Dial	DIN	Weatherproof (DMW)
0.2-1bar, 3-15psig	Dual	53300100R	53310100R	53320100R
0-2bar, 0-30psig	Dual	53301200R	53311200R	T.B.A
0-4bar, 0-60psig	Dual	53301300R	53311300R	T.B.A
0-8bar, 0-120psig	Dual	53301400R	53311400R	53321400R
0.2-1bar	0-100%	53309000R	53319000R	53329000R
3-15psig	0-100%	53309100R	53319100R	53329100R
20-100kPa	0-100%	53309200R	53319200R	53329200R

Options to special order: Captured bleed version of handwheel manostat suitable for natural gas applications available. Factory fitting of a reduction gearbox to handwheel manostat (change "00R" to "96R"). Yoke mounting for Weatherproof Manostat (change "00R" to "10R"). Special scale calibrations for Dial Manostats. Alternative pneumatic connections. Low pressure versions of standard models.

WatsonSmith

Keison Products
P.O. Box 2124, Chelmsford
CM1 3UP, England

Tel: +44 (0) 1245 600560
Fax: +44 (0) 1245 600030
Email: sales@keison.co.uk

www.keison.co.uk

IMI
A subsidiary of IMI plc

1998
THE QUEEN'S AWARD FOR EXPORT ACHIEVEMENT

LLOYD'S REGISTER QUALITY ASSURANCE ISO9001
Registered in England 1691122

UKAS QUALITY MANAGEMENT 001

Appendix 4


Druck
PDCR 800 SERIES
General Purpose
Pressure Transducers
Type PDCR 800 Series
High Accuracy
± 0.1% BSL for ranges to 900 psi
Negligible hysteresis and repeatability
Excellent overpressure capability
Greater than 4 times rated pressure
Good thermal stability
± 1.5% total error band -5° to +175°F
Customized versions available
PDCR 800 Series

PDCR 800 SERIES

Every PDCR 800 transducer is based on a high performance pressure sensor (core) which has subsequently been completed for a specific application by the addition of an electron beam welded pressure connector and an electrical connector assembly. The core itself is an accurate pressure transducer incorporating a high integrity silicon diaphragm and titanium module, a pcb assembly and advanced compensation techniques which give excellent performance over extended temperature ranges. The final assembly is electron beam welded and encapsulated. These cores are produced in large quantities and following automatic calibration over the whole temperature range and to three times the nominal pressure range all the data is stored in the computer data base.

The benefits are a high performance to cost ratio series of the transducers listed below, including the core which can be selected and adapted in many different ways and supplied on short delivery.

Type number and specification

PDCR 800/801 - Basic core
PDCR 810/811 - General purpose
PDCR 820/821 - General purpose
PDCR 830/831 - Depth
PDCR 860/861 - Integral connector

This type numbering system denotes the following details:-

PDCR 8XX

- Compensated temperature range
  - **0** 32° to 122°F (0° to 50°C)
  - **1** -5° to +175°F (-20° to + 80°C)
- Backend construction & electrical connection
  - e.g. **2**: teflon cable and reference tube
- 800 transducer series

Please refer to temperature effects, ordering information, assembly diagram and installation drawings to fulfill your requirements.

STANDARD SPECIFICATIONS

Operating pressure ranges
1, 2.5, 5, 10, 20, 30, 50, 100, 150, 200, 300, 500 and 900 psi gauge.
Other pressure units may be specified e.g., ins. H_2O, kPa, etc.
Absolute, differential and sealed gauge transducers are available.
For higher ranges refer to PDCR 610/9000 data sheets.

Negative pressure
All transducers will accurately respond to pressures below gauge (negative pressures) and will operate with a vacuum applied. The reference side of the PDCR 82X is suitable for pressures up to 30 psig.

Overpressure
The rated pressure range can be exceeded by the following multiples causing negligible calibration change:-
10 x for 1 and 2.5 psi ranges
6 x for 5 psi range
4 x for 10 psi range and above.
Reference side: 30 psi maximum
For higher differential pressures refer to PDCR 10/L/900 data sheets.

Burst pressure
In excess of 10 x rated pressure.

Positive pressure media
Fluids compatible with quartz and titanium.

Reference pressure media
Dry, non-corrosive, non-conducting gases.
For liquid pressure media on reference, refer to PDCR 120/WL data sheet.

Conducting pressure media
When operating with a conducting pressure media use a fully floating system or ground the +Ve supply.
If this method is not practicable please refer to PDCR 900 data sheet.

Transduction principle
Integrated silicon strain gauge bridge.

Excitation voltage
10 Volts @ 5mA nominal.

Output voltage
17mV for 1 psi range
25mV for 2.5 psi range
50mV for 5 psi range
100mV for 10 psi range and above.
The above outputs are for 10 Volts and are proportional to excitation voltage.
For amplified outputs please refer to PDCR 130/135 data sheet.

Common mode voltage
Typically + 6.5 Volts with respect to the -Ve supply at 10 Volts excitation.

Output impedance
2000 ohms nominal.

Load impedance
Greater than 100K ohms for quoted performance.

Resolution
Infinite.

Combined non-linearity, hysteresis and repeatability
±0.1% B.S.L. for all ranges.

Zero offset
±3mV maximum.

Span setting
± 10mV maximum. Units of the same range are matched to closer than ± 3mV.

Operating temperature range
-5° to +175°F (-20° to + 80°C) standard.
This temperature range can be extended from -65°F (-54°C) to 250°F (120°C) for PDCR 82X and PDCR 86X.

Temperature effects

PDCR 8X0
±0.5% total error band 32° to 122°F (0° to 50°C) for 2.5 psi ranges and above.
±0.7% total error band 32° to 122°F (0° to 50°C) for 1 psi range.
N.B. PDCR 830 ±0.3%, 30° to 86°F (-2° to +30°C)

PDCR 8X1
±1.5% total error band -5° to +175°F (-20° to + 80°C) for 2.5 ranges and above.
For -65° to +250°F (-54° to +125°C) temperature range please refer to manufacturer. Typical thermal zero and span coefficients of ±0.009%/°F (±0.015%/°C)

Natural frequency
28 kHz for 5 psi increasing to 360 kHz for 500 psi.
For more detailed information please refer to manufacturer.

Acceleration sensitivity
0.006% F.S./g for 5 psi decreasing to 0.0002% F.S./g for 500 psi.

Mechanical shock
1000g for 1ms half sine pulse in each of 3 mutually perpendicular axis will not affect calibration.

Vibration
Response less than 0.05% F.S./g at 30g peak 10Hz-2kHz, limited by 0.5 in. double amplitude (MIL-STD Proc 514.2-2 Curve L).

Weight
3.5 oz nominal.

Electrical Connection

PDCR 81X, 82X
3 ft. integral cable supplied

PDCR 83X
3ft. Vented cable supplied as standard. Continuous lengths up to 500 ft. are available. Please refer to manufacturer for larger lengths.

PDCR 86X
6 pin Bayonet receptacle, PTIH-10-6P or equivalent (Hermetic stainless) to MIL-C-26482.
Mating connector type PT06A-10-6S or equivalent not supplied.

Pressure connection
$^1/_4$" NPT Flat end
$^7/_{16}$" UNF ($^1/_4$ A.N.) as MS33656-4
$^1/_8$" NPT with bulkhead mount (as shown on drawing PDCR 82X)
Flush fitting (M14 x 1.5 thread) - see example installation drawing on back page.
Depth cone (fitted as standard on PDCR 83X)
Others available on request.

Continuing development sometimes necessitates specification changes without notice.

Ordering information

Please state the following:

(1) Type number

PDCR 8XX

- 0 32° to 122°F (0° to 50°C)
- 1 -5° to +175°F (-20° to + 80°C

- 0 basic core
- 1 integral vented cable and boot
- 2 teflon cable & reference tube
- 3 depth back end with integral vented cable which incorporates a Kevlar strain relieving core
- 6 integral connector

(2) Operating pressure range
(3) Pressure connection
(4) Pressure media

For non-standard requirements please specify in detail.

SPECIFICATION OPTIONS

The following summarizes the possibilities and for further details and ordering information please contact our Sales Office.

1. Parameter selection

Every PDCR 800 series transducer is calibrated not only to its nominal full range pressures, but to two times and three times this pressure and also the temperature effects of zero and span are monitored at five temperatures between -5° to +175°F (-20° to +80°C). All this information is stored in a computer and enables us, where it is important, to optimize the performance parameters to suit specific applications. Selection can either be for improved performance in accuracy or temperature drift from standard transducers or to optimize certain parameters by using the transducers in the overrange condition.

2. Improved accuracy

The standard linearity and hysteresis is ±0.1% B.S.L., but this can be improved to ±0.05% B.S.L., or even better by selection. In some cases this may result in a reduction of the full scale output.

3. Higher overload pressure

The lowest overload pressure for standard devices is 400% but this can be increased up to 1000% where necessary. This will reduce the full scale output and increase the zero drift with temperature unless this is maintained by selection.

4. Higher output

All cores can be overranged by three times nominal full scale, giving outputs of up to 300mV for most ranges. This will improve the zero stability, reduce the overload, and the linearity will be slightly degraded.

N.B. The calibration data available for transducers operating in overload condition is limited to 1000 psi maximum.

5. Excitation voltage

The transducers can be operated from any d.c. excitation up to 12 Volts maximum. The output is proportional to excitation, but the exact offset and span should be measured at the desired excitation.

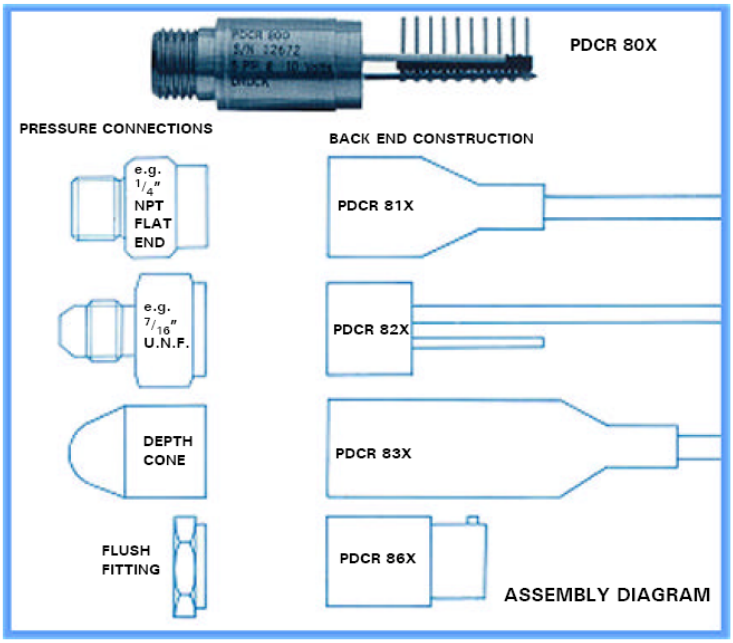

6. Improved temperature effects

Improved thermal error bands can be selected from the data base.
e.g. ±0.3% 32° to 122°F (0° to 50°C)
±1.0% -5° to 175° F (-20° to +80°C)
Other error bands over different temperature ranges can also be selected.

7. Improved zero stability

Thermal zero shift and long term zero stability are improved proportionally with overload.

8. Long term stability

The standard PDCR 800 series offers typically 0.2% F.S. per year stability at 10 Volt operation, but this can be improved considerably by operating in the overrange condition at a reduced supply voltage.

9. Thermal hysteresis

The calibration of a standard transducer at room temperature will repeat within 0.2% F.S. after cycling through the full temperature range.

10. Rationalization

The transducers can be selected such that both the zero offset and the full scale output are matched to better than 1% F.S. where interchangeability is important.

11. Extended temperature range

Transducers are available which will operate between -65° to +250° F (-54° to +125°C).

Please refer to PDCR 82X2 product note.

12. Shunt cal.

This facility is available by connecting an external resistor across the appropriate connection. The thermal coefficient of this Shunt cal. signal is typically 0.0025%/°F.

13. Calibration print out

Available on request relating to selected parameters above.

Examples of alternative specifications based upon a standard 150 psig transducer

Operating pressure range psi	Overload X.F.S.	Accuracy B.S.L. % F.S.	Output with 10 Volt excitation
100	X6	±0.06%	70mV
150	X4(600 psi)	±0.1%	100mV
300	X2	±0.15%	200mV
450	X1.3	±0.2%	300mV

The above example illustrates the various specification performances when using the standard 150 psig core. e.g. used at 300 psi continuously, the overload is X2, accuracy is ± 0.15% B.S.L. and output 200mV.

150 psig	X4(600 psi)	±0.06%	100mV

The above example can be selected if ±0.06% is required with 100mV output for ranges up to 300 psi.

INSTALLATION DRAWINGS

Dimensions: inches

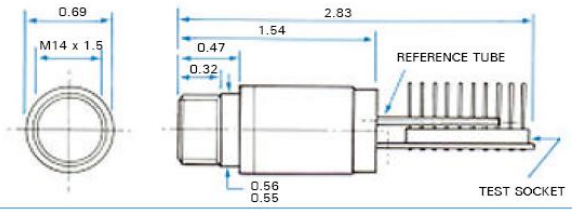

Electrical connection

Test socket	PDCR 80X	
k	1	Output negative
f	3	Supply negative
e	4	Supply positive
j	5	Output positive

PDCR 80X

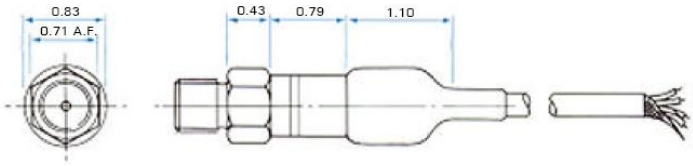

Electrical connection
6 Core shielded/vented cable

Red	Supply positive
White	Supply negative
Yellow	Output positive
Blue	Output negative
Shield	N/C to transducer body

Any other cores not connected.

PDCR 81X

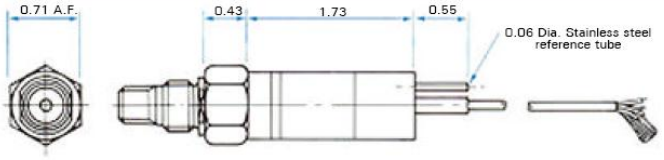

Electrical connection
4 Core teflon shielded cable

Red	Supply positive
Blue	Supply negative
Yellow	Output positive
Green	Output negative
Shield	N/C to transducer body

PDCR 82X

Pressure Connection

Illustrated front end depth cone fitted as standard.

This incorporates a hydraulic damper to protect the device from high pressure pulses caused by underwater impact.

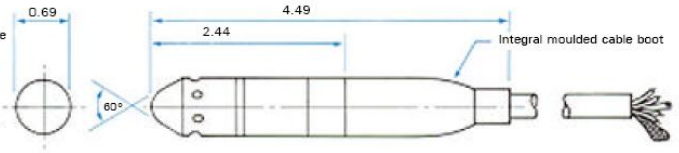

Electrical connection
6 Core shielded/vented cable

Red	Supply positive
White	Supply negative
Yellow	Output positive
Blue	Output negative
Black, Shield	To transducer body

Any other cores not connected.

PDCR 83X

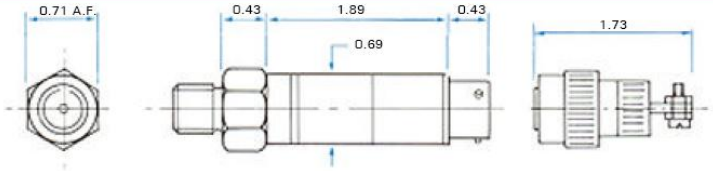

Electrical connection

Pin A	Supply positive
Pin B	Output positive
Pin C	Output negative
Pin D	Supply negative

PDCR 86X

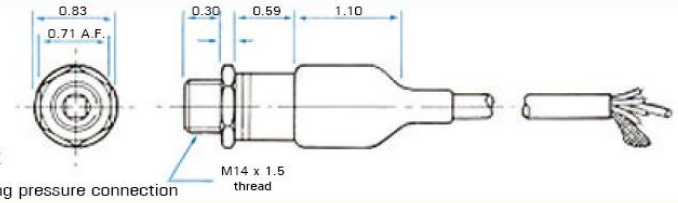

e.g. PDCR 81X
with flush fitting pressure connection

Electrical connection
6 Core shielded/vented cable

Red	Supply positive
White	Supply negative
Yellow	Output positive
Blue	Output negative
Shield	N/C to transducer body

Any other cores not connected.

Druck Incorporated
4 Dunham Drive
New Fairfield, CT06812
Tel: (203)-746-0400
Fax: (203)-746-2494
E-Mail: usa.sales@druck.com
http://www.druckinc.com

Representative:

Appendix 5

The following figures describe changes in the hydraulic properties of SS/2, SS/3 and SS/4, as estimated by HYDRUS-1D, from drainage data gathered during drying cycles 1 and 3. The samples have been arranged in order of increasing bulk density and each sample has two figures associated with it. The first figure shows the total volume of water filled pores at tension. These figures demonstrate that pores of all effective diameters were changed during the wetting and drying process, not just those visible as cracks. With these graphs, a table is shown that gives the parameters of the van Genuchten-Mualem Equation that were estimated by HYDRUS-1D and their 95 % confidence intervals i.e. there is a 95 % probability that the 'true' value lies between the limits quoted. The second figure in each pair shows this information graphically, alongside the measured drainage data.

SS/2

Low density group

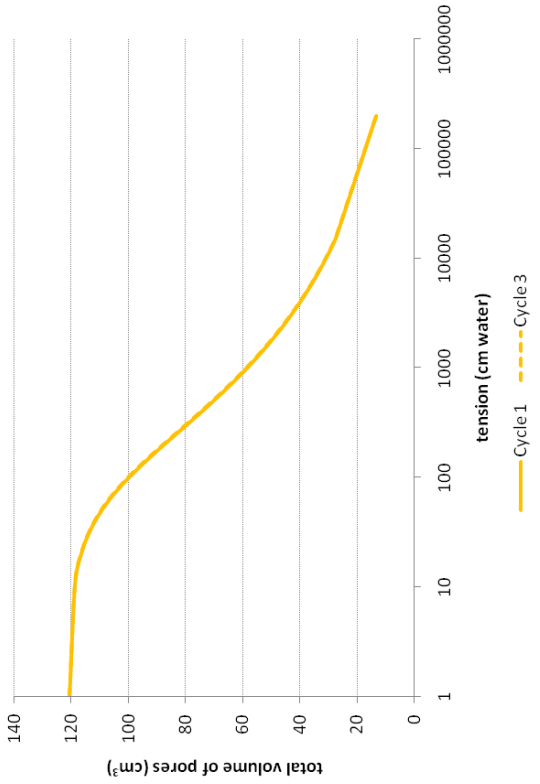

SS/2	cycle 1	*lower*	*upper*	cycle 3	*lower*	*upper*
bulk density (g cm^{-3})	**1.20E+00**			**1.20E+00**		
alpha	**1.30E-02**	*8.44E-03*	*1.75E-02*	**1.27E-02**	*1.20E-02*	*1.35E-02*
n	**1.28E+00**	*1.27E+00*	*1.29E+00*	**1.28E+00**	*1.26E+00*	*1.29E+00*
K_{sat} (cm s^{-1})	**2.03E-07**	*1.51E-07*	*2.54E-07*	**3.10E-05**	*2.42E-05*	*3.78E-05*
l	**7.83E-05**	*-4.81E-02*	*4.83E-02*	**1.14E+01**	*1.05E+01*	*1.23E+01*
R^2 drainage	**9.96E-01**			**9.96E-01**		

Figure 60.SS/2, sample 1. Total volume of water filled pores during drainage cycles 1 and 3.

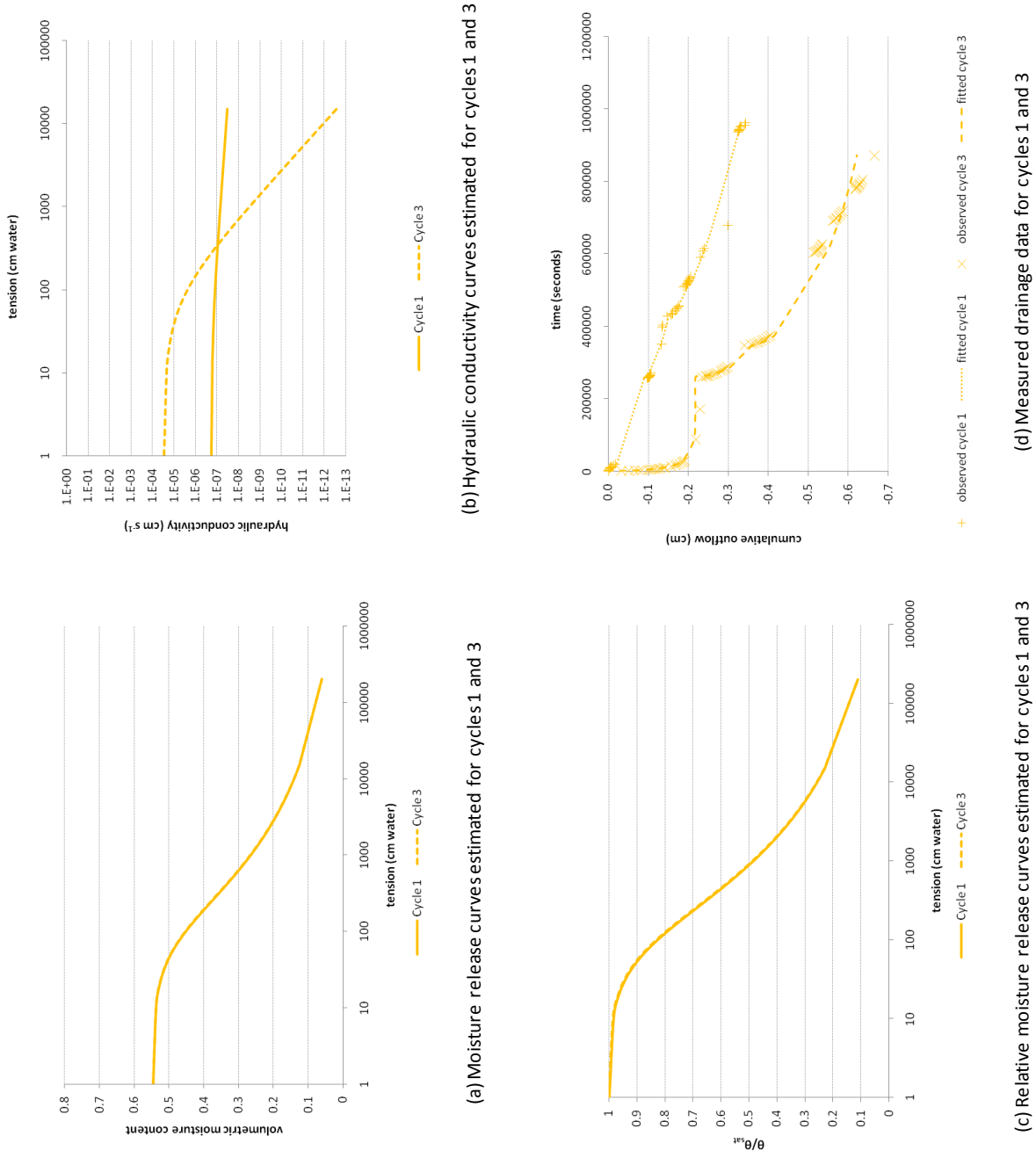

Figure 61. SS/2, sample 1. Hydraulic properties estimated with HYDRUS-1D.

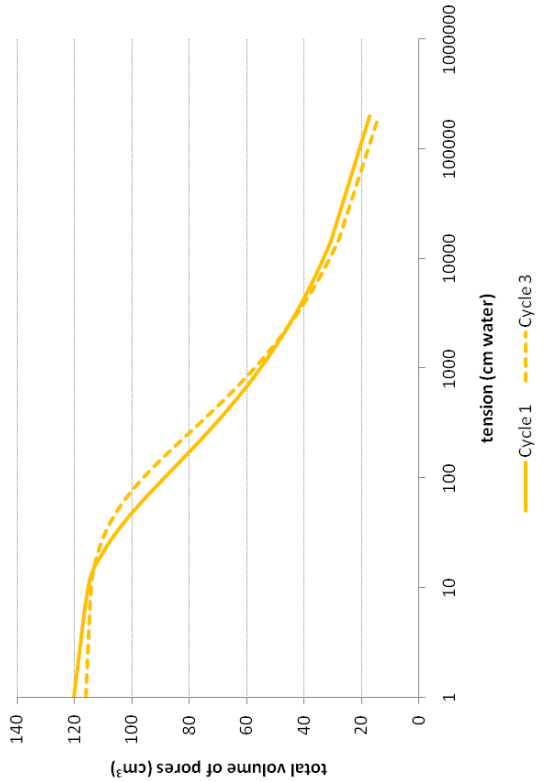

SS/2	cycle 1	*lower*	*upper*	cycle 3	*lower*	*upper*
bulk density (g cm^{-3})	**1.23E+00**			**1.25E+00**		
alpha	**1.49E-02**	*4.16E-03*	*2.56E-02*	**1.34E-02**	*1.26E-02*	*1.43E-02*
n	**1.27E+00**	*1.25E+00*	*1.29E+00*	**1.27E+00**	*1.26E+00*	*1.28E+00*
K_{sat} (cm s^{-1})	**4.12E-07**	*3.00E-07*	*5.24E-07*	**1.40E-05**	*1.22E-05*	*1.59E-05*
l	**2.00E-02**	*-2.52E+00*	*2.56E+00*	**8.06E+00**	*7.39E+00*	*8.73E+00*
R^2 drainage	**9.96E-01**			**9.98E-01**		

Figure 62. SS/2, sample 2. Total volume of water filled pores during drainage cycles 1 and 3.

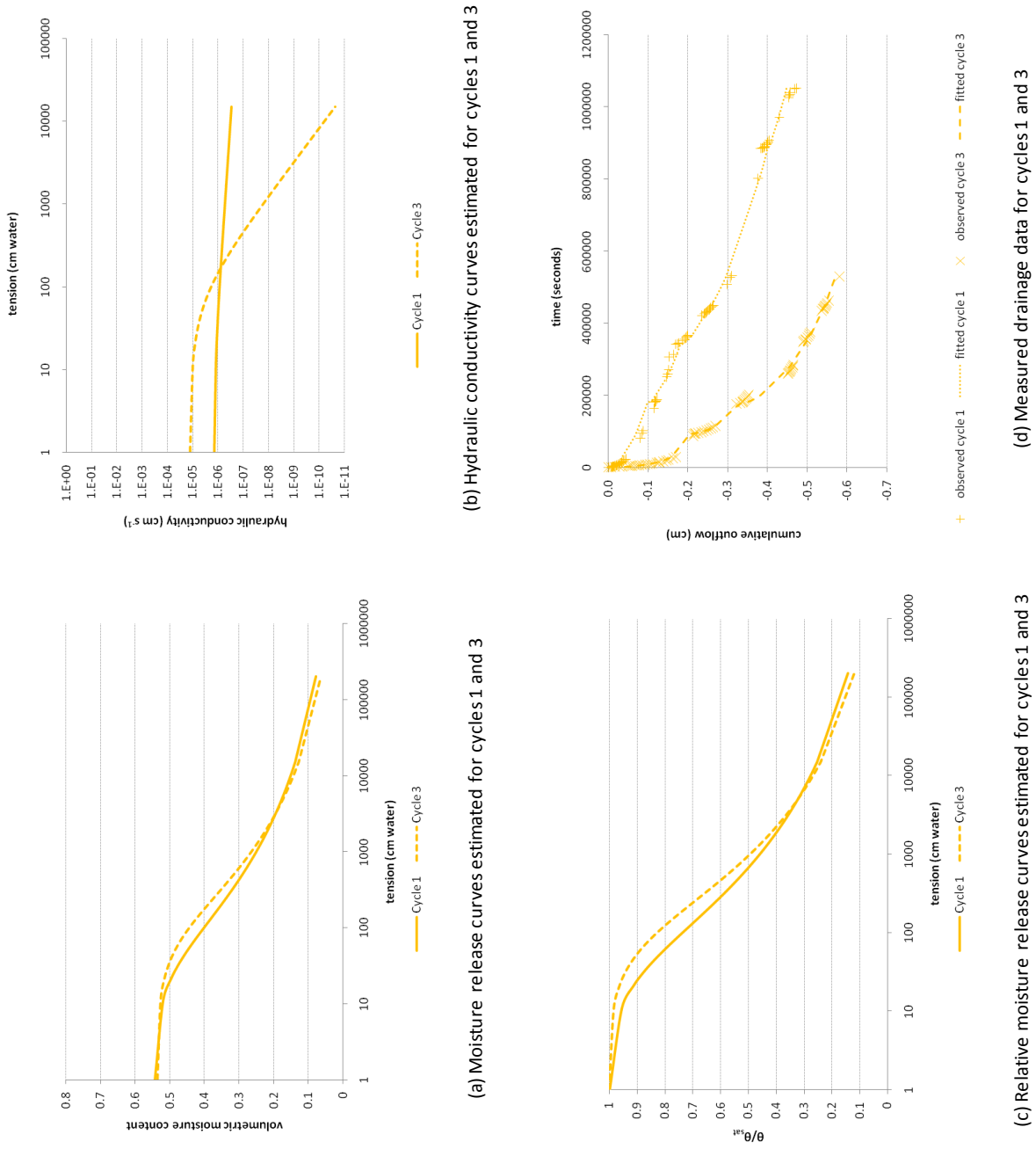

Figure 63. SS/2, sample 2. Hydraulic properties estimated with HYDRUS-1D.

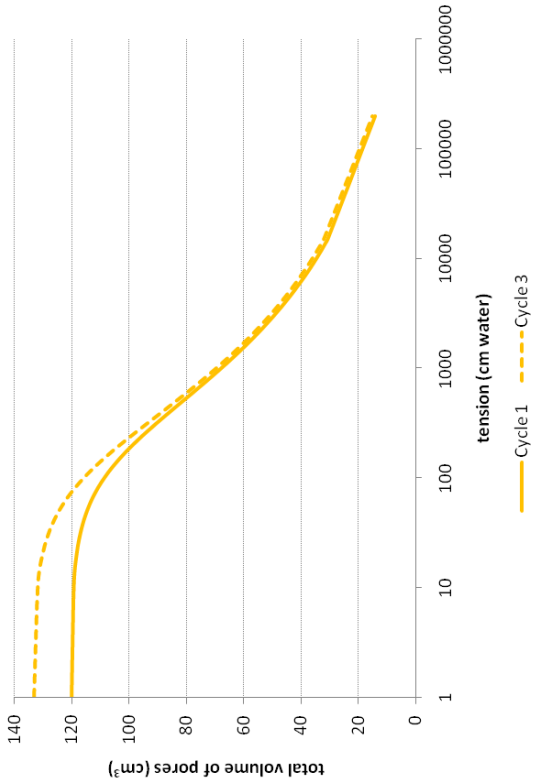

SS/2	cycle 1	*lower*	*upper*	cycle 3	*lower*	*upper*
bulk density (g cm^{-3})	**1.23E+00**			**1.16E+00**		
alpha	**6.29E-03**	*6.04E-03*	*6.54E-03*	**8.98E-03**	*8.15E-03*	*9.82E-03*
n	**1.30E+00**	*1.29E+00*	*1.30E+00*	**1.29E+00**	*1.28E+00*	*1.31E+00*
K_{sat} (cm s^{-1})	**6.40E-07**	*5.38E-07*	*7.42E-07*	**8.04E-06**	*5.28E-06*	*1.08E-05*
l	**1.81E+01**	*1.62E+01*	*1.99E+01*	**1.01E+01**	*8.20E+00*	*1.21E+01*
R^2 drainage	**9.99E-01**			**9.91E-01**		

Figure 64. SS/2, sample 3. Total volume of water filled pores during drainage cycles 1 and 3.

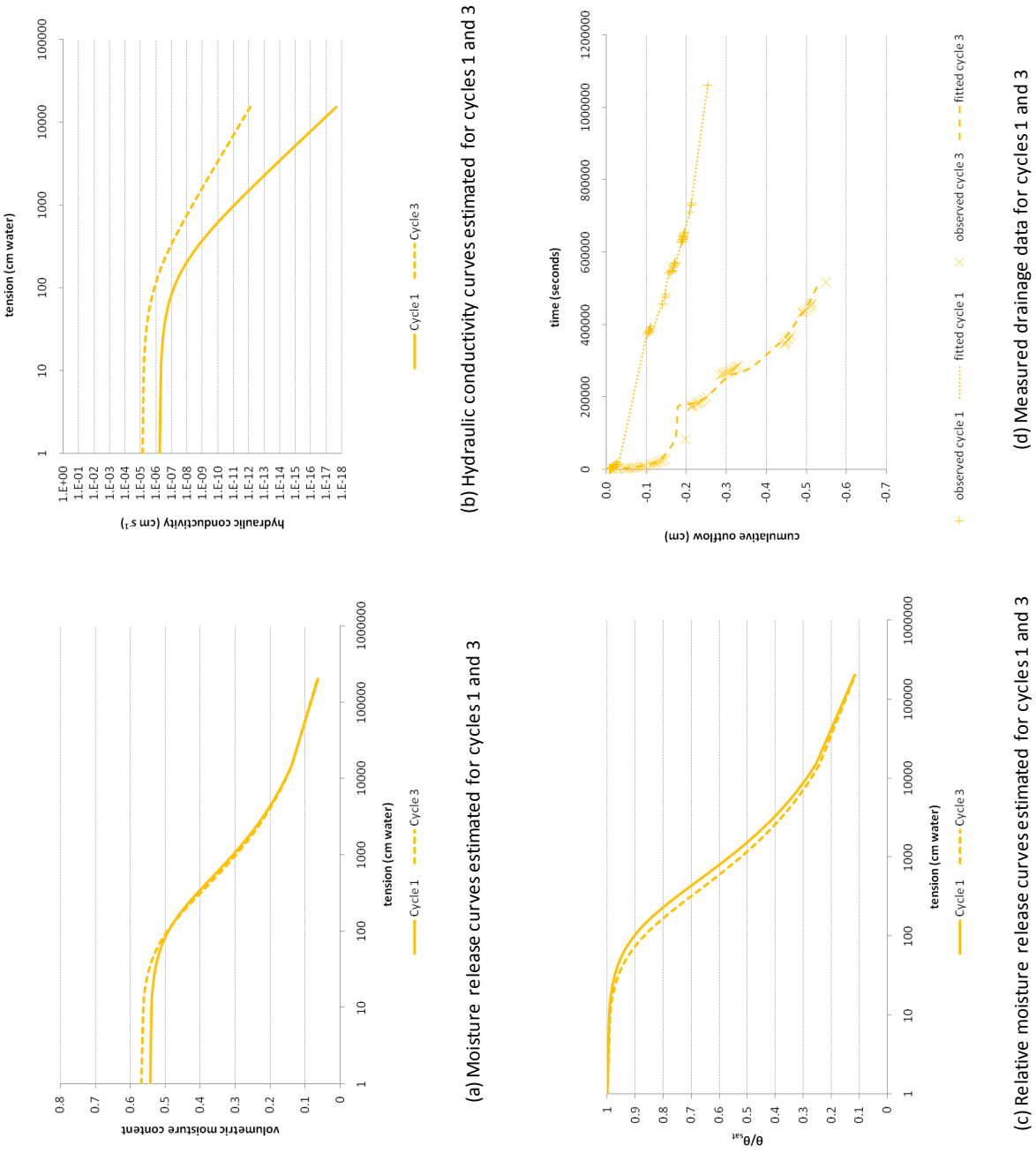

Figure 65. SS/2, sample 3. Hydraulic properties estimated with HYDRUS-1D.

Medium density group

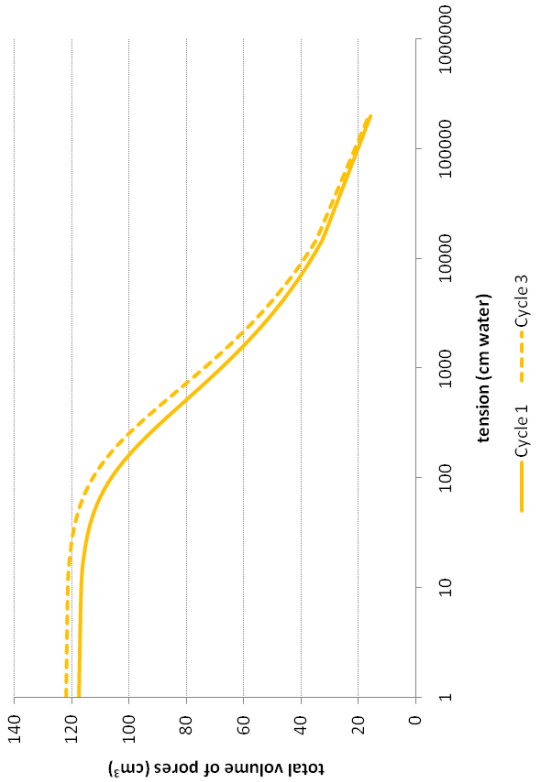

SS/2	cycle 1	*lower*	*upper*	cycle 3	*lower*	*upper*
bulk density (g cm^{-3})	**1.35E+00**			**1.33E+00**		
alpha	**6.64E-03**	*-6.66E-02*	*7.99E-02*	**5.18E-03**	*3.84E-03*	*6.52E-03*
n	**1.28E+00**	*9.36E-01*	*1.63E+00*	**1.29E+00**	*1.28E+00*	*1.31E+00*
K_{sat} (cm s^{-1})	**1.98E-08**	*-8.94E-08*	*1.29E-07*	**4.09E-07**	*2.15E-07*	*6.04E-07*
l	**5.22E-03**	*-4.49E+01*	*4.49E+01*	**2.38E+00**	*-1.47E+00*	*6.23E+00*
R^2 drainage	**9.16E-01**			**9.92E-01**		

Figure 66. SS/2, sample 4. Total volume of water filled pores during drainage cycles 1 and 3.

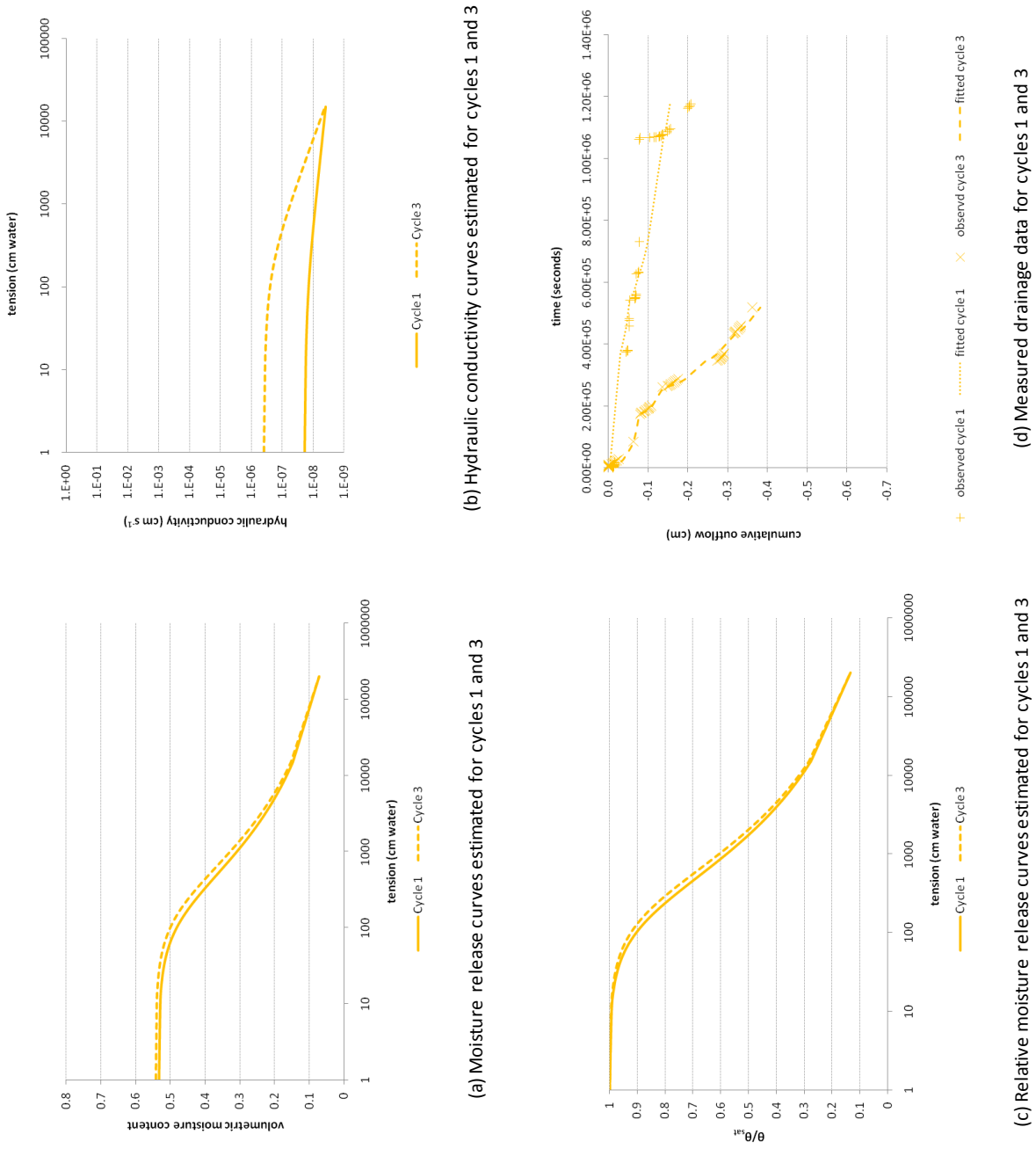

Figure 67. SS/2, sample 4. Hydraulic properties estimated with HYDRUS-1D.

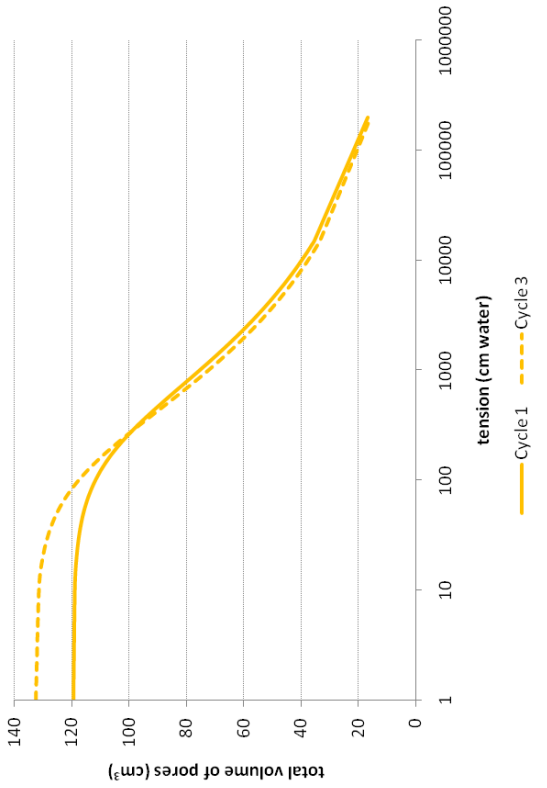

SS/2	cycle 1	*lower*	*upper*	cycle 3	*lower*	*upper*
bulk density (g cm^{-3})	**1.39E+00**			**1.31E+00**		
alpha	**4.41E-03**	*4.18E-03*	*4.64E-03*	**7.68E-03**	*7.36E-03*	*8.00E-03*
n	**1.29E+00**	*1.29E+00*	*1.30E+00*	**1.29E+00**	*1.28E+00*	*1.29E+00*
K_{sat} (cm s^{-1})	**1.73E-06**	*1.19E-06*	*2.28E-06*	**2.56E-06**	*1.99E-07*	*2.96E-06*
l	**4.33E+01**	*2.35E+00*	*4.80E+01*	**1.44E+01**	*1.32E+01*	*1.56E+01*
R^2 drainage	**9.95E-01**			**9.98E-01**		

Figure 68. SS/2, sample 5. Total volume of water filled pores during drainage cycles 1 and 3.

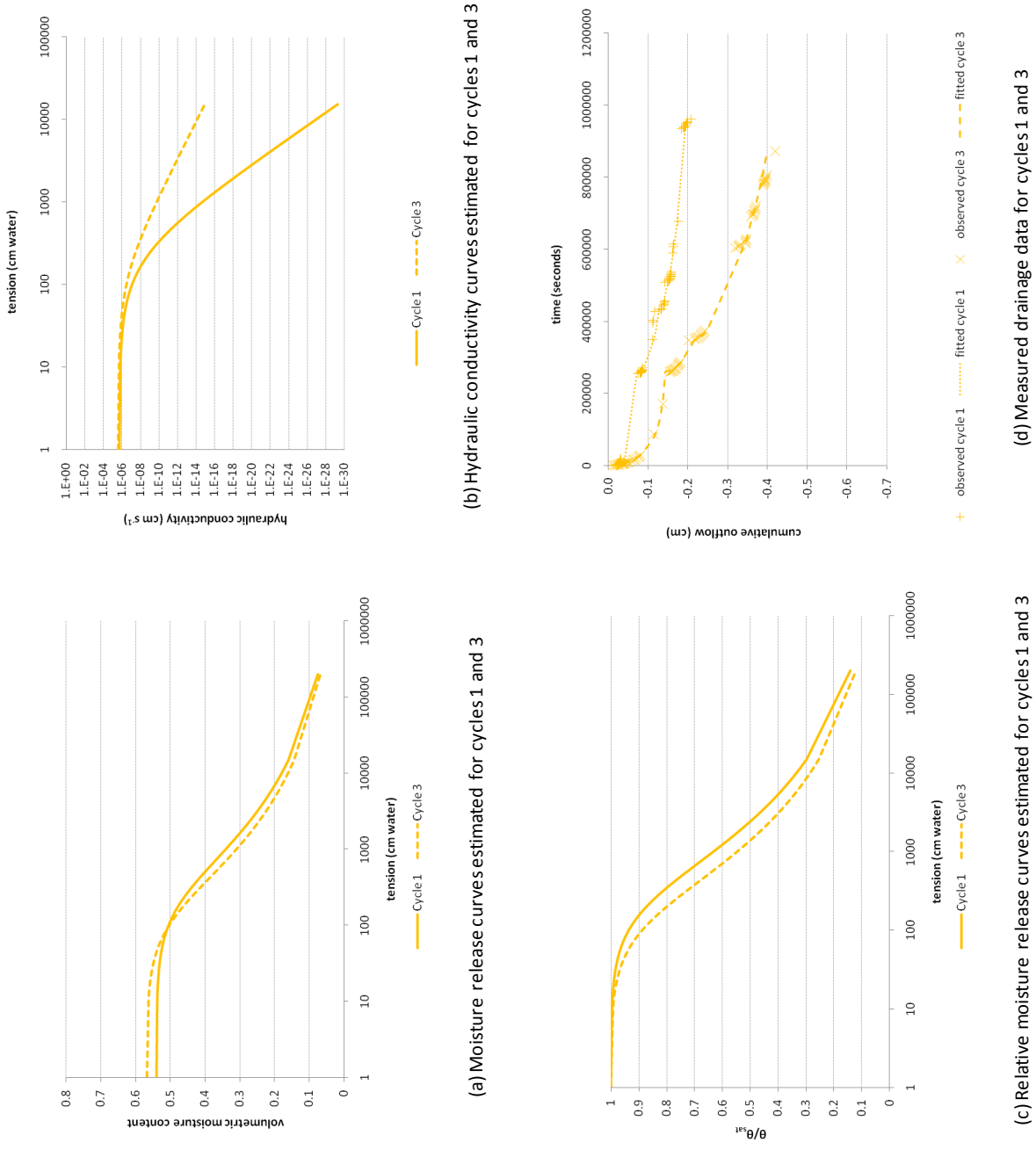

Figure 69. SS/2, sample 5. Hydraulic properties estimated with HYDRUS-1D.

High density group

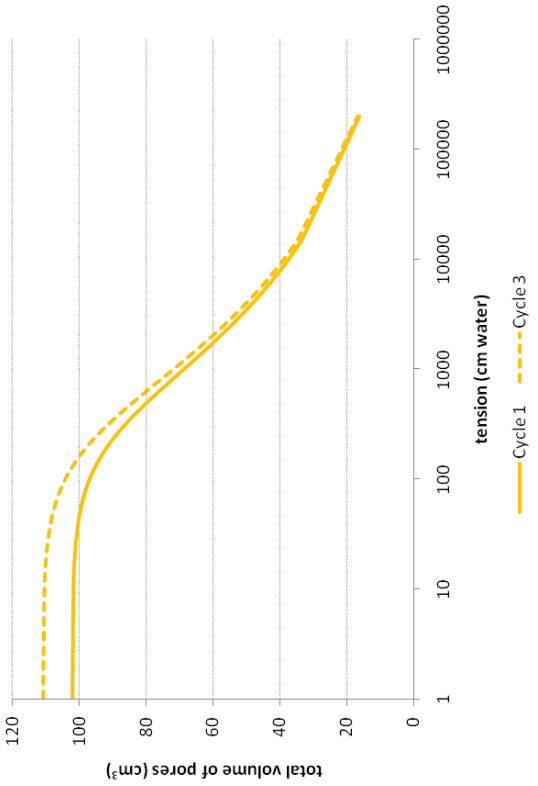

SS/2	cycle 1	*lower*	*upper*	cycle 3	*lower*	*upper*
bulk density (g cm^{-3})	**1.48E+00**			**1.42E+00**		
alpha	**3.59E-03**	*3.39E-03*	*3.78E-03*	**4.20E-03**	*3.69E-03*	*4.70E-03*
n	**1.27E+00**	*1.27E+00*	*1.28E+00*	**1.28E+00**	*1.27E+00*	*1.29E+00*
K_{sat} (cm s^{-1})	**3.29E-07**	*2.36E-07*	*4.22E-07*	**7.61E-07**	*5.07E-07*	*1.02E-06*
l	**2.86E+01**	*2.40E+01*	*3.31E+01*	**7.28E+00**	*4.67E+00*	*9.88E+00*
R^2 drainage	**9.98E-01**			**9.94E-01**		

Figure 70. SS/2, sample 6. Total volume of water filled pores during drainage cycles 1 and 3.

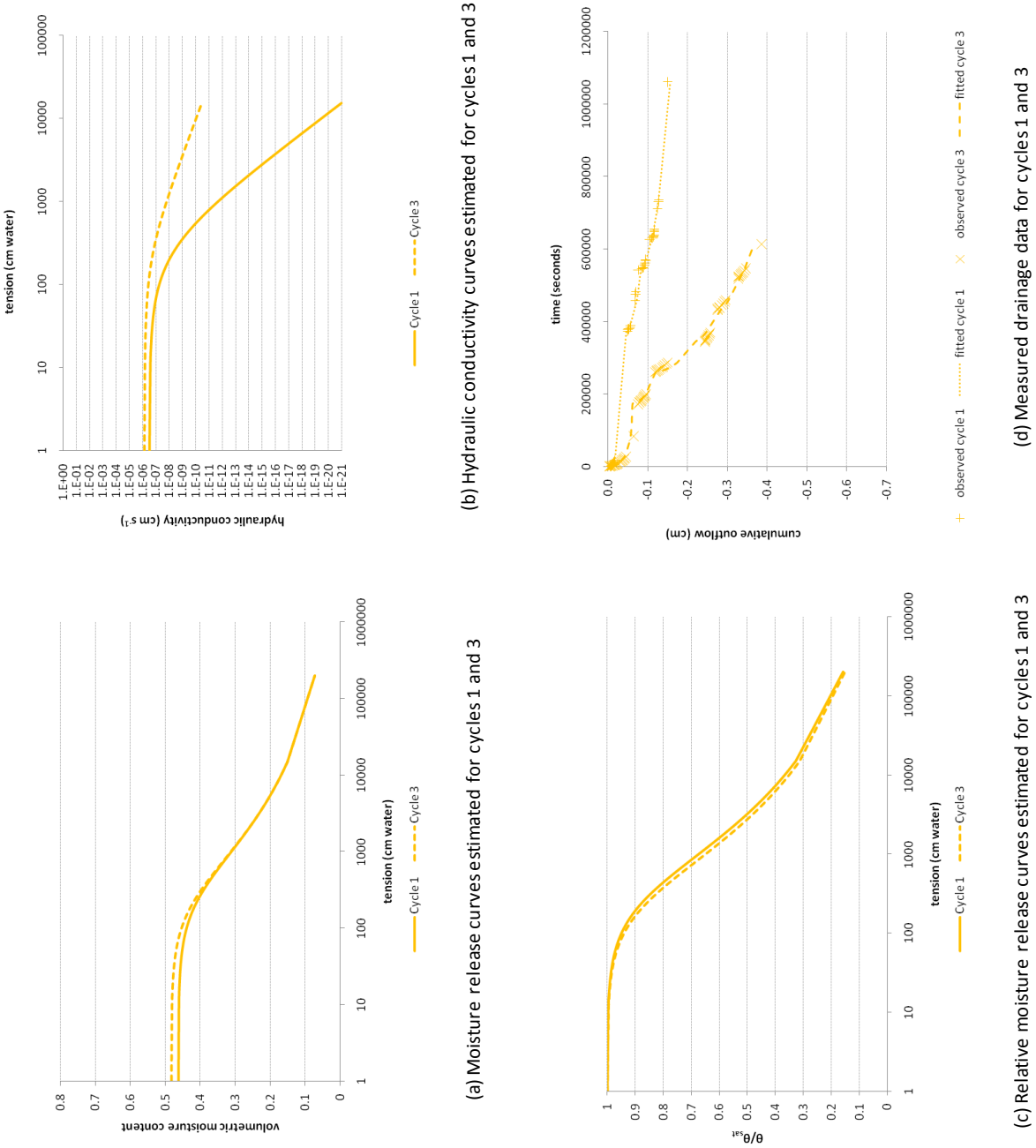

Figure 71. SS/2, sample 6. Hydraulic properties estimated with HYDRUS-1D.

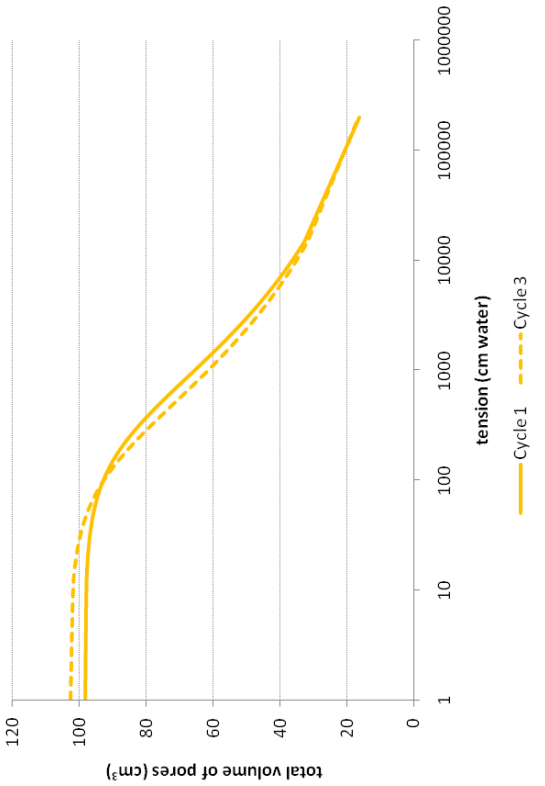

SS/2	cycle 1	*lower*	*upper*	cycle 3	*lower*	*upper*
bulk density (g cm^{-3})	**1.48E+00**			**1.45E+00**		
alpha	**3.98E-03**	*3.67E-03*	*4.29E-03*	**7.31E-03**	*6.71E-03*	*7.91E-03*
n	**1.27E+00**	*1.26E+00*	*1.27E+00*	**1.25E+00**	*1.25E+00*	*1.26E+00*
K_{sat} (cm s^{-1})	**5.44E-06**	*2.76E-06*	*8.13E-06*	**5.37E-06**	*4.05E-06*	*6.70E-06*
l	**3.17E+01**	*2.70E+01*	*3.64E+01*	**7.03E+00**	*5.72E+00*	*8.34E+00*
R^2 drainage	**9.98E-01**			**9.96E-01**		

Figure 72. SS/2, sample 7. Total volume of water filled pores during drainage cycles 1 and 3.

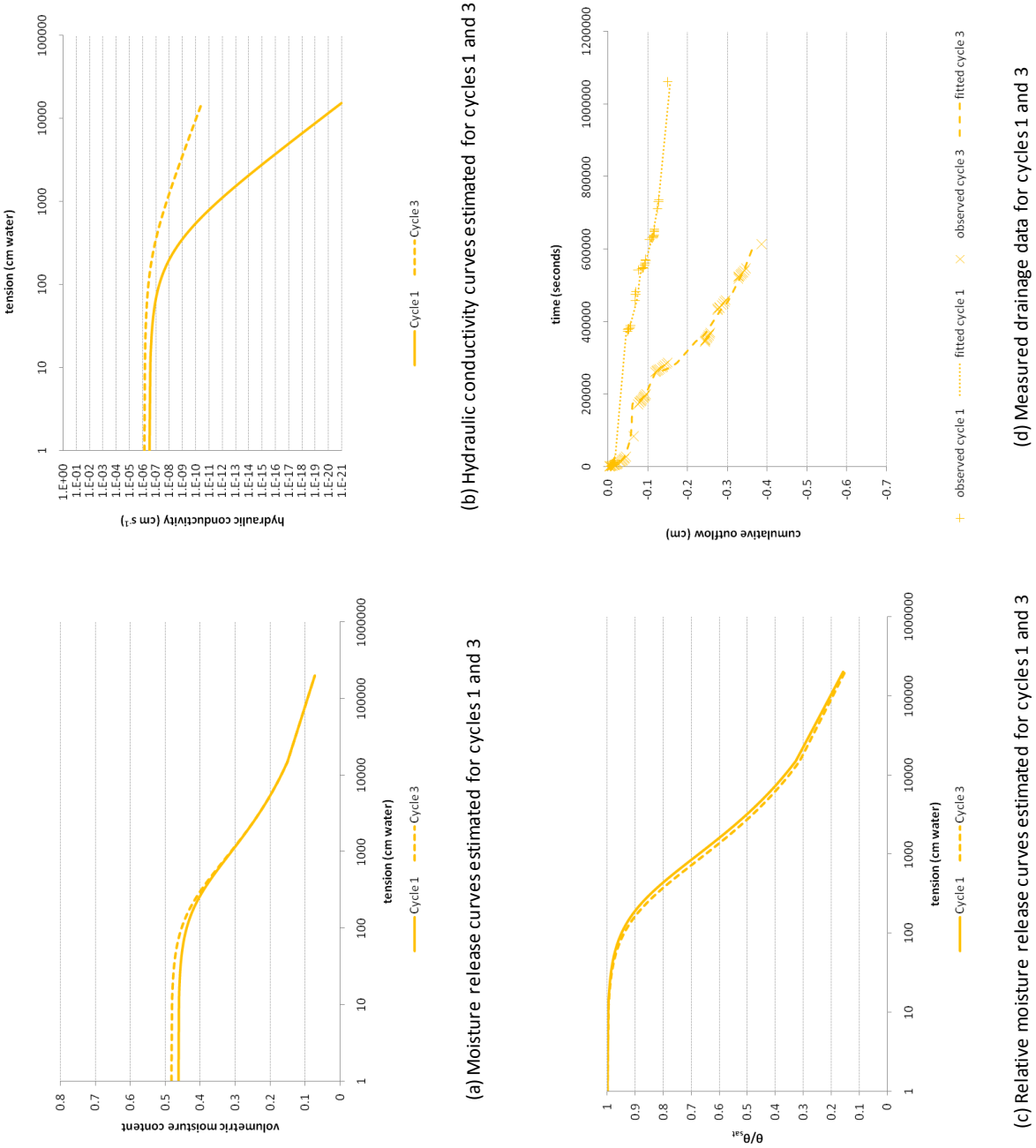

Figure 73. SS/2, sample 7. Hydraulic properties estimated with HYDRUS-1D.

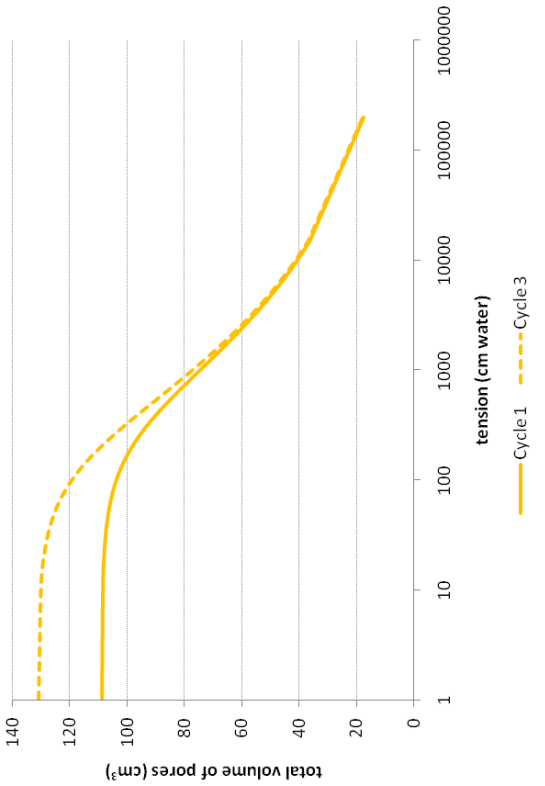

SS/2	cycle 1	*lower*	*upper*	cycle 3	*lower*	*upper*
bulk density (g cm^{-3})	**1.60E+00**			**1.45E+00**		
alpha	**3.29E-03**	*2.86E-03*	*3.73E-03*	**6.12E-03**	*5.61E-03*	*6.63E-03*
n	**1.28E+00**	*1.27E+00*	*1.28E+00*	**1.28E+00**	*1.27E+00*	*1.29E+00*
K_{sat} (cm s^{-1})	**7.69E-08**	*6.72E-08*	*8.65E-08*	**3.01E-06**	*1.97E-06*	*4.04E-06*
l	**2.13E-04**	*-4.74E-02*	*4.79E-02*	**1.48E+01**	*1.23E+01*	*1.74E+01*
R^2 drainage	**9.96E-01**			**9.93E-01**		

Figure 74. SS/2, sample 8. Total volume of water filled pores during drainage cycles 1 and 3.

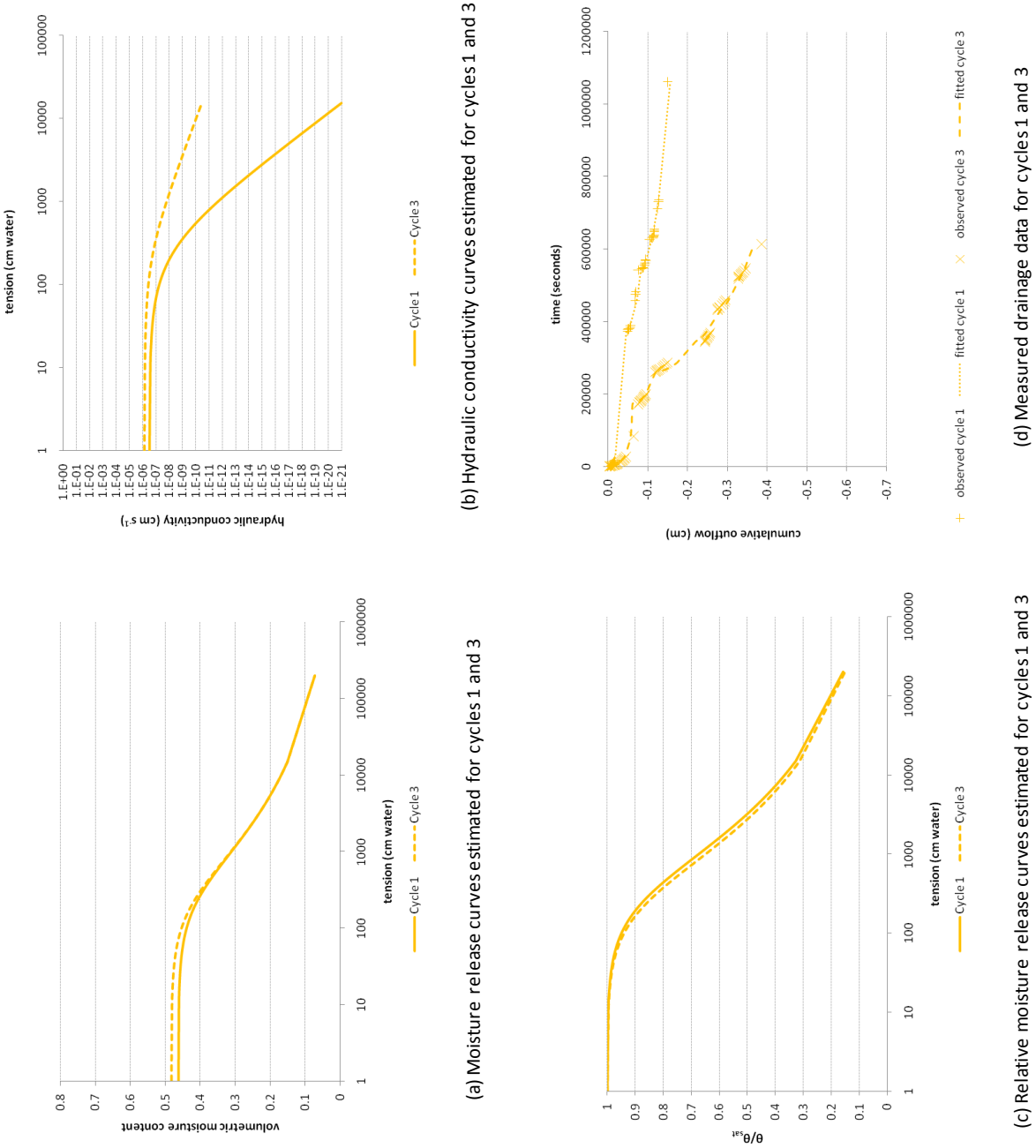

Figure 75. SS/2, sample 8. Hydraulic properties estimated with HYDRUS-1D.

SS/3

Low density group

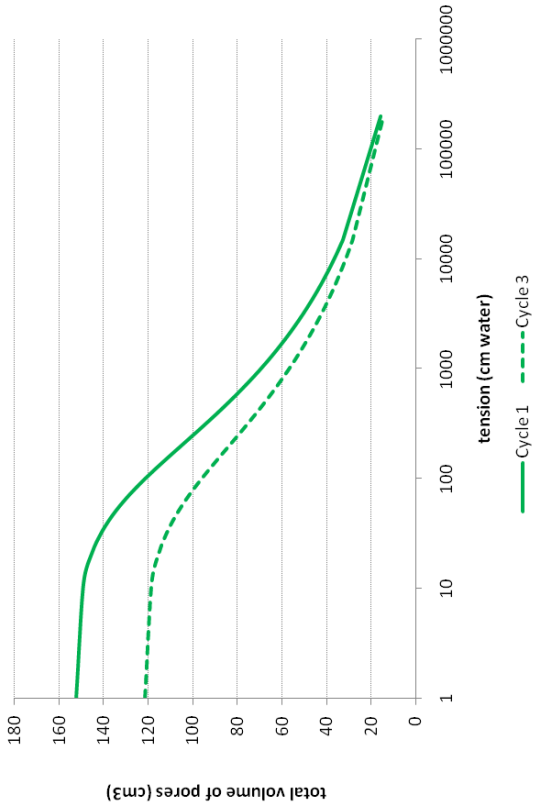

SS/3	cycle 1	*lower*	*upper*	cycle 3	*lower*	*upper*
bulk density (g cm^{-3})	**8.96E-01**			**1.04E+00**		
alpha	**1.62E-02**	*1.48E-02*	*1.77E-02*	**1.85E-02**	*1.71E-02*	*1.98E-02*
n	**1.28E+00**	*1.27E+00*	*1.29E+00*	**1.26E+00**	*1.25E+00*	*1.26E+00*
K_{sat} (cm s^{-1})	**2.61E-03**	*9.73E-04*	*4.24E-03*	**5.23E-03**	*2.38E-03*	*8.08E-03*
l	**3.71E+01**	*3.29E+01*	*4.14E+01*	**3.27E+01**	*2.96E+01*	*3.59E+01*
R^2 drainage	**9.91E-01**			**9.93E-01**		

Figure 76. SS/3, sample 1. Total volume of water filled pores during drainage cycles 1 and 3.

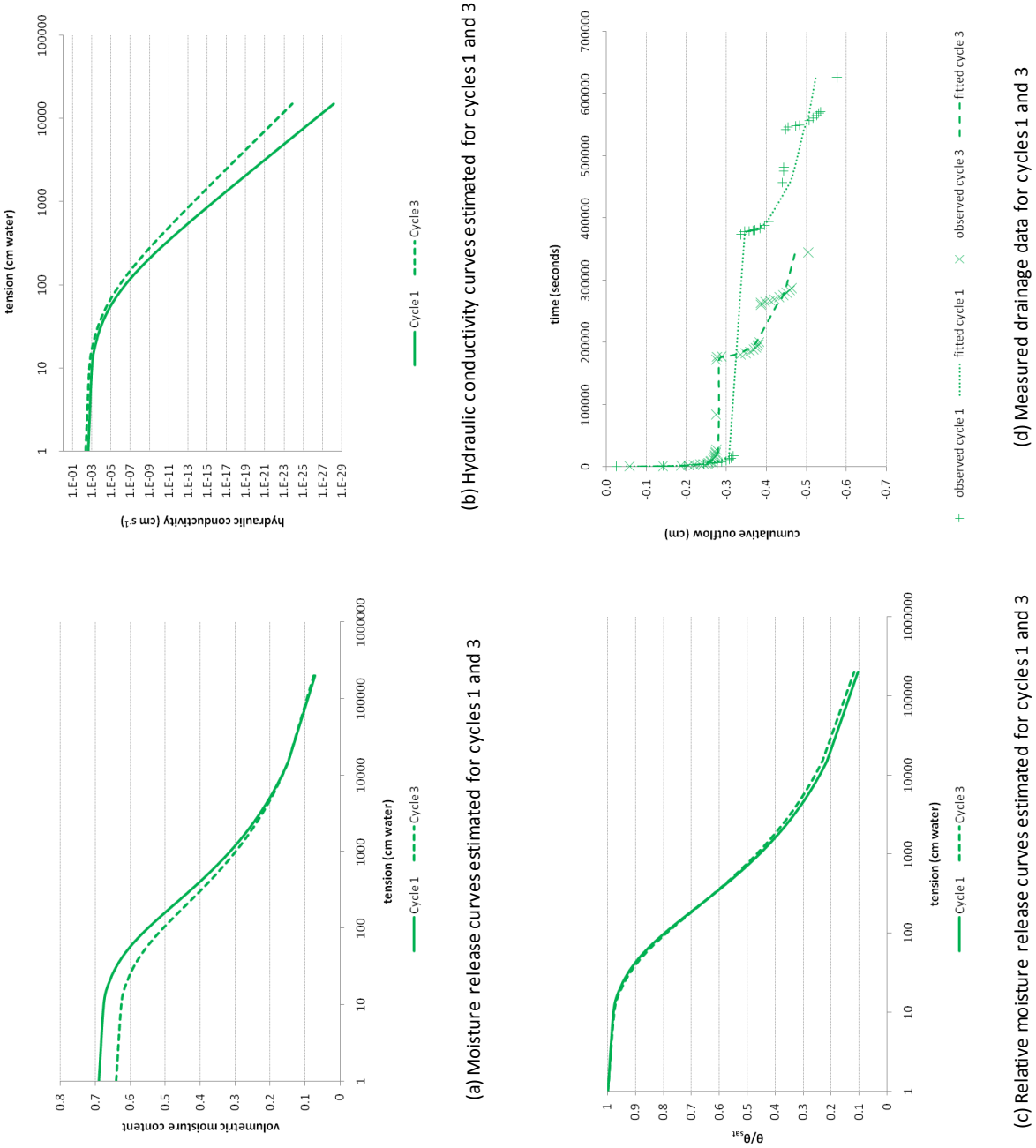

Figure 77. SS/3, sample 1. Hydraulic properties estimated with HYDRUS-1D.

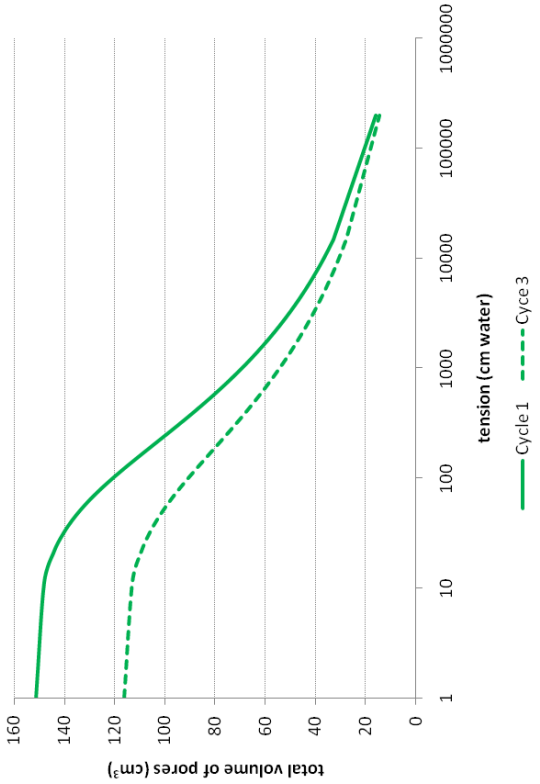

SS/3	cycle 1	*lower*	*upper*	cycle 3	*lower*	*upper*
bulk density (g cm^{-3})	**9.11E-01**			**1.08E+00**		
alpha	**1.61E-02**	*1.44E-02*	*1.77E-02*	**2.08E-02**	*1.99E-02*	*2.18E-02*
n	**1.27E+00**	*1.26E+00*	*1.29E+00*	**1.25E+00**	*1.24E+00*	*1.25E+00*
K_{sat} (cm s^{-1})	**1.22E-03**	*7.79E-04*	*1.67E-03*	**4.39E-03**	*3.20E-03*	*5.58E-03*
l	**2.99E+01**	*2.80E+01*	*3.18E+01*	**3.15E+01**	*3.02E+01*	*3.28E+01*
R^2 drainage	**9.88E-01**			**9.97E-01**		

Figure 78. SS/3, sample 2. Total volume of water filled pores during drainage cycles 1 and 3.

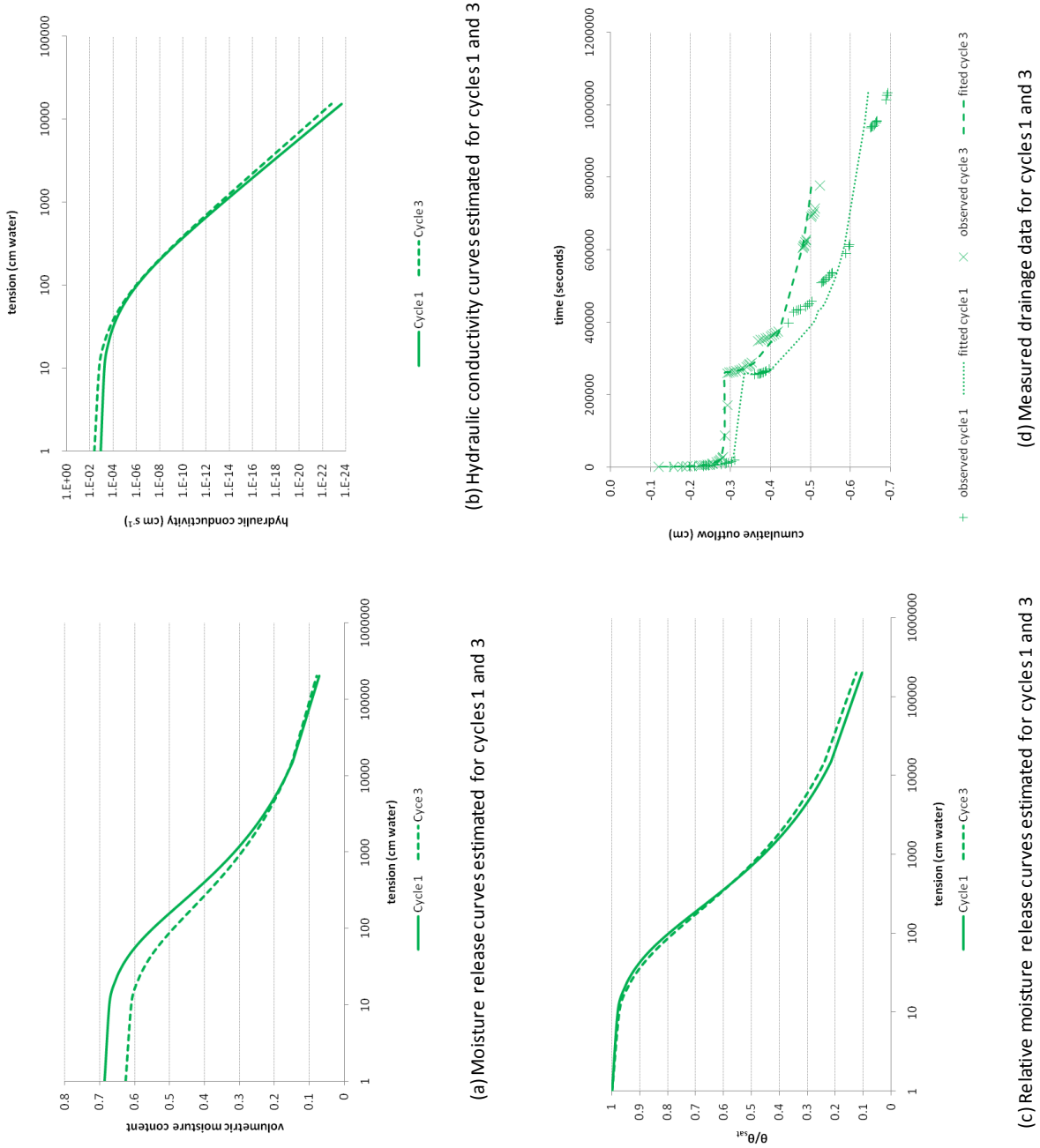

Figure 79. SS/3, sample 2. Hydraulic properties estimated with HYDRUS-1D.

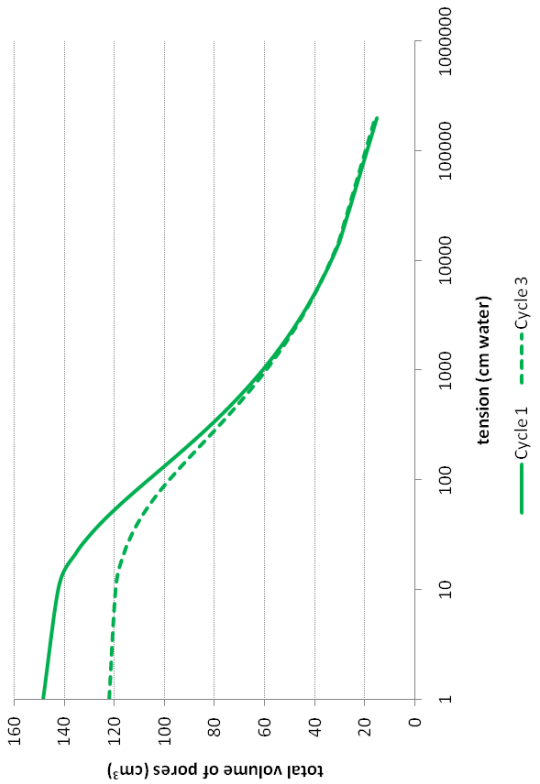

SS/3	cycle 1	*lower*	*upper*	cycle 3	*lower*	*upper*
bulk density (g cm^{-3})	**9.49E-01**			**1.08E+00**		
alpha	**3.05E-02**	*2.68E-02*	*3.41E-02*	**1.74E-02**	*1.66E-02*	*1.83E-02*
n	**1.26E+00**	*1.24E+00*	*1.27E+00*	**1.25E+00**	*1.25E+00*	*1.26E+00*
K_{sat} (cm s^{-1})	**7.04E-03**	*3.54E-03*	*1.05E-02*	**7.66E-04**	*6.09E-04*	*9.23E-04*
l	**2.26E+01**	*2.06E+01*	*2.46E+01*	**2.05E+01**	*1.96E+01*	*2.15E+01*
R^2 drainage	**9.92E-01**			**9.97E-01**		

Figure 80. SS/3, sample 3. Total volume of water filled pores during drainage cycles 1 and 3.

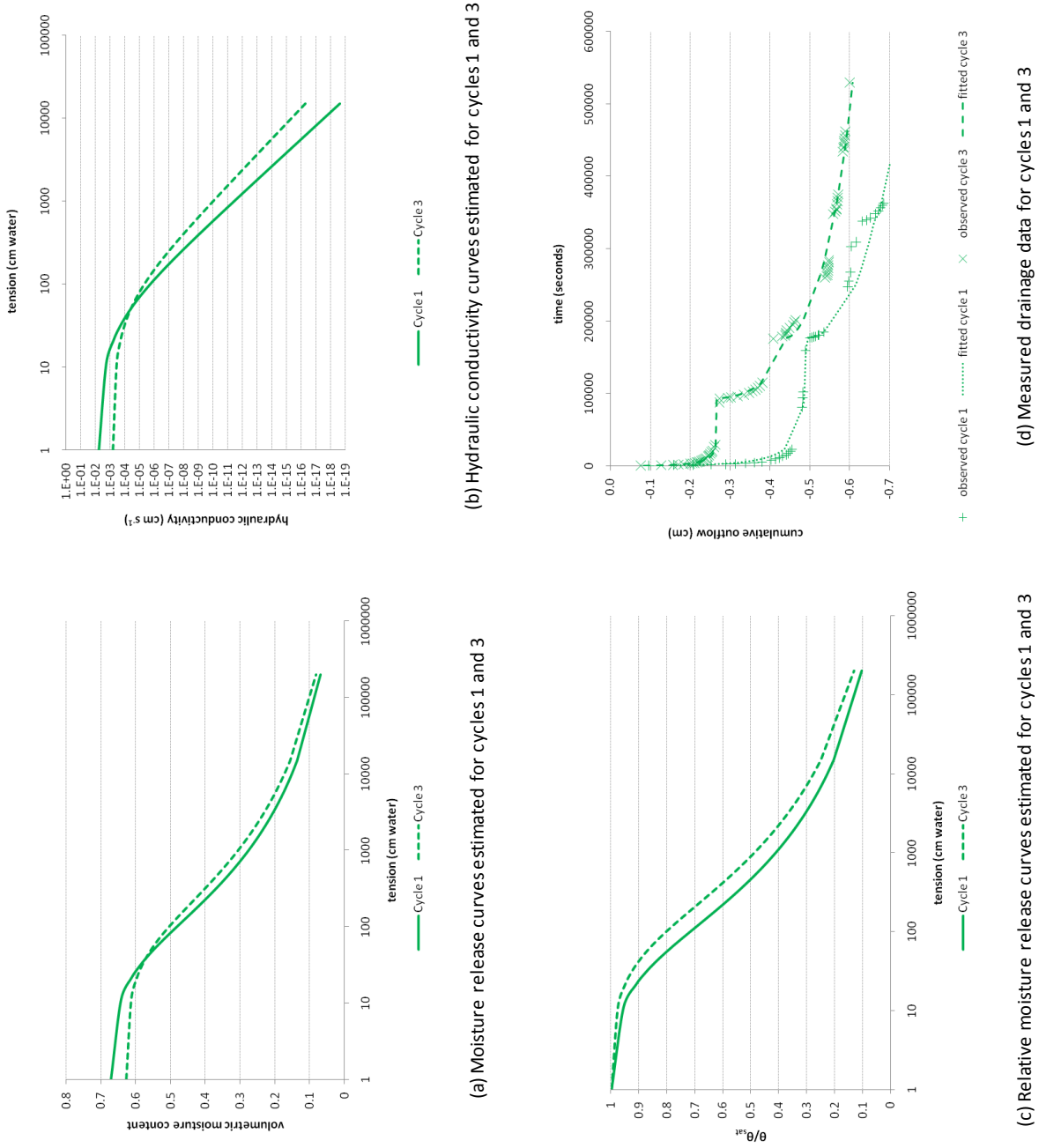

Figure 81. SS/3, sample 3. Hydraulic properties estimated with HYDRUS-1D.

Medium density group

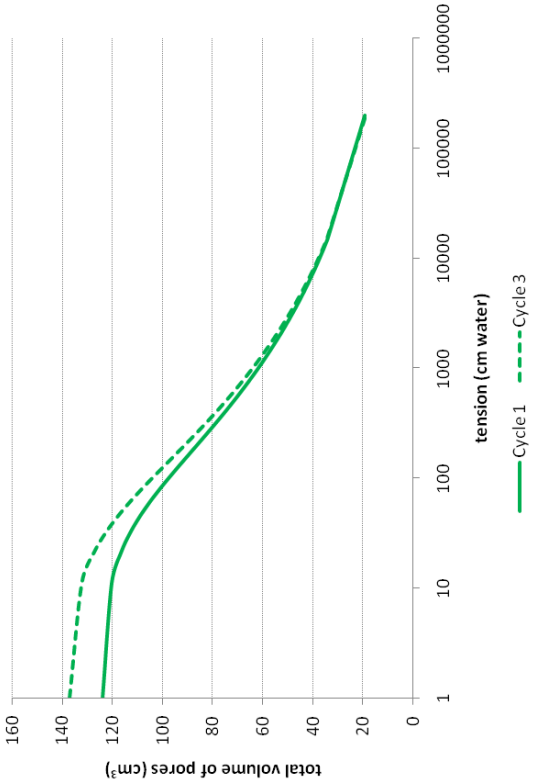

SS/3	cycle 1	*lower*	*upper*	cycle 3	*lower*	*upper*
bulk density (g cm^{-3})	**1.27E+00**			**1.20E+00**		
alpha	**2.34E-02**	*2.22E-02*	*2.45E-02*	**2.72E-02**	*2.49E-02*	*2.95E-02*
n	**1.22E+00**	*1.22E+00*	*1.22E+00*	**1.23E+00**	*1.22E+00*	*1.23E+00*
K_{sat} (cm s^{-1})	**6.67E-05**	*5.89E-05*	*7.45E-05*	**2.66E-04**	*1.99E-04*	*3.32E-04*
l	**1.80E+01**	*1.73E+01*	*1.86E+01*	**2.18E+01**	*2.08E+01*	*2.28E+01*
R^2 drainage	**9.99E-01**			**9.98E-01**		

Figure 82. SS/3, sample 4. Total volume of water filled pores during drainage cycles 1 and 3.

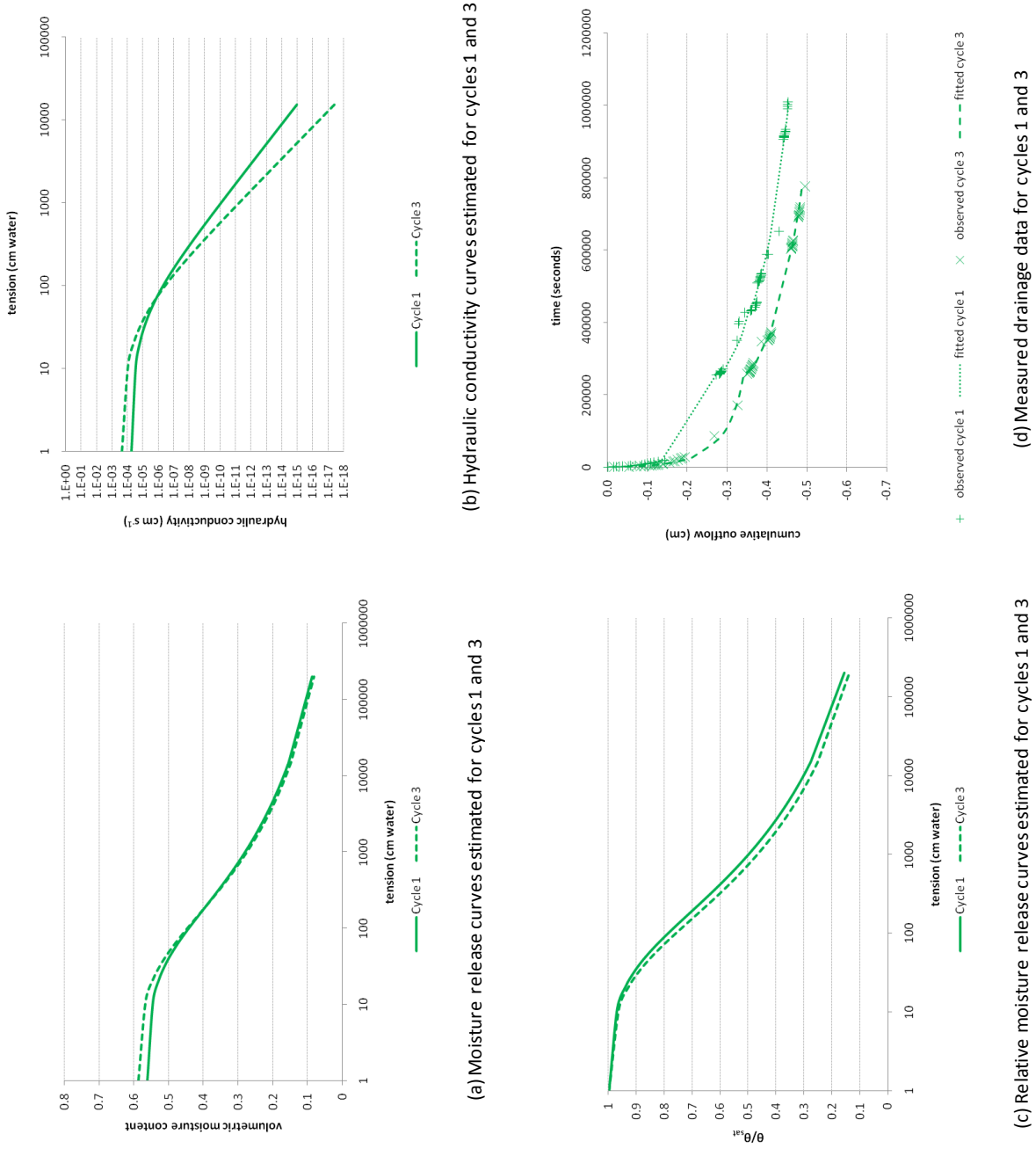

Figure 83. SS/3, sample 4. Hydraulic properties estimated with HYDRUS-1D.

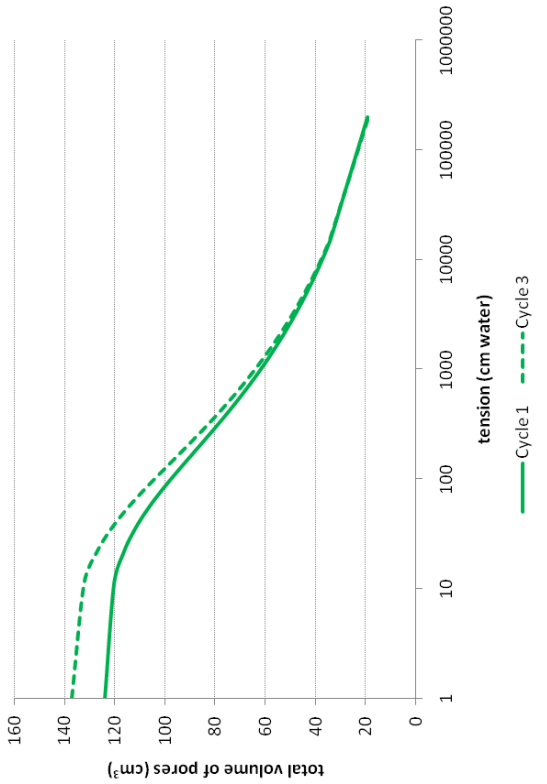

SS/3	cycle 1	*lower*	*upper*	cycle 3	*lower*	*upper*
bulk density (g cm^{-3})	**1.27E+00**			**1.20E+00**		
alpha	**2.34E-02**	*2.22E-02*	*2.45E-02*	**2.72E-02**	*2.49E-02*	*2.95E-02*
n	**1.22E+00**	*1.22E+00*	*1.22E+00*	**1.23E+00**	*1.22E+00*	*1.23E+00*
K_{sat} (cm s^{-1})	**6.67E-05**	*5.89E-05*	*7.45E-05*	**2.66E-04**	*1.99E-04*	*3.32E-04*
l	**1.80E+01**	*1.73E+01*	*1.86E+01*	**2.18E+01**	*2.08E+01*	*2.28E+01*
R^2 drainage	**9.99E-01**			**9.98E-01**		

Figure 84. SS/3, sample 5. Total volume of water filled pores during drainage cycles 1 and 3.

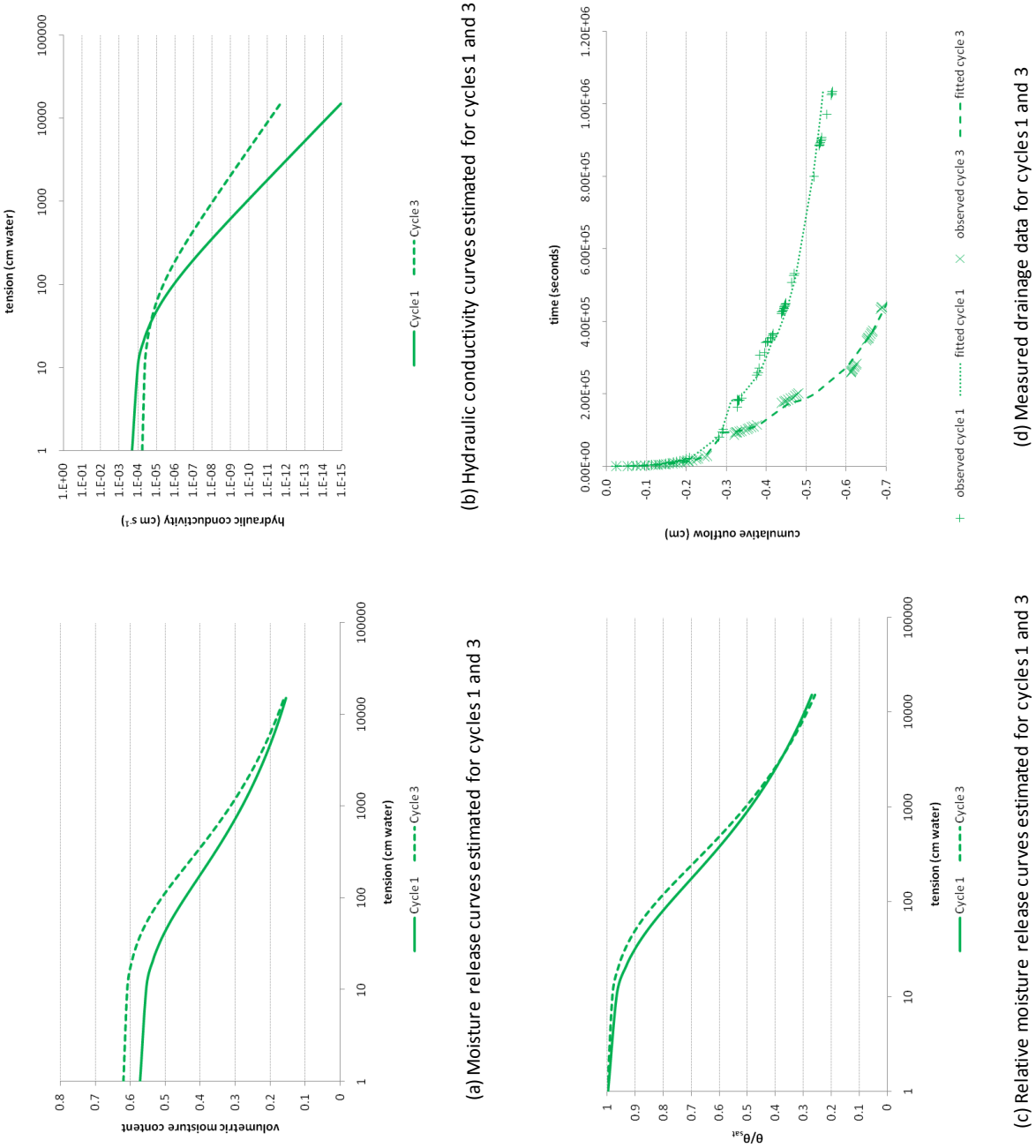

Figure 85. SS/3, sample 5. Hydraulic properties estimated with HYDRUS-1D.

High density group

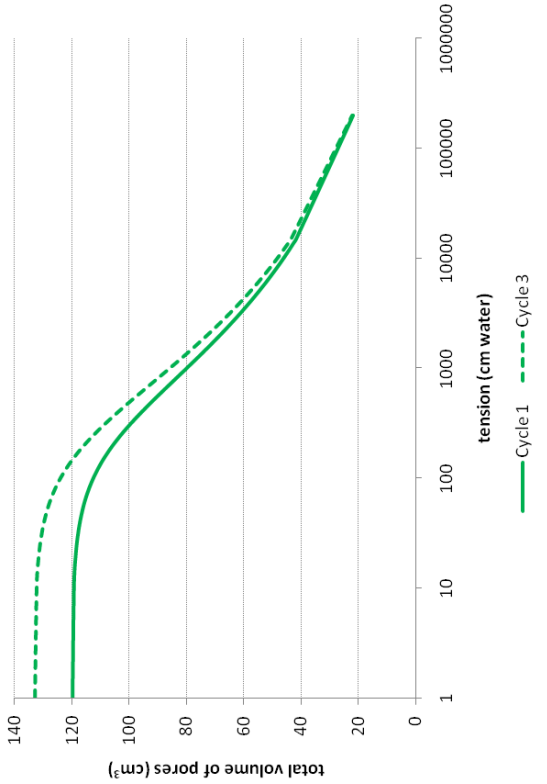

SS/3	cycle 1	*lower*	*upper*	cycle 3	*lower*	*upper*
bulk density (g cm^{-3})	**1.35E+00**			**1.27E+00**		
alpha	**4.52E-03**	*3.01E-03*	*6.03E-03*	**4.87E-03**	*4.54E-03*	*5.20E-03*
n	**1.25E+00**	*1.24E+00*	*1.26E+00*	**1.26E+00**	*1.25E+00*	*1.26E+00*
K_{sat} (cm s^{-1})	**1.59E-07**	*1.10E-07*	*2.09E-07*	**2.64E-06**	*1.86E-06*	*3.42E-06*
l	**7.16E-03**	*-3.74E+00*	*3.76E+00*	**2.25E+01**	*1.96E+01*	*2.54E+01*
R^2 drainage	**9.94E-01**			**9.95E-01**		

Figure 86. SS/3, sample 6. Total volume of water filled pores during drainage cycles 1 and 3.

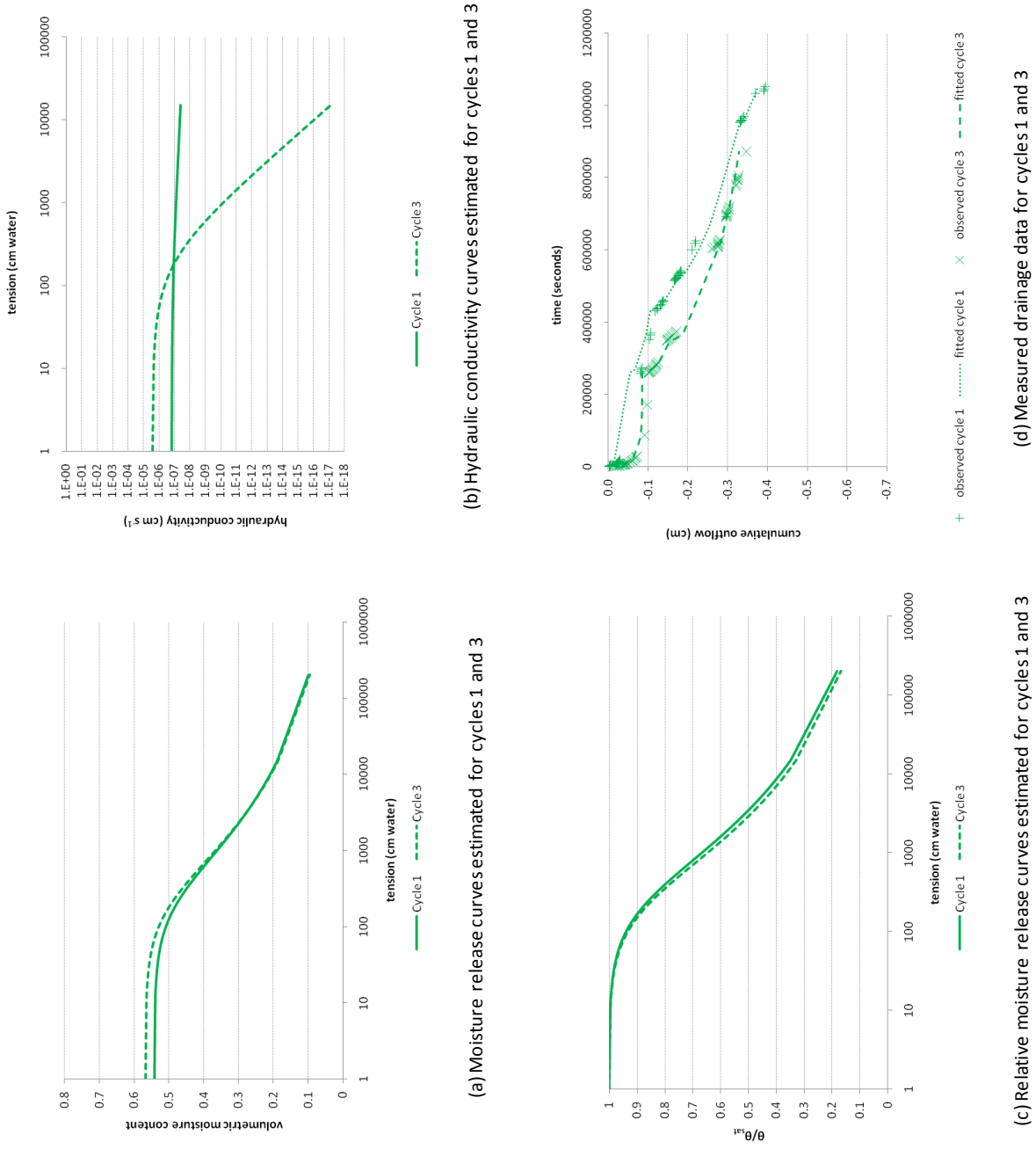

Figure 87. SS/3, sample 6. Hydraulic properties estimated with HYDRUS-1D.

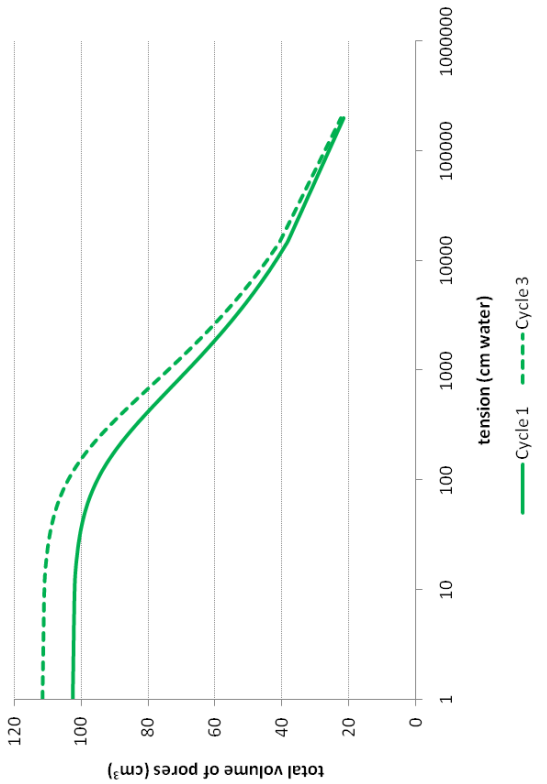

SS/3	cycle 1	*lower*	*upper*	cycle 3	*lower*	*upper*
bulk density (g cm^{-3})	**1.44E+00**			**1.38E+00**		
alpha	**5.80E-03**	*2.23E-03*	*9.37E-03*	**5.40E-03**	*4.97E-03*	*5.83E-03*
n	**1.22E+00**	*1.20E+00*	*1.23E+00*	**1.23E+00**	*1.22E+00*	*1.23E+00*
K_{sat} (cm s^{-1})	**6.39E-08**	*3.90E-08*	*8.89E-08*	**9.11E-06**	*5.86E-06*	*1.24E-05*
l	**7.49E-02**	*-7.00E+00*	*7.15E+00*	**1.58E+01**	*1.32E+01*	*1.83E+01*
R^2 drainage	**9.98E-01**			**9.96E-01**		

Figure 88. SS/3, sample 7. Total volume of water filled pores during drainage cycles 1 and 3.

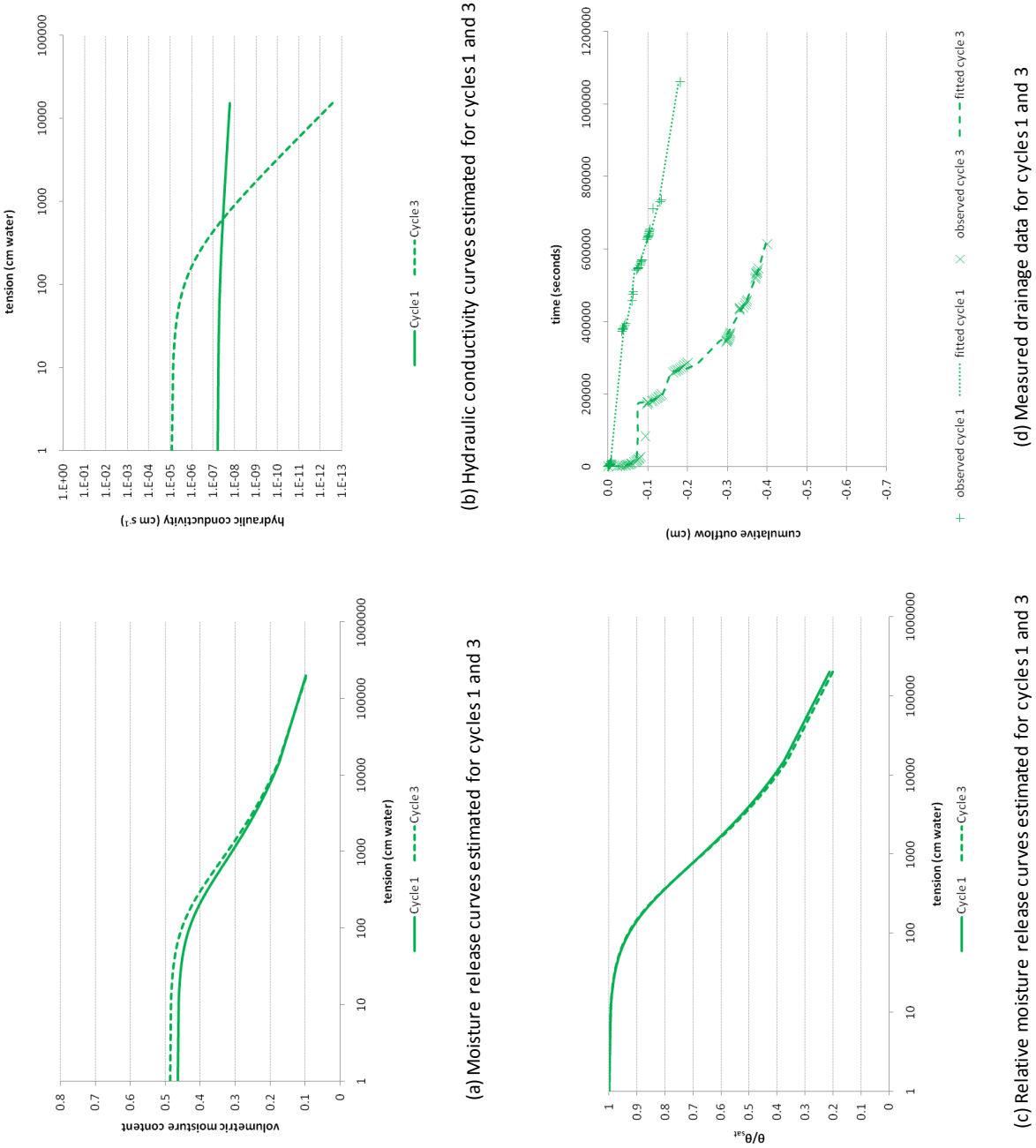

Figure 89. SS/3, sample 7. Hydraulic properties estimated with HYDRUS-1D.

SS/4

Low density group

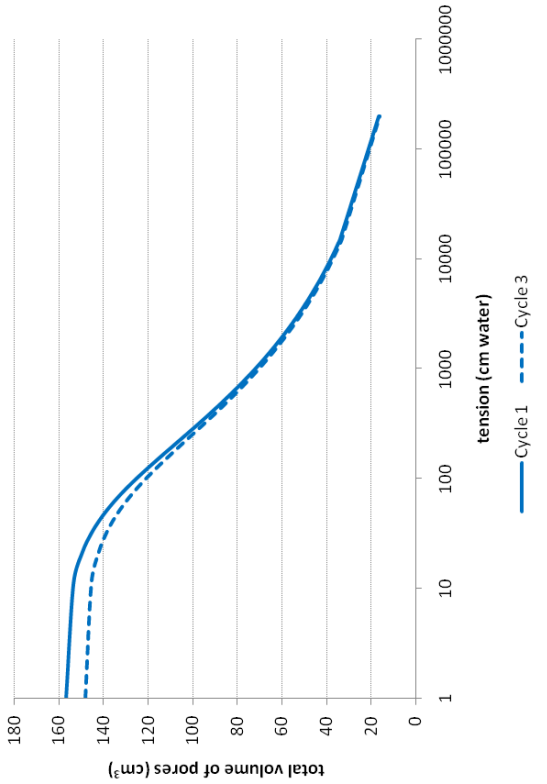

SS/4	cycle 1	*lower*	*upper*	cycle 3	*lower*	*upper*
bulk density (g cm^{-3})	**8.99E-01**			**9.37E-01**		
alpha	**1.60E-02**	*1.54E-02*	*1.66E-02*	**1.41E-02**	*1.32E-02*	*1.50E-02*
n	**1.28E+00**	*1.28E+00*	*1.29E+00*	**1.28E+00**	*1.27E+00*	*1.29E+00*
K_{sat} (cm s^{-1})	**6.09E-02**	*3.84E-02*	*8.33E-02*	**3.16E-03**	*1.71E-03*	*4.61E-03*
l	**6.16E+01**	*5.86E+01*	*6.45E+01*	**3.97E+01**	*3.69E+01*	*4.25E+01*
R^2 drainage	**9.98E-01**			**9.90E-01**		

Figure 90. SS/4, sample 1. Total volume of water filled pores during drainage cycles 1 and 3.

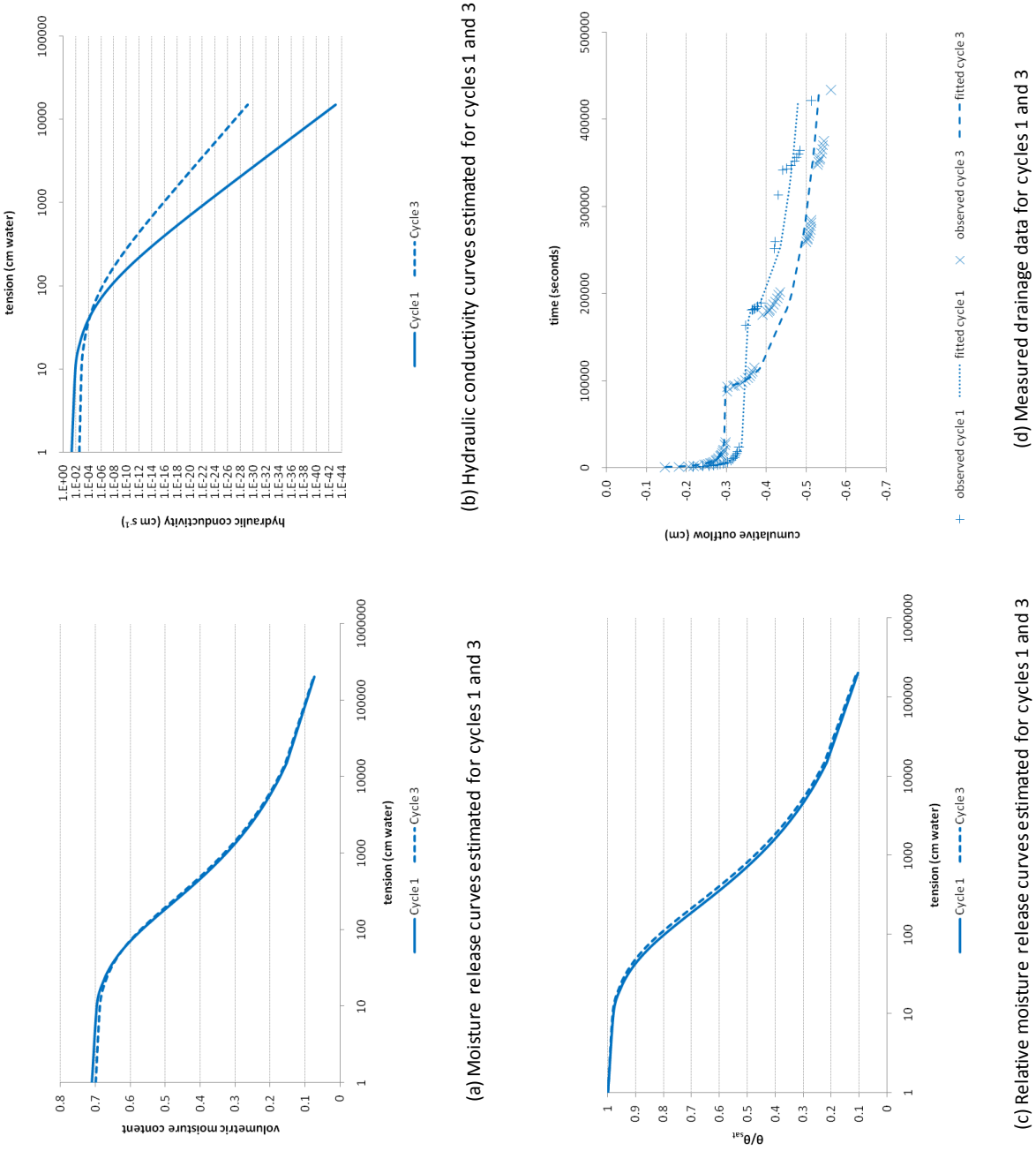

Figure 91. SS/4, sample 1. Hydraulic properties estimated with HYDRUS-1D.

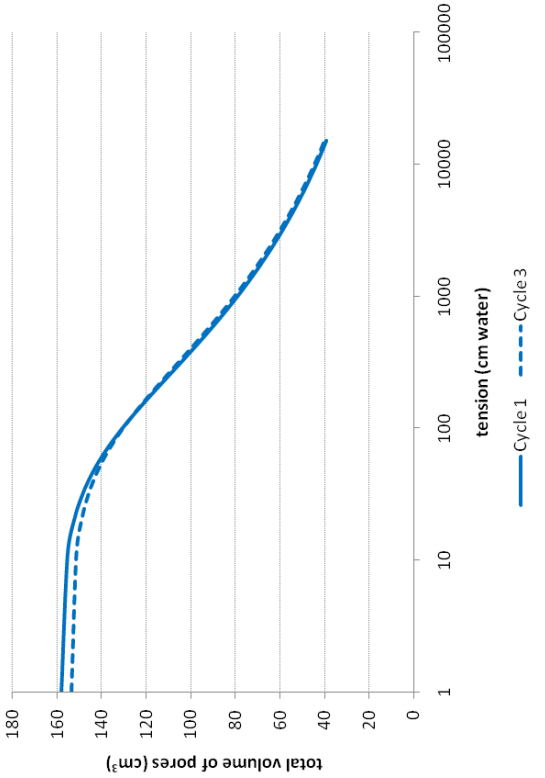

SS/4	cycle 1	*lower*	*upper*	cycle 3	*lower*	*upper*
bulk density (g cm^{-3})	**9.05E-01**			**9.24E-01**		
alpha	**1.41E-02**	*1.27E-02*	*1.54E-02*	**1.18E-02**	*1.14E-02*	*1.21E-02*
n	**1.26E+00**	*1.25E+00*	*1.27E+00*	**1.26E+00**	*1.26E+00*	*1.27E+00*
K_{sat} (cm s^{-1})	**3.51E-03**	*1.20E-03*	*5.83E-03*	**1.74E-03**	*1.34E-03*	*2.13E-03*
l	**4.85E+01**	*4.37E+01*	*5.33E+01*	**5.78E+01**	*5.60E+01*	*5.96E+01*
R^2 drainage	**9.88E-01**			**9.97E-01**		

Figure 92. SS/4, sample 2. Total volume of water filled pores during drainage cycles 1 and 3.

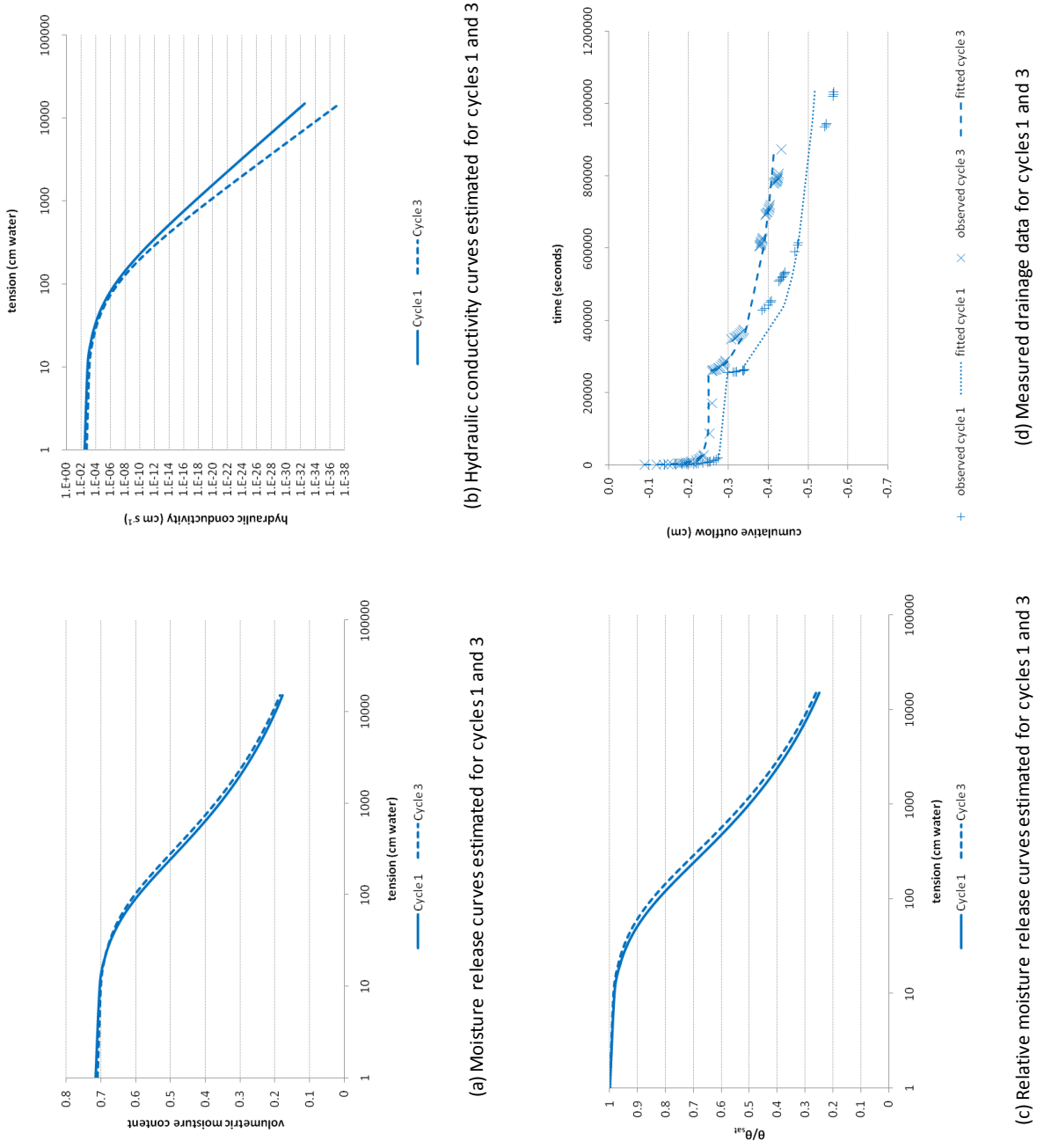

Figure 93. SS/4, sample 2. Hydraulic properties estimated with HYDRUS-1D.

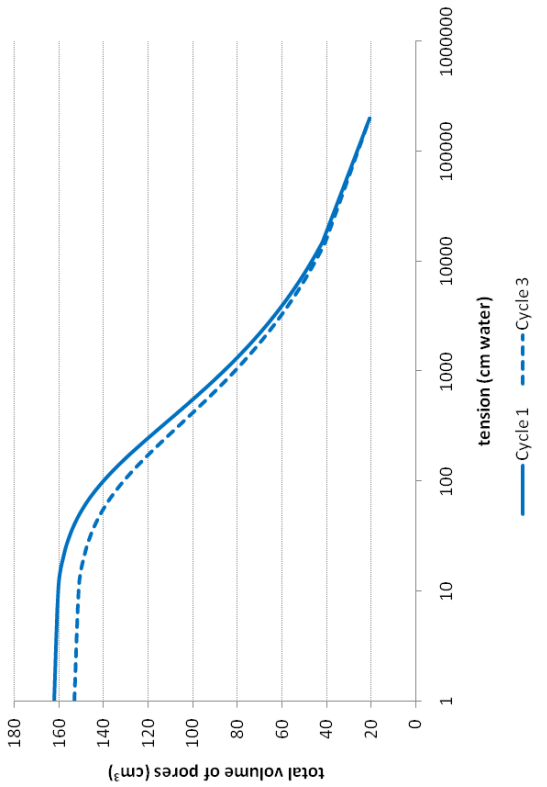

SS/4	cycle 1	*lower*	*upper*	cycle 3	*lower*	*upper*
bulk density (g cm^{-3})	**9.24E-01**			**9.62E-01**		
alpha	**9.97E-03**	*9.50E-03*	*1.04E-02*	**1.10E-02**	*1.03E-02*	*1.16E-02*
n	**1.27E+00**	*1.26E+00*	*1.27E+00*	**1.26E+00**	*1.25E+00*	*1.27E+00*
K_{sat} (cm s^{-1})	**5.70E-05**	*4.90E-05*	*6.49E-05*	**7.61E-04**	*5.41E-04*	*9.81E-04*
l	**3.90E+01**	*3.80E+01*	*4.00E+01*	**4.94E+01**	*4.72E+01*	*5.16E+01*
R^2 drainage	**9.96E-01**			**9.92E-01**		

Figure 94. SS/4, sample 3. Total volume of water filled pores during drainage cycles 1 and 3.

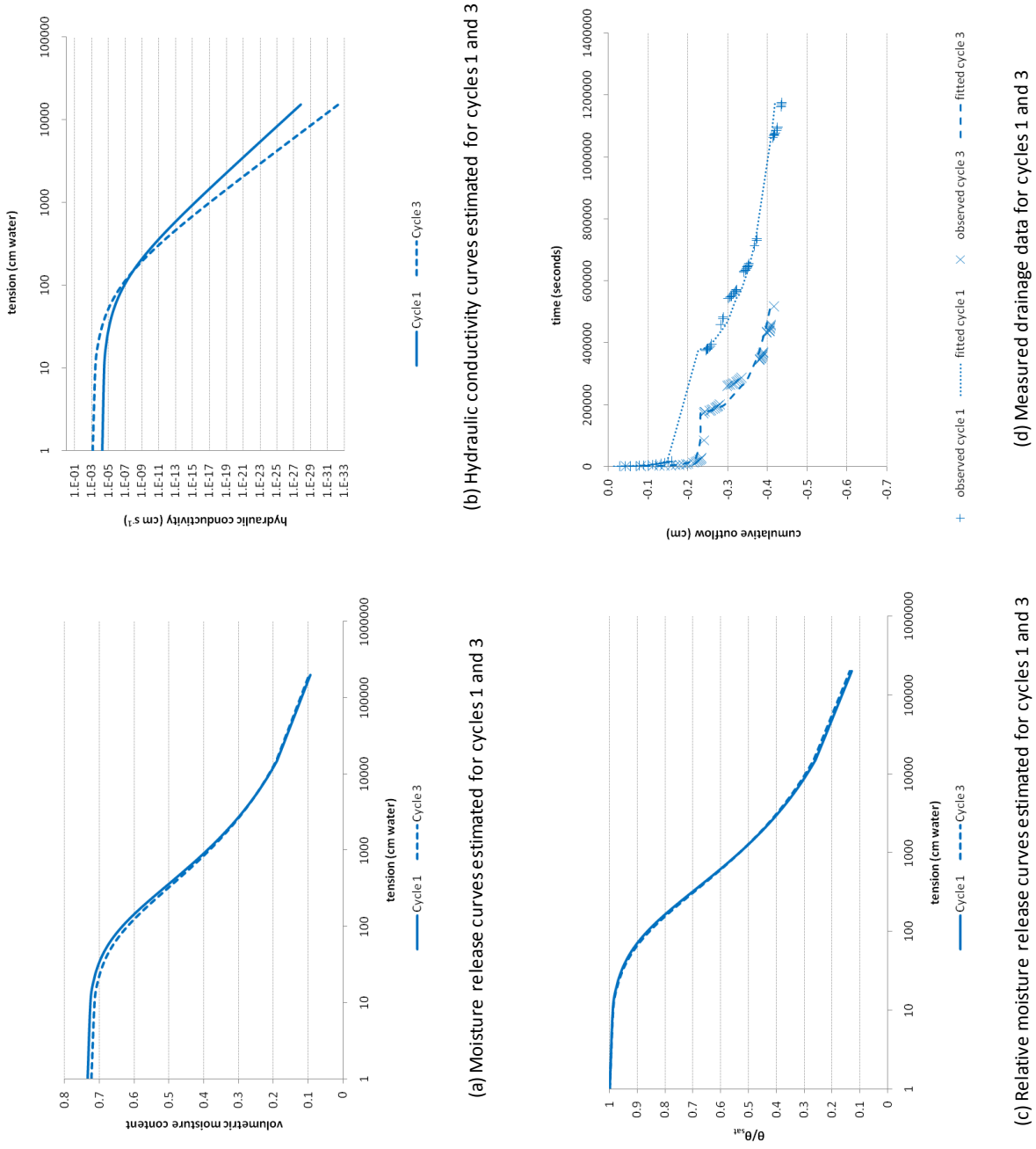

Figure 95. SS/4, sample 3. Hydraulic properties estimated with HYDRUS-1D.

Medium density group

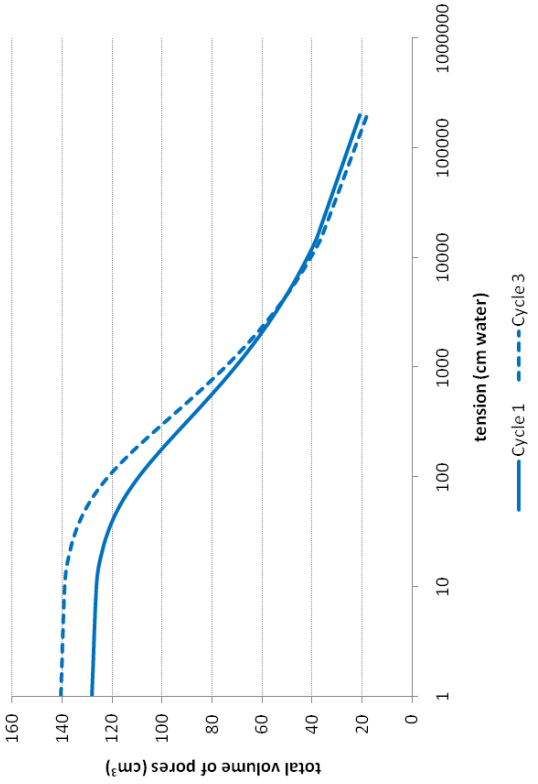

SS/4	cycle 1	*lower*	*upper*	cycle 3	*lower*	*upper*
bulk density (g cm^{-3})	**1.32E+00**			**1.10E+00**		
alpha	**1.27E-02**	*1.21E-02*	*1.34E-02*	**9.87E-03**	*9.69E-03*	*1.01E-02*
n	**1.23E+00**	*1.23E+00*	*1.24E+00*	**1.27E+00**	*1.27E+00*	*1.27E+00*
K_{sat} (cm s^{-1})	**2.43E-04**	*1.71E-04*	*3.15E-04*	**5.75E-05**	*5.27E-05*	*6.23E-05*
l	**3.94E+01**	*3.70E+01*	*4.18E+01*	**3.21E+01**	*3.12E+01*	*3.31E+01*
R^2 drainage	**9.96E-01**			**9.99E-01**		

Figure 96. SS/4, sample 4. Total volume of water filled pores during drainage cycles 1 and 3.

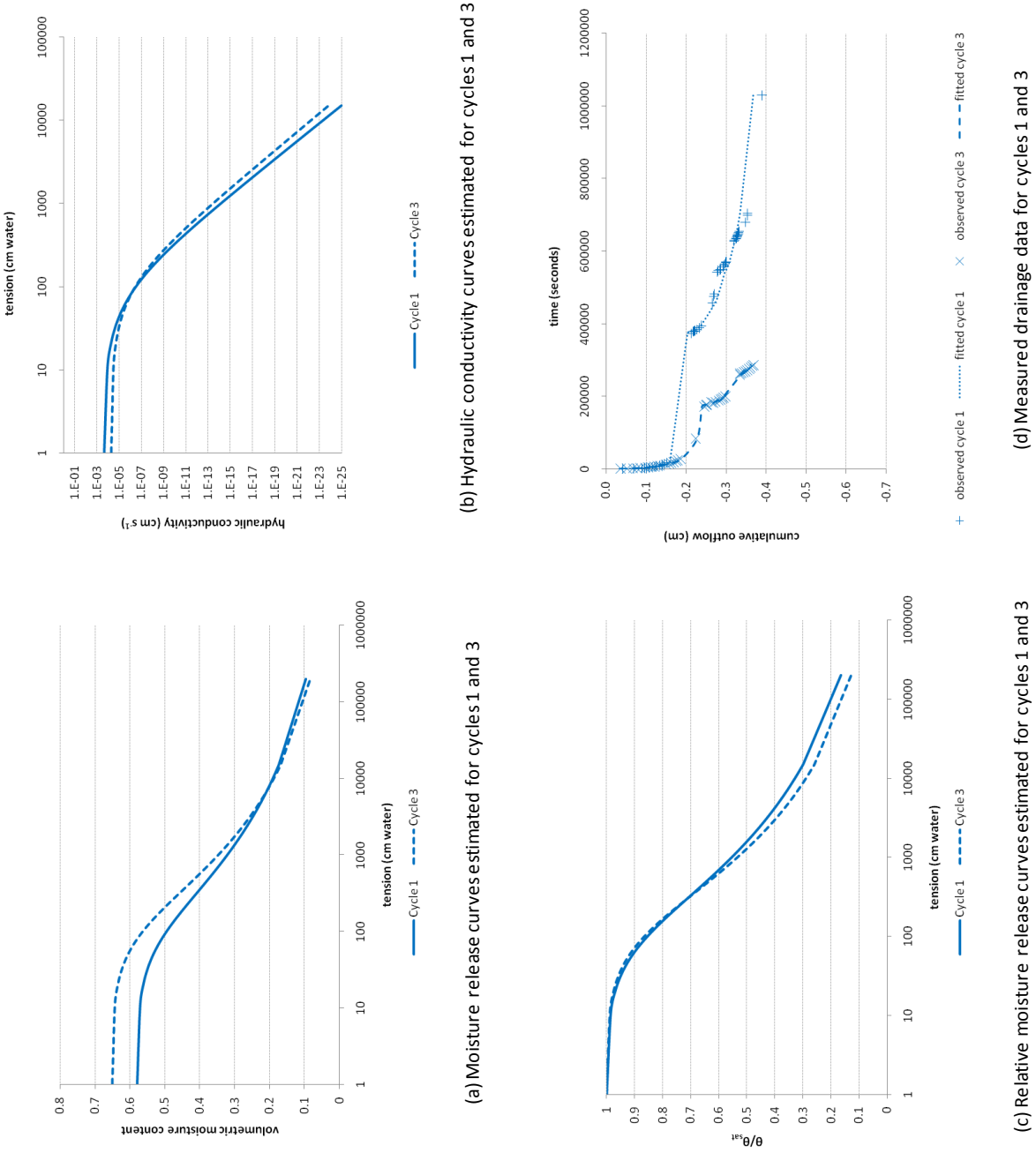

Figure 97. SS/4, sample 4. Hydraulic properties estimated with HYDRUS-1D.

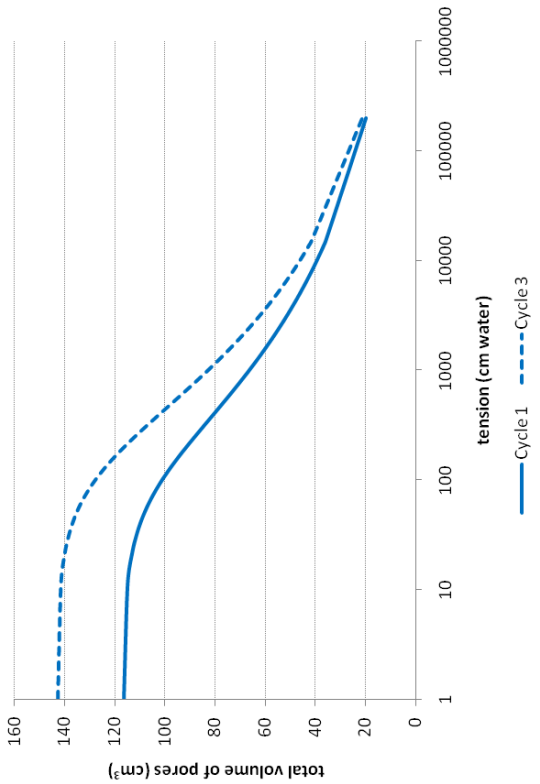

SS/4	cycle 1	*lower*	*upper*	cycle 3	*lower*	*upper*
bulk density (g cm^{-3})	**1.32E+00**			**1.18E+00**		
alpha	**1.11E-02**	*1.04E-02*	*1.18E-02*	**7.70E-03**	*6.95E-03*	*8.44E-03*
n	**1.22E+00**	*1.22E+00*	*1.23E+00*	**1.25E+00**	*1.25E+00*	*1.26E+00*
K_{sat} (cm s^{-1})	**3.23E-05**	*2.45E-05*	*4.02E-05*	**7.16E-06**	*5.83E-06*	*8.49E-06*
l	**2.44E+01**	*2.26E+01*	*2.61E+01*	**2.43E+01**	*2.20E+01*	*2.67E+01*
R^2 drainage	**9.96E-01**			**9.95E-01**		

Figure 98. SS/4, sample 5. Total volume of water filled pores during drainage cycles 1 and 3.

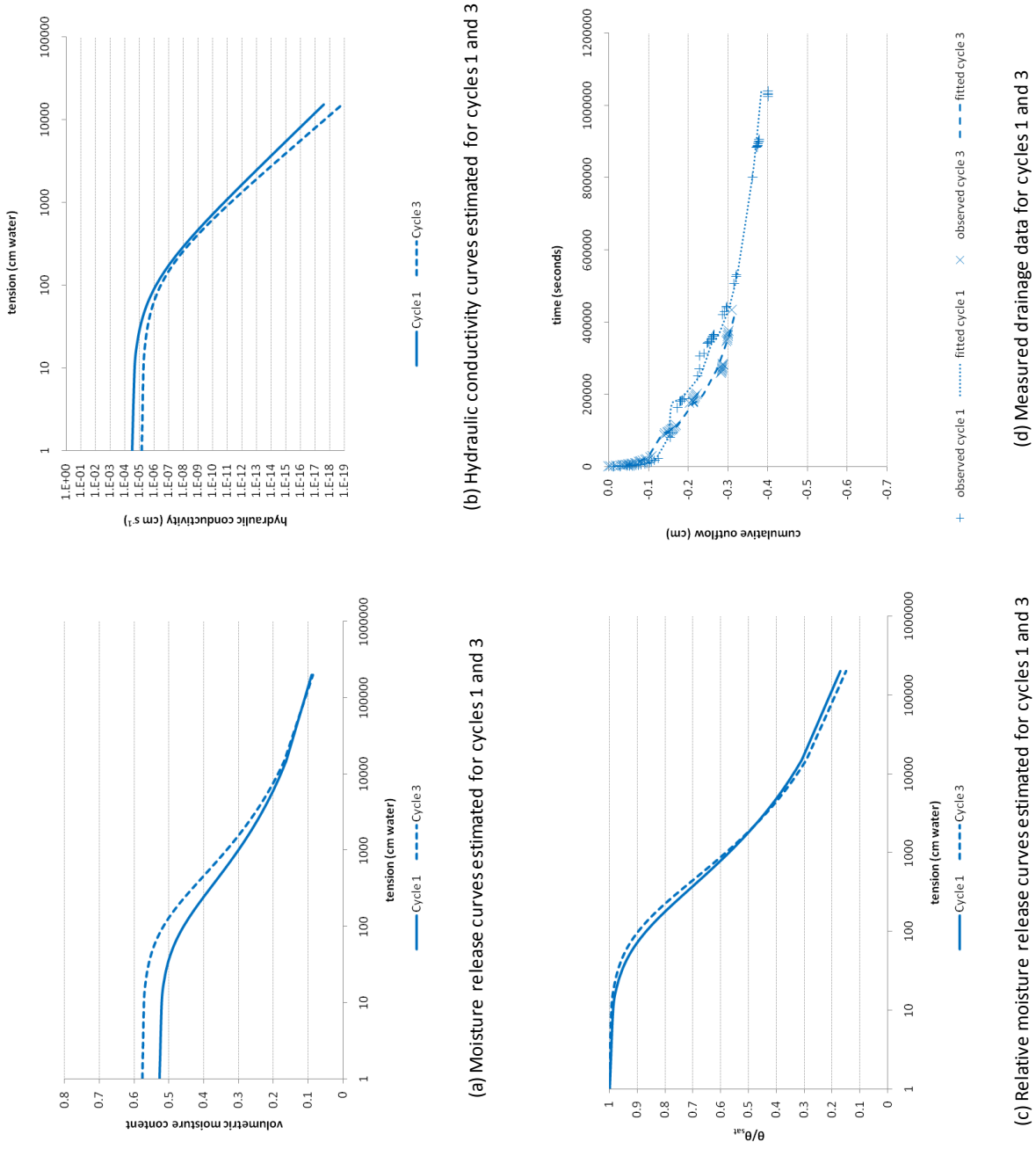

Figure 99. SS/4, sample 5. Hydraulic properties estimated with HYDRUS-1D.

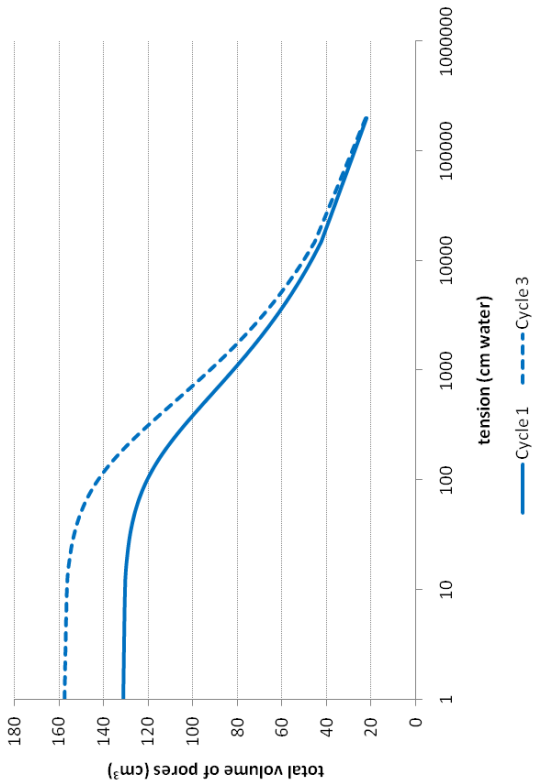

SS/4	cycle 1	*lower*	*upper*	cycle 3	*lower*	*upper*
bulk density (g cm^{-3})	**1.35E+00**			**1.21E+00**		
alpha	**6.05E-03**	*5.65E-03*	*6.44E-03*	**6.77E-03**	*6.66E-03*	*6.88E-03*
n	**1.25E+00**	*1.25E+00*	*1.25E+00*	**1.27E+00**	*1.26E+00*	*1.27E+00*
K_{sat} (cm s^{-1})	**3.57E-06**	*2.67E-06*	*4.47E-06*	**8.41E-06**	*7.82E-06*	*9.00E-06*
l	**3.14E+01**	*2.89E+01*	*3.40E+01*	**3.98E+01**	*3.90E+01*	*4.06E+01*
R^2 drainage	**9.94E-01**			**9.99E-01**		

Figure 100. SS/4, sample 6. Total volume of water filled pores during drainage cycles 1 and 3.

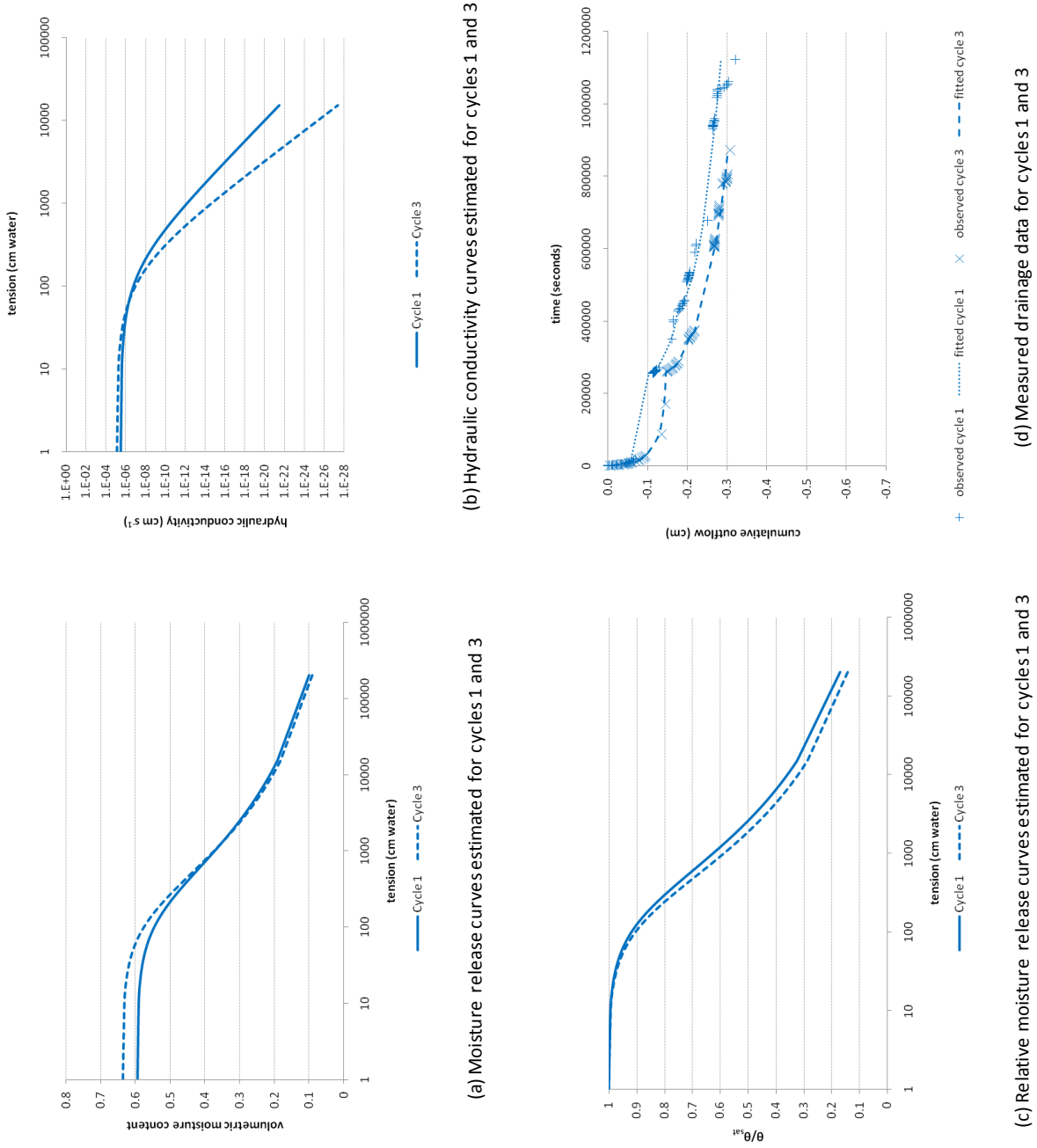

Figure 101. SS/4, sample 6. Hydraulic properties estimated with HYDRUS-1D.

High density group

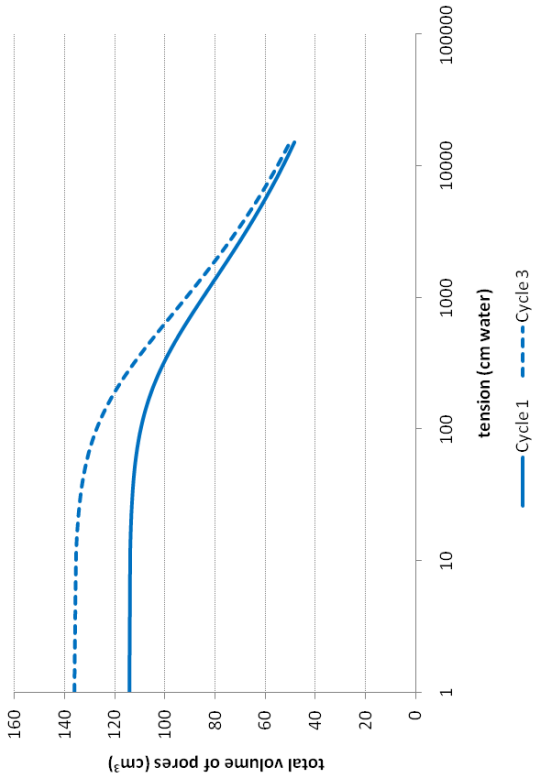

SS/4	cycle 1	*lower*	*upper*	cycle 3	*lower*	*upper*
bulk density (g cm^{-3})	**1.40E+00**			**1.27E+00**		
alpha	**3.25E-03**	*1.86E-03*	*4.64E-03*	**5.12E-03**	*4.84E-03*	*5.39E-03*
n	**1.22E+00**	*1.21E+00*	*1.23E+00*	**1.23E+00**	*1.22E+00*	*1.23E+00*
K_{sat} (cm s^{-1})	**1.37E-07**	*8.28E-08*	*1.91E-07*	**5.14E-06**	*3.95E-06*	*6.33E-06*
l	**4.34E-03**	*-6.22E-01*	*6.30E-01*	**3.16E+01**	*2.87E+01*	*3.44E+01*
R^2 drainage	**9.96E-01**			**9.96E-01**		

Figure 102. SS/4, sample 7. Total volume of water filled pores during drainage cycles 1 and 3.

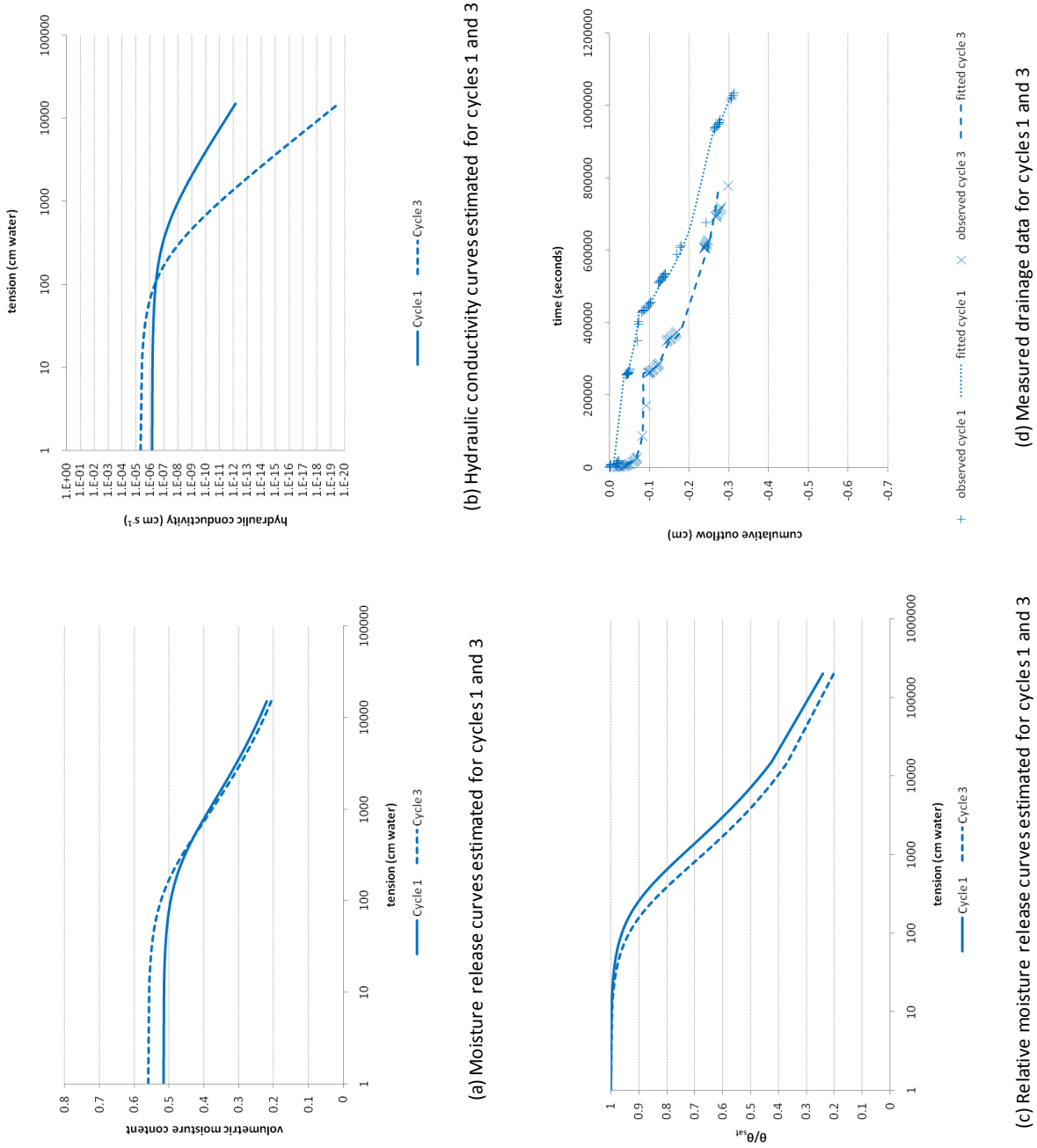

Figure 103. SS/4, sample 7. Hydraulic properties estimated with HYDRUS-1D.

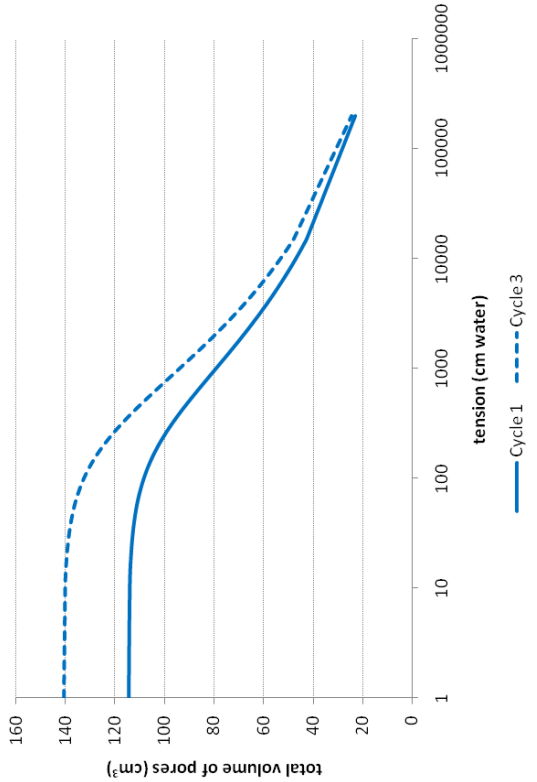

SS/4	cycle 1	*lower*	*upper*	cycle 3	*lower*	*upper*
bulk density (g cm^{-3})	**1.43E+00**			**1.28E+00**		
alpha	**4.08E-03**	*3.50E-03*	*4.67E-03*	**4.19E-03**	*3.96E-03*	*4.43E-03*
n	**1.24E+00**	*1.23E+00*	*1.24E+00*	**1.26E+00**	*1.26E+00*	*1.26E+00*
K_{sat} (cm s^{-1})	**4.48E-07**	*3.04E-07*	*5.92E-07*	**2.74E-06**	*2.38E-06*	*3.11E-06*
l	**1.80E+01**	*1.36E+01*	*2.24E+01*	**5.35E+01**	*5.02E+01*	*5.67E+01*
R^2 drainage	**9.96E-01**			**9.98E-01**		

Figure 104. SS/4, sample 8. Total volume of water filled pores during drainage cycles 1 and 3.

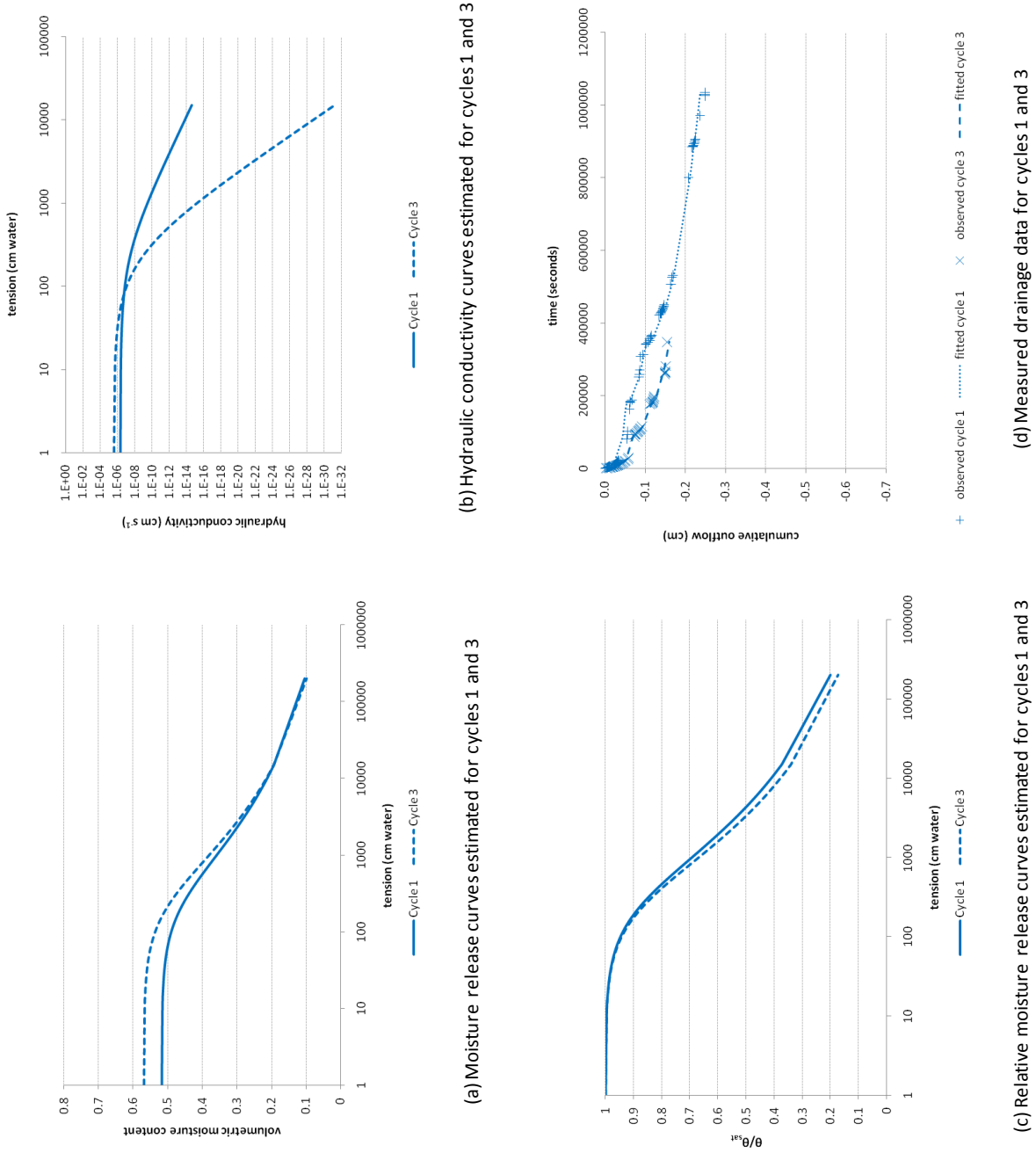

Figure 105. SS/4, sample 8. Hydraulic properties estimated with HYDRUS-1D.

Appendix 6

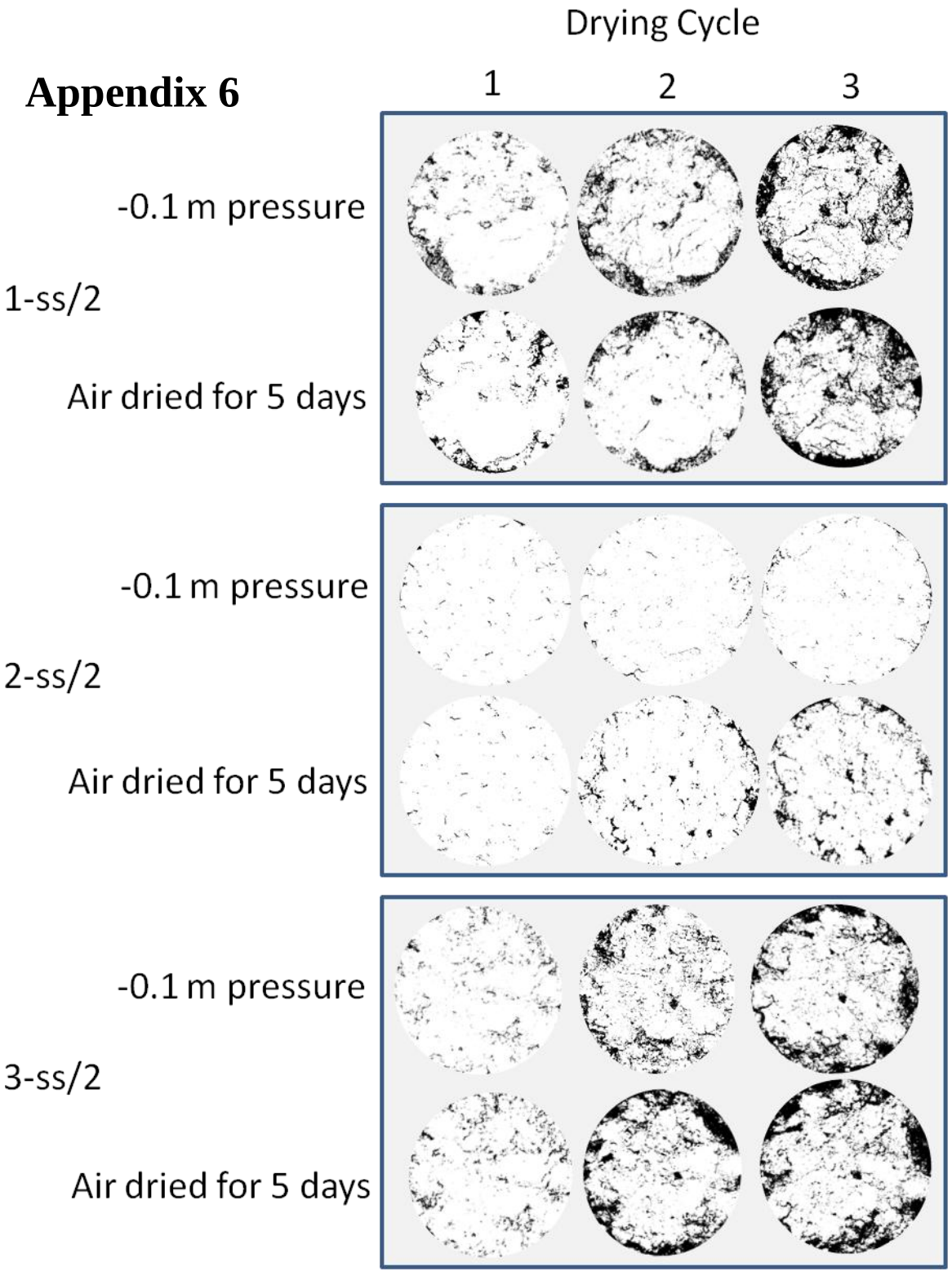
Drying Cycle
1
2
3
-0.1 m pressure
1-ss/2
Air dried for 5 days
-0.1 m pressure
2-ss/2
Air dried for 5 days
-0.1 m pressure
3-ss/2
Air dried for 5 days

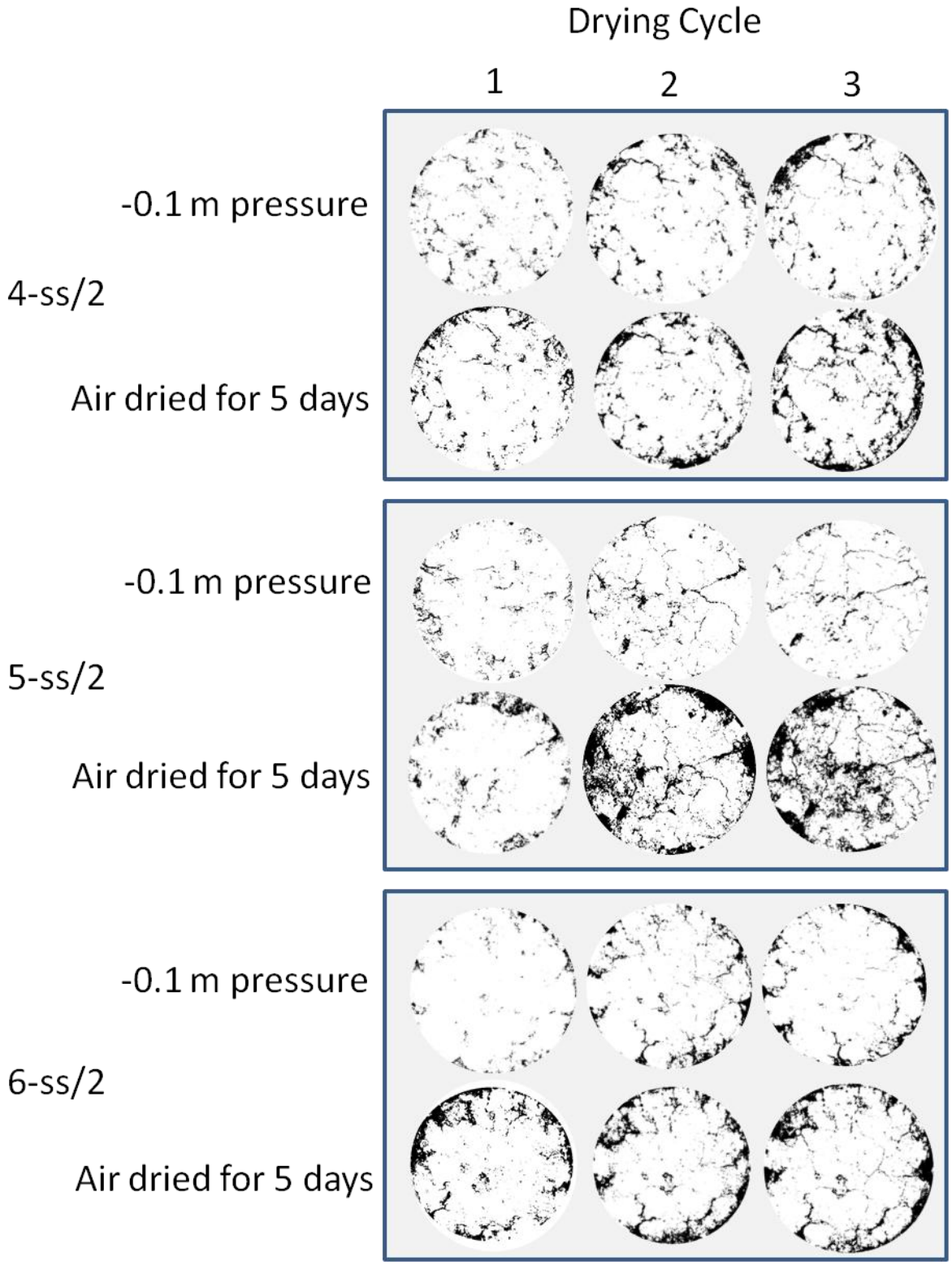
Drying Cycle
1
2
3
-0.1 m pressure
4-ss/2
Air dried for 5 days
-0.1 m pressure
5-ss/2
Air dried for 5 days
-0.1 m pressure
6-ss/2
Air dried for 5 days

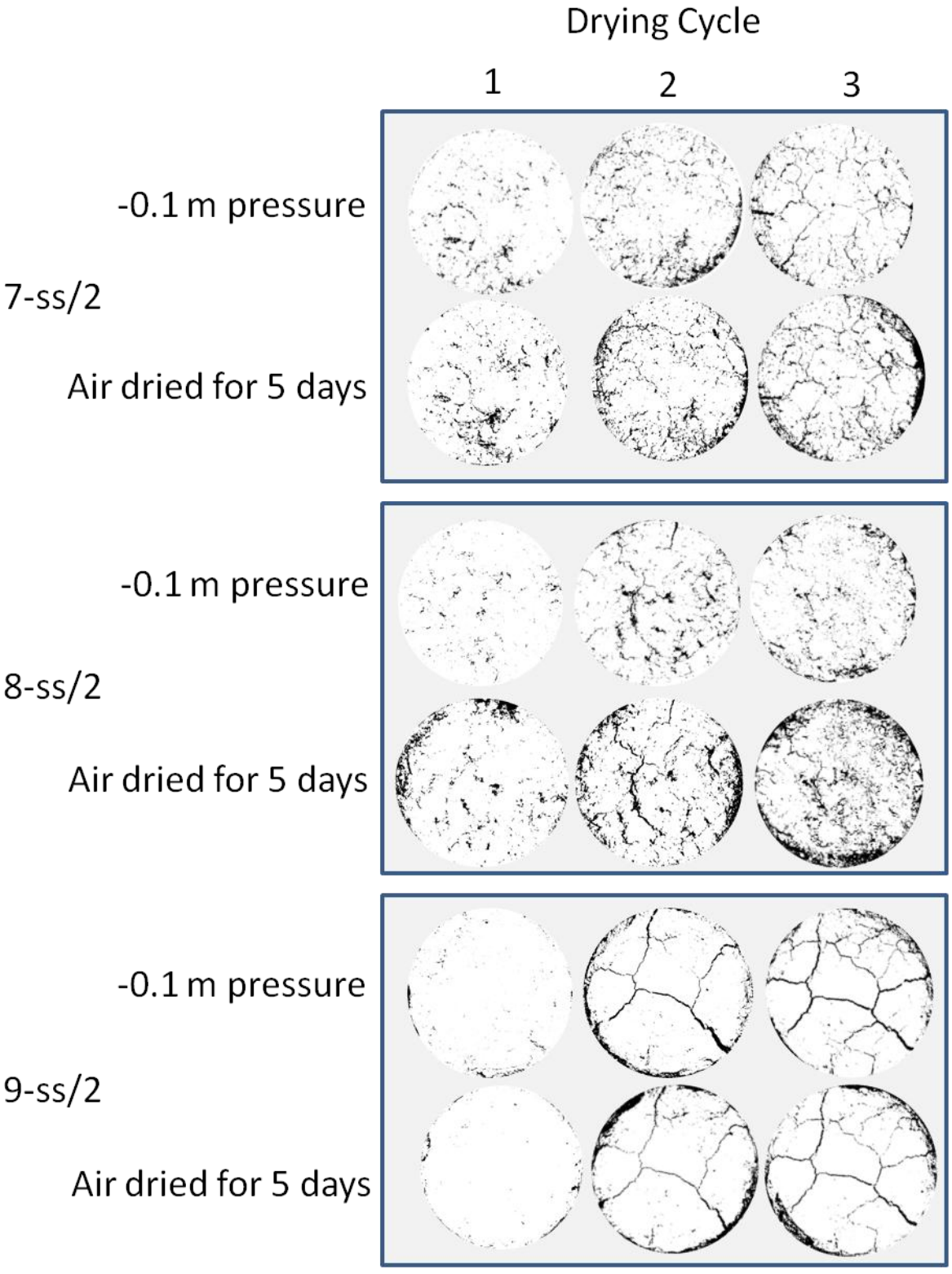
Drying Cycle
1
2
3
-0.1 m pressure
7-ss/2
Air dried for 5 days
-0.1 m pressure
8-ss/2
Air dried for 5 days
-0.1 m pressure
9-ss/2
Air dried for 5 days

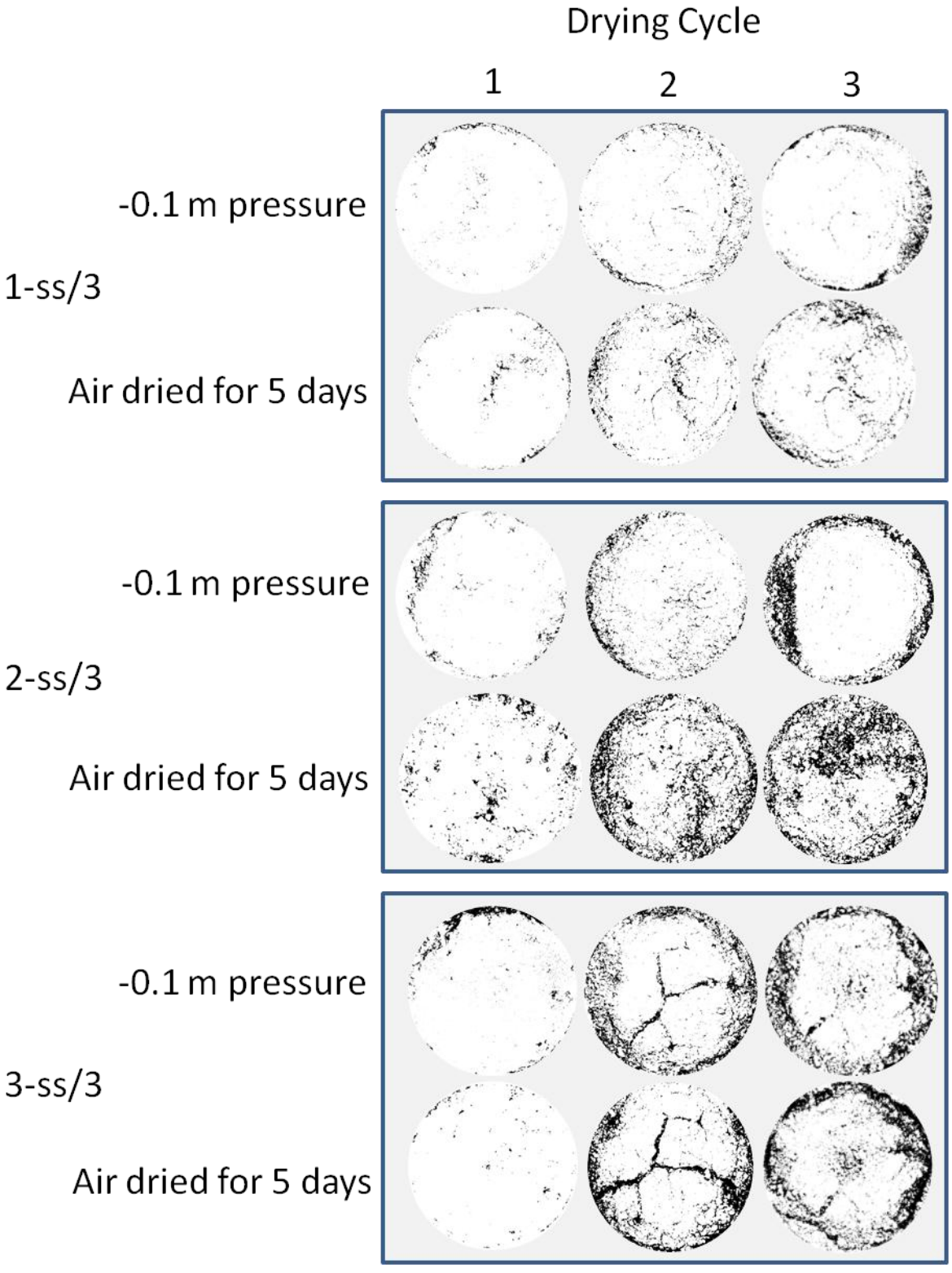
Drying Cycle
1
2
3
-0.1 m pressure
1-ss/3
Air dried for 5 days
-0.1 m pressure
2-ss/3
Air dried for 5 days
-0.1 m pressure
3-ss/3
Air dried for 5 days

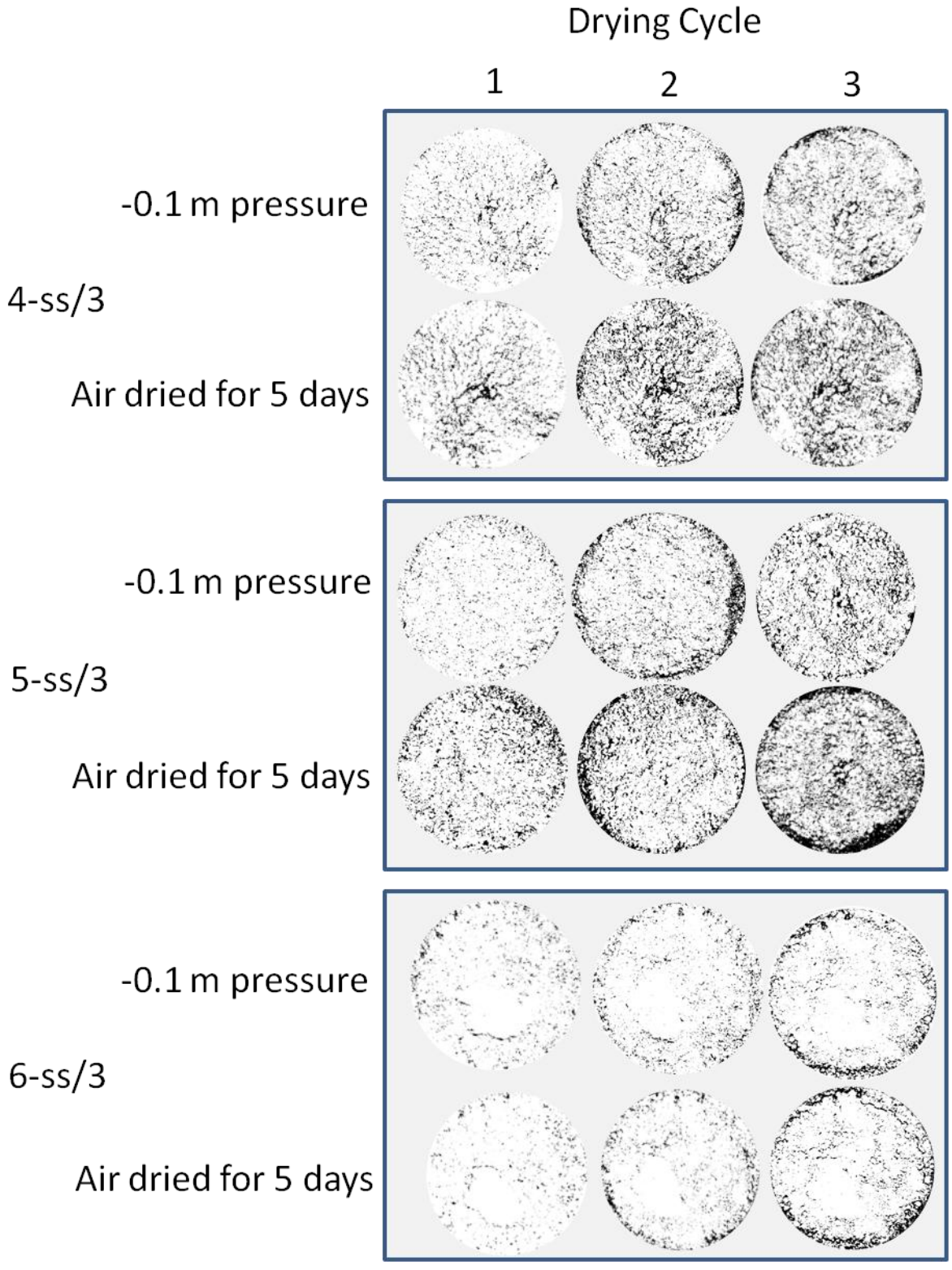
Drying Cycle
1
2
3
-0.1 m pressure
4-ss/3
Air dried for 5 days
-0.1 m pressure
5-ss/3
Air dried for 5 days
-0.1 m pressure
6-ss/3
Air dried for 5 days

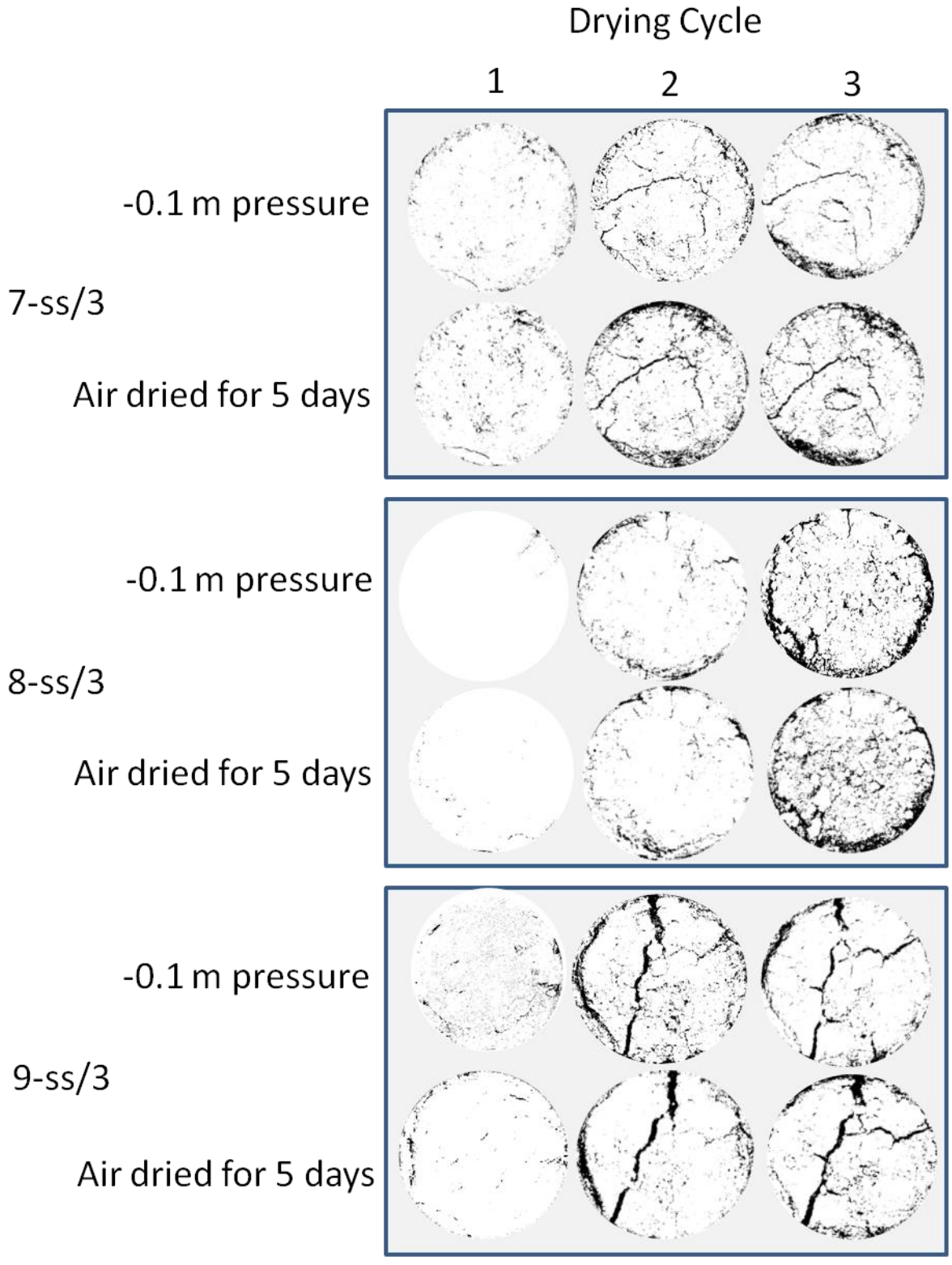
Drying Cycle
1
2
3
-0.1 m pressure
7-ss/3
Air dried for 5 days
-0.1 m pressure
8-ss/3
Air dried for 5 days
-0.1 m pressure
9-ss/3
Air dried for 5 days

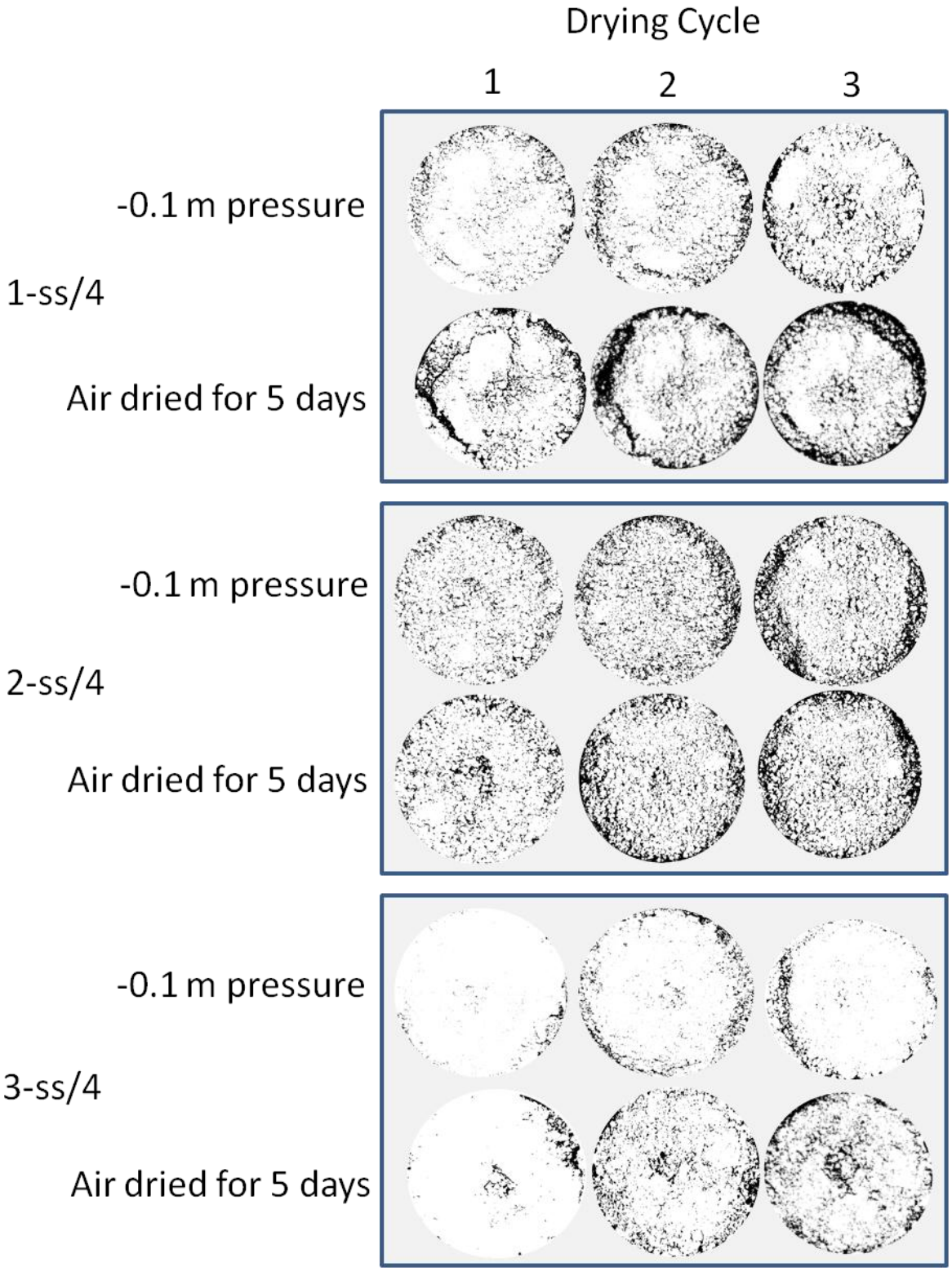
Drying Cycle
1
2
3
-0.1 m pressure
1-ss/4
Air dried for 5 days
-0.1 m pressure
2-ss/4
Air dried for 5 days
-0.1 m pressure
3-ss/4
Air dried for 5 days

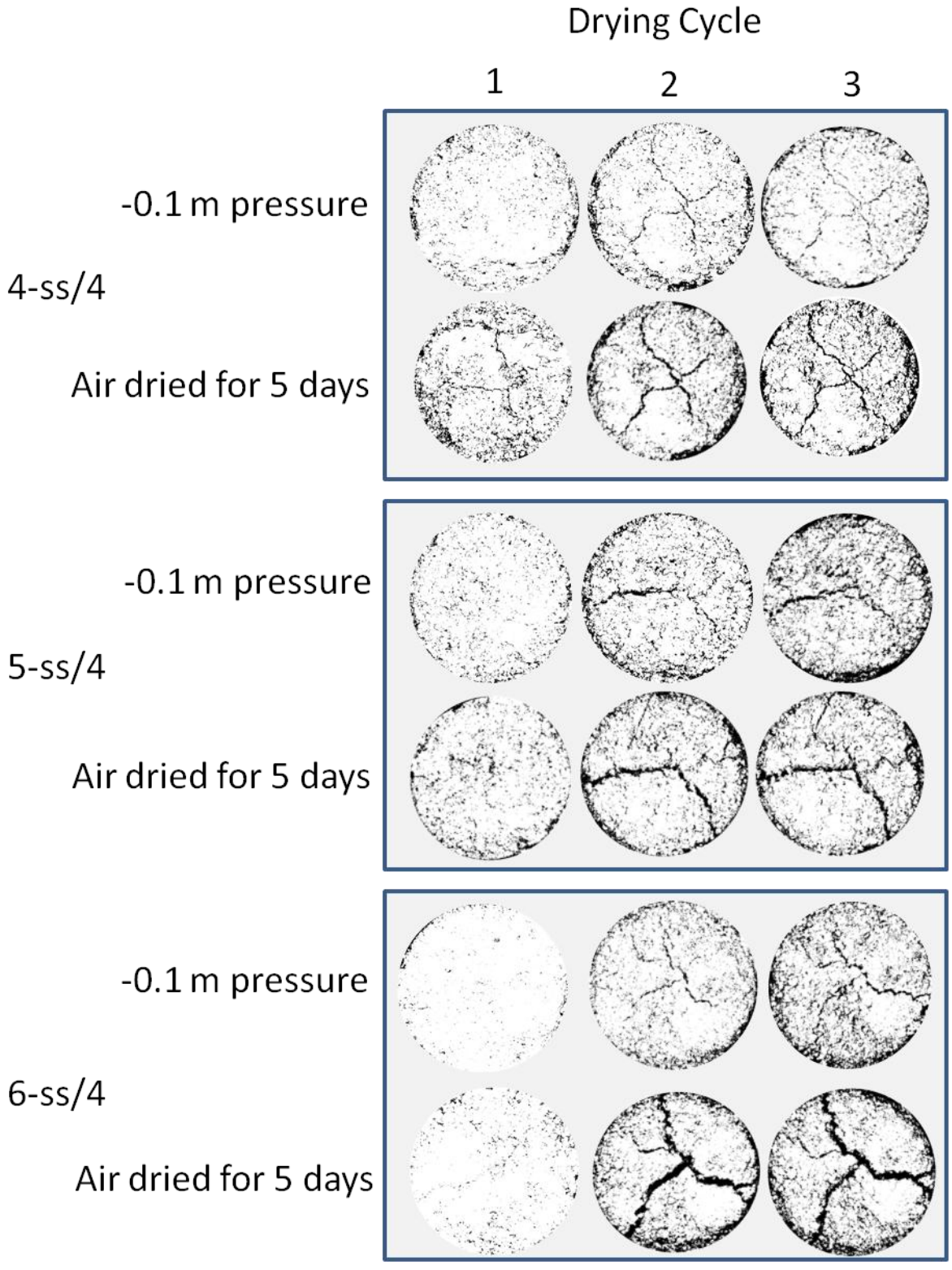
Drying Cycle
1
2
3
-0.1 m pressure
4-ss/4
Air dried for 5 days
-0.1 m pressure
5-ss/4
Air dried for 5 days
-0.1 m pressure
6-ss/4
Air dried for 5 days

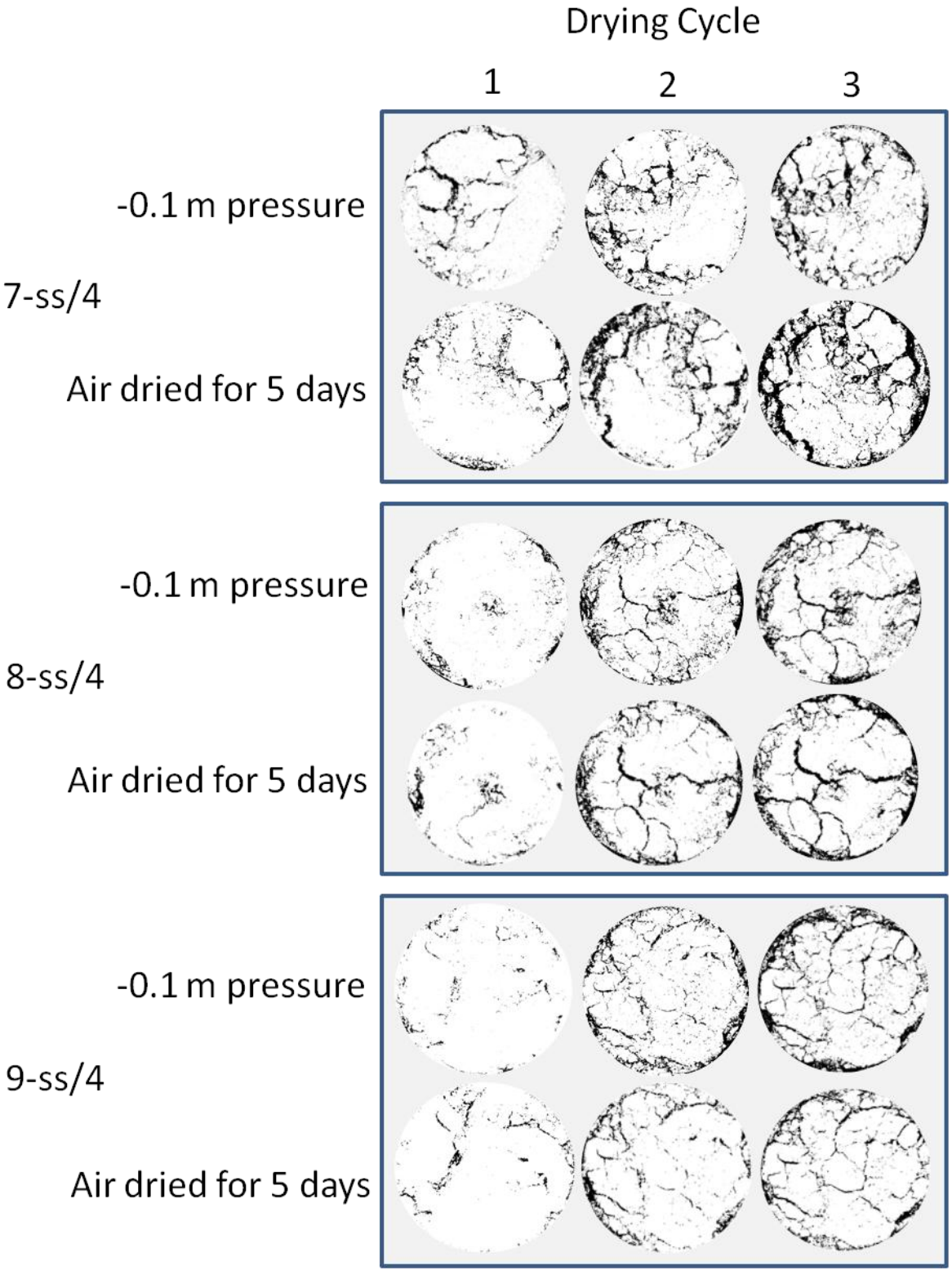
Drying Cycle
1
2
3
-0.1 m pressure
7-ss/4
Air dried for 5 days
-0.1 m pressure
8-ss/4
Air dried for 5 days
-0.1 m pressure
9-ss/4
Air dried for 5 days